DOCTOR OF PHILOSOPHY

Investigations into the biotechnological applications of dielectrophoresis.

Burt, Julian Paul Hillhouse

Award date:
1990

Awarding institution:
Bangor University

PAGE/PAGES
EXCLUDED
UNDER
INSTRUCTION
FROM
UNIVERSITY

A Thesis submitted to the University of Wales
in candidature for the degree of
Doctor of Philosophy

Investigations into the Biotechnological Applications of Dielectrophoresis

by

Julian Paul Hillhouse Burt B.Sc.

School of Electronic Engineering Science,
University of Wales,
Bangor, Gwynedd.

May 1990

ACKNOWLEDGEMENTS

I would like to take this opportunity of thanking all my friends and members university staff, both academic and technical, who have given their invaluable assistance during the course of this work.

I am particularly grateful to my supervisor Professor Ron Pethig for his constant enthusiasm, advice and encouragement and to Mr Peter Whittington and Drs Mike Norton and Neil George of Warren Spring Laboratory for their interest and support during this project.

I am also indebted to Dr. Peter Gascoyne for his help and encouragement during my visit to the M.D. Anderson Cancer Center, Houston, Texas, U.S.A. and for making the time I spent there so rewarding and enjoyable.

I would also like to express my thanks to Dr Alan Doyle for allowing me to spent some time at the European Collection of Animal Cell Cultures, Porton Down, U.K. and to his staff, in particular Ms. Sally Booth whose patience and care in growing cells was invaluable.

My thanks also go to my colleagues Talal Al-Ameen, Jonathan Price, Takashi Inoue, Jeremy Hawkes, Myles Capstick, Geoff Archer and Jonathan Bonnett for their friendship and useful discussions and to Brian Bolton and Stewart Clark (E.C.A.C.C., Porton Down), Phil Parsonage (Warren Spring Laboratory, Stevenage), Robyn Rhea and Jamileh Noshari (M.D. Anderson Cancer Center, Houston), John Tame, David Whitehead, Gwyn Williams and John Berry for their technical support

I would also like to gratefully acknowledge the award of an SERC-CASE research studentship in collaboration with Warren Spring Laboratory, Stevenage, U.K. and the financial support of the National Foundation for Cancer Research (U.S.A).

SUMMARY

The dielectrophoretic force experienced by a range of cell types has been examined with the aim of investigating possible applications of dielectrophoresis to Biotechnology. Measurements of the dielectrophoretic response of cells used a new optical measurement system developed to provide a rapid, simple and accurate method for studying the dielectrophoretic behaviour of micro-organisms over the frequency range 1Hz to 4MHz.

The cell types used in these experiments were bacteria, mammalian cells and a range of Friend Murine Erythroleukaemia cell lines.

It has been found that the dielectrophoretic response of a particle may be described in three distinct regions. At frequencies below 200Hz the dielectrophoretic force is found to be greatly influenced by the presence of a net surface charge on the cells, causing a large, hitherto unobserved, collection at low frequencies. Over the mid-frequency range (200Hz to 10kHz) the collection is found to be controlled by the effective conductivity of the cells whereas above 10kHz the dielectrophoretic response is dictated by the dielectric permittivity of the cells.

Investigations into the effects of suspending medium conductivity on the dielectrophoretic response showed that for frequencies below 1MHz the magnitude of the force reduced with increasing media conductivity and became directed away from the regions of high field intensity when the media conductivity was greater than that of the cells.

Experiments using mammalian cell lines revealed that on the chemically-induced transformation of a cell line from a cancerous state to a near-normal state, an increase in the effective surface conductivity of the cell occurs. This is thought to be related to an increase in membrane rigidity, associated with the increased membrane content of fatty acid molecules such as cholesterol and protein cross-linking effects. A similar effect was also seen in HeLa cells exposed to formaldehyde.

The implications of these results to the biotechnological applications of dielectrophoresis are also discussed.

CONTENTS

CHAPTER 1

INTRODUCTION

Over the past 15 years biotechnological industries have undergone massive and rapid expansion as a result of advances in genetic engineering and fermentation technology. To aid British industries in this growth, the Department of Trade and Industry initiated the Biological Separations Club (BIOSEP) with the aim of creating a fund of information on biotechnological processes as well as co-ordinating research projects of common interest to participating companies. One area of interest was the "Downstream Processing" a product undergoes during its manufacture. The origin of the majority of biotechnological products is the large scale growth of specific cell lines. These lines are usually genetically engineered to over-produce a required chemical or protein. The full recovery process of a product from the fermented cell suspension (broth) depends on whether the chemical is retained within the grown cell or secreted into the growth medium. In all cases the grown cells have, at some time, to be removed from their suspending media. Current separation methods rely on the use of centrifugation or filtration. Both of these processes are time consuming and suffer from a number of drawbacks such as the binding of filters. A State of the Art Report (Bowden and Whittington, 1986) which studied novel separation technologies, compared alternative methods of particle separation including electrophoresis and the magnetic seeding of cell lines. The report recommended a programme of work to study the potential applications of a phenomenon known as dielectrophoresis to biotechnological processes, in particular cell separation.

Dielectrophoresis can be defined as the induced motion of matter, charged or uncharged, in non-uniform a.c. or d.c. electric fields. This should not be confused with the more common technique of electrophoresis where particles experience a free charge related force in the

presence of uniform electric fields. Observations of the dielectrophoretic effect date back to 1923 when Hateschek and Thorne reported that particles suspended in a narrow field system migrated towards the field-producing electrodes. Similar observations were reported by Soyenoff (1931) when studying the coalescence of coal dust suspended in toluene. However, the first major study of this phenomenon was not until 1951 when Herbert Pohl published his paper entitled "The Motion and Precipitation of Suspensoids in Divergent Electric Fields". Pohl called the effect "Dielectrophoresis" and concluded that the magnitude of the dielectrophoretic force experienced by particles was dependent on the dielectric properties of the particles rather than the presence of any free charges associated with the particle.

The nature of the dielectrophoretic force can be described by means of the following example. Figure1.1(a) shows two particles, one charged and the other uncharged, suspended in an uniform electric field. The charged particle will experience a net Coulombic force towards the electrode of opposite polarity (in this example the cathode). Coulombic forces also act on dipoles within the neutral particle causing the particle to become polarised. Due to the uniform nature of the electric field, the force on the induced positive polarisation charge (given by F=q.E where q is the charge and E is the electric field strength) is equal and opposite to the force on the negative polarisation charge resulting in a net cancellation of the forces on the particle. If the same neutral particle is suspended in a non-uniform electric field (figure 1.1(b)) it undergoes a similar polarisation process. However, in this case the unequal electric field strength on each side of the particle, caused by the non-uniform form of the field, gives rise to a net translational force towards the region of strongest field (about the point-like cathode in figure 1.1(b)). A dielectrophoretic force will also act upon a charged particle suspended in a non-uniform field where the net force experienced by the particle is the vector sum of the dielectrophoretic and coulombic forces on the particle. As the dielectrophoretic force is always directed towards the region of highest field strength, so the polarity of the electric field may be changed without affecting the magnitude or direction of the force enabling a.c. as well as d.c. electric fields to

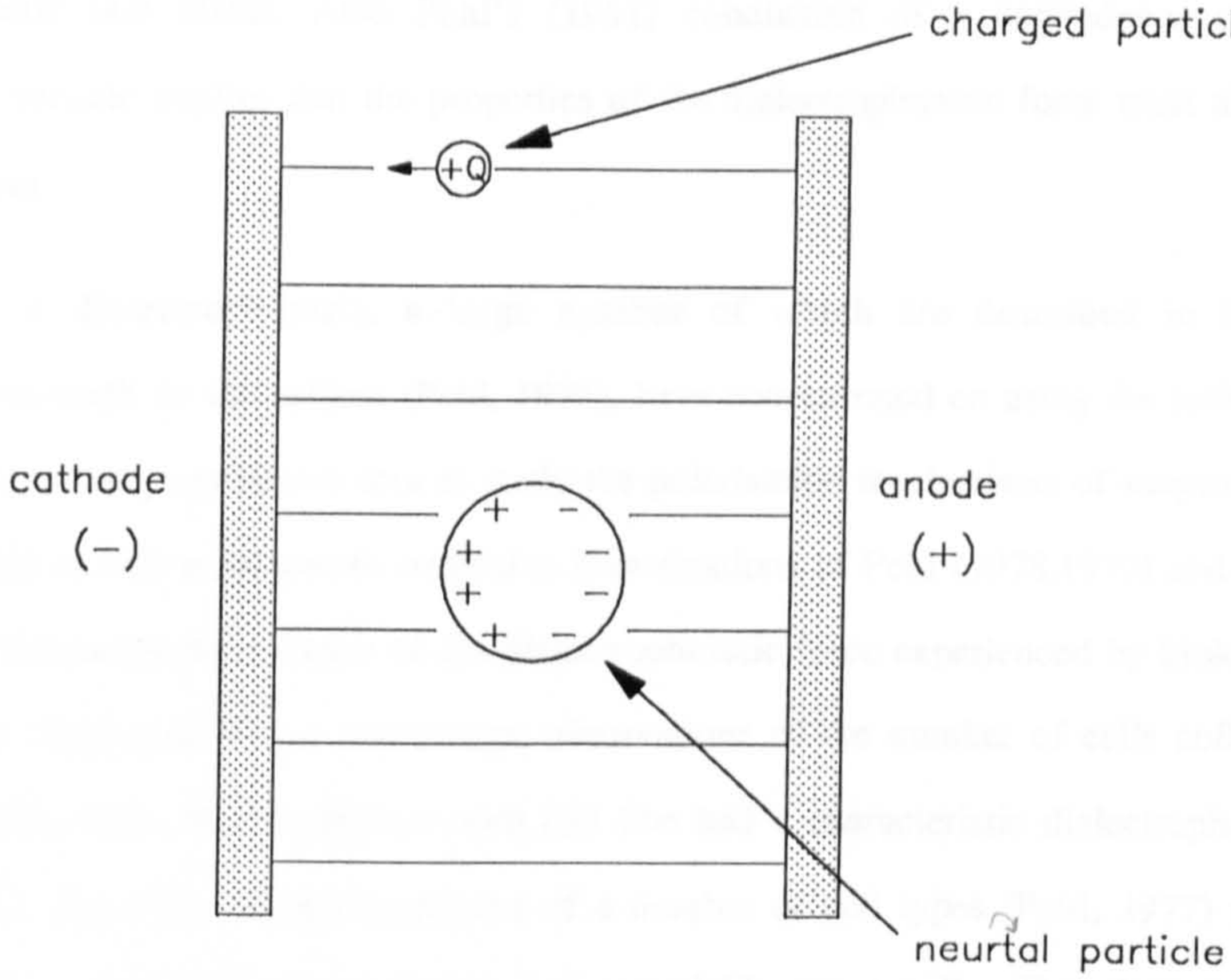

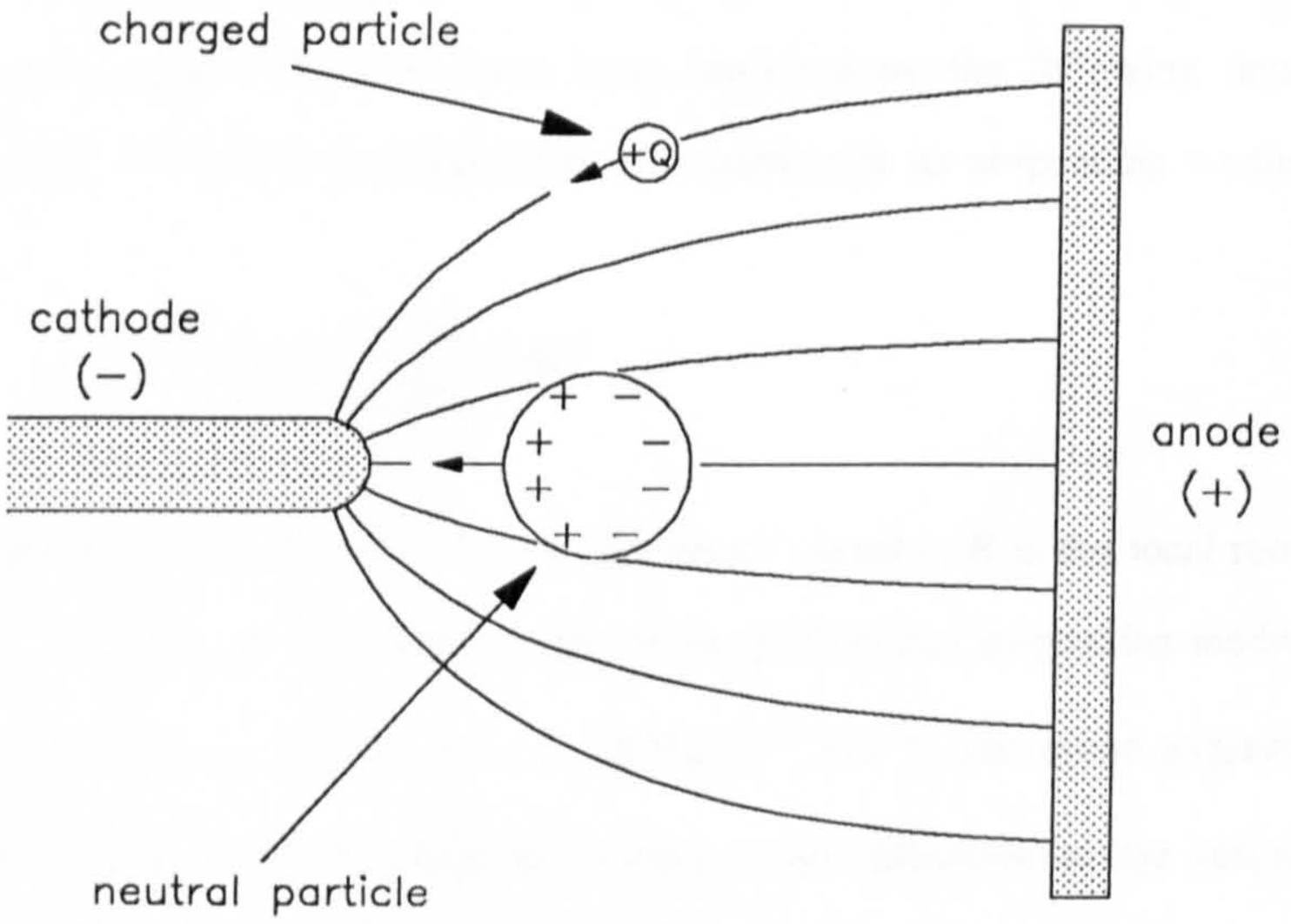

Figure 1.1 A comparison of the behaviour of neutral and charged particles suspended in (a) a uniform electric field and (b) a non-uniform electric field.

be used to generate this effect. Also Pohl's (1951) conclusion of a dependence on the polarisability of a particle implies that the properties of the dielectrophoretic force must also be frequency dependent.

Previous studies of dielectrophoresis, a large number of which are described in Pohl's comprehensive monograph on the subject (Pohl, 1978), have concentrated on using the technique of dielectrophoresis as an investigative tool to study the polarisation mechanisms of suspensions. Of particular interest to this work are the extensive investigations of Pohl (1978,1977) and other co-workers on the frequency dependence of the dielectrophoretic force experienced by biological cells under various conditions. Using microscope observations of the number of cells collected at platinum electrodes, Pohl discovered that each cell line had a characteristic dielectrophoretic response. Figure 1.2 shows the collection spectra of a number of cell types (Pohl, 1977) along with a comparison of the response of viable and non-viable yeast cells. The characteristic differences in the dielectrophoretic responses of these cells implies that dielectrophoresis may be used in the large scale detection and characterisation of cell lines. To date the differences in the collection spectra of particles have been explained by the following dependence of the dielectrophoretic force on the polarisability of a particle in its suspending medium (Pohl,1978):

$$\mathbf{F} = \frac{1}{2} v \varepsilon_o \varepsilon_m \frac{\varepsilon_p - \varepsilon_m}{\varepsilon_p + 2\varepsilon_m} \nabla |\mathbf{E}|^2$$

where v is the volume of the cell, ∇ is the del vector operator, $\mathbf{E}$ is the local root mean squared electric field, ε_p and ε_m are the permittivities of the particle and suspending medium respectively and ε_o is the permittivity of free space ($\varepsilon_o = 8.85 \times 10^{-12}$ Fm^{-1}). The above expression shows that the magnitude of the force is essentially related to the difference in the permittivities of the particle and the suspending medium. Using this approach, it has been possible to broadly explain the presence of a number of peaks in the dielectrophoretic collection spectrum of chloroplasts (Pethig, 1979) as well as explaining the presence of regions of zero collection observed in the spectrum.

Fig 1.2.

Dielectrophoresis has also been studied with more commercial applications in mind. Pohl (1958) developed a small-scale continuous separator for the removal of PVC polymers from benzene/tetrachloromethane mixtures. A semi-continuous separator has also been developed by Sasaki and Dunthorpe (1984) for the particulate cleaning of lubricating oils using d.c. (10kV) electric fields. Various other small-scale separators have been developed for the removal of particles such as magnesium oxide and other minerals from solution (Lin and Benguigui 1982, Lin et al 1979). The largest separation system (up to $50m^3$) has been developed by Hall and Brown (1966). Their batch system uses a combination of electrophoretic and dielectrophoretic forces to remove particles from hydraulic, lubricating, fuel and transformer oils.

A common factor in all previous studies of the dielectrophoretic effect is the use of low conductivity ($<10^{-5}Sm^{-1}$) suspending mediums. It has long been known (Pohl, 1978) that the dielectrophoretic force is reduced in magnitude in the presence of conducting solutions. This poses a considerable problem for biological separation since a typical suspending medium for cells usually contains an equivalent to 150mM sodium chloride concentration to maintain an osmolarity equal to that of the cell interior as well as containing a number of different species of ions essential for maintaining cell viability. The ionic nature of biological solutions implies a typical conductivity of $1.5Sm^{-1}$ for cell suspending media (Bowden and Whittington, 1986). In overcoming the problems of a conducting medium, it is essential to first determine the parameters which control the magnitude and direction of the dielectrophoretic force. The early stages of the work described here concentrate on the development of a novel optical technique for measuring the dielectrophoretic responses of various cell types with increased speed and accuracy over previously used techniques. Having developed a prototype optical measurement system capable of studying the response of a number of bacteria, investigations turned to the relationship between the conductivities of the bacteria *Micrococcus lysodeikticus* and its suspending medium with respect to the properties of the dielectrophoretic force. Experiments were carried out using various medium conductivities as well as altering the properties of the bacteria by treatment with the enzyme lysozyme.

Further development of the optical measurement system enabled the theoretical prediction of a conductivity dependence in the dielectrophoretic force at frequencies below 10kHz to be verified. Also observed with the improved system was a large, previously unreported, dielectrophoretic response for applied fields below 100Hz in frequency. This response, measured in bacteria, yeasts and silicon powder, is explained in terms of the effective conductivity of the suspended particles.

Investigations into the possible applications of dielectrophoresis to high-cost, low-yield product manufacture and process control allowed a study of the dielectrophoretic responses of a range of mammalian cells to be made with particular attention being paid to the effects of the preserving agent formaldehyde on the collection of human cervical carcinoma, HeLa, cells. Utilising the results of previous experiments, the final set of experiments were aimed at investigating the more subtle changes that occur when chemically inducible erythroleukaemia cells undergo the transformation from a near-normal to a cancerous state.

The work described here investigates a small number of the many possible applications of dielectrophoresis to biotechnology. Through investigations of the fundamental parameters determining the dielectrophoretic force and by the development of a novel measurement system it has been possible to compile a comprehensive body of knowledge concerning the factors affecting the applications of dielectrophoresis using electric fields below 10 MHz and as a result of this, a number of interesting observations of the electrical properties of various cell systems have also been possible.

1.2 References

Bowden, C.P. and Whittington, P.N. (1986) *The Application of Novel Technologies to Biotechnological Separation*. BIOSEP/SAR6/86 Warren Spring Laboratory, Stevenage, U.K.

Hall, H.J. and Brown, R.F. (1966) Electrostatic Removal of Impurities from a Liquid of High Resistivity. *Lubrication Eng.* **22** 488.

Hateschek, E. and Thorne, P.C.L. (1923) Metal Sols in Non- dissociating Liquids Part1. Nickel in Toluene and Benzene. *Roy. Soc. Proc.* **103** 276-284.

Lin, I.J., Yaniv, I. and Zimmels, Y. (1979) On the Separation of Minerals in High Gradient Electric Fields. *13th International Mineral Processing Conference, Warsaw* 81-103.

Lin, I.J. and Benguigui, L. (1982) High Gradient Electric Field Separation and Dielectric Filtration of Fine Particles. *Proc. World Filtr. Cong.* **1** 177-185.

Pethig, R. (1979) *Dielectric and Electronic Properties of Biological Materials*. J. Wiley and Son, Chichester.

Pohl, H.A. (1951) The Motion and Precipitation of Suspensoids in Divergent Electric Fields. *J. Appl. Phys.* **22** 869-871.

Pohl, H.A. (1958) Some Effects of Non-uniform Fields on Dielectrics. *J. Appl. Phys.* **29** 1182-1189.

Pohl, H.A. (1977) Dielectrophoresis: Applications to the Characterisation and Separation of Cells. In *Methods of Cell Separation* (ed.) N. Catsimpoolas. Plenum Press, London.

Pohl, H.A. (1978) *Dielectrophoresis*. Cambridge University Press, Cambridge.

Sasaki, A and Dunthorpe O.M. (1984) *Filtration and Separation* Nov.-Dec. 407-410. (From Bowden and Whittington, 1986).

Soyenoff, J. (1931) Hydrocarbons as Dispersion Media: A review. *J. Phys. Chem.* **35** 2993-3002.

CHAPTER 2

BACKGROUND THEORY; DIELECTRICS, DIELECTROPHORESIS AND CELL STRUCTURE

2.1 Introduction

Presented in this chapter is the necessary background theory and information on the dielectric properties of materials, the dielectrophoretic force and cell structure used in chapters 3 to 6. Also included in this chapter is a brief overview of the general dielectric properties of cell systems together with the discussion of a suitable model with which to analyse these properties. The topics are discussed only briefly in this chapter, but a list of some of the many previous publications (section 2.9) which cover the subjects in much greater detail is also included.

2.2 Dielectric Permittivity

Consider two parallel metal plates of area A and separated by a vacuum at a distance d apart (figure 2.1). On the application of a potential difference, V, across the plates, a charge, Q_o, is created on the facing surfaces such that

$$Q_o = C_o V \qquad 2.1$$

where C_o is the capacitance of the plates. By Gauss's Law the field between the plates must be proportional to the charge density on the plates, therefore

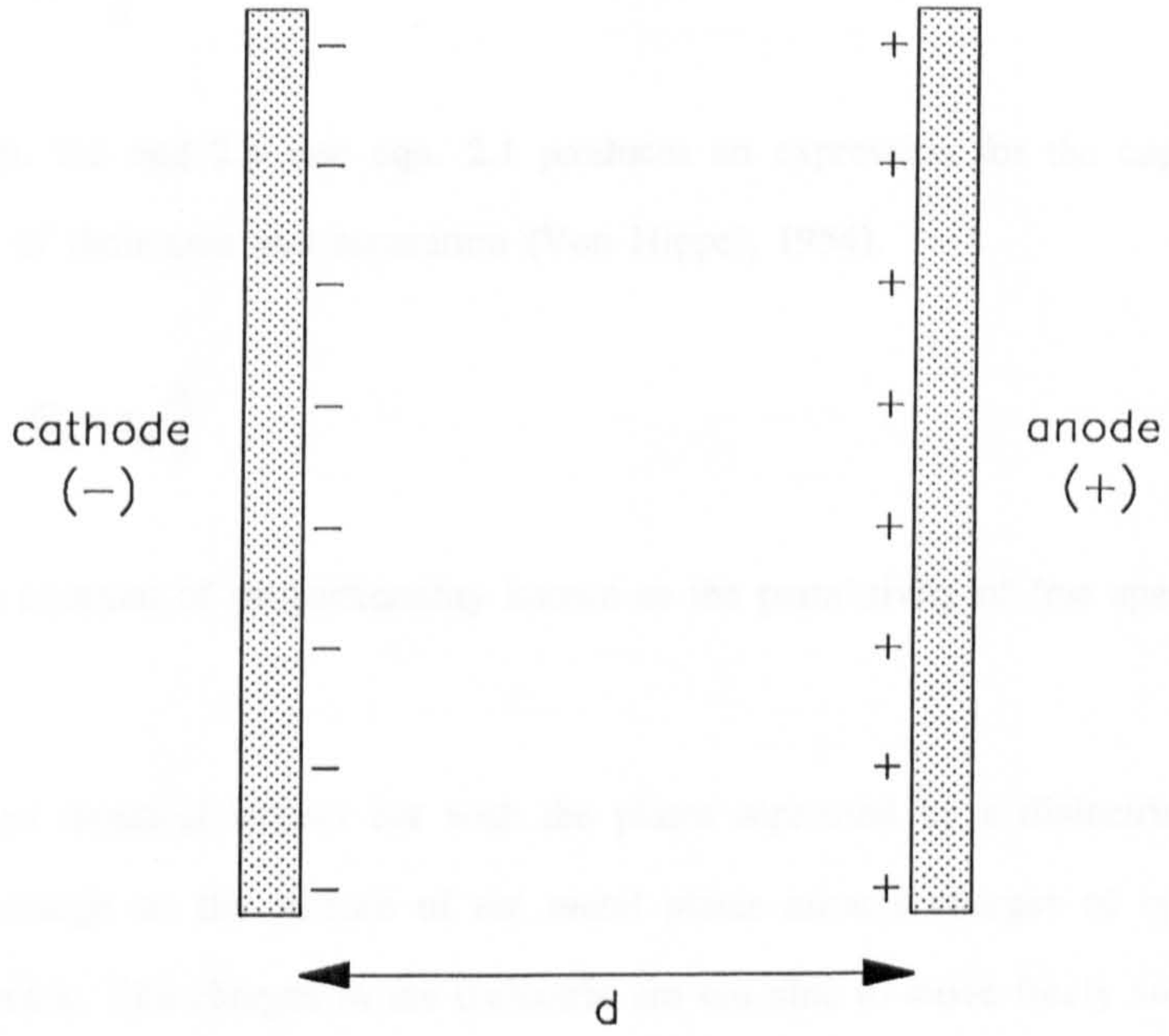

Figure 2.1 A parallel plate capacitor with plates of area A and separated by a distance d.

$$E \alpha \frac{Q_o}{A} \qquad 2.2$$

Also, for a parallel plate system the electric field strength E can be expressed as follows:

$$E = \frac{V}{d} \qquad 2.3$$

Substituting eqn. 2.2 and 2.3 into eqn. 2.1 produces an expression for the capacitance of the plates in terms of their area and separation (Von Hippel, 1954).

$$C_o = \varepsilon_o \frac{A}{d}$$

where ε_o is the constant of proportionality known as the permittivity of free space ($\varepsilon_o = 8.85 \times 10^{-12}$ Fm^{-1})

Now consider an identical system but with the plates separated by a dielectric material. The presence of a charge on the surface of the metal plates attracts charges of opposite polarity within the dielectric. The charges in the dielectric are not able to move freely and participate in conduction processes. However, they are able to move by small amounts under the influence of an electrostatic force causing a net build up of charge on the surface of the dielectric (figure 2.2). The charge built up on the dielectric cancels the charge on the plates of the capacitor allowing extra charge to flow onto the plates in order to maintain a constant potential difference (eqn. 2.1). Therefore, the presence of a dielectric increases the amount of charge stored on the capacitor plates by an amount equal to the degree of polarisation of the dielectric.

$$Q_{total} = Q_o + Q_{polarisation}$$

Therefore, for a constant applied voltage

$$C_{o\,total} = C_o + C_{polarisation} = \varepsilon_o \frac{A}{d} + \varepsilon_o \varepsilon_r \frac{A}{d}$$

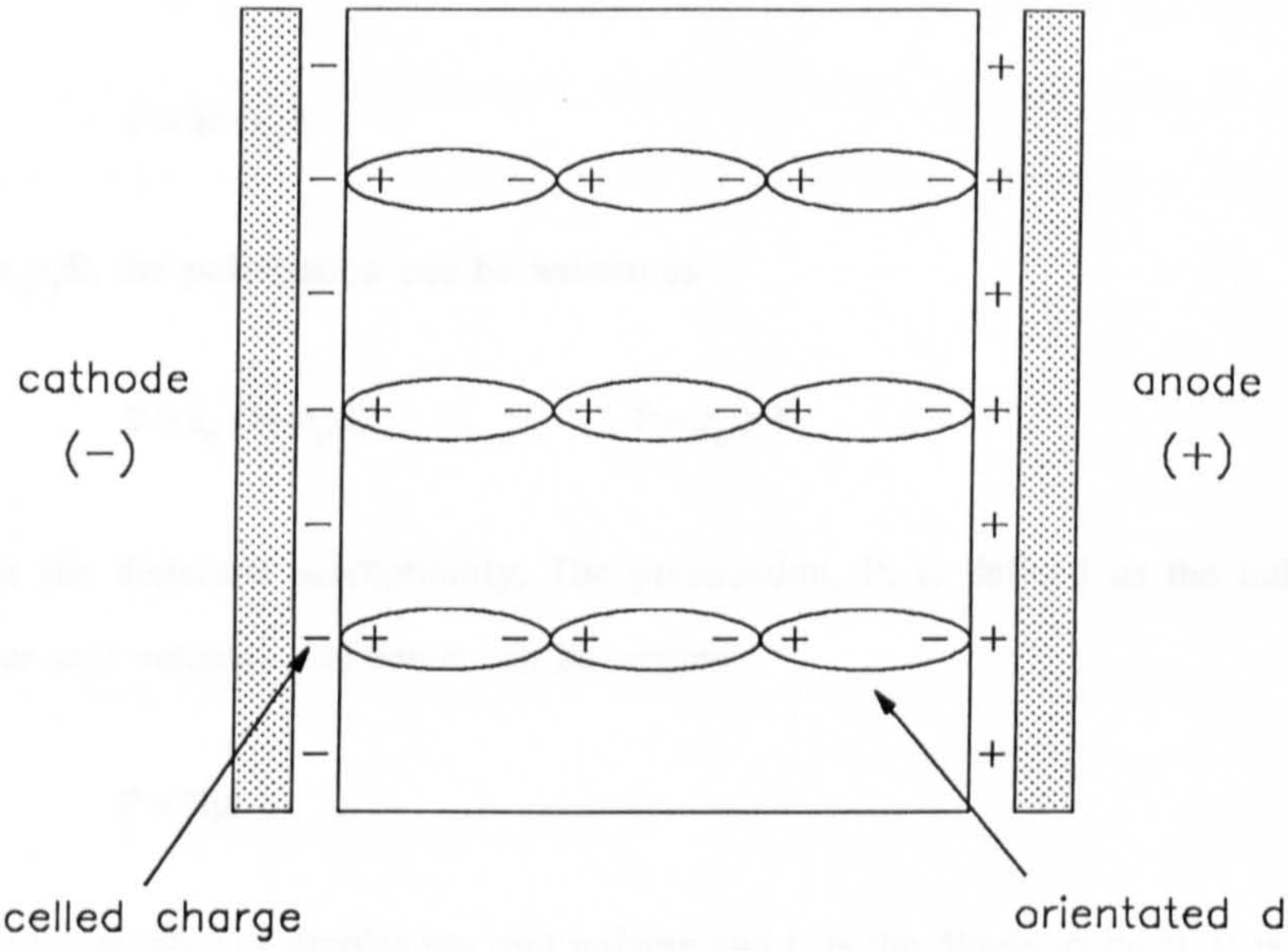

Figure 2.2 Two parallel plates separated by a dielectric to form a capacitor. Orientated dipoles within the dielectric effectively cancel a proportion of the charge on the metal plates.

where ε_r is the relative permittivity of the dielectric compared to that of free space.

To further understand the nature of the dielectric permittivity, the two plates should be described in electrostatic terms. The charge density (or polarisation, **P**) on the dielectric surface is equal to the total charge density on the plate (or Electric flux density, **D**) minus the charge required to maintain the potential difference between the plates.

$$\mathbf{P} = \mathbf{D} - \varepsilon_o \mathbf{E}$$

Since $\mathbf{D}=\varepsilon_o\varepsilon_r\mathbf{E}$, the polarisation can be written as

$$\mathbf{P} = \varepsilon_o (\varepsilon_r - 1)\mathbf{E} \quad ; \quad \mathbf{P} = \varepsilon_o \chi \mathbf{E} \qquad 2.4$$

where χ is the dielectric susceptibility. The polarisation, **P**, is defined as the induced dipole moment per unit volume and hence can be written

$$\mathbf{P} = N\mu$$

where N is the number of dipoles per unit volume and μ is the dipole moment. μ is the product of the polarisability of a dipole, α, and the local field strength about the dipole, E_L. Therefore, the relative permittivity of a dielectric (from eqn. 2.4) can be written as

$$\varepsilon_r = 1 + \frac{N\alpha E_L}{\varepsilon_o E} \quad ; \quad \alpha = \frac{P}{E} \qquad 2.5$$

This general relationship can be simplified (Allison, 1971) to arrive at the Claussus Mosotti equation (eqn. 2.6) for high degrees of crystal symmetry or complex molecular disorder.

$$\frac{\varepsilon_r - 1}{\varepsilon_r + 2} = \frac{N\alpha}{3\varepsilon_o} \qquad 2.6$$

2.3 The Complex Dielectric Permittivity

Now Consider the effect of applying a step voltage at time t=0 to the parallel plate capacitor in figure 2.2. Initially the dipoles within the dielectric will be randomly orientated and hence the polarisation, P, of the dielectric will be zero. The application of a step voltage causes the dipoles to align. This, however, is not an instantaneous process as the dipoles will experience some inertia. The rate of change in polarisation can be assumed to be proportional to the difference between the maximum possible polarisation and the actual polarisation and so can be written in terms of a first order differential equation

$$\frac{dP}{dt} = \frac{1}{\tau}(\chi E - P) \qquad 2.7$$

where τ is the constant of proportionality and both E and P are time dependent. Solving eqn. 2.7 using the integrating factor $\exp(t/\tau)$ the following relationship is obtained

$$P \exp(t/\tau) = \chi E \exp(t/\tau) + C \qquad 2.8$$

where C is the constant of integration. In defining a step voltage the polarisation at t=0 must be zero, therefore substituting t=0 into eqn 2.8 allows C to be found.

$$C = -\chi E$$

Hence the polarisation, P, can be described in the time domain as

$$P = \chi [1 - \exp(t/\tau)] E \qquad 2.9$$

Equation 2.9 predicts that, on the application of a step field, the polarisation will approach its maximum value exponentially at a rate determined by τ.

Solving eqn. 2.7 by a similar technique for the case of a sinusoidal field, $E=E_o\exp(j\omega\tau)$, (where ω represents the angular frequency of the voltage) the following frequency domain description of the polarisation can be obtained.

$$P = \frac{\chi E}{1+j\omega\tau} \qquad 2.10$$

Since in general

$$P = \chi \varepsilon_o E$$

for the sinusoidal case substituting $\varepsilon_o\chi = (\varepsilon_r\varepsilon_o - \varepsilon_o)$ into eqn. 2.10 reveals the total permittivity to be a complex term, ε^*.

$$\varepsilon^* = \varepsilon' - j\varepsilon'' \qquad 2.11$$

where

$$\varepsilon' = \varepsilon_o + \frac{\varepsilon_o(\varepsilon_s - 1)}{1+\omega^2\tau^2} \qquad 2.12$$

$$\varepsilon'' = \frac{\omega\tau\varepsilon_o(\varepsilon_s - 1)}{1+\omega^2\tau^2} \qquad 2.13$$

For the case of a d.c. voltage across the capacitor plates shown in figure 2.2, $\omega=0$ and the complex permittivity reduces to $\varepsilon^*=\varepsilon_s$. ε_s therefore has the physical meaning of the steady state d.c. permittivity.

By considering the energy storage properties of a dielectric in an a.c. field and introducing the first law of thermodynamics (conservation of energy) it has been shown (Frohlich, 1958) that the imaginary term, ε'', in the complex permittivity is a measure of the loss of energy from the field.

The frequency dependence of both ε' and ε'' is shown in figure 2.3. The equations describing this frequency variation (eqns. 2.12 and 2.13) are commonly referred to as the Debye equations, after the work of Debye (1929) who originally described the frequency dependence of polarisation processes analytically. Eqns. 2.12 and 2.13 can also be explained in terms of the

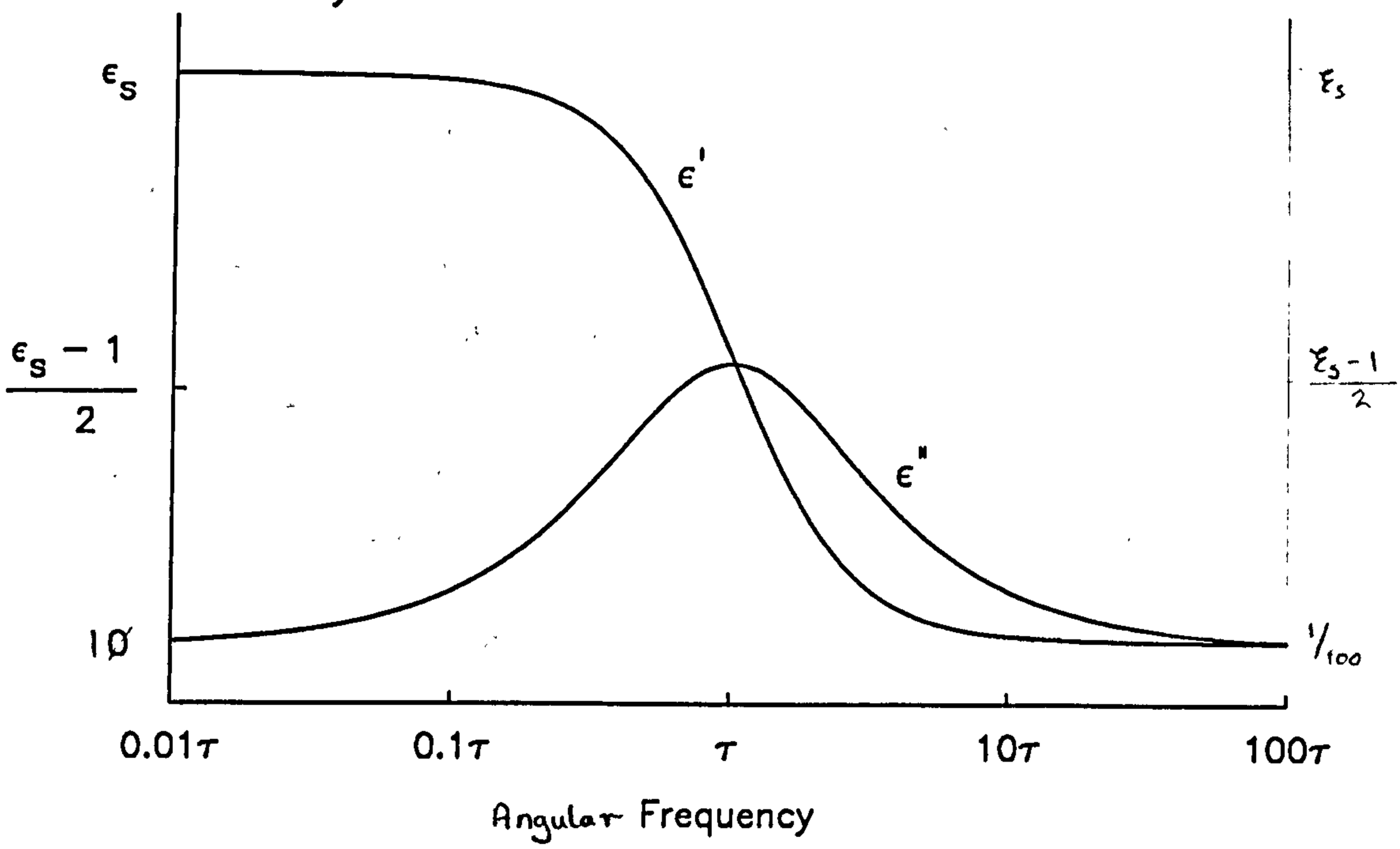

Figure 2.3 The variation in both the real and imaginary permittivity as described by the Debye equations (eqns. 2.12 and 2.13).

movement of a dipole and the energy stored by the dipole. If the dipoles within a dielectric align with a field taking a characteristic time, τ, to orientate, say 1 second, then on the application of an alternating voltage with a period of 100 seconds the dielectric stores the field energy for 99% of the period and loses energy for the 1 second it takes to orientate with the field. Therefore the energy stored per cycle (ε') is close to a maximum whereas the energy lost per cycle (ε'') is close to its minimum value. As the frequency of the applied field is increased, the dipole is aligning for a greater percentage of the periodic time causing the energy storage to be decreased whilst giving rise to an increase in energy lost. When the applied field period is equal to τ the the dipole will orientate in phase with the field and the energy stored will equal the energy lost. This frequency is referred to as the relaxation frequency and is the maximum field frequency at which the dipole can fully align with the field. At frequencies above the relaxation frequency the dipole cannot orientate fully, hence both the stored energy and the lost energy decrease until at frequencies where the period is much less than τ the dipole does not align with the field to any degree and so does not contribute to the overall polarisation process.

Substituting the complex permittivity into the a.c. form of Ohm's law allows an equivalent electrical circuit for the dielectric to be found.

$$j\omega C^* = j\omega\varepsilon_o\varepsilon'\frac{A}{d} + \omega\varepsilon_o\varepsilon''\frac{A}{d} = G + j\omega C$$

The presence of both a real and imaginary term in the admittance of the dielectric signifies a conductance in parallel with the energy storing capacitance. Figure 2.4(a) shows the equivalent circuit for a dielectric where the capacitor has an effective permittivity of ε' and the conductance provides a frequency dependent measure of the energy loss (ε'').

$$C = \varepsilon_o\varepsilon'\frac{A}{d} \qquad ; \qquad G = \sigma_{a.c.}\frac{A}{d}$$

where

$$\sigma_{a.c.} = \varepsilon_o\varepsilon''\omega$$

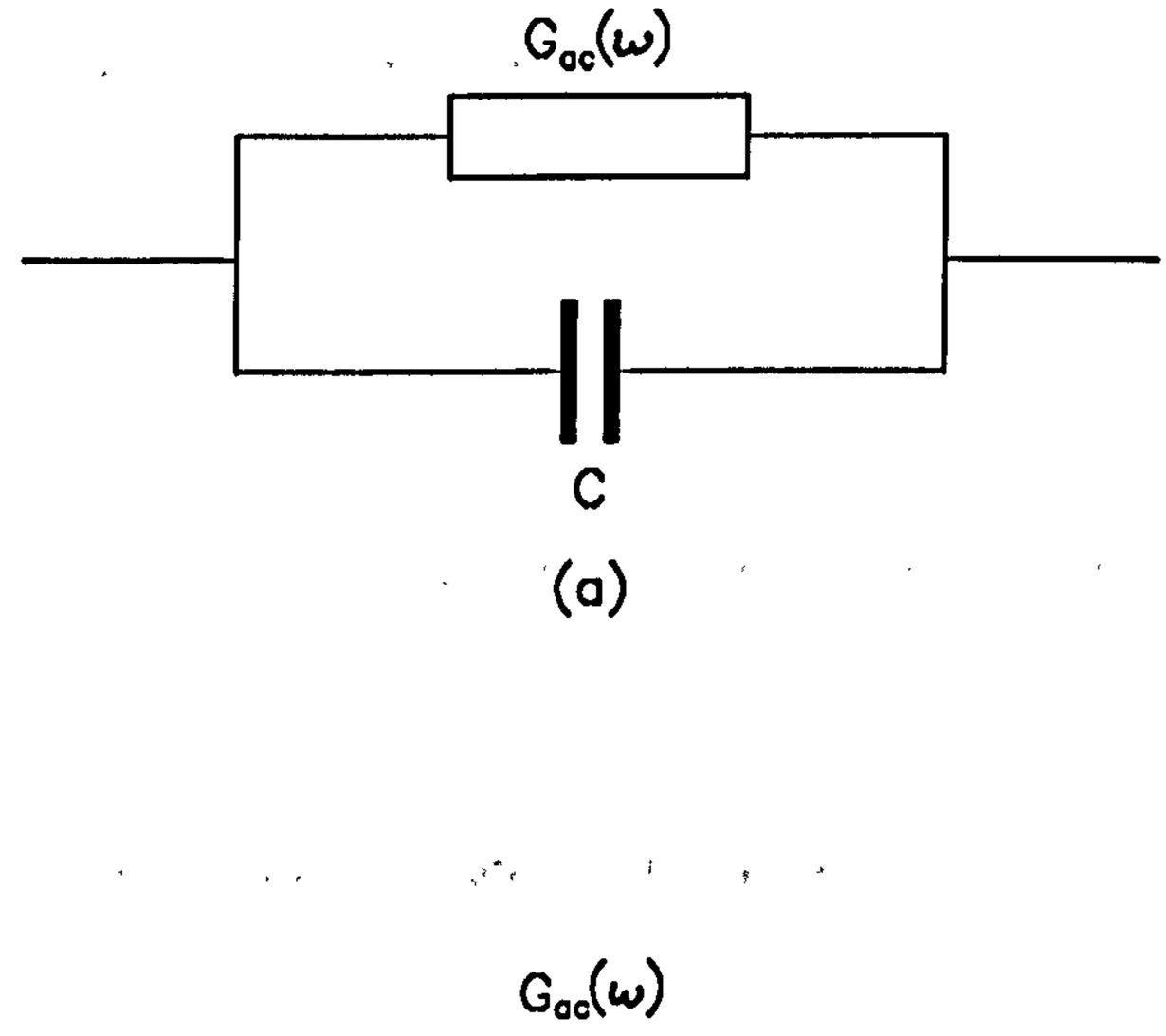

Figure 2.4 The equivalent electrical circuit for a dielectric (a) without and (b) with the presence of a component of d.c. conductivity.

Shown in figure 2.4(b) is the effect of any ionic conductive path through the dielectric. This appears as a frequency independent conductance also in parallel with the capacitance.

Substituting σ_{ac} into the complex permittivity, ε^*, a more convenient form of the complex permittivity of a dielectric is obtained.

$$\varepsilon^* = \varepsilon_o \varepsilon' - j\frac{\sigma_{a.c.}}{\omega} \qquad 2.14$$

It is this form of eqn. 2.11 that will be used to describe the complex permittivity in all further discussions.

2.4 Polarisation Mechanisms and Dielectric Relaxation

In section 2.2 the permittivity of a material was found to be dependent on the polarisability of the dielectric (eqn. 2.6). In general there are three basic polarisation processes which contribute to the polarisability. The first of these, referred to as orientational polarisation, α_o, occurs only in polar materials which, by definition, contain permanent dipoles in their structure arising from the separation of charged molecular groups within the material. Examples of molecules exhibiting this form of polarisability are Dimethylsulphoxide (DMSO) and hydrogen cyanide (HCN) as shown in figure 2.5. On the application of an electric field to such molecules the charged regions experience Coulombic forces causing the dipolar molecule to align with the field.

A second form of polarisation, atomic polarisation, α_a, occurs from the displacement of differently charged ions in a crystal lattice. An imposed electric field will cause positive ions to move relative to the negative ions inducing a dipole moment and associated polarisation in the dielectric.

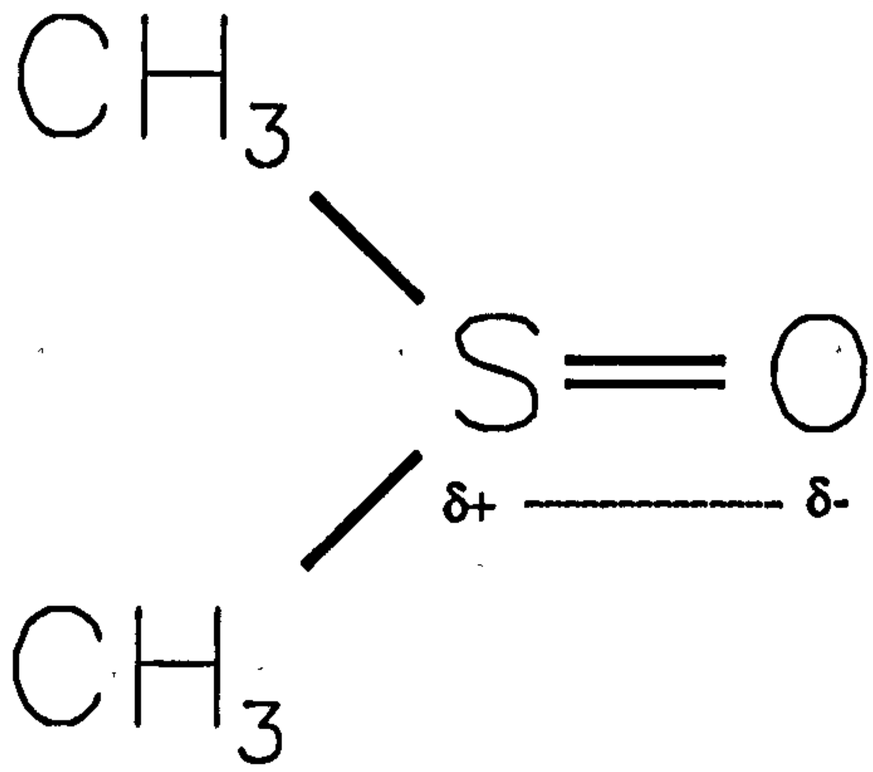

Dimethylsulphoxide (DMSO)

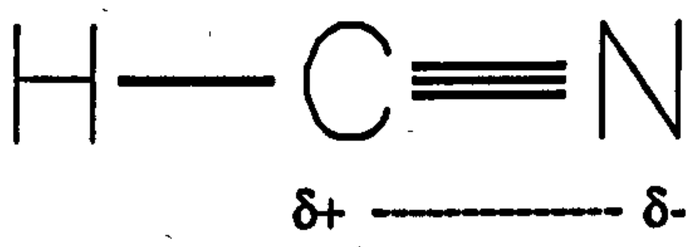

Hydrogen Cyanide (HCN)

Figure 2.5 Diagrams of the structure of dimethylsuphoxide and hydrogen cyanide showing the separation of charge causing the molecules to possess permanent dipoles.

The final polarisation effect is that which occurs at an atomic scale. Electronic polarisation, α_e, is the most common form of polarisation and arises from the field-induced displacement of the electron distribution around an atomic nucleus. This displacement, of around 10^{-8} Angstroms, occurs in all atoms.

A less obvious polarisation mechanism occurs at the interface of two dielectrics. This is referred to as interfacial or Maxwell–Wagner polarisation after the work of Maxwell (1892) and Wagner (1914, 1924). Figure 2.6 shows this situation in terms of a parallel plate capacitor containing two dielectrics of differing thickness, d_1 and d_2, and differing conductivity and permittivity, ε_1, σ_1 and ε_2, σ_2. The capacitor can be described in terms of the equivalent circuit also shown in figure 2.6 where

$$C_1 = \varepsilon_o \varepsilon_1 \frac{A}{d_1} \qquad C_2 = \varepsilon_o \varepsilon_2 \frac{A}{d_2}$$

$$R_1 = \frac{d_1}{A\sigma_1} \qquad R_2 = \frac{d_2}{A\sigma_2}$$

Solving the differential equations for the current flow through the circuit reveals that on the application of a step voltage to the circuit the voltages V_1 and V_2 increase exponentially to their maximum value with a time constant τ as given by

$$V_1 = \frac{VR_1}{R_1+R_2}\left(1-\left[\frac{\tau-R_2C_2}{\tau}\right]\exp(-t/\tau)\right)$$

$$V_2 = \frac{VR_2}{R_1+R_2}\left(1-\left[\frac{\tau-R_1C_1}{\tau}\right]\exp(-t/\tau)\right)$$

where

$$\tau = \frac{R_1R_2(C_1+C_2)}{R_1+R_2}$$

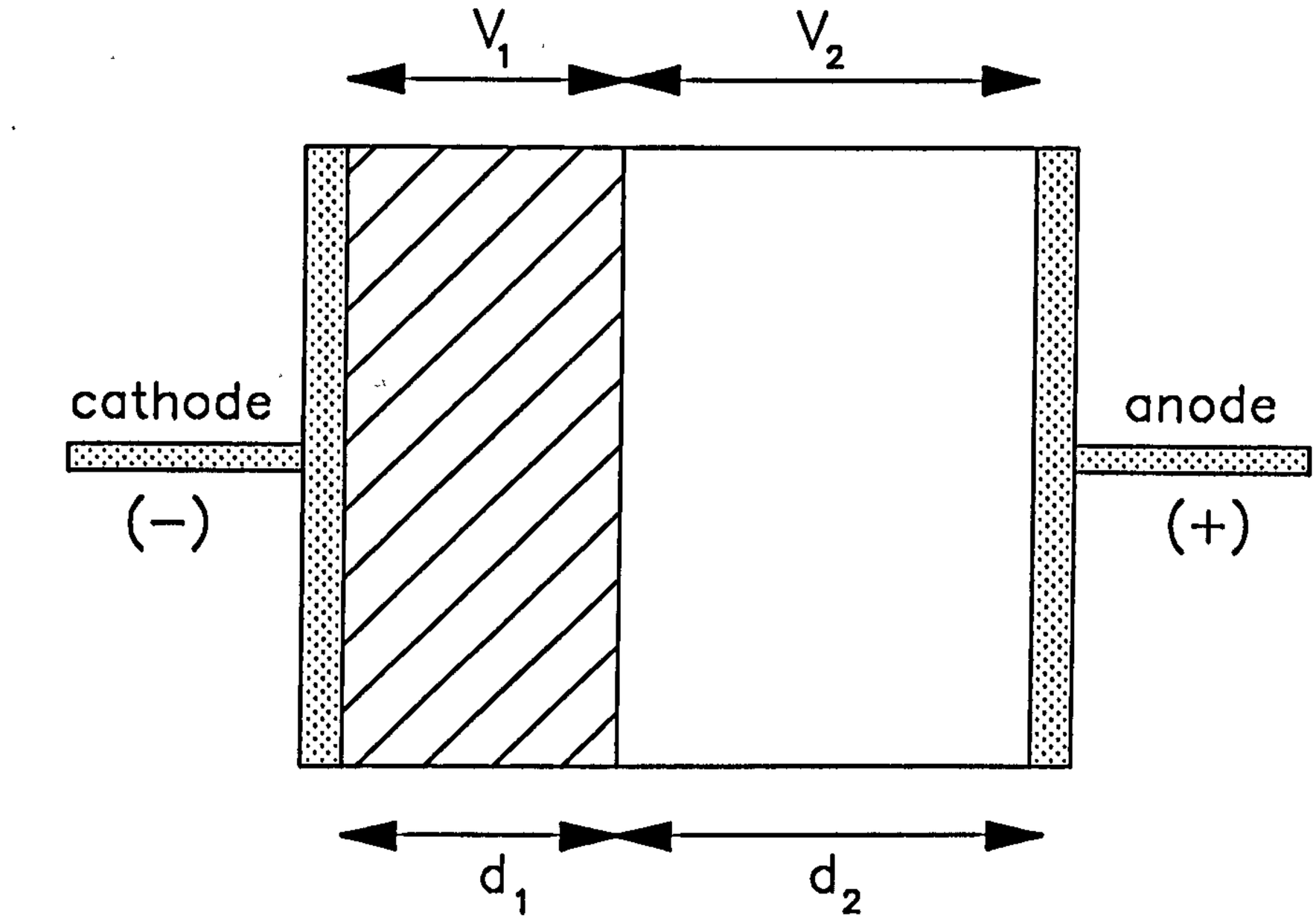

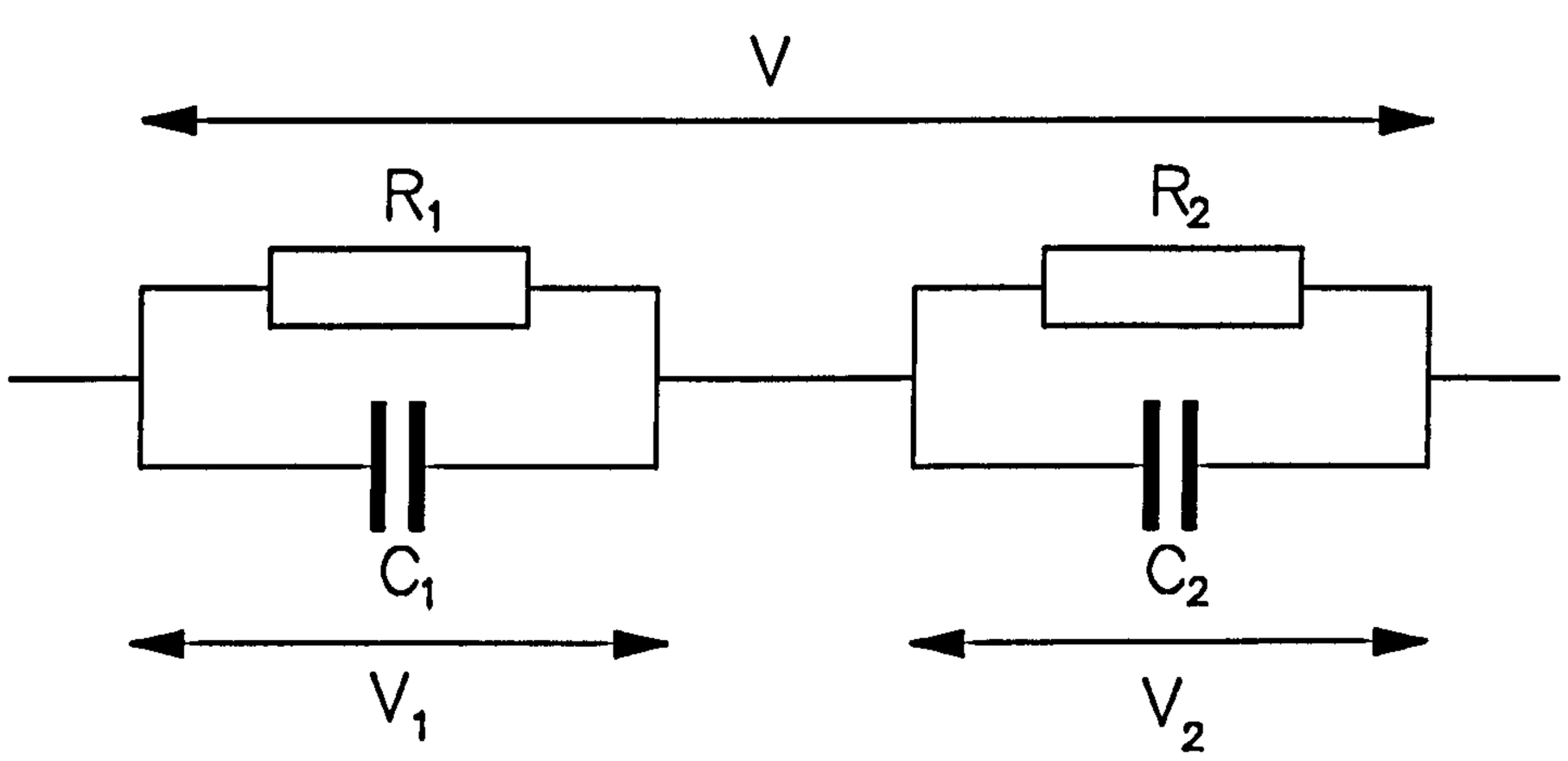

Figure 2.6 A parallel plate capacitor separated by two differing dielectrics of respective thickness d_1 and d_2 along with its equivalent electrical circuit.

The total a.c. impedance of the circuit can be calculated as

$$Z_{total} = Z_1 + Z_2 = \frac{(R_1 + R_2)(1 + j\omega\tau)}{(1 + j\omega\tau_1)(1 + j\omega\tau_2)}$$

where τ_1 and τ_2 are the characteristic relaxation times of each dielectric given by

$$\tau_i = R_i C_i = \frac{\varepsilon_i}{\sigma_i}$$

The above impedance can be written in terms of a capacitance with a complex permittivity

$$\frac{1}{Z} = j\omega e_o \varepsilon^* \frac{d}{A}$$

Solving for ε^* reveals the following expression for the effective permittivity of the capacitor

$$\varepsilon^* = \varepsilon' - j\varepsilon''$$

where

$$\varepsilon' = \frac{d(\tau_1 + \tau_2 - \tau + \omega^2 \tau_1 \tau_2 \tau)}{\varepsilon_o A (R_1 + R_2)(1 + \omega^2 \tau^2)}$$

$$\varepsilon'' = \frac{d - d(\omega^2 \tau_1 \tau_2 + \omega^2 \tau (\tau_1 + \tau_2))}{\omega e_o A (R_1 + R_2)(1 + \omega^2 \tau^2)}$$

These equations are of the same form as the Debye equation described in section 2.3. By applying the conditions that as ω tends to zero so ε^* tend to ε_s (d.c. or maximum permittivity) and as ω tend to infinity ε^* approaches ε_∞ (high-frequency or minimum permittivity) the following relationships can be derived

$$\varepsilon_s = \frac{d(\tau_1+\tau_2-\tau)}{\varepsilon_o A(R_1+R_2)} \qquad \varepsilon_\infty = \frac{d\tau_1\tau_2}{\varepsilon_o A(R_1+R_2)\tau}$$

The above equations show that at the interface between two dielectrics a Debye type relaxation occurs with a relaxation time and complex permittivity which is dependent on the dielectric properties and physical dimensions of each dielectric. In addition to the Debye-type of dispersion caused by interfacial polarisation, an extra frequency-dependent conductance occurs through the interface giving an effective complex interfacial permittivity of

$$\varepsilon_{interfactial} = \varepsilon_\infty + \frac{\varepsilon_s-\varepsilon_\infty}{1+j\omega\tau} - j\frac{\sigma}{\omega}$$

where

$$\sigma = \frac{d}{A}(R_1+R_2)^{-1}$$

The overall effect of each polarisation is cumulative so that the total polarisability can be given as

$$\alpha_{total} = \alpha_{interfacial} + \alpha_{orientation} + \alpha_{atomic} + \alpha_{electronic}$$

Therefore, the polarisability of a dielectric is a maximum at d.c. and reduces through each dispersion process with increasing frequency to reach a minimum at frequencies above the relaxation frequency for any electronic polarisation process. Figure 2.7 shows a typical variation in ε' and ε'' with frequency for a dielectric exhibiting a number of relaxation processes. Below approximately 1Hz the effect of any d.c. conductivity is seen to influence the loss term ε'' but has no effect on ε'. The effects of interfacial polarisation can extend from 1Hz to around 10MHz depending on the nature of the interface. On increasing the frequency of the electric field imposed on the dielectric the effects of permanent dipole relaxations are observed (1MHz to 1GHz). Permanent dipoles are usually large compared to the induced dipoles involved in atomic and electronic polarisation and so give a larger change in permittivity (dielectric increment). The

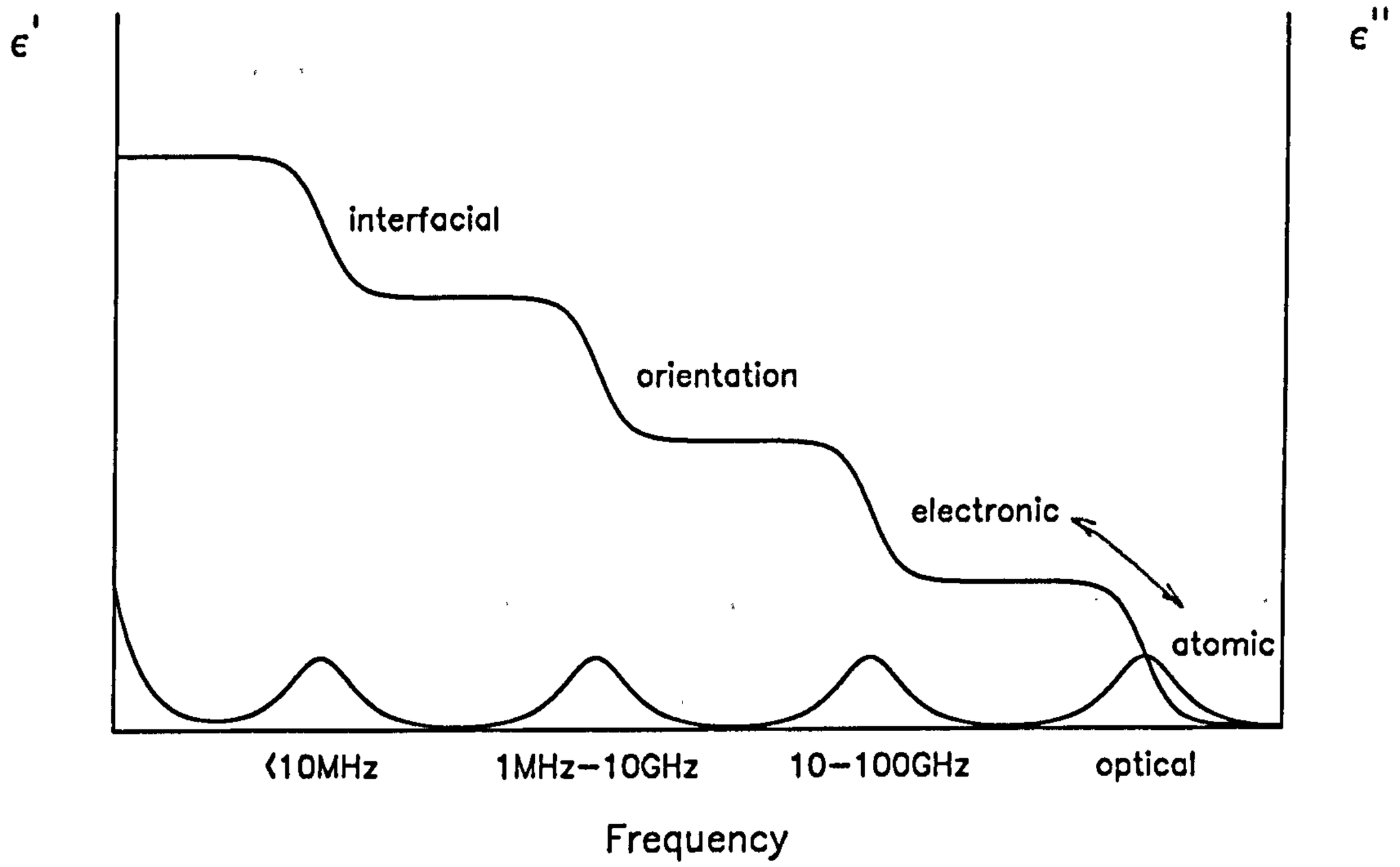

Figure 2.7 The frequency variation in ε' and ε'' for a typical dielectric exhibiting a number of relaxation processes.

next relaxation or dispersion mechanism is that of atomic polarisation followed by the smallest dispersion due to electronic polarisation which occurs at optical frequencies. Above this relaxation the permittivity of the dielectric approaches that of free space.

2.5 The Dielectrophoretic Force

In a static electric field the net force on a dipole is given by

$$\mathbf{F} = (\boldsymbol{\mu} \cdot \nabla)\mathbf{E} \qquad 2.15$$

where μ is the dipole moment vector, ∇ is the del vector operator and $\mathbf{E}$ is the external electric field. For a homogeneous isotropically polarisable dielectric the total dipole moment is given as

$$\mu_{total} = \mu v = \alpha v \mathbf{E}$$

where v is the volume of the dielectric and α, as discussed earlier, is its polarisability.

The force on a dielectric body can thus be written as

$$\mathbf{F} = \alpha v (\mathbf{E} \cdot \nabla)\mathbf{E} = \frac{1}{2}\alpha v \nabla |\mathbf{E}|^2 \qquad 2.16$$

Eqn. 2.16 shows the force to be proportional to the term $\nabla |E|^2$. This term describes the magnitude E^2 and the direction of the force. The factor E^2 is independent of the sign of the field and thus is a scalar term. Therefore to maximise the force, F, a large field strength along with a strongly divergent field (large ∇) is required.

Equation 2.16 also shows a direct relationship between the polarisability, α, and the dielectrophoretic force. The calculation of a suitable value for the polarisability comes from considering Laplace's equation (Von Hippel, 1954). Consider the situation of a homogeneous, isotropically polarisable, dielectric sphere of radius a and permittivity ε_p suspended in a homogeneous, isotropically polarisable, medium of infinite extent (permittivity ε_m) as

represented in figure 2.8. The dipole moment of the sphere is given by $\mu=Pv$ where P is the polarisation per unit volume. The field distribution produced by the sphere is radial and hence can be described by Laplace's equation using spherical co- ordinates

$$\nabla^2 V = \frac{\delta^2 V}{\delta r^2} + \frac{z}{r}\frac{\delta V}{\delta r} + \frac{1}{r^2}\frac{\delta^2 V}{\delta \theta^2} + \frac{1}{r^2}\frac{\cos\theta}{\sin\theta}\frac{\delta V}{\delta \theta} = 0$$

where V is the electric potential and θ r and z describe the position of a point in the field. The potential of the field inside, V_i, and outside, V_o, the sphere can be described by the following relationships

$$V_o = \left(\frac{A}{r^2} - Br\right)\cos\theta \qquad V_i = \left(\frac{C}{r^2} - Dr\right)\cos\theta$$

By taking into account the boundary conditions that when r=a the field potential and flux density are continuous, then

$$V_o = V_i \qquad \varepsilon_p \frac{\delta V_{gi}}{\delta r} = \varepsilon_m \frac{\delta V_{go}}{\delta r}$$

At an infinite distance from the sphere the applied field, E_o, is undisturbed hence

$$V_o = -E_o r\cos\theta = -E_o z\cos\theta$$

and at the origin (chosen as the centre of the dielectric sphere) the potential is finite so the field within the sphere is given by

$$E_1 = \frac{3\varepsilon_m E_o}{\varepsilon_p + 2\varepsilon_m}$$

The polarisability is equal to the polarisation divided by the field strength, so

$$\alpha = \varepsilon_o(\varepsilon_p - \varepsilon_m)\frac{E_{gi}}{E_{go}}$$

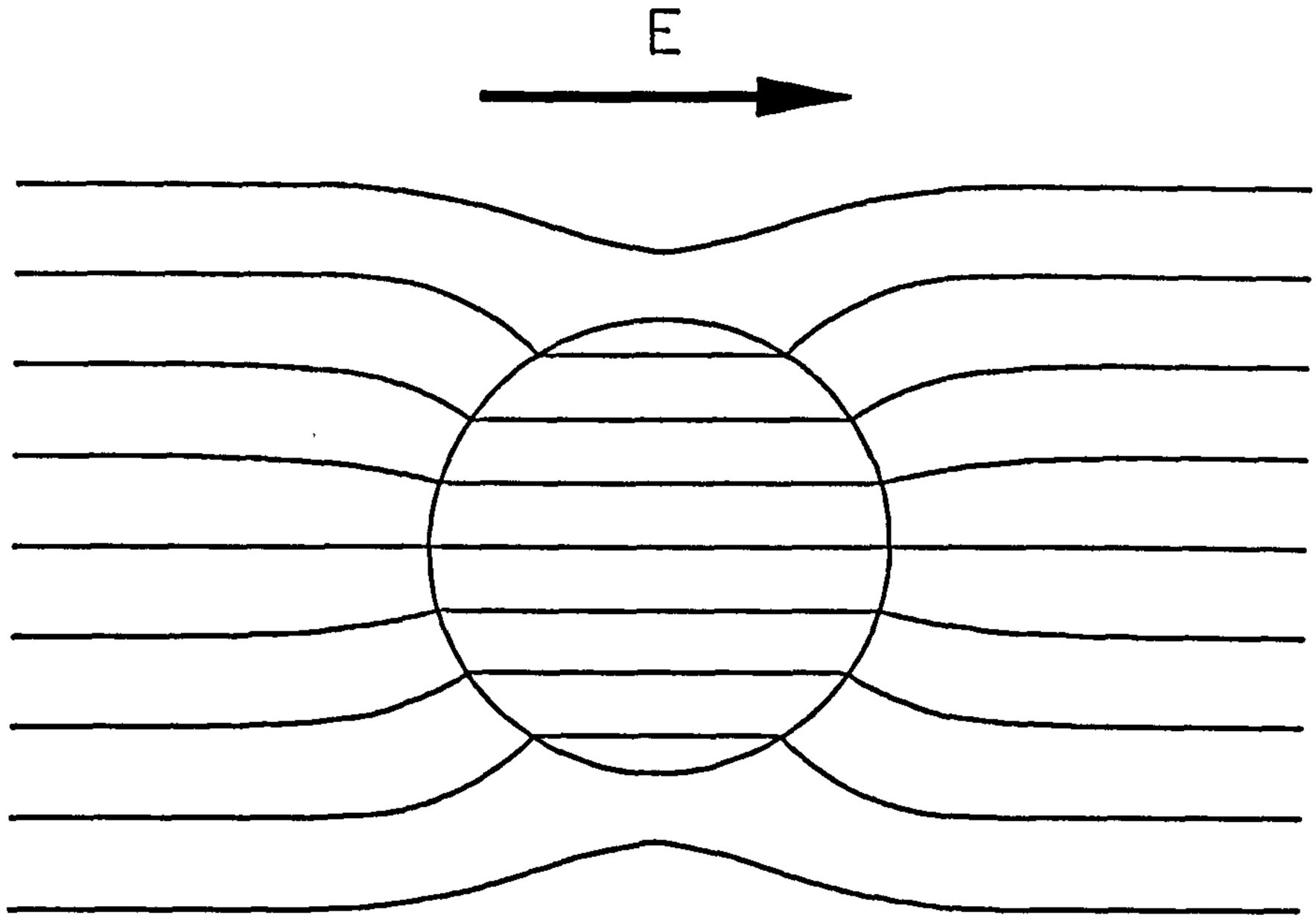

Figure 2.8 The interaction of a dielectric sphere with an applied homogeneous electric field.

and the polarisability of the suspended sphere is given by

$$\alpha = \varepsilon_o \varepsilon_m \frac{\varepsilon_p - \varepsilon_m}{\varepsilon_p + 2\varepsilon_m} \qquad 2.17$$

Equation 2.17 can be extended using a depolarisation factor A to describe suspended ellipsoids

$$\alpha = \varepsilon_o \varepsilon_m \frac{\varepsilon_p - \varepsilon_m}{\varepsilon_p + A\varepsilon_m}$$

Therefore, assuming very dilute suspensions of ellipsoids the dielectrophoretic force on the suspended sphere can be written as

$$\mathbf{F} = \frac{3V}{2} v \varepsilon_o \varepsilon_m \frac{\varepsilon_p - \varepsilon_m}{\varepsilon_p + 2\varepsilon_m} \nabla |E|^2 \qquad 2.18$$

It is this general form of equation 2.16 which has been used in different forms to describe the majority of dielectrophoretic measurements to date. In chapters 3 to 6 this formula is examined experimentally and its limitation are discussed. Suggestions for its improvement when used to describe the dielectrophoresis of colloidal particles are also made..

2.6 Cell Structure

In these studies 3 cell types have been investigated, bacteria, yeasts and mammalian cells. The bacteria are classified as prokaryote having no recognised internal organelles and with a cytoplasm (interior of the cell) made up of the various nutrients, enzymes, proteins and essential genetic material of the cell. The yeast and mammalian cells, possessing a well characterised internal organisation, are classified as eukaryote. Cells can be discussed in terms of their cytoplasmic content, membrane structure and cell wall structure.

2.6.1 Cell Interior

As mentioned above, the bacterial cytoplasm is a mixture of all the necessary materials for growth. Also suspended in the cytoplasm is the genetic material of the bacteria, the chromosomes, which are essentially closed loops of extensively folded DNA (deoxyribonucleic acid). The chromosomes are attached to the interior surface of the plasma membrane which encloses the whole cell. The cytoplasm also contains numerous ribosomes, small rounded bodies made up of proteins and RNA (ribonucleic acid), which are the sites of protein manufacture within the bacteria. In the ribosomes small RNA molecules attach to amino acids and, via coding RNA molecules, assemble the appropriate amino acids to create required proteins. Food is stored in the cytoplasm in the form of insoluble granules of the polymer poly-B-hydroxybutyrate, which provides a source of both carbon and energy. It has also been noted that some strains of bacteria contain very basic internal membranes which enclose various substances such as gases or photosynthetic apparatus.

Eukaryotic cells, such as yeasts and mammalian cells, have a much more complex cytoplasmic organisation consisting of many separate membrane enclosures. The main component of the eukaryotic cytoplasm is the nucleus. This is a membrane enclosure which contains the genetic information of the cell in the form of chromosomes as in bacteria. Information is converted from DNA into RNA and passes through pores in the nucleic membrane to direct protein synthesis within the cytoplasm. A second component in common with bacteria are the ribosomes for protein synthesis.

The cytoplasm of eukaryotic cells also contains a complex transport system made up of extensive, membranous, tubules called the endoplasmic reticulum which allows proteins and other molecules to be directed about the cell interior.

Mitochondria are present in virtually all eukaryotic cells and play an important role in the breakdown and synthesis of carbohydrates, fats and amino acids. Mitochondria contain DNA, RNA and ribosomes and are self reproducing using information gained from the nucleus. The mitochondria are surrounded by two membranes, the inner one is extensively folded to provide

a large surface area for the attachment of enzymes for the catalysis of electron transport reactions in the production of ATP, the principle energy storage molecule in cells. Other membranous constituents of the cell interior include lysomes for the digestion of small molecules and chloroplasts in photosynthetic cells.

2.6.2 Cell Membranes

Membranes are essential to cellular life in enclosing the contents of an organelle or whole cell. However, membranes are more than passive barriers, they also act as highly selective filters and are able to maintain unequal concentrations of ions on either side yet at the same time allow certain large molecules to pass through. All biological membranes share a similar structure, including the plasma membrane which encloses the whole cell and to which particular attention will be paid.

Figure 2.9 shows a schematic, three dimensional, view of a small section of a cell membrane. Approximately 50% of the mass of the plasma membrane is due to lipid molecules. Three major types of lipid are found in membranes, phospholipids (the most abundant), cholesterol (not present in bacterial membranes), and glycolipids. All are amphipatic with a hydrophilic, polar, region and a hydrophobic region. When amphipatic molecules are surrounded by an aqueous environment they tend to aggregate so as to bury the hydrophobic regions and leave the hydrophilic regions exposed to water. In the case of cells the lipid molecules hide the hydrophobic regions by forming a bilayer as shown in figure 2.10. These bilayers have a high degree of fluidity which allows for the movement of individual lipid molecules within the plane of the membrane. However, it is rare for molecules to migrate from one side of the bilayer to the other. Cholesterol is incorporated within the bilayer to provide a degree of rigidity. The cholesterol molecule is a small rigid molecule which is able to orientate itself between phospholipid molecules in the bilayer, with its polar head close to the polar head group of the phospholipid. The rigid steroid ring tail of the cholesterol molecule interacts with the fatty acid chain of the phospholipid to immobilise the parts of the fatty acid chain close to the polar head of the lipid. Glycolipids are found on the outer surface of the plasma membrane and are similar

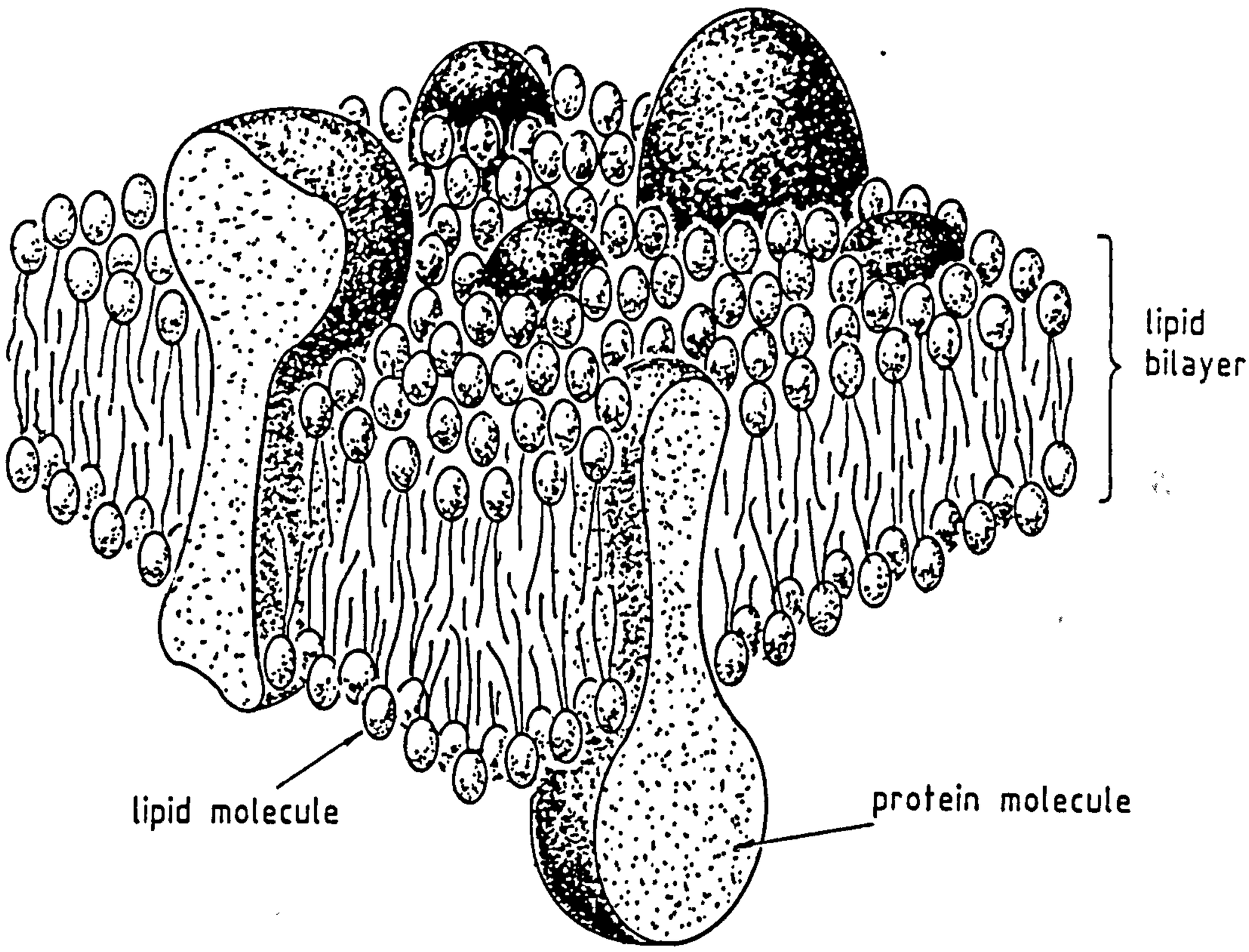

Figure 2.9 A schematic three dimensional view of a small section of cell membrane approximately 10nm square.

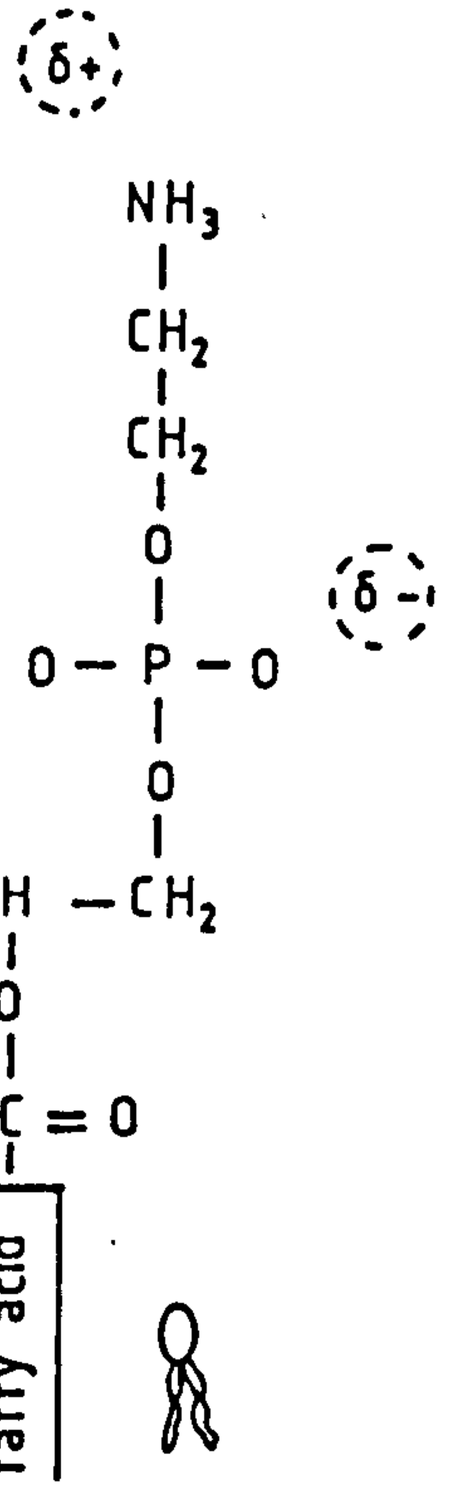

Phosphatidyl - ethanolamine

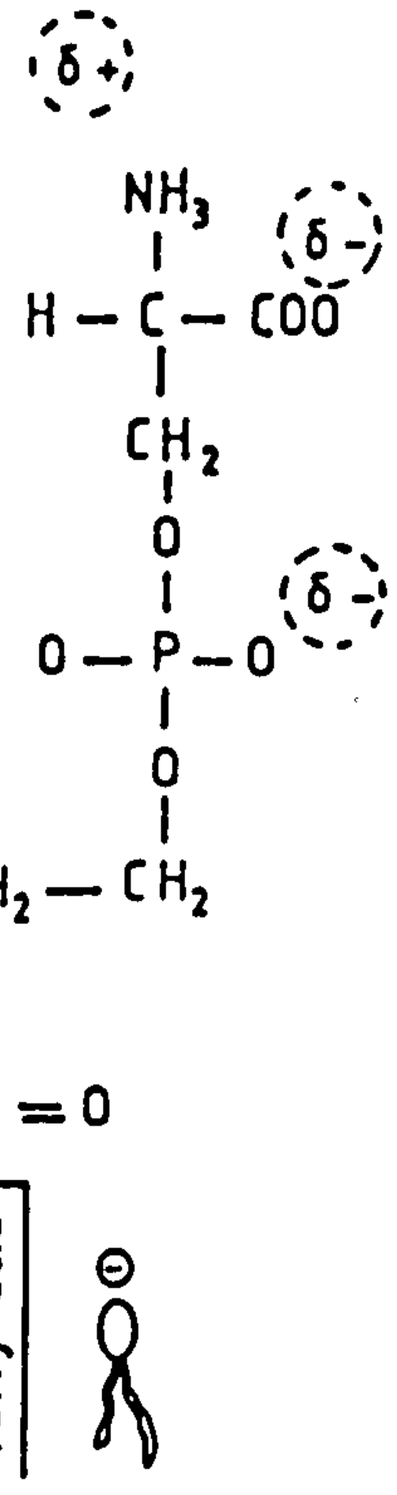

Phosphatidyl - serine

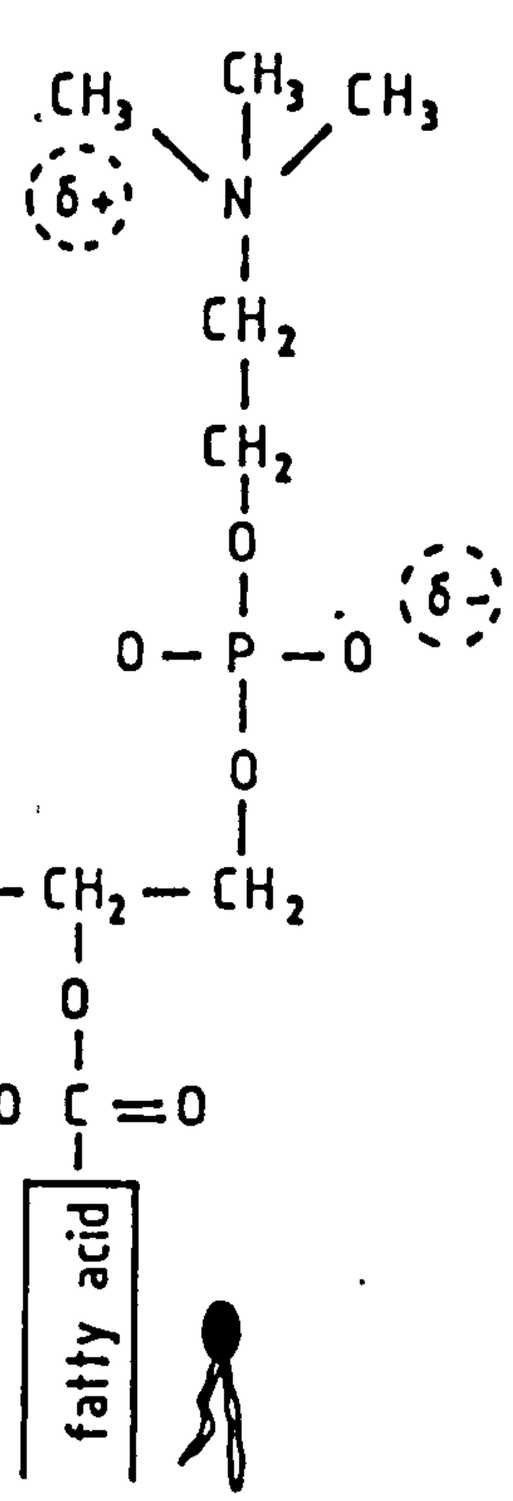

Phosphatidyl - choline

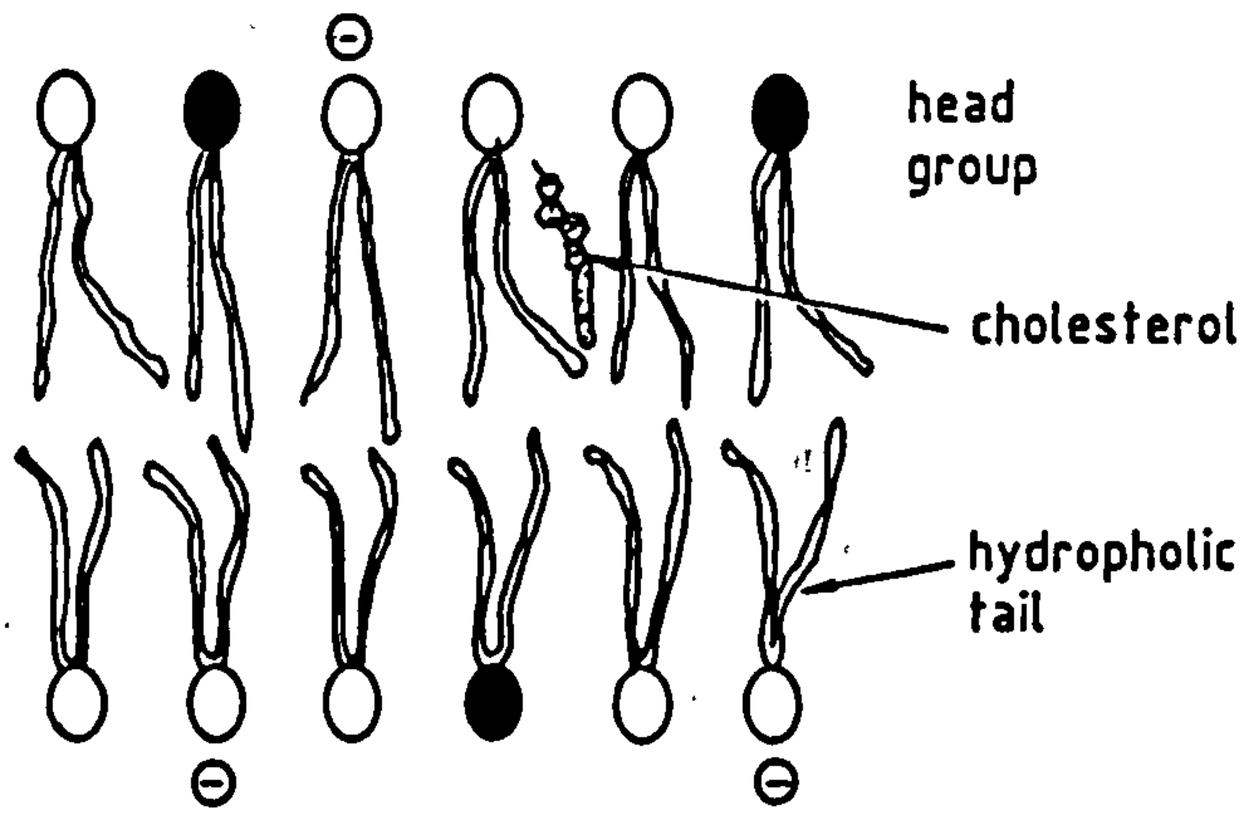

Lipid bilayer

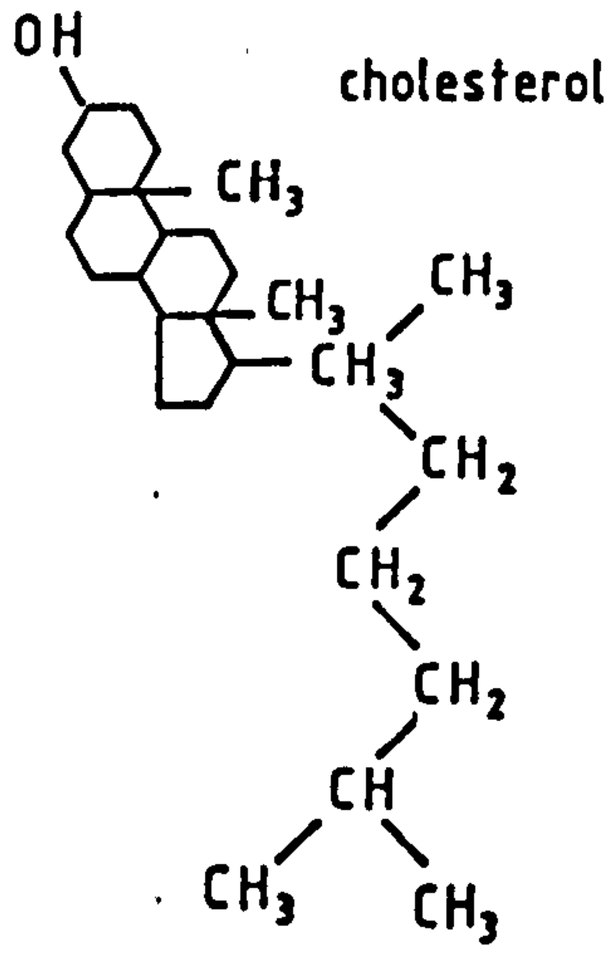

Figure 2.10 The formulas and symbols of the three major membrane phospholipids and cholesterol together with a schematic illustration showing the asymmetrical distribution of lipids within a typical cell membrane.

to phospholipids with two hydrocarbon chain tails, but have a head group consisting of one or more sugar residues. The exact function of these lipids is not known. However, one group of glycolipids, the gangliosides, contain one or more sialic acid residues which gives the molecule a net negative charge.

Whereas the basic structure of biological membranes is determined by the lipid bilayer their functions are carried out largely by the membrane proteins. Membrane proteins are inserted (figure 2.11) directly into the lipid bilayer and are usually amphipatic. The hydrophobic regions of the protein interact with the fatty acid chains of the phospholipid and the hydrophilic regions are exposed to water on one or usually both sides of the bilayer. However, because of the fluidity of the membrane, these proteins are able in most cases to move laterally within the plane of the membrane.

The proteins are made of sequences of amino acids and also contain carbohydrate at their terminations, usually in the form of covalently bonded sugar or sialic acid residues located on the outer surface of the membrane. This region of high carbohydrate concentration close to the surface of the cell is referred to as the cell glycocalyx.

The hydrophobic interior of the lipid bilayer helps the membrane to serve as an impermeable barrier to polar molecules, so preventing most of the water soluble contents of the cell escaping. In biological membranes the controlled movement of molecules across the membrane is carried out by the membrane proteins. Small non-polar molecules and water are able to diffuse through the membrane. However, larger molecules and polar molecules have to travel across the membrane via transport proteins. There are three principle mechanisms for membrane transport, all involve the movement of molecules through channels in the membrane formed by the proteins. The simplest form of transport is passive diffusion of large molecules through protein channels. In this case the concentration gradient of the molecule governs the direction of transport. A more complex form of transport is involved for the movement of polar molecules, where not only does a concentration gradient determine the direction of travel but an electrochemical gradient, provided by the transmembrane potential, also acts on the molecule.

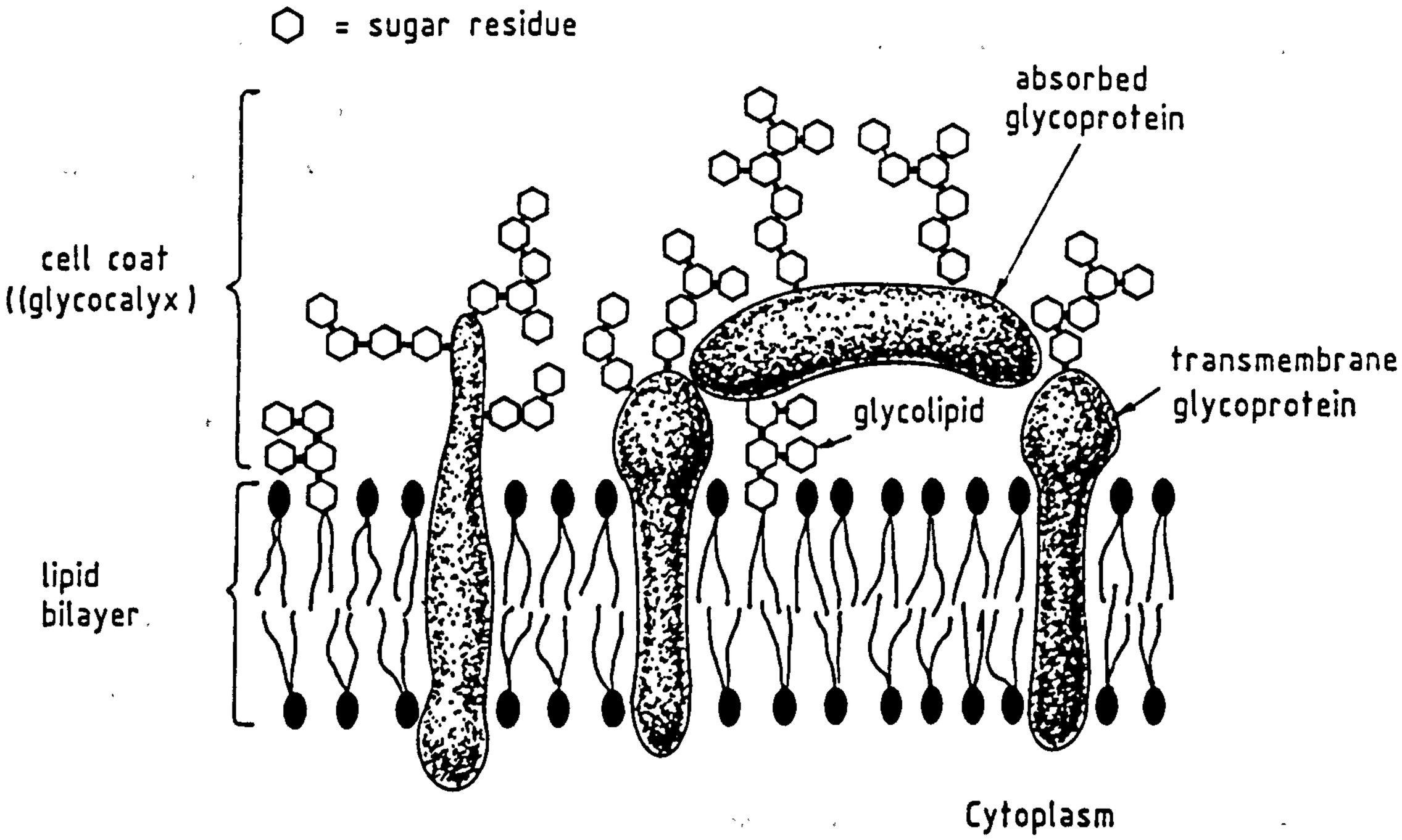

Figure 2.11 A schematic diagram of a typical cell membrane showing the presence of proteins within the membrane as well as the cell glycocalyx.

The difference in electrochemical potential across biological membranes is caused by the well documented sodium-potassium pump mechanism which provides the third means of membrane transport referred to as active transport. The Na^+-K^+ pump protein system maintains a higher concentration of sodium ions outside the membrane than inside while simultaneously maintaining a higher concentration of potassium ions inside the cell. This movement and regulation of ion concentrations involves the use of energy stored in the form of ATP and converted by the enzyme ATPase. The regulation of ion movement provides an electrochemical potential difference across the membrane where the interior of the cell is approximately 70mV more negative than the exterior of the cell.

2.6.3 Cell Wall

In order to protect the delicate plasma membrane surrounding the cell from variations in environment both bacteria and yeasts also posses a rigid cell wall which encloses the plasma membrane. In bacteria the cell wall is formed from a polymer, peptidoglycan, which comprises of polysaccharide backbone chains with alternate glucosaminic and muramic acid residues. Attached to some or all of the muramic acid residues are short chain amino acids which can link to amino acid residues on adjacent peptidoglycan chains. This cross-linking gives rise to a giant hollow molecule which completely encloses the plasma membrane. A similar structure occurs on the surface of yeasts from the crosslinking of glucan and mannan polymer chains.

The cell walls of bacteria provide a means of classifying between two categories of bacteria. The Gram classification uses a staining technique to distinguish between bacteria with (gram negative) and without (gram positive) an outer membrane covering the cell wall. Gram positive bacteria have a thick peptidoglycan layer which is interspersed with teichoic acids around the plasma membrane, whereas gram negative bacteria have a considerably thinner peptidoglycan cell wall between the plasma membrane and an outer membrane. The outer membrane is composed of phospholipids , proteins and lipoprotiens with a unique polymer lipopolysaccharide on the outer surface. The cell wall has many other uses apart from providing mechanical

strength. For example, it can store essential ions e.g. magnesium by attraction to the many ionisable groups within the porous cell wall as well as acting as a molecular sieve to protect the plasma membrane from harmful molecules such as antibiotics.

2.7 Dielectric Properties of Cells

The complex structure of a cell (described in section 2.6) gives rise to many individual polarisation mechanisms. These polarisations can be categorised as being associated with either the cell exterior, the cell membrane or the cell interior and are observed as three distinct dispersions referred to as the α β and γ dispersions. Although the many molecular structures within the cell produce individual dispersions their effect on the overall dielectric properties of the cell are not always noticeable. Figure 2.12 shows the approximate magnitudes and frequencies of the α β and γ dispersions.

When exposed to low-frequency electric fields (Hz) the cell exhibits a maximum permittivity far in excess of any permittivity observed for a homogeneous system. On increasing the frequency of the electric field a large dispersion is observed at around 1kHz with a dielectric increment of around 10^6. This dispersion has been observed for all colloidal particles studied. The cause of this large dispersion is considered to be the relaxation of the electrical double layer which exists around the cell. When suspended in an aqueous medium all particles acquire a net surface charge, usually negative, and in the case of a cell this is enhanced by the presence of negatively charged head groups on some lipids as well as various acid and sugar residues on the membrane surface. The surface charge attracts mobile, oppositely charged, ions (counter-ions) from within the suspending medium. This layer of ions is referred to as the double layer of the cell, the cell surface forming one, negatively charged, layer and the ions the second positively charged diffuse layer. On the application of an electric field to this double layer system, the 'cloud' of ions around the cell is displaced about the centre of the cell forming a very large induced dipole as shown in an exaggerated form in figure 2.13, with a characteristic displacement relaxation time. The relaxation time of such a dispersion is usually around 1kHz and is controlled by factors

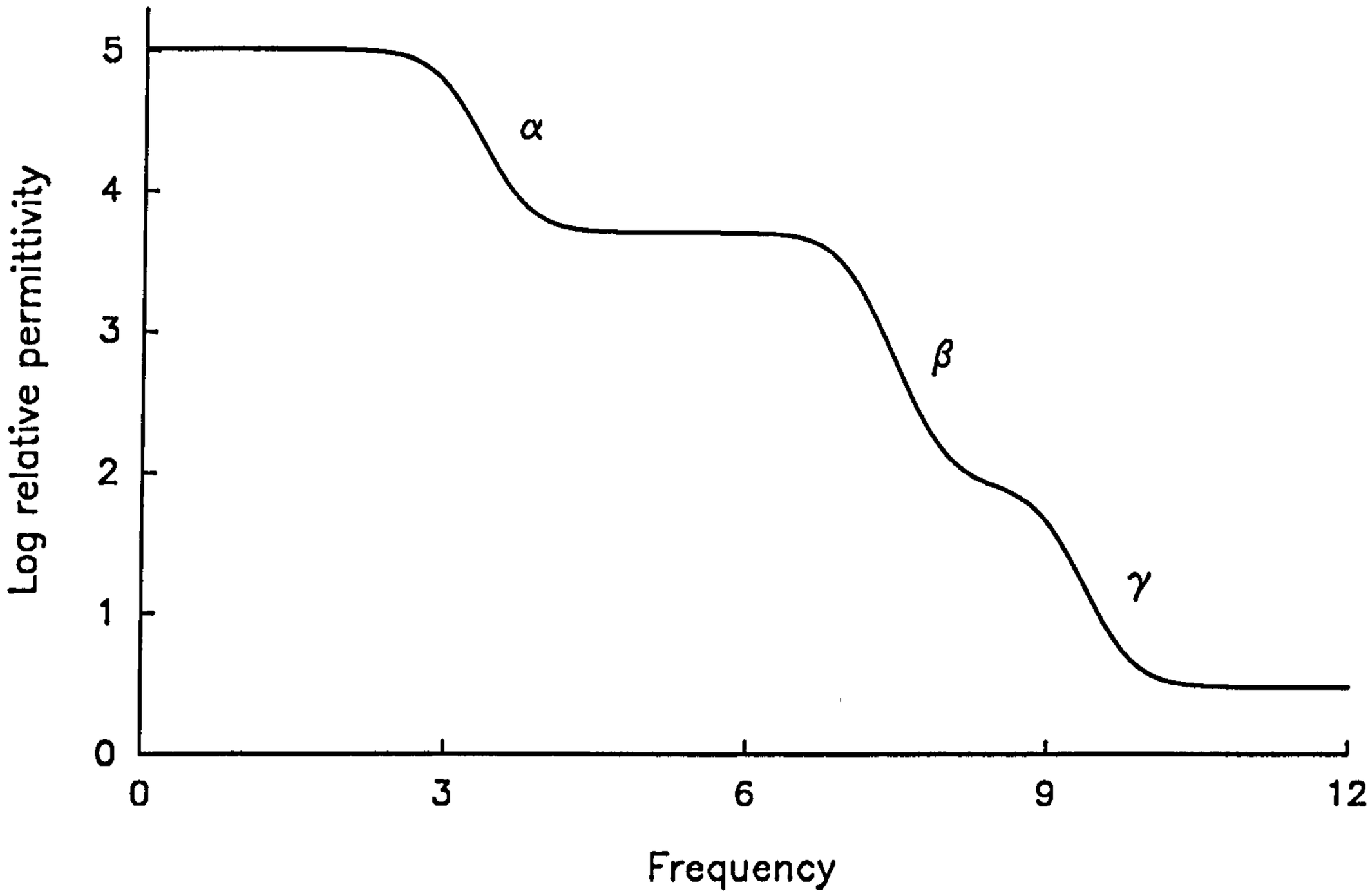

Figure 2.12 The frequency variation in the complex permittivity of a typical cell showing the presence of the three distinct α, β and γ dispersions.

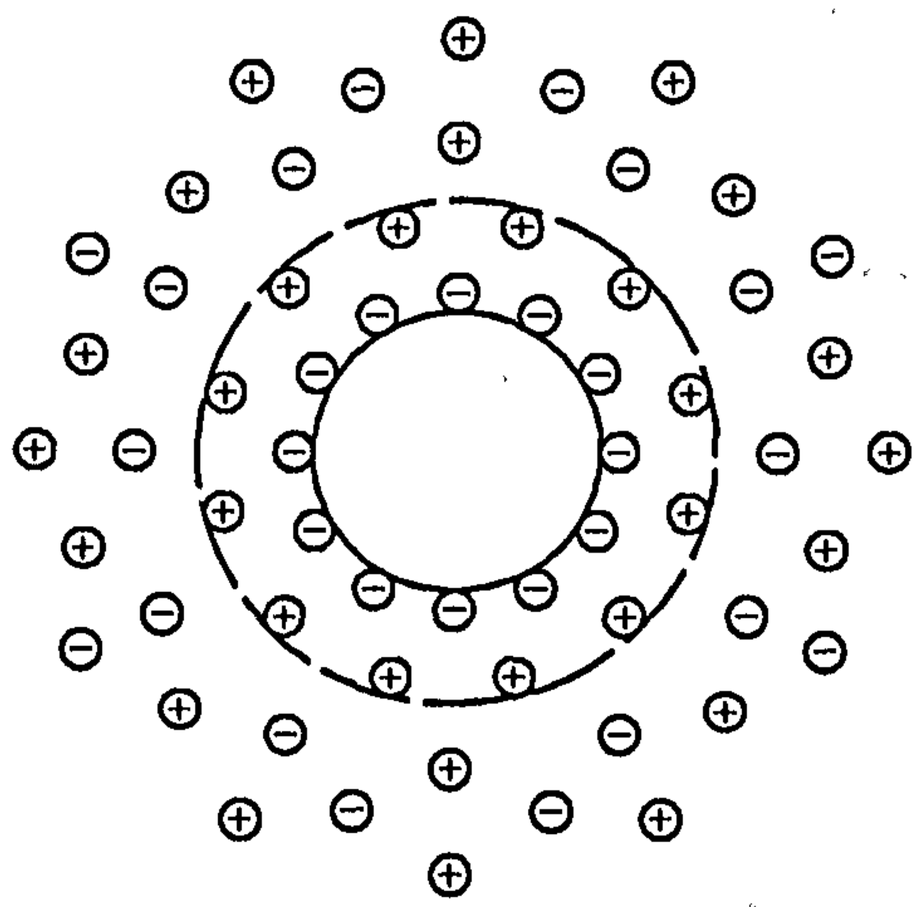

(a)

E

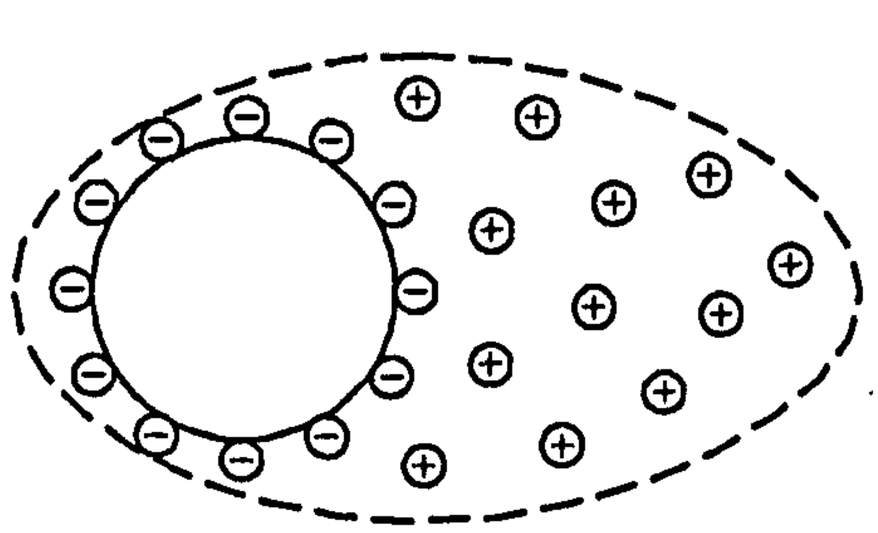

(b)

Figure 2.13 The presence of a diffuse double layer around a particle (a) before and (b) after the application of an electric field. The displacement of ions shown here is greatly exaggerated.

such as surface charge density, ionic mobility, and ionic concentration in the suspending medium and on the cell surface. This α dispersion is discussed in greater detail in chapter 4, where its effect on the dielectrophoretic force is examined.

The low permeability of the plasma membrane to ions and other polar molecules implies that it can be considered electrically as a dielectric rather than a conductor. The dielectric properties of the plasma membrane are usually described in terms of a capacitance and resistance per unit area. The average thickness of a lipid bilayer membrane is around 5nm and the permittivity of the phospholipids which make up the bilayer is around $2.5\varepsilon_o$. This gives an average membrane capacitance of around $0.5\mu Fcm^{-2}$. The widely held textbook value of membrane capacitance is $1.0\mu Fcm^{-2}$, which was originally found by extracelluar electrode measurements. However, transmembrane electrode techniques have found the membrane capacitance to probably be no more than $0.6\mu Fcm^{-2}$, with the lateral electrophoresis of proteins within the plane of the membrane affecting the effective permittivity of the membrane (Pethig and Kell 1987). In parallel with this capacitance must be some degree of conductivity caused by the movement of ions through the membrane, either by diffusion or via the membrane transport proteins. A typical membrane resistance is around 20 ohm m^{-2} (Asami, 1989) which for a membrane thickness of 5nm is equivalent to a conductivity of $0.25nSm^{-1}$. At low frequencies an applied electric field is unable to penetrate the plasma membrane due to the high resistance and reactance of the membrane, as shown in figure 2.14(a). In this case the cytoplasm of the cell is shielded from the applied field and the cell appears to the electric field as a solid sphere with dielectric properties equal to those of the membrane. As the frequency of the electric field is increased the reactance of the membrane decreases and, at frequencies above around 1-10MHz, the membrane reactance effectively short-circuits the membrane resistance allowing the electric field to penetrate the cell. Now the cell appears as a sphere with a radius equal to that of the cell minus the membrane thickness and with dielectric properties equal to those of the cell cytoplasm, as shown in figure 2.14(b). The mechanism for the charge build up on the surface of the cell is identical to that of the interfacial, Maxwell-Wagner, polarisation described earlier in this chapter. In the case of a cell membrane there are two interfaces; one between the

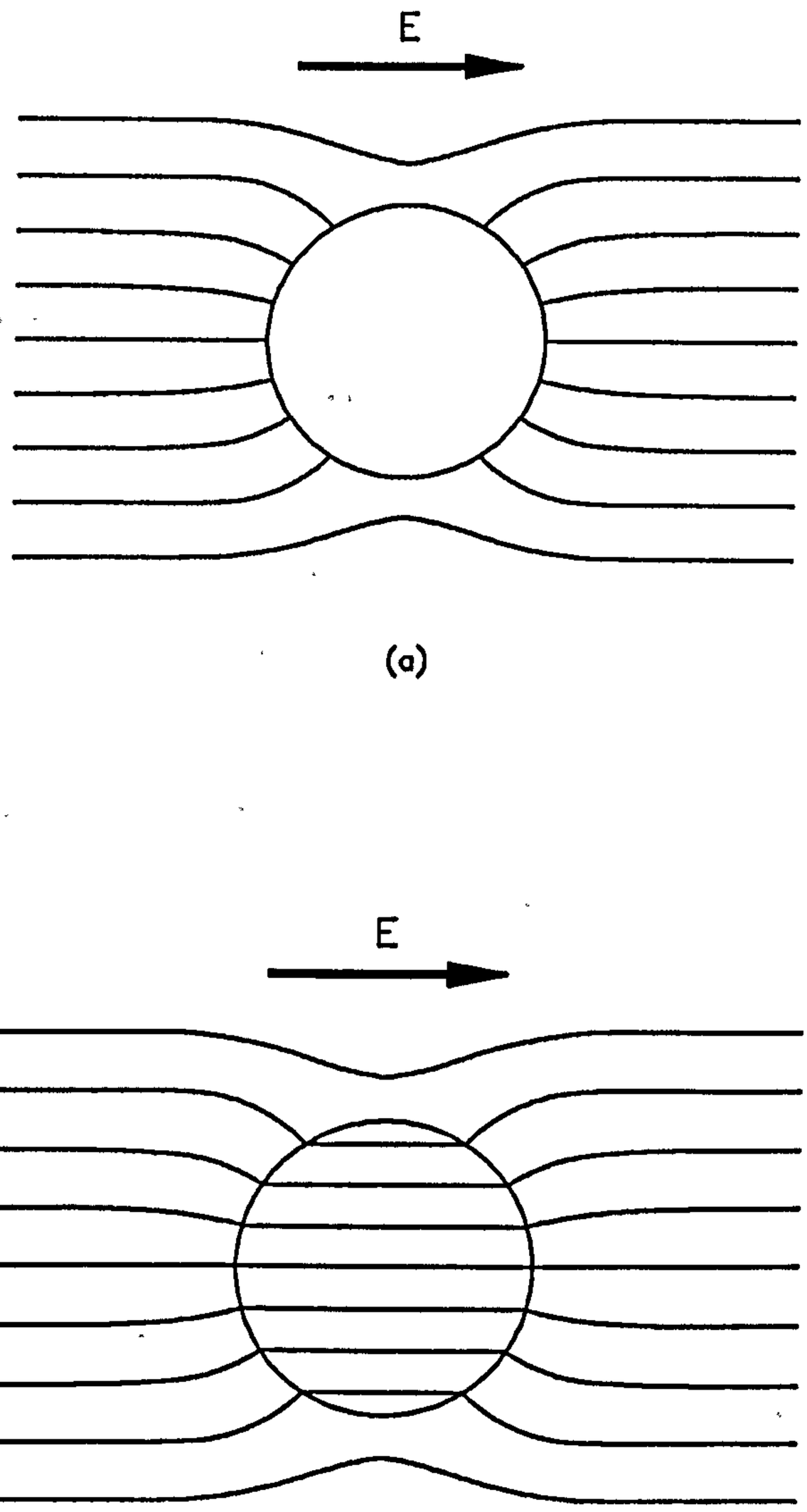

Figure 2.14 The interaction of a typical cell with an applied homogeneous electric field at (a) low and (b) high frequencies.

suspending medium and the outer surface of the membrane and one between the inner surface and the cytoplasm. If the dielectric properties of the suspending medium and cytoplasm are similar (as is usually the case to maintain cell viability) the dispersion due to the inner interface will not be observed due to the inability of the electric field to penetrate the cell. It has also been noted that this membrane or β dispersion is not a single relaxation process but may contain relaxations attributed to the rotation of protein molecules within the plane of the membrane (Kell and Harris, 1985).

Increasing the frequency of the applied electric field further reveals a number of small dispersions due to the many different molecular structures of the constituents of the cell cytoplasm. The final major dispersion observed in cells occurs at around 0.1-1GHz and is associated with the relaxation of water molecules bound to the various protein molecules within the cytoplasm. This γ relaxation is at a lower frequency to that of normal bulk water, which occurs at around 20GHz, and reveals differences in the freedom of movement of bound water molecules to free water molecules.

2.8 The Shelled Sphere Model of a Cell

In order to simplify the investigation of the complex dielectric properties of a cell suspension it is advantageous to employ a suitable model of a cell. In general cells are ovoid in shape and therefore can be simplified to be spherical. In 1924 Fricke derived the following equation to describe the dielectric properties of spherical particles of permittivity ε_{12} and conductivity σ_{12} suspended in a dielectric medium of conductivity σ_2 and permittivity ε_2:

$$\frac{K-K_1}{K+2K_1}=\rho\frac{K_2-K_1}{K_2+2K_1} \qquad 2.19$$

Here, K, K_1 and K_2 represent the complex conductivity of the suspension, particle and medium respectively where ρ is the volume fraction of the suspension taken up by the cells. The complex conductivity of a dielectric is equivalent to the complex permittivity and is essentially a rearrangement of eqn. 2.14.

$$K = j\omega\varepsilon^* = \sigma_{a.c.} + j\omega\varepsilon_o\varepsilon'$$

If a single sphere is used to represent a suspended cell then only one relaxation mechanism can be modelled. As discussed in the previous section there are at least three dielectric relaxations observable in a typical cell. Therefore the structure of the cell must be considered in extending this model.

The cytoplasm of a cell consists of a mixture of ions, enzymes and proteins as discussed earlier. The cytoplasm has a ionic concentration equivalent to 150mM NaCl and so can be modelled as a single sphere of radius a and conductivity $1.5Sm^{-1}$ (equivalent to 150mM NaCl). The permittivity of the cytoplasm depends on the exact contents of the cell but is usually around $80\varepsilon_o$. Enclosing the cytoplasm is the plasma membrane. The permittivity of the lipid bilayer membrane is around $2.5\varepsilon_o$ being largely determined by the lipid content of the membrane. The conductivity of the membrane is determined by the degree of ion transport through protein channels in the membrane and is usually around $0.25nSm^{-1}$ (Asami, 1989). Therefore, a typical cell can be modelled as a conducting sphere, representing the cell cytoplasm, surrounded by an insulating shell of thickness r (typically r = 5nm) representing the plasma membrane such that the sum of a and r is equal to the radius of the cell.

The shelled sphere model of a dielectric system was also used by Fricke (1936) to determine the surface conductivity of particles. Each phase of the system will contribute to the overall complex conductivity of the model. Therefore, the complex conductivity of the cell in eqn. 2.19 can be rewritten as

$$K_2' = K_3 \frac{(2K_3 + K_2)(a+r)^3 - 2(K_3 - K_2)a^3}{(2K_3 + K_2)(a+r)^3 + (K_3 - K_2)a^3} \qquad 2.20$$

where K_2 and K_3 are the cytoplasmic and membrane complex conductivities, respectively. Schwan (1957) also arrives at eqn. 2.19 from Maxwell's equations (1892) when investigating the dielectric properties of a shelled sphere model of a single cell. In Schwan's case, K, K_1 and K_2 refer to the total cell, membrane and cytoplasm conductivity, respectively. The volume fraction term, ρ, becomes the fraction of the total cell volume taken up by the cytoplasm volume;

$$\rho = \frac{(a-r)^3}{r^3}$$

In Schwan's case (1957) eqn 2.20 can be simplified to

$$K_2' = \frac{K_2 + 2K_3 \frac{r}{a}}{1 + \frac{r}{a}\frac{K_2}{K_3}}$$

for r<a, as is the case in a typical cell.

Therefore, using the general formula of eqn. 2.19 it is possible to analyse the dielectric properties of any number of phases by the inclusion of substitutions of a similar form to eqn. 2.20.

The single shelled model has been extended by the addition of a second shell around the cell to introduce the effects of a cell wall and surface charge polarisations (Pohl, 1978). Workers such as Asami (1989) and Morgan (1987) have introduced a second, inner, shell around the cytoplasm sphere to represent the effects of, for instance, a nuclear membrane. The processes of increasing the number of shells in the model have been discussed by Irimajiri et al (1979) where a system with n shells is discussed.

2.9 References

Sections 2.2 to 2.4

Allison, J. (1971) *Electronic Engineering Materials and Devices.* McGraw-Hill, London.

Bueche, F. (1986) *Introduction to Physics for Scientists and Engineers.* 4th ed. McGraw-Hill, New York.

Debye, P. (1929) *Polar Molecules.* Chemical Book Company, New York.

Frohlich, H. (1958) *Theory of Dielectrics.* 2nd ed. Clarendon Press, Oxford.

Hayt, W. H. (1981) *Engineering Electromagnetics.* 4th ed. Mc Graw-Hill, New York.

Maxwell, J. C. (1892) *Electricity and Magnetism.* Clarendon Press, Oxford.

Pethig, R. (1979) *Dielectric and Electronic Properties of Biological Materials.* J. Wiley and sons, Chichester.

Von Hippel, A. R., (1954) *Dielectrics and Waves.* Mc Graw-Hill, New York.

Wagner, K. W. (1914) The After-effect in Dielectrics, *Arch Elektrotech* 2 371-387.

Wagner, K. W. (1924) *Die Isoliertoffe der Elektrotechnik.* Ed. H. Schering. Springer, Berlin. (from Pethig, 1979)

Section 2.5

Pethig, R. (1979) *Dielectric and Electronic Properties of Biological Materials.* J. Wiley and sons, Chichester.

Pohl, H. A., (1978) *Dielectrophoresis.* Cambridge University Press, Cambridge.

Von Hippel, A. R. (1954) *Dielectrics and Waves.* Mc Graw- Hill, New York.

Section 2.6

Alberts, B., Bray, D., Lewis, J., Raff, M., Roberts, K. and Watson, J. D. (1983) *Molecular Biology of the Cell.* Garland, New York.

Ambrose, E. J. and Easty, D. M. (1978) *Cell Biology.* Nelson and sons, London.

Freshney, R. I. (1987) *Culture of Animal Cells.* Alan R. Liss Inc, New York.

Morgan, J. R. (1978) *Dielectrophoretic Studies on Biological Materials.* University of Wales Ph. D. thesis.

Rose, A. H. and Harrison, J. S., (1969) *The Yeasts, volume 1: Biology of yeasts.* Academic Press, U.K.

Singleton, P. and Sainsbury, D. (1981) *Introduction to Bacteria.* J. Wiley and sons, Chichester.

Section 2.7

Asami, K., Takahashi, Y. and Takashima, S. (1989) Dielectric Properties of Mouse Lymphocytes and Erythrocytes. *Biochim. Biophys. Acta* **1010** 49-55.

Kell, D. B., and Harris C. M. (1985) On the Dielectrically Observable Consequence of the Diffusional Motions of Lipids and Proteins in Membranes. *Eur. Biophys. J.* **12** 181-197.

Pethig, R., and Kell, D.B. (1987) The Passive Electrical Properties of Biological Systems: Their Significance in Physiology, Biophysics and Biotechnology. *Phys. Med. Biol.* **32** 933-970.

Polk, C. and Postow, E. (eds) (1986) *CRC Handbook of Biological Effects of Electromagnetic Fields.* CRC Press, Florida.

Schwan, H.P. (1957) Electrical properties of Tissue and Cell Suspensions. In *Advances in Biological and Medical Physics.* Academic Press, New York.

Schwan, H. P. (1988) Dielectric Spectroscopy and Electro-rotation of Biological Cells. *Ferroelectrics* **86** 205-223.

Section 2.8

Asami, K., Takahashi, Y. and Takashima, S, (1989) Dielectric Properties of Mouse Lymphocytes and Erythrocytes. *Biochim. Biophys. Acta* **1010** 49-55.

Fricke, H. (1924) A Mathematical treatment of the Electric Conductivity and Capacity of Disperse Systems. *Physical Rev.* **24** 575-587.

Fricke, H. and Curtis, H. J. (1936) The Determination of Surface Conductance from Measurements on Spherical Particles. *J. Phys. Chem.* **40** 715-722.

Irimajiri, A., Hanai, T. and Inouye, A. (1979) A Dielectric Theory of "Multi-Stritified Shell" Model with its Application to a Lymphoma Cell. *J. Theor. Biol.* **78** 251-269.

Maxwell, J. C. (1892) *Electricity and Magnetism.* Clarendon Press, Oxford.

Morgan, H., Ginzburg, M. and Ginzburg, B. Z. (1987) Dielectric Properties of the Halophilic Bacteria Halobacterium Halobium and H. Marismortui with Reference to the Conductivities and Permittivities of the Cytoplasmic Membrane and Intracellular Phases. *Biochim. Biophys. Acta* **924** 54-66.

Pohl, H. A. (1978) *Dielectrophoresis.* Cambridge University Press, Cambridge.

Schwan, H.P. (1957) Electrical properties of Tissue and Cell Suspensions. In *Advances in Biological and Medical Physics.* Academic Press, New York.

Schwan, H. P. (1988) Dielectric Spectroscopy and Electro-rotation of Biological Cells. *Ferroelectrics* **86** 205-223.

CHAPTER 3

STUDIES OF THE DIELECTROPHORETIC BEHAVIOUR OF BACTERIA AND THE DESIGN OF A NEW OPTICAL MEASUREMENT SYSTEM

3.1 Introduction

The quantitative measurement of the dielectrophoretic force has been the cause of much concern since the existence of the dielectrophoretic effect was first reported by Pohl (1951). The traditional method for measuring particulate dielectrophoresis (Pohl, 1978) is to observe an electrode through a microscope and to estimate, usually via time-sequenced photographs for each measurement frequency, the rate at which the particles under investigation collect at the electrode. This method is time-consuming, non-precise and can be problematical for small cells such as bacteria. To overcome the short-comings in conventional techniques a number of new measurement methods have been proposed, the most notable of which has been dielectrophoretic levitation first reported by Jones (Jones and Kallio 1979, Jones and Kraybill 1986, Feeley and McGovern 1986, Kaler and Jones 1989). Other methods include the direct measurement of the dielectrophoretic force on a large particle (Pohl and Pethig, 1977), particle velocity measurement (Stoicheva and Dimitrov, 1986), quasi-elastic light scattering (Kaler et al, 1988) and the combination of levitation and impedance measurement (Bahaj and Bailey, 1985).

In the studies described in this chapter a new optical technique for the measurement of the dielectrophoretic collection rate was used. This new method, based on monitoring changes in the

light absorbance properties of a particle suspension, as particles are collected at an electrode array, has allowed measurements which hitherto would have taken a full day to complete using conventional methods to be carried out in approximately 20 minutes. The speed at which measurements can be made using the new optical system makes it ideal for the study of biological cells which must be kept alive during experiments since changes in their physiological state can adversely effect any experimental results.

To investigate the possible applications of dielectrophoresis to biotechnology, a detailed knowledge of the dielectrophoretic collection spectrum of biological particles (in this case cells) is required. In these experiments the biotechnologically important bacteria *Escherichia coli* and *Bacillus subtilis* along with the bacteria *Micrococcus lysodeikticus* were studied. *M. lysodeikticus* has been the subject of much biophysical investigation. In particular the dielectric studies of Einolf and Carstensen (1969) and the surface charge investigations of Price and Pethig (1986) make this bacteria an ideal cell with which to examine the bioelectrical processes which determine the dielectrophoretic response of a cell. The experiments described in this chapter were aimed at investigating the frequency dependence of the dielectrophoretic collection rate of biological cells over the frequency range 20Hz to 4MHz and the relationship between this frequency dependence and the electrical conductivity and permittivity of the cell and suspending medium. Particular attention was paid to the effects of medium conductivity on the collection rate which is reported (Pohl, 1978) to diminish as the conductivity of the suspending medium is increased. This would impose severe limitations on the possible application of dielectrophoresis as a means of primary cell separation where a typical cell culture medium has a high electrical conductivity (approximately 1.0Sm^{-1}, Bowden and Whittington, 1986).

3.2 Materials and Methods

3.2.1 Optical Measurement System

The design of the optical chamber and collecting electrodes is shown in figure 3.1. The microelectrodes were fabricated on a glass substrate in a four stage process. First a seed layer

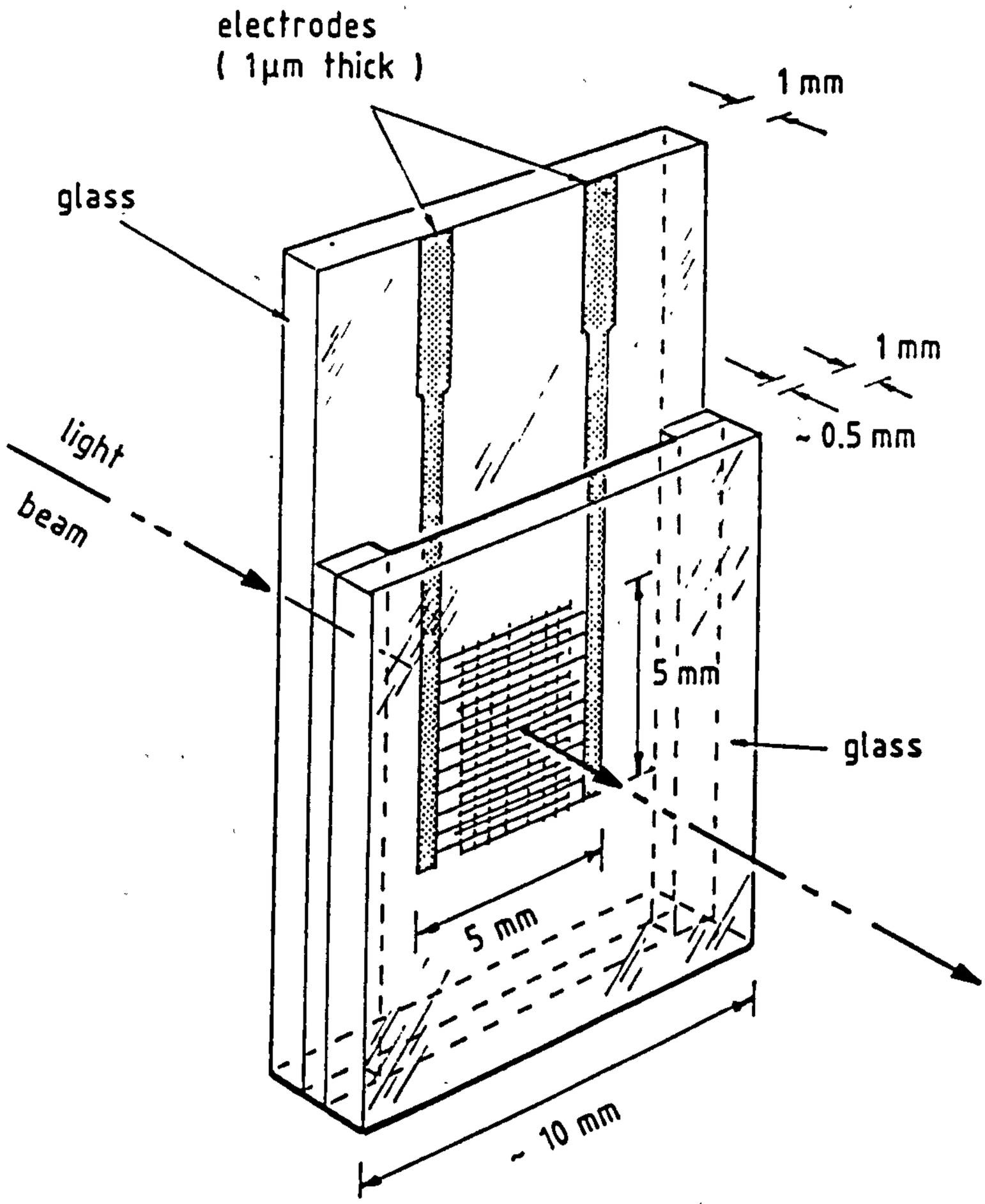

Figure 3.1 Design of the optical cell and micro-electrodes.

of chrome was sputtered onto the glass. The chrome adheres strongly to the substrate forming a good anchor for a second, 1μm thick, layer of sputtered copper (which does not adhere well to glass). The electrode structure was then etched into the chrome/copper surface of the substrate using standard photolithographic techniques. The final stage of fabrication was the electrochemical deposition of a 0.2μm layer of gold onto the etched electrodes. This provided an inert layer over the copper to avoid the presence of copper ions, which are known to be toxic to some cell lines (George, 1986), from entering any cell suspension used as well as to extend the experimental lifetime of the electrodes. A second glass plate was then placed over the electrodes to produce a small sample chamber of around 0.5mm depth. The sample chamber was then filled with a suspension of the cells to be studied and its optical absorbance was measured, using a standard, large beam spectrophotometer (Unicam SP8-100, SP6-400), as a function of time for various frequencies of an applied voltage to the electrodes. The analysing light beam passing through the sample chamber and electrode array was approximately 3mm x 5mm. Sinusoidal voltages were applied to the electrodes using a signal generator (Farnell LFM 3) and all changes in optical absorbance were monitored at a fixed wavelength of 450nm. The initial absorbance of the filled chamber was typically 0.5.

The field-producing electrodes were of a castellated, interdigitated, geometry as shown in figure 3.2. This design was chosen for the high degree of field non-uniformity produced while simplifying the production of the photolithographic mask used in the manufacturing processes. Figure 3.2 also shows the electric field equipotentials for a 20V signal applied to the electrodes as obtained by a solution of Laplace's equation using a finite-difference computational method (Vitkovitch, 1966). The field strength produced in the plane of the electrodes, close to the substrate, varies from $0.8MVm^{-1}$ to $80kVm^{-1}$. In the bulk solution the field will extend radially from the electrodes producing a non-uniform field throughout the sample chamber directed towards the electrodes with the highest field strengths at the tips of the electrode castellations.

For frequencies where the polarisability of the cells under investigation exceeds that of their suspending medium, the cells will experience a dielectrophoretic force towards, and be collected at, the castellated tips of the electrodes. Figure 3.3 shows this collection in a series of

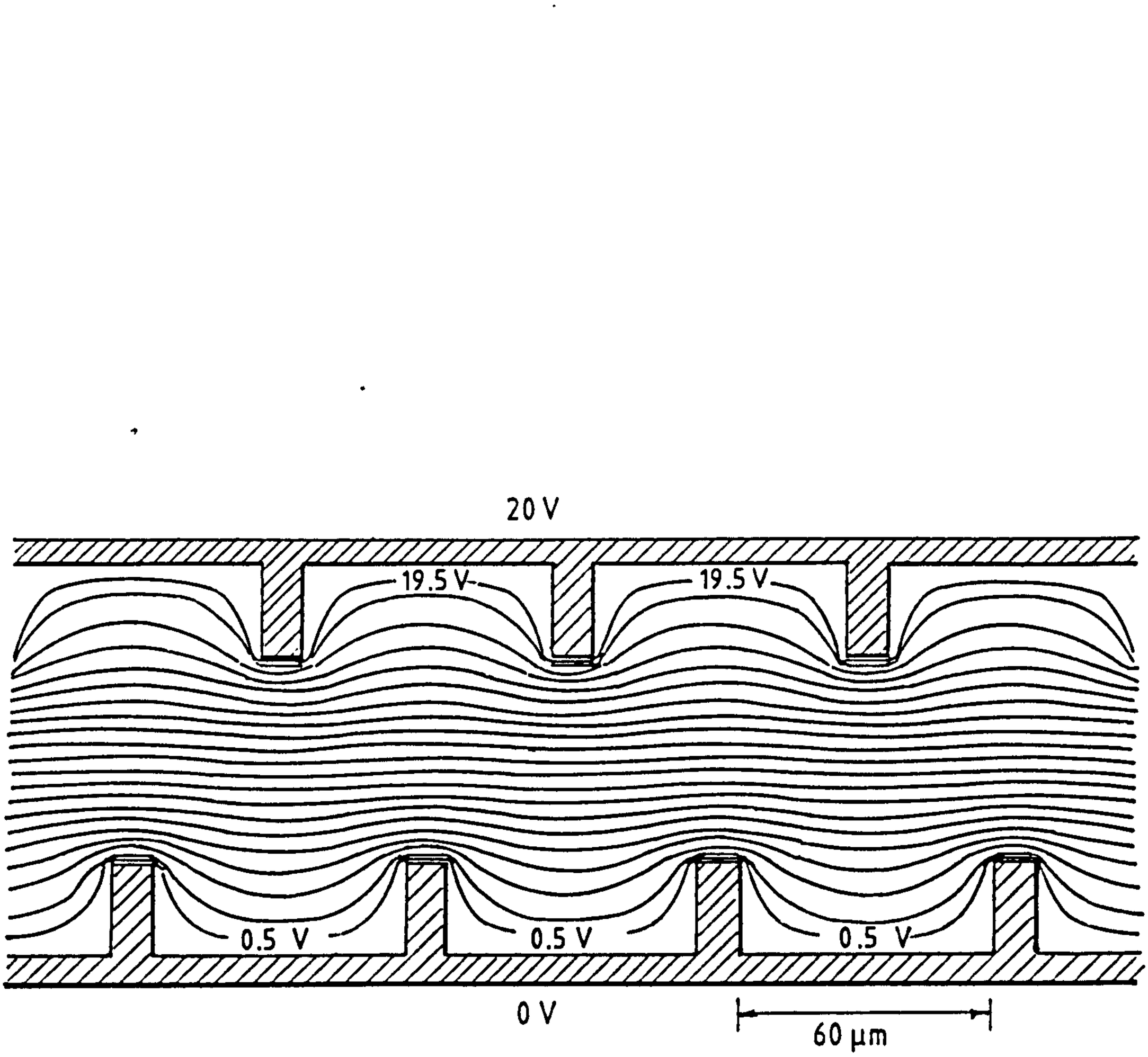

Figure 3.2 Magnified view of castellated electrode design. The equipotentials are plotted at 1V intervals, apart from the 0.5V and 19.5V potentials, for the case of a 20V signal applied to the electrodes.

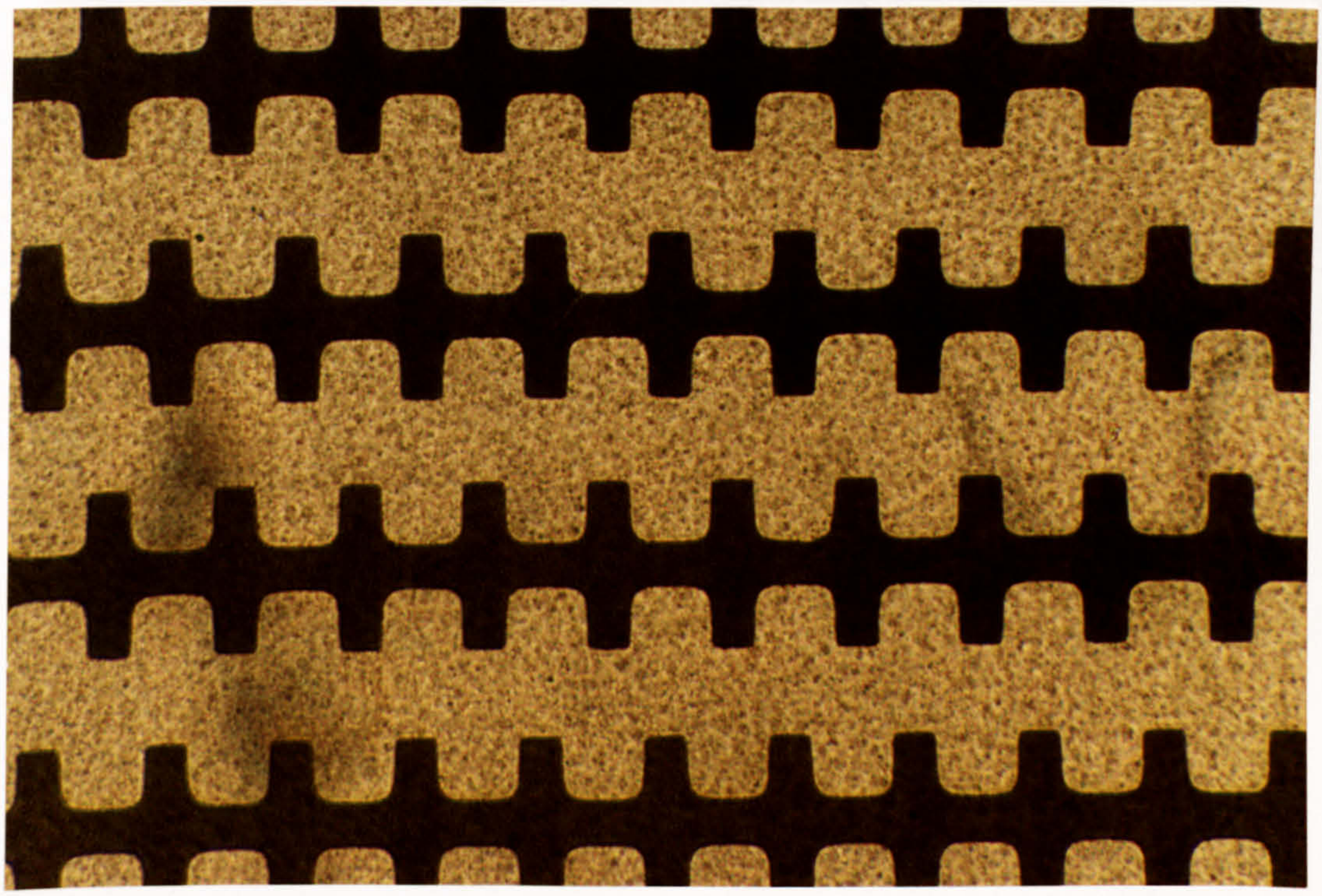

Figure 3.3(a) Microscope magnification (x130) of the micro-electrode configuration and a suspension of *M. lysodeikticus* in 280mM mannitol solution before the signal was applied.

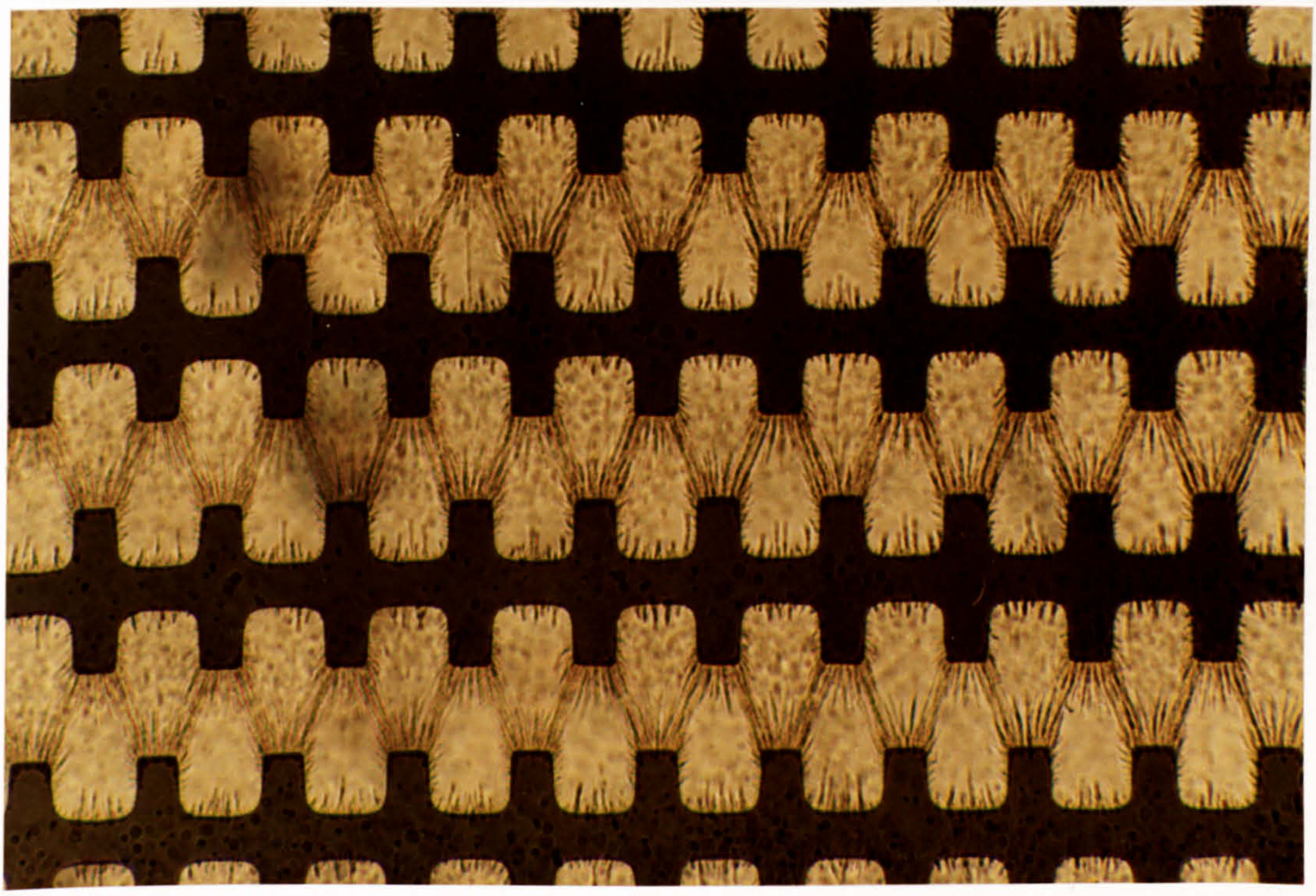

Figure 3.3(b) 60 seconds after the application of a 100kHz, 10V peak-peak sinusoidal signal.

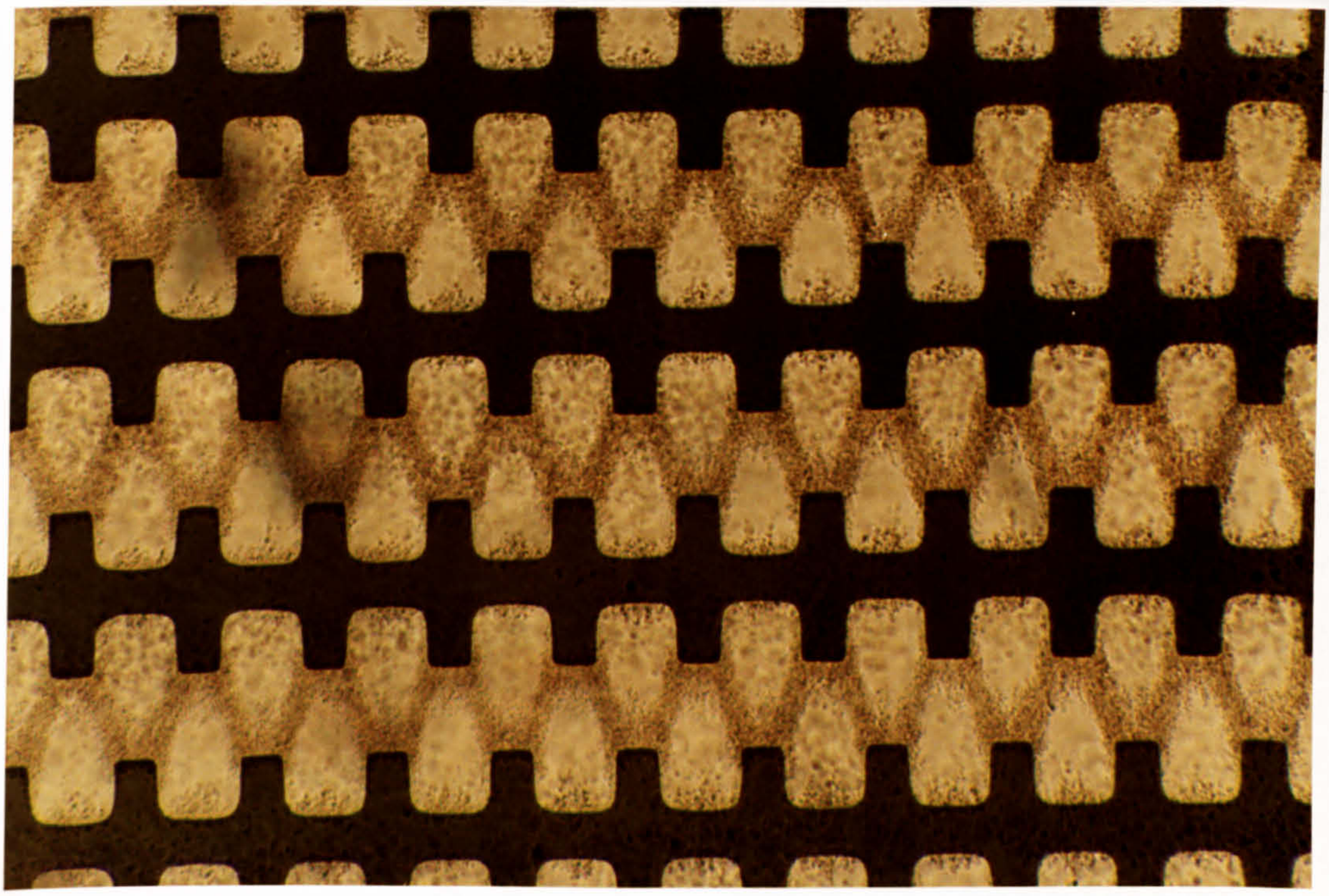

Figure 3.3(c) 10 seconds after the signal was subsequently removed.

photographs taken using a x130 microscope magnification of the electrode array. The photograph in figure 3.3(a) shows the uniform distribution of *M. lysodeikticus* suspended in a 280mM mannitol solution. On the application of a 100kHz 10V peak-peak sinusoidal signal to the electrodes, the cells begin to collect at the electrode tips and are removed from the bulk solution causing a decrease in the optical absorbance of the bulk solution. Figure 3.3(b) shows such a collection 60 seconds after the application of the signal to the electrodes. The decrease in optical absorbance is clearly seen together with an increased absorbance about the electrode tips. If the absorbance is determined over a sufficiently large area then, for relatively low cell concentrations and a short optical pathlength, the reduction in absorbance of the bulk solution is the dominant effect. The collection of cells at the electrodes is enhanced by electric field-induced cell-cell interactions taking place in the bulk solution that give rise to 'pearl chain' formations (due to the local deformation of the applied electric field by the cells) which increase the effective volume of the cells. These pearl chains collect together and extend across the inter-electrode spacing (figure 3.3(b)). On the removal of the applied voltage the cells, under the influence of Brownian motion and cell-cell electrostatic repulsion, disperse from the electrodes. Figure 3.3(c) shows the distribution of cells 10 seconds after the field producing voltage is removed from the electrode, whilst after a further 60 seconds the cells return to a uniform distribution as seen in figure 3.3(a).

The 3 stages of the dielectrophoretic collection process as seen in figure 3.3 can also be observed in the temporal variation in the optical absorbance of the system. Figure 3.4 shows a typical variation in absorbance for a suspension of *M. lysodeikticus* on the application of a 100kHz 10V peak-peak sinusoidal signal to the electrodes. A rapid reduction in absorbance is observed on the initial application of the voltage followed by a more gradual reduction over the next minute. Microscope observations have shown that as the voltage is applied the cells in the immediate vicinity of the electrodes are collected rapidly and this gives rise to the initial sharp decrease in absorbance observed. The subsequent slower absorbance change is due to the movement of cells from the bulk solution to the electrodes. These cells collect across the inter-electrode spacing in long pearl chains to form the extended 'w' formation across the

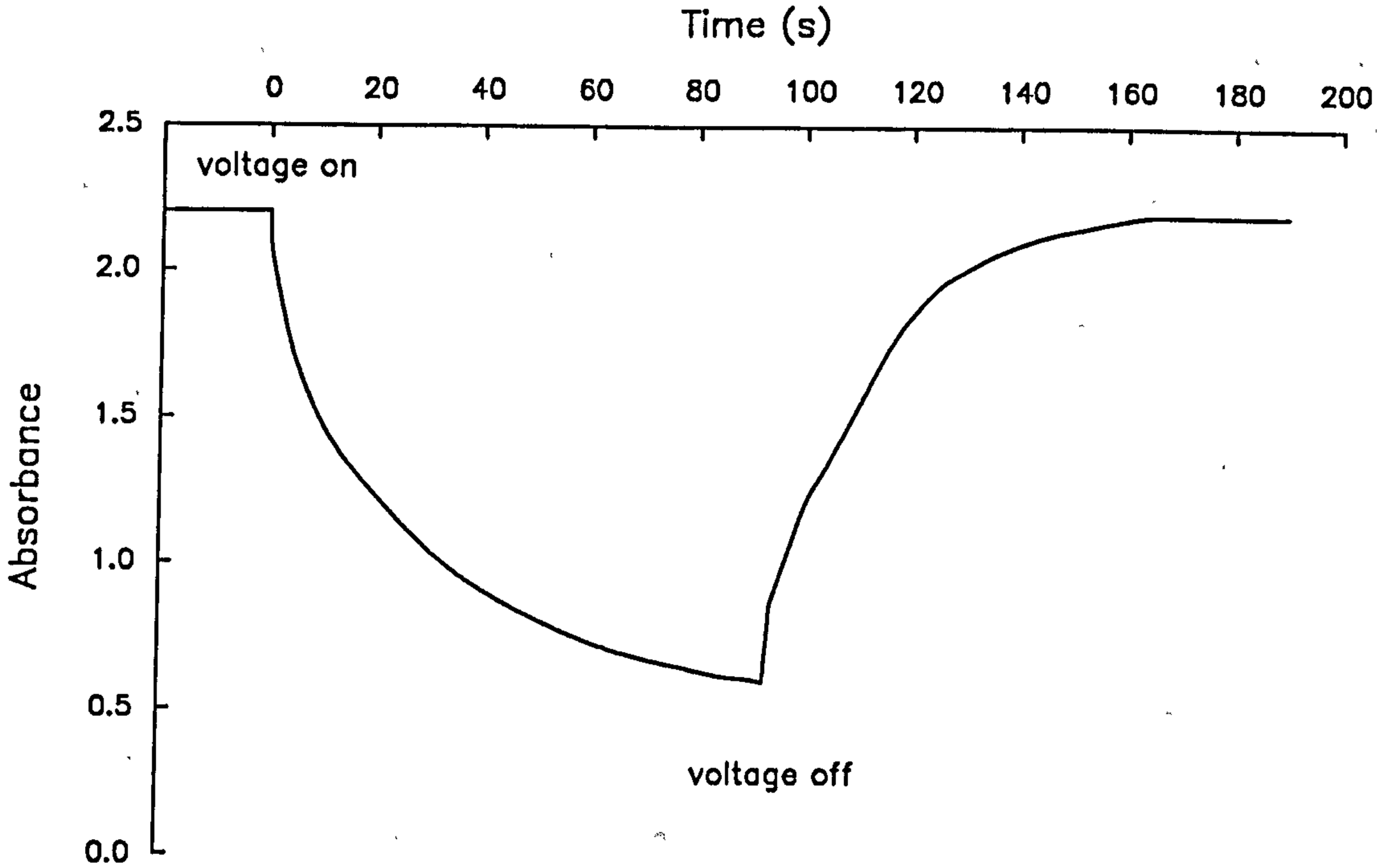

Figure 3.4 The temporal variation of the 450nm absorbance of *M. lysodeikticus* suspended in 280mM mannitol solution on the application and removal of a 100kHz, 10V peak-peak sinusoidal signal.

electrode tips seen in figure 3.3(b). The formation of cell chains across the electrode gaps give rise to areas of increasing absorbance which have the effect of causing an apparent reduction in the rate of change of absorbance.

On the removal of the applied voltage an immediate and rapid increase in absorbance is observed. This correlates with the appearance of normal Brownian motion (suppressed by the polarising influence of the electric field), rapid dispersion of cells from the electrodes and the breakdown of pearl chain formations as seen in figure 3.3(c). This rapid dispersal of cells and the breakdown of pearl chain formations is considered to arise from electrostatic repulsion associated with cell-cell and cell-substrate interactions. Price and Pethig (1986) reported a cell surface charge density of $-1.5\mu Ccm^{-2}$ for *M. lysodeikticus*. The presence of a net surface charge causes cells to be repelled from each other as well as from the negatively charged glass substrate. The initial increase in absorbance as cells disperse is followed by a more gradual rate of increase and probably results from the natural diffusion of cells into the bulk solution.

To obtain the dielectrophoretic collection spectra presented in the following sections of this chapter, plots of the form of figure 3.4 were obtained for applied sinusoidal voltages from 20Hz to 4MHz at 6V peak-peak in magnitude. The dielectrophoretic collection rate can be considered as equal to the rate of removal of cells from the sample suspension and hence, by Beer's law (chapter 4), to the rate of change in optical absorbance. The following figures (3.5-3.8) are based on the reduction in optical absorbance occurring in the first 4 seconds after the application of the field-producing voltage. Although taking measurements after 40 second reveals an identical response for *M. lysodeikticus* the excessive presence of pearl chain formations around the electrode tips can cause erroneous results when cells of differing shape, such as *B. subtilis*, are studied. To aid reproducibility of results a fresh sample of cell suspension was used for each frequency measurement with the optical chamber being rinsed with deionised water before each reading to remove all traces of previous samples.

3.2.2 Cell Suspensions

Cell suspensions were obtained in freeze dried form (Sigma, U.K.) and were used either directly in this form or grown in culture. Dried cells were resuspended in 150mM NaCl at 25°C for 1 hr. to rehydrate. Cultured cells were grown for 48hrs (stationary phase) in a general undefined medium containing $3gl^{-1}$ Malt extract, $3gl^{-1}$ yeast extract, $10gl^{-1}$ glucose and $5gl^{-1}$ bacteriological peptone by a shake flask method from a 1µl loop inoculum. Cells were harvested from their rehydrating or growth medium by centrifugation (100 x g for 5minutes), washed 3 times and resuspended to an optical density of 0.5 at 450nm in 280mM mannitol (equivalent to 150mM NaCl). The mannitol solution provided an osmotically balanced suspending medium which greatly reduced the leakage of ions across the cell membrane, as well as having a low conductivity and being non-digestible by the cells.

M. lysodeikticus protoplasts were produced by breaking down the outer, polysaccharide, cell wall of the bacteria with a high osmotic pressure solution of lysozyme. The intact cells were washed as described above and then resuspended in 2ml 0.8M sucrose solution. To this suspension 70µl of a solution ($10mg\ ml^{-1}$) of chicken egg-white lysozyme (Sigma U.K.) was added and left to react at room temperature. The lysing reaction was monitored by measuring the optical density as a function of time and was found to reach completion after approximately 2hrs. The high osmotic pressure was required to prevent the plasma membrane from bursting when the protective cell wall of the intact cell was destroyed. The change in optical absorbance produced by the dielectrophoretic collection of the protoplasts was around 5 times less than that produced by the intact cells. (scanning electron micrographs reveal approximately a 50% reduction in volume on lysozyme treatment). For this reason measurements were made on protoplast suspensions that were 5 times the concentration of intact cells. Before measurement the cells were suspended and washed three times in 0.8M sucrose solution.

3.3 Dielectrophoretic Response of Bacteria

Figure 3.5 shows the dielectrophoretic collection spectra of the bacteria *Micrococcus lysodeikticus*, *Escherichia coli* and *Bacillus subtilis*. This graph demonstrates an important feature of the dielectrophoretic effect on micro-organisms, namely that different species exhibit different, characteristic, frequency responses. The results for *M. lysodeikticus* and *E. coli* share a similar form, that of a low collection rate at 20Hz rising quickly to a peak at 40 Hz for *E. coli* and 100Hz for *M. lysodeikticus*. After this low-frequency peak in collection the response for *M. lysodeikticus* rapidly reduces until 1kHz whereupon the collection begins to gradually increase to a constant rate at frequencies above 10kHz until a steady decrease is observed above 500kHz. The response for *E. coli* reduces gradually from the low-frequency peak to reach a constant collection rate at 5kHz until at high frequencies, above 100kHz, the response reduces to virtually zero at 4MHz. *B. subtilis* shows a different response to *E. coli* and *M. lysodeikticus*; from 20Hz to 200Hz a constant collection is observed, above 200Hz this increases to a peak at 1kHz and then reduces to a constant rate at 4kHz before rapidly rising to a second, high-frequency, peak at 1MHz after which a reduction in collection occurs.

3.4 Effect of Medium Conductivity on the Collection of *M. lysodeikticus*

As observed by Pohl (1978) and discussed by Bowden and Whittington (1986) an increase in medium conductivity reduces the magnitude of the dielectrophoretic response until at conductivities equivalent to those of a typical cell growth medium the force is non-existent. Figure 3.6 shows the effect of increased medium conductivity on the collection on *M. lysodeikticus*. The mannitol solution used in the previous section, and the first graph of figure 3.6, has a conductivity similar to that of deionised water (10^{-3}-$10^{-4}$$Sm^{-1}$). Cells suspended in this medium display a large, low-frequency, peak in collection and a large response at higher frequencies. The addition of NaCl to a concentration of 1mM (equivalent to 0.01Sm^{-1}) causes a dramatic reduction in the low-frequency collection peak as well as a shift in its frequency from 100Hz to 200Hz. At higher frequencies the dielectrophoretic response is reduced by a

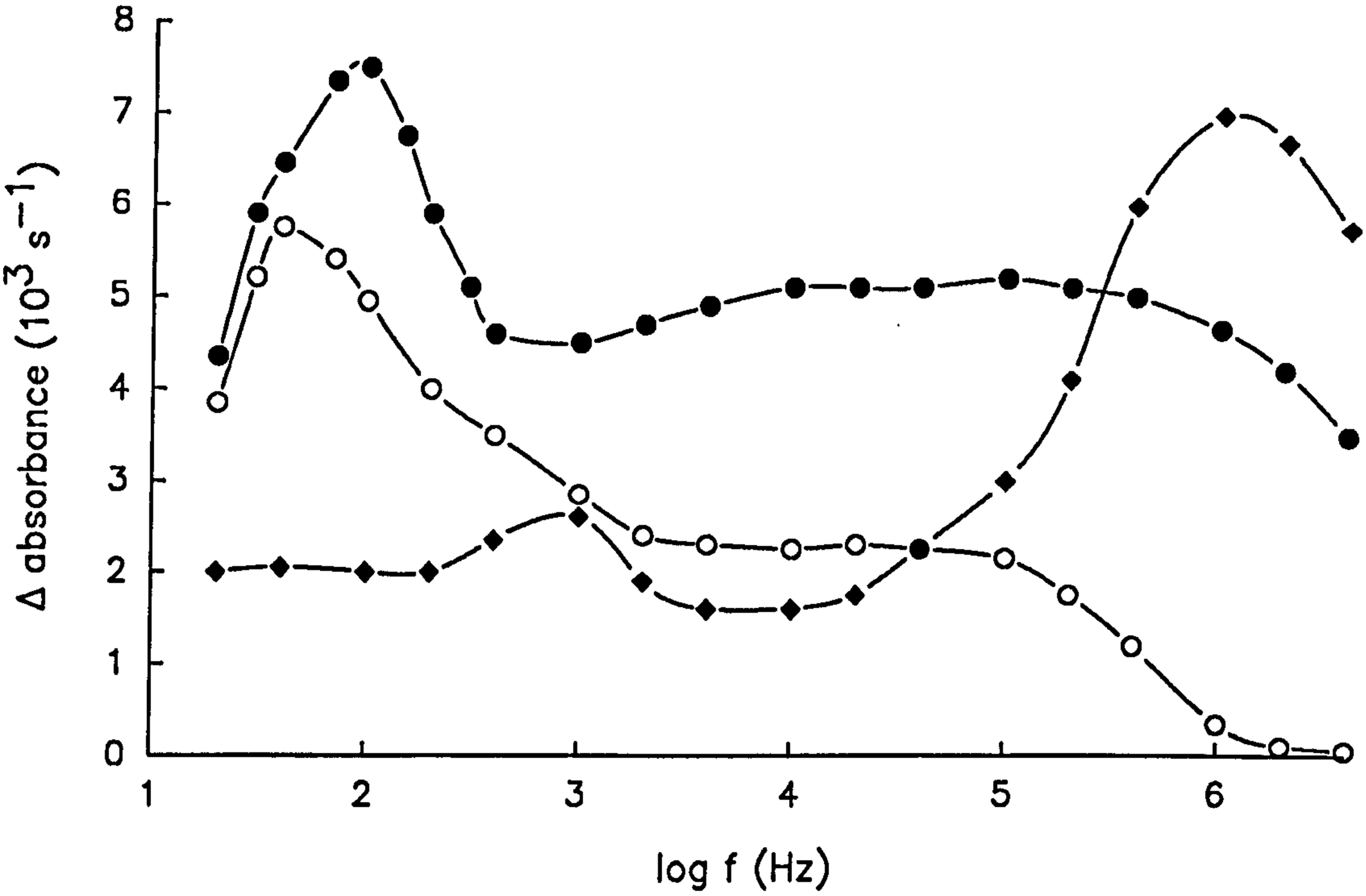

Figure 3.5 The frequency dependence of the dielectrophoretic collection rate of *M. lysodeikticus* (●), *E. coli* (O) and *B. subtilis* (◆) suspended in 280mM mannitol solution. The applied signal was 6V peak-peak.

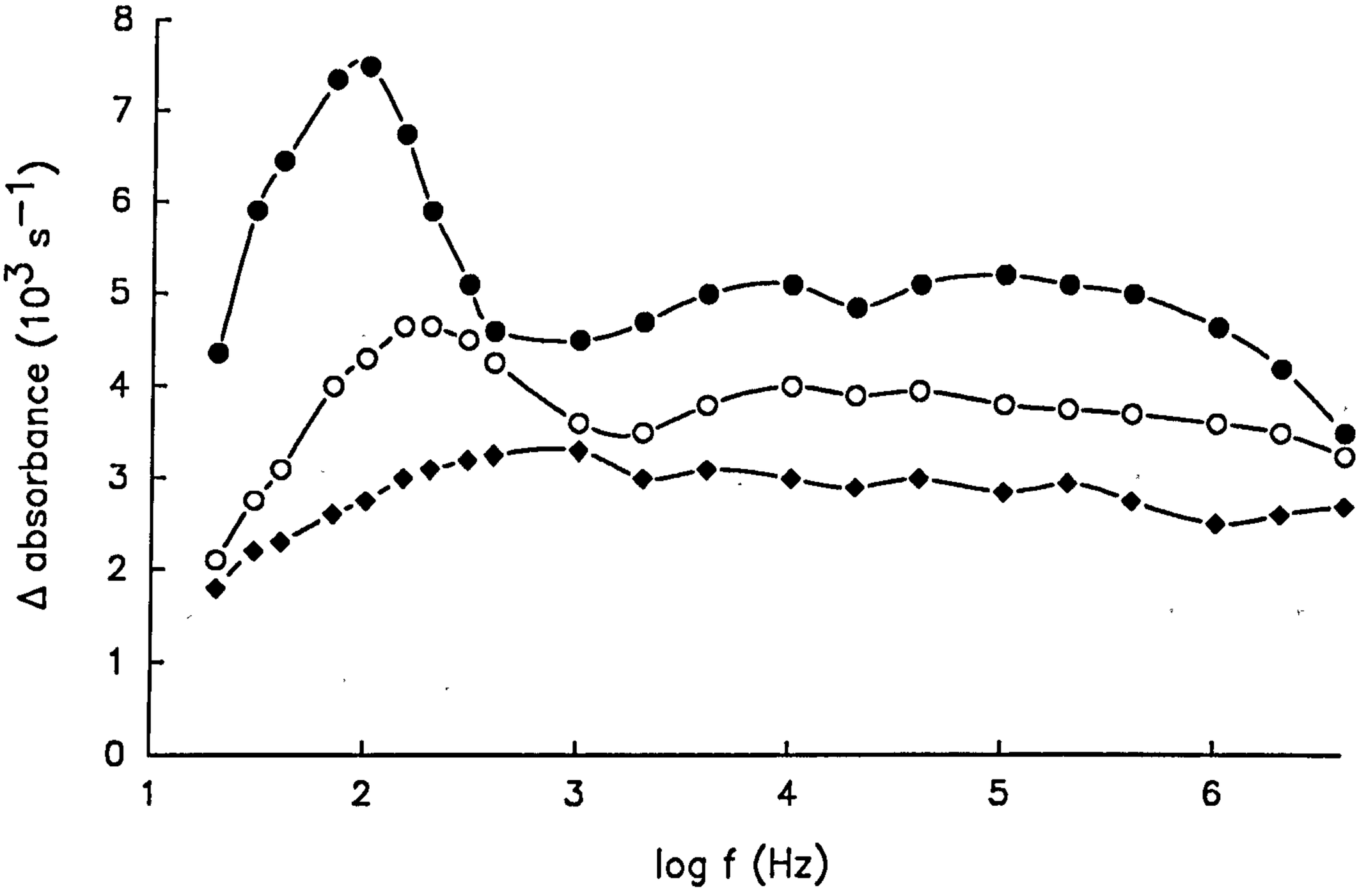

Figure 3.6 Frequency dependence of the dielectrophoretic collection rate of *M. lysodeikticus* suspended in 280mM mannitol (●), mannitol + 1mM NaCl (O), and mannitol + 2mM NaCl (◆) for a 6V peak-peak applied sinusoidal signal.

constant factor of approximately 1.3. The further addition of sodium chloride to a concentration of 2mM ($0.02Sm^{-1}$) causes a further reduction and virtual removal of the low-frequency peak which is now shifted to 600Hz. As before, a reduction by a further factor of 1.3 is observed in the collection rate above 1kHz.

To further investigate the effect of medium conductivity on the dielectrophoretic force the collection of *M. lysodeikticus* at 10kHz was measured as a function of medium conductivity from 0-$1Sm^{-1}$ by the addition of sodium chloride to the mannitol suspending medium. The observed variation in dielectrophoretic force, figure 3.7, shows a reduction in collection from 0 to $0.2Sm^{-1}$ at which point the dielectrophoretic force is reduced to zero. Above $0.2Sm^{-1}$ the response becomes increasingly negative until from $0.45Sm^{-1}$ to $1.0Sm^{-1}$ a constant, negative, collection rate is measured. Microscope observations of this negative effect, observed by an increase in optical absorbance on the application of an electric field, show that it corresponds to the apparent repulsion of the bacteria from the electrodes towards the areas of lowest field intensity. Also shown in figure 3.7 is a calculated theoretical response for the variation in collection for increasing suspending medium conductivity (section 3.6).

3.5 Dielectrophoretic Study of the Protoplasts of *M. lysodeikticus*

It is known (Pethig and Kell, 1987) that for frequencies below around 1MHz an electric field applied to a cell will not penetrate through its insulating plasma membrane. Therefore the electrical properties of the cell which determine the form of its dielectrophoretic response below 1MHz are likely to be associated with the surface of the cell. The surface of bacteria differ from that of other cells by the presence of a protective polysaccharide cell wall over the plasma membrane. Treatment with a solution of lysozyme removes the cell wall to leave the bacteria protoplast with a lipid bilayer surface containing the various membrane proteins of the bacteria.

Figure 3.8 shows the dielectrophoretic response of protoplasts of *Micrococcus lysodeikticus* at a concentration five times that of the intact *micrococcus*. The spectrum shows a large collection at low frequencies which reduces as the field frequency is increased until a region of constant

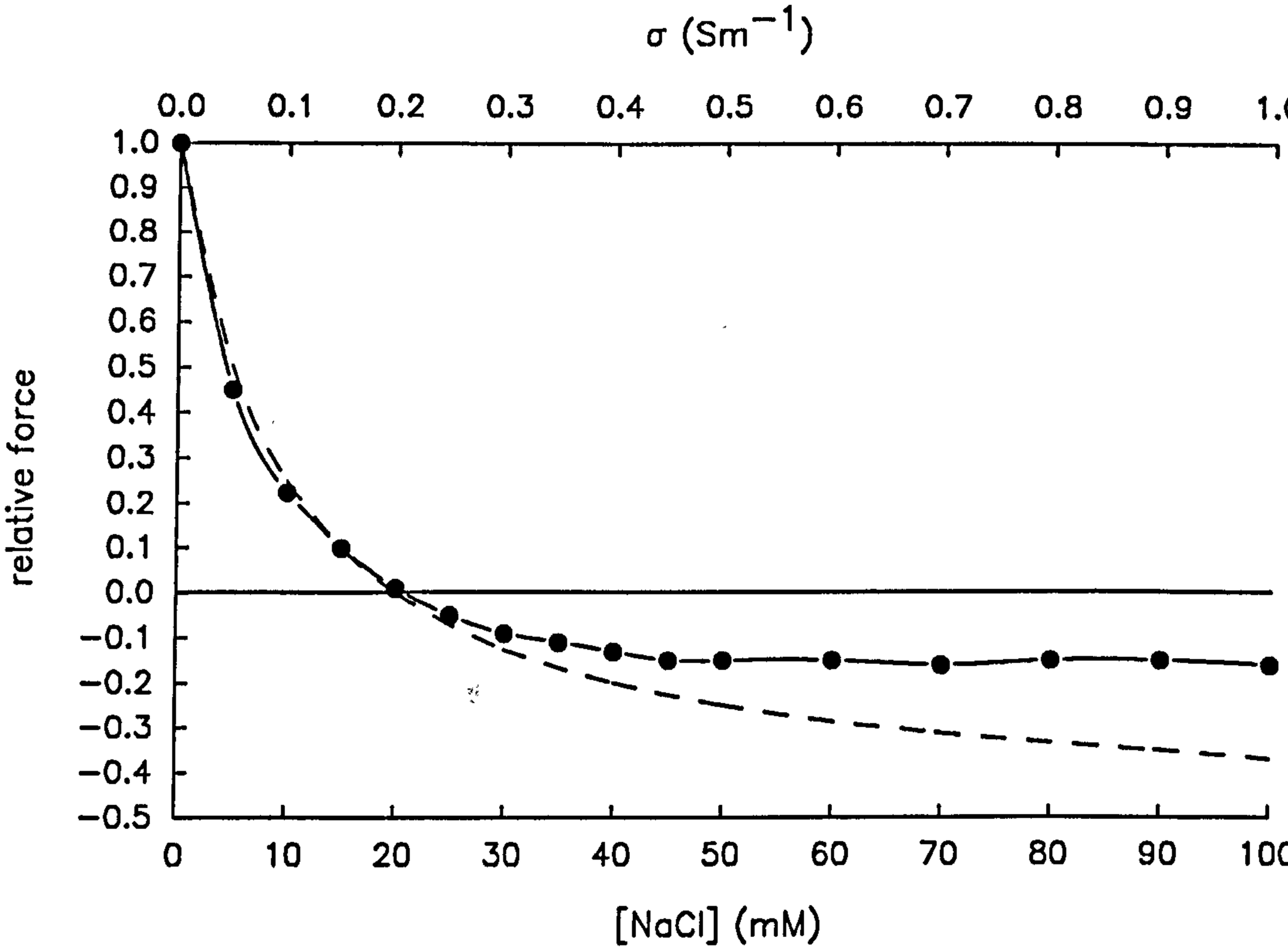

Figure 3.7 The theoretical and experimental variation of the dielectrophoretic force as a function of solution conductivity, normalised for 280mM mannitol. Theoretical data calculated from eqn. 3.7 for the case of σ_p=0.2Sm^{-1}.

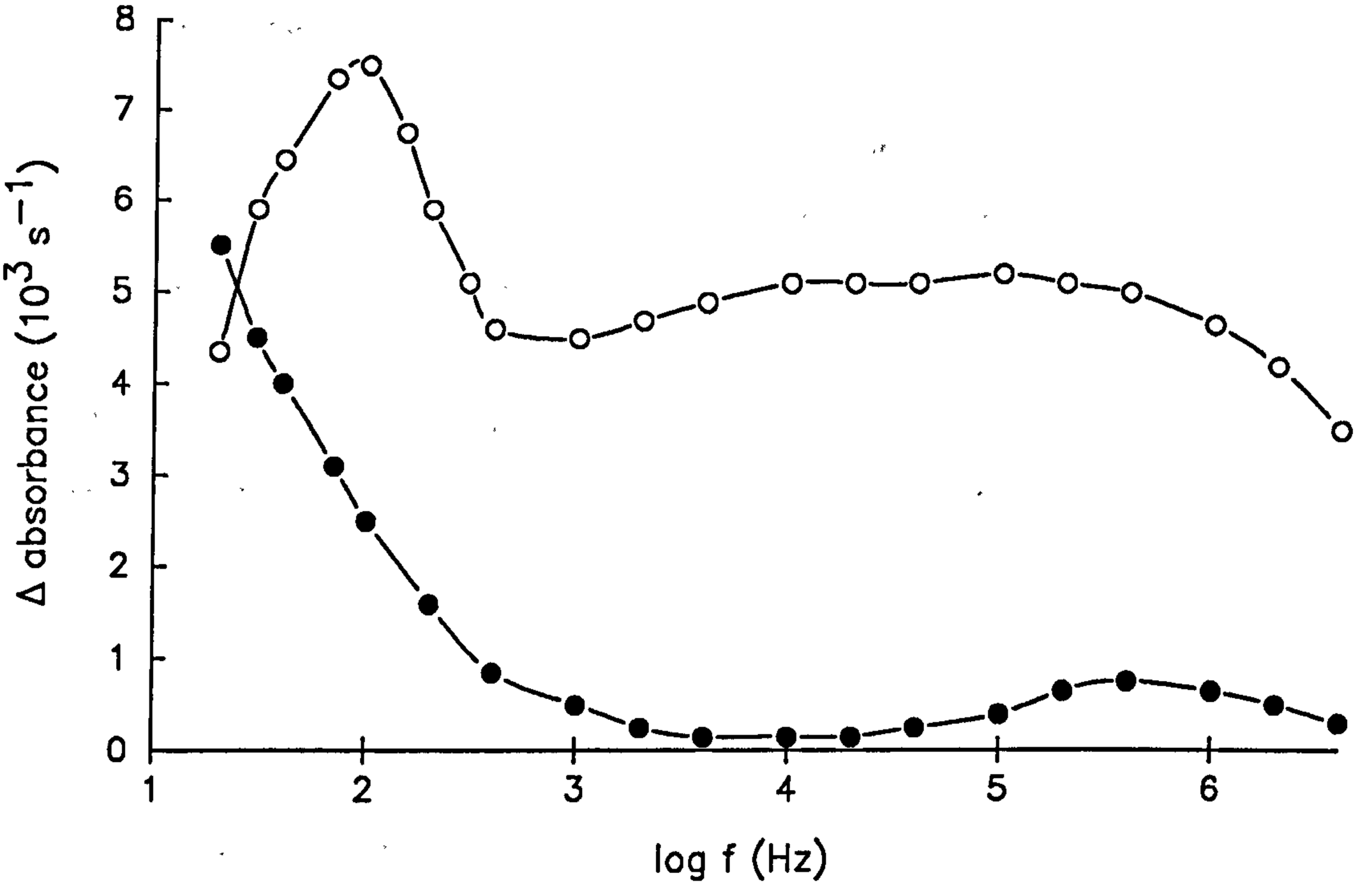

Figure 3.8 The frequency dependence of the dielectrophoretic response of protoplasts of *M. lysodeikticus* (●) in 0.8M mannitol (at 5 times the concentration of the results of figure 3.5) for a 6V peak-peak applied sinusoidal signal. Also shown is the dielectrophoretic response of intact *M. lysodeikticus* (O) as given in figure 3.5.

collection is observed from about 2kHz to 40kHz. Above 40kHz the collection increases to a peak at 400kHz before the now familiar decrease in collection at frequencies of 1MHz and above. Also shown in figure 3.8 is the dielectrophoretic collection spectrum of the intact bacteria (figure 3.5) for comparison.

3.6 Discussion

The bacterial collection spectra given in figure 3.5 highlight an important feature of the dielectrophoretic effect namely that different species exhibit different, characteristic, frequency responses. In chapter 2 a general expression was derived for the magnitude of the dielectrophoretic force experienced by particles (Pohl, 1978). This derivation makes use of the well documented theoretical dipole moment of an ideally polarisable homogeneous sphere of known volume in an infinite ideal dielectric medium (von Hippel, 1954) to arrive at the following relationship:

$$F = \frac{3Y}{2} v \varepsilon_o \varepsilon_m \frac{\varepsilon_p - \varepsilon_m}{\varepsilon_p + 2\varepsilon_m} \nabla |E|^2 \quad 3.1$$

where v is the particle volume, ε_m and ε_p are the medium and particle permittivity respectively, ∇ is the del vector operator and E is the local root mean square field strength.

Equation 3.1 predicts a constant force with no variation or frequency dependence. For very low conductivity particles and medium a frequency dependence can be introduced by considering the dielectric relaxation processes of the particles and medium, as discussed in chapter 2. However, the introduction of a dielectric relaxation implies the use of particles and media with a degree of conductivity, and in this case the permittivity of the medium and particle become complex terms as given below.

$$\varepsilon_m^* = \varepsilon_o \varepsilon_m - j\frac{\sigma_m}{\omega} \qquad \varepsilon_p^* = \varepsilon_o \varepsilon_p - j\frac{\sigma_p}{\omega} \quad 3.2$$

Pohl (1978) suggested that only the real part of the now complex force equation should be considered. After further consideration of the complex force and its theoretical derivation Jones and Kallio (1979) reported the following, widely excepted, force equation for real dielectrics:

$$\mathbf{F}=\frac{\partial \mathbf{r}}{2}\mathbf{v}\,\mathrm{Re}\left(\varepsilon_o\varepsilon_m\frac{\varepsilon_p^*-\varepsilon_m^*}{\varepsilon_p^*+2\varepsilon_m^*}\right)\nabla|\mathbf{E}|^2=\frac{\partial \mathbf{r}}{2}\mathbf{v}\,\alpha\,\nabla|\mathbf{E}|^2 \qquad 3.3$$

Equation 3.3 has also been derived using different methods by Benguigui and Lin (1982) and Saur (1985). However, the expansion of the polarisability term, α (chapter 2), has produced several confusing expressions for the polarisability of the suspended particles. A more understandable form of α (Al-Ameen, 1989) can be obtained by the introduction of a depolarisation factor A and the use of the identity

$$K=\frac{(1-A)}{A}$$

in eqn. 3.3 to obtain the following expression

$$\alpha=(K+1)\,\varepsilon_m\frac{\omega^2(\varepsilon_p-\varepsilon_m)(K\varepsilon_m+\varepsilon_p)+(\sigma_p-\sigma_m)(K\sigma_m+\sigma_p)}{\omega^2(K\varepsilon_m+\varepsilon_p)^2+(K\sigma_m+\sigma_p)^2} \qquad 3.4$$

For spherical particles the factor A has a value of 1/3 and by using the identity

$$\tau=\frac{\varepsilon_p+2\varepsilon_m}{\sigma_p+2\sigma_m}\varepsilon_o \qquad 3.5$$

the full expansion of the polarisability, α, in equation 3.3 becomes

$$\alpha=\varepsilon_m\left[\frac{\omega^2\tau^2}{1+\omega^2\tau^2}\left(\frac{\varepsilon_p-\varepsilon_m}{\varepsilon_p+2\varepsilon_m}\right)+\frac{1}{1+\omega^2\tau^2}\left(\frac{\sigma_p-\sigma_m}{\sigma_p+2\sigma_m}\right)\right]\varepsilon_o \qquad 3.6$$

Although eqn. 3.6 is derived for the case of an ideal dielectric particle in an infinite ideal dielectric medium, it may be considered valid for the low conductivity media and cell concentrations used in the experiments described in this chapter.

To compare the experimental dielectrophoretic spectra with those predicted by eqn. 3.6 it is easiest to adopt the single shelled sphere model for a cell as discussed in chapter 2. Figure 3.9 shows such a model where the inner sphere represents the cytoplasm of the bacteria and is assigned a permittivity ε_i and conductivity σ_i. Surrounding the cytoplasm is a thin shell symbolising the cellular membrane with permittivity and conductivity ε_s and σ_s respectively. The whole cell is suspended in a medium with a complex permittivity described by the permittivity and conductivity ε_m and σ_m. The medium used in the experiments described here was a 280mM mannitol solution which had a conductivity slightly above that of the deionised water used in making up the solution ($\sigma_m=10^{-3}$-$10^{-4}Sm^{-1}$) and a permittivity close to that of water ($\varepsilon_m=80\varepsilon_o$). In his investigations into the resistance of bacterial membranes Carstensen (1967) found, using a model which ignored the cell wall of a bacteria, that the resistance of *M. lysodeikticus* membranes could be as high as 10^{-4} ohm m^2 (corresponding to a membrane conductivity of around $5 \times 10^{-5}Sm^{-1}$). The capacitance of cellular membranes has been found by a number of workers to be almost universally around 1.0 μFcm^{-2} (Schwan 1957, Fricke et al 1956) corresponding to a membrane permittivity of around $5\varepsilon_o$. The cytoplasm of a cell has a high ionic concentration, primarily potassium ions, resulting in an effective cytoplasmic conductivity of around 2 Sm^{-1} (Tempest, 1969). The permittivity of the cytoplasm, like the suspending medium, is similar to that of water ($\varepsilon_m=80\varepsilon_o$). Substituting these values into the single shell model equations given in section 2.8 and using a typical membrane thickness of around 5nm and a cell radius of approximately 1μm the dielectric properties of the bacterial model can be found. The substitution of the model particle permittivity and conductivity into eqn. 3.6 reveals the theoretical collection spectra shown in figure 3.10. The permittivities and conductivities used here have been arrived at through investigations into the dielectric properties of cells suspended in conducting media usually of near physiological strength. However, Einolf and Carstensen (1969) point out that these values are dependent on the movement of ions in

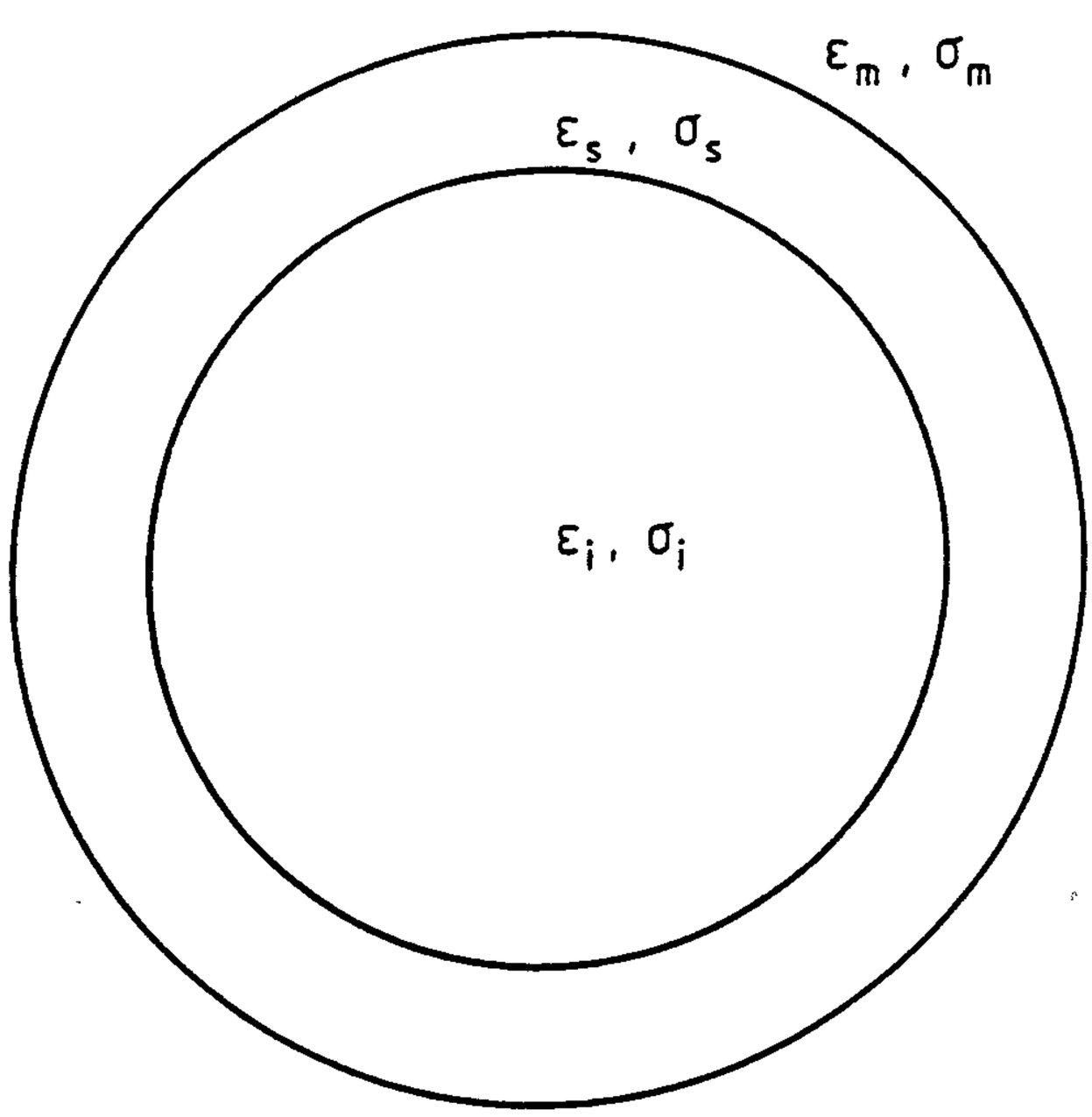

Figure 3.9 A single shelled sphere model of a bacteria. ε_m and σ_m represent the dielectric properties of the suspending media, ε_s and σ_s symbolise the dielectric properties of the cell membrane and the properties of the cytoplasm are described by the parameters ε_i and σ_i.

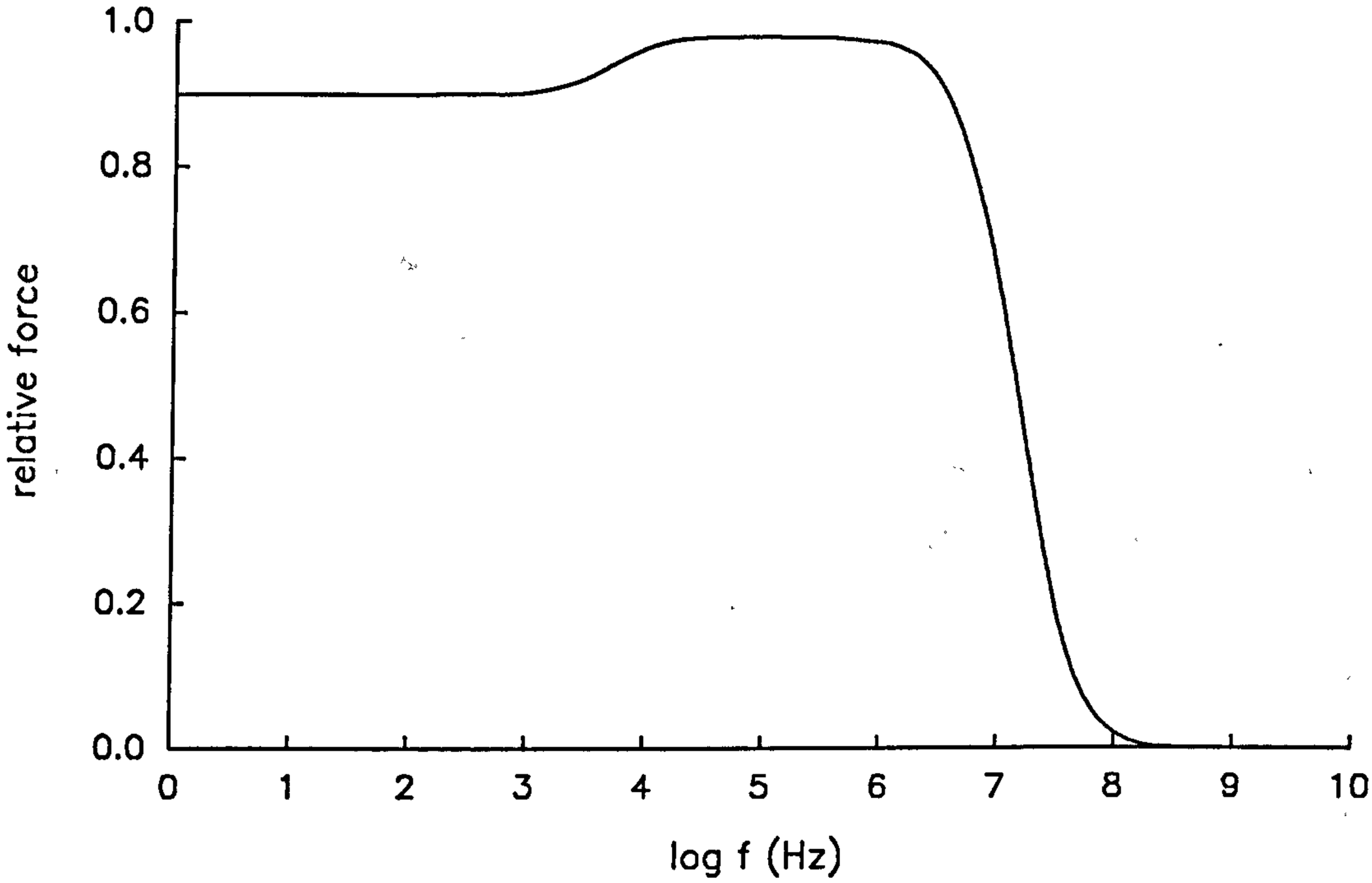

Figure 3.10 The variation in the relative dielectrophoretic force as a function of applied frequency as described by eqn. 3.6 using a single shelled sphere model of a bacteria. $\varepsilon_m=\varepsilon_i=80\varepsilon_o$, $\varepsilon_s=5\varepsilon_o$, ($\varepsilon_o=8.85\times10^{-12}Fm^{-1}$), $\sigma_m=7\times10^{-4}Sm^{-1}$, $\sigma_s=5\times10^{-5}Sm^{-1}$ and $\sigma_i=2.0Sm^{-1}$.

each phase of the system, especially the membrane and related cell wall. In the experiments described in this chapter the ionic concentration of the cell suspending media have been kept as low as possible and hence the figures used in the above analysis must be regarded as approximations to the exact values of each parameter. However, they serve to illustrate the mechanisms which control the magnitude of the dielectrophoretic force.

Figure 3.10 shows that at low frequencies (10Hz -10kHz) the collection rate is constant until at around 10kHz the response is observed to increase, reaching a constant higher collection rate at around 100kHz. This can be explained by the examination of eqn. 3.6 which predicts that where $\omega\tau<1$ the magnitude of the dielectrophoretic force is controlled by the difference in the particle and medium conductivity, whereas at frequencies where $\omega\tau>1$ the force is dictated by the difference in the particle and medium permittivities. Substituting the effective conductivity and permittivity of the model bacteria together with those of the suspending medium into eqn. 3.5 shows that τ has a value of around 2×10^{-5}s at frequencies below 1MHz and hence $\omega\tau=1$ at 50kHz. At frequencies below around 1MHz the shelled sphere model of the bacteria predicts the effective conductivity of the cell to be around 0.001 Sm-1, which is greater than that of the suspending medium and hence causes a large collection below 50kHz. Also predicted below 1MHz is an effective cell permittivity of around 2000. Since the difference between the particle and medium permittivity is larger than the difference between the particle and medium conductivity, the dielectrophoretic force increases at frequencies above 50kHz. The change in the dielectrophoretic force at around 50kHz corresponds to the Maxwell-Wagner type relaxation that occurs at the interface between the suspending medium and the outer surface of the bacterial membrane. The decrease in the dielectrophoretic response above 1MHz can also be explained in terms of a Maxwell-Wagner type dispersion. In this case the relaxation occurs at the interface between the inner surface of the membrane and the cytoplasm at approximately 10MHz, and the dielectrophoretic force is seen to reduce in conjunction with the decrease in the effective permittivity of the bacteria. The observation of two interfacial relaxations can explain the peak in collection measured for *B. subtilis* and to a lesser extent in the response of *M. lysodeikticus* protoplasts. However, the separation of these two interfacial relaxations is not usually observed

in dielectric measurements since the conductivity of the suspending medium is normally comparable to the conductivity of the cell cytoplasm and therefore both relaxations occur at similar frequencies. The presence of two interfacial polarisations has previously been reported by Zhang et al (1984) for the case of polystyrene microcapsules filled with potassium chloride solutions suspended in a medium with a lower conductivity than the interior of the capsules.

It is interesting to note, however, that the theoretical collection spectra described above does not predict the peak in the collection observed for all three bacteria in the frequency range 50Hz to 1kHz. Microscope observations reveal this peak to be caused by a combination of increased low-frequency collection, the disruption of pearl chain formation by the slight electrophoretic movement of cells in low-frequency fields and the collection of cells along the length of the electrodes rather than across the inter-electrode gap.

The effects of medium conductivity can also be explained by the examination of eqn. 3.6. For frequencies where $\omega\tau<1$ the term $\omega^2\tau^2/(1+\omega^2\tau^2)$ becomes close to zero, hence eqn 3.6 can be rewritten as

$$\alpha = \varepsilon_o \varepsilon_m \frac{\sigma_p - \sigma_m}{\sigma_p + 2\sigma_m} \qquad 3.7$$

Figure 3.6 shows the effect of increasing the medium conductivity of *micrococcus*. The decrease in collection rate on the addition of sodium chloride can be predicted by eqn. 3.7. The reduction in the low-frequency peak in collection can be explained by the presence of convection currents and low-frequency electrode effects associated with extended electrical double layers in low conductivity solutions.

Figure 3.7 reveals the full relationship between medium conductivity and the dielectrophoretic force. As the conductivity of the medium is increased the effective polarisability, α, decreases until the polarisability, and hence force, becomes zero when the medium conductivity is equal to the particle conductivity. For the case of the medium conductivity being greater than that of the particle, the polarisability becomes negative and the dielectrophoretic force is reversed and

directed away from the regions of high field intensity. The measurements given in figure 3.7 show the conductivity of the particle to be approximately $0.2Sm^{-1}$ since a 20mM NaCl solution suspending medium produces zero collection. It is of interest to note that this conductivity is in excellent agreement with the value of $0.19Sm^{-1}$ obtained by Carstensen et al (1965) from dielectric measurements in the range 10Hz to 10kHz. An effective conductivity of this magnitude was interpreted in terms of a shelled sphere model of the micro-organism consisting of a highly conducting cell wall surrounding a membrane of high resistivity enclosing the cytoplasm. At frequencies lower than that of the Maxwell-Wagner relaxation at the inner surface of the cell, external electric fields are not able to penetrate across the cell membrane into the conducting interior of a viable cell (Pethig and Kell, 1987) and so the overall effective cell conductivity is governed by the electrical properties of the cell wall and membrane. Carstensen et al (1965) concluded that an overall effective conductivity for *M. lysodeikticus* of around $0.2Sm^{-1}$ could be interpreted in terms of the shelled sphere model if a conductivity of $0.9Sm^{-1}$ was assigned to the outer cell wall. This relatively high conductivity was attributed to the presence of mobile counter ions for the fixed charges in the cell wall, an effect noted by Carstensen et al (1965) to be dependent on the conductivity of the suspending medium.

In their analysis of the low-frequency dielectric properties of colloidal particles in electrolytes, Schwan et al (1962) concluded that these properties were related to the particles having an effective surface conductance and capacitance, with the conductance consisting of one frequency dependent and one frequency independent component. The frequency dependent component varied little with changes in suspending medium conductivity, whereas the frequency independent component increased with increasing medium conductivity. With respect to eqn. 3.6 these effects would result in the parameter σ_p increasing and ε_p decreasing with increasing σ_m. This in turn could explain the divergence between experiment and theory in figure 3.7, where the dielectrophoretic force at the higher medium conductivities is larger than predicted using dielectric data.

The domination of the electrical properties of the bacterial cell wall in determining the dielectrophoretic force at low frequencies can be demonstrated by comparing the response of

intact *micrococcus* with its protoplasts, as shown in figure 3.8. Protoplasts are bacteria which have lost their porous, highly conductive, cell wall but still retain the bacterial phospholipid bilayer and membrane protein surface. The dielectric data of Einolf and Carstensen (1969) shows this loss of the cell wall to cause a 40 fold reduction in cell conductivity together with a reduction in volume by a factor of 8. The collection spectrum for protoplasts shows a collection rate of approximately 0.15 mAs^{-1}, after correction for volume. Relative to intact cells a reduction in collection of a factor of 34 is observed, which is comparable to the factor of 40 predicted by dielectric measurement. The presence of a peak in the dielectrophoretic response at around 100kHz to 1MHz for protoplasts confirms the validity of the single shell bacteria model used earlier in this section, which ignored the presence of a cell wall

The protoplast spectrum also reveals information of significance in the low-frequency, 20Hz to 1kHz, range. Figure 3.8 shows no low-frequency peak in collection but a continued increase with decreasing frequency. Microscope observations of protoplast collection reveals a reduction in low-frequency electrode effects, such as convection currents, together with a more definite collection of cells at electrodes rather than in pearl chains at frequencies below 200Hz. As discussed in the next chapter, it is thought that the large low-frequency collection observed for protoplasts is the true shape of a low-frequency collection spectrum rather than the peak observed for intact *micrococcus*, which is an artefact related to electrode and pearl chain effects.

3.7 References

Al-Ameen, T.A.K. (1990) *Theoretical and Practical Aspects of Dielectrophoresis.* University of Wales Ph.D thesis.

Bahaj, A.S. and Bailey, A.G. (1985) The Relationship Between Dielectrophoretic and Impedance Responses of Dielectric Particles Immersed in Aqueous Media. *IEEE Trans. on Industry Applications* **IA-21 5** 1300-1305.

Benguigui, L. and Lin, I.J. (1982) More About the Dielectrophoretic Force. *J. Appl. Phys.* **52** 1141-1143.

Bowden, C.P. and Whittington, P.N. (1986) *The Application of Novel Technologies to Biotechnological Primary Separation.* BIOSEP/SAR6/86. Warren Spring Laboratory, Stevenage, U.K.

Carstensen, E.L., Cox, H.A., Mercer, W.B. and Natale, L.A. (1965) Passive Electrical Properties of Microorganisms, I: Conductivity of *Escherichia Coli* and *Micrococcus Lysodeikticus. Biophys. J.* **5** 289-300.

Carstensen, E.L. (1967) Passive Electrical Properties of Microorganisms, II: Resistance of the Bacterial Membrane. *Biophy. J.* 7 493-503.

Einolf, C.W. and Carstensen, E.L. (1969) Passive Electrical Properties of Microorganisms, IV: Studies of the Protoplasts of *Micrococcus Lysodeikticus. Biophys. J.* **9** 634-643.

Feeley, C.M. and McGovern, F. (1986) Microcomputer-based Measurement of Bubble Dielectrophoresis, *J. Phys. E: Sci. Instrum.* **19** 923-927.

Fricke, H., Schwan, H.P., Li, K. and Bryson, V. (1956) A Dielectric Study of the Low-conductance Surface Membrane of *E. Coli. Nature* **177** 134-135.

George, N. (1986) University of Birmingham Ph.D. Thesis.

Jones, T.B. and Kallio, G.A. (1979) Dielectrophoretic Levitation of Spheres and Shells. *J. Electrostatics* **6** 207-224.

Jones, T.B. and Kraybill, J.P. (1986) Active Feedback-controlled Dielectrophoretic Levitation. *J. Appl. Phys.* **60** 1247-1252.

Kaler, K.V.I.S., Fritz, O.G. and Adamson, R.J. (1988) Dielectrophoretic Velocity Measurements Using Quasi-elastic Light Scattering. *J. Electrostatics* **21** 193-204.

Kaler, K.V.I.S. and Jones, T.B. (1989) Dielectrophoretic Spectra of Single Cells Determined by Feedback Controlled Levitaion. *Biophys. J.* **57** 173-182

Pethig, R. and Kell, D.B. (1987) The Passive Electrical Properties of Biological Systems: Their Significance in Physiology, Biophysics and Biotechnology. *Phys. Med. Biol.* **8** 933-970.

Pohl, H.A. (1951) The Motion and Precipitation of Suspensoids in Divergent Electric Fields. *J. Appl. Phys.* **22** 869-871

Pohl, H.A. and Pethig, R. (1977) Dielectric Measurement Using Non-uniform Electric Fields (Dielectrophoretic) Effects. *J. Phys. E: Sci Instrum.* **10** 190-193.

Pohl, H.A. (1978) *Dielectrophoresis.* Cambridge University Press, Cambridge.

Price, J.A.R. and Pethig, R. (1986) Surface Charge Measurements on *Micrococcus Lysodeikticus* and the Catalytic Implications for Lysozyme. *Biochim. Biophys. Acta* **889** 128-135.

Sauer, F.A. (1985) Interaction Forces Between Microscopic Particles in an External Electromagnetic Field. In *Interactions Between Electromagnetic Fields and Cells* (eds.) Chiabrera, A., Nicolini, C. and Schwan, H.P., Plenum, London.

Schwan, H.P. (1957) Electrical Properties of Tissue and Cell Suspensions. *In Advan. Biol. Med. Phys.* Academic Press, New York.

Schwan, H.P., Schwarz, G. Maczak, J. and Pauly, H. (1962) On the Low-Frequency Dielectric Dispersion of Colloidal Particles in Electrolyte Solutions. *J. Phys. Chem.* **66** 2626-2635.

Stoicheva, N. and Dimitrov, D.S. (1986) Frequency Effects in Protoplast Dielectrophoresis. *Electrophoresis* **7** 339- 341.

Tempest, D.W. (1969) Quantitaive Relationships Between Inorganic Cations and Anionic Polymers in Growing Bacteria *Symp. Gen. Microbiol.* 19 87-111.

Vitkovitch, D. (1966) *Field Analysis.* Van Nostrand, London.

Von Hippel, A.R. (1954) *Dielectrics and Waves.* Wiley, New York.

Zhang, H.Z., Sekine, K., Hanai, T. and Koizumi, N. (1984) Dielectric Approach to Polystyrene Microcapsule Analysis and the Application to the Capsule Permeability to Potassium Chloride. *Colloid and Polymer Sci.* **262** 513-520.

CHAPTER 4

THE LOW-FREQUENCY DIELECTROPHORETIC COLLECTION OF COLLOIDAL SUSPENSIONS AND AN IMPROVED OPTICAL MEASUREMENT SYSTEM

4.1 Introduction

In the previous chapter an optical system for measuring the dielectrophoretic collection rate was described. This system, though capable of providing useful information on the dielectrophoretic response of bacteria, cannot be successfully used to measure larger cell types (also of biotechnological importance) such as yeast or mammalian cells which typically have a diameter of around 10μm. Described in this chapter is an improved optical system capable of measuring particles up to 40μm in diameter. This system employs the same fundamental principle of observing a change in the optical absorbance of a cell suspension as cells are dielectrophoretically collected at a set of electrodes (chapter 3). However, with a redesigned optical sample chamber and the addition of specialised instrumentation a stand-alone dielectrophoresis spectrometer has been constructed.

Among the advantages of the improved system, discussed in detail in section 4.6, is the ability to quantitatively measure the dielectrophoretic response of particles at frequencies as low as 1Hz, at least 1.5 decades lower in frequency than any previously reported study of dielectrophoresis. In this chapter particular attention is shown to the measurement of the

low-frequency dielectrophoretic response of the bacteria *M. lysodeikticus* and two strains of yeast. To verify an observed large low–frequency collection in the frequency range 1Hz to 10kHz as universal to all particles, the collection spectrum of silicon powder was also measured to provide a simple model of a colloidal suspension. To further investigate the effects of medium conductivity on the dielectrophoretic response a defined strain of yeast, NCYC 1110, was studied over a frequency band from 10Hz to 4MHz and for a range of medium conductivities.

4.2 Materials and Methods

4.2.1 Optical Chamber

The test particles were suspended in the optical chamber shown in figure 4.1 and subjected to the non-uniform electric field generated by two castellated electrode arrays placed 1mm apart. The optical absorbance of the particle suspension was monitored by means of a light beam of cross-section 0.9mm x 7mm passing through the middle of the two glass sides of the chamber that separate the electrode arrays. All of the emerging light beam was detected using a large area ($1cm^2$) photodiode. The electrodes were of the same castellated design described in chapter 3. However, in this case the electrodes were based on an 80μm rather than a 40μm grid and were fabricated from 17μm copper clad printed circuit board using standard photolithographic techniques. The circuit board substrate was 'paxolin'. Fibreglass substrates were found to be unsuitable due to the presence of ionisable chemical groups whose negative charge repelled the test particles from the electrode arrays. The interdigitated castellated electrodes were again chosen for their simplicity of design, and because of the high degree of field non-uniformity produced not only within the vicinity of electrode tips but also extending radially into the sample chamber.

On applying a voltage to the electrodes the suspended particles were pulled by the dielectrophoretic force into the plane of the electrode arrays and collected between the interdigitated electrodes. Such removal of particles from the bulk solution was detected as a decrease in the optical absorbance of the suspension and is a measure of the dielectrophoretic

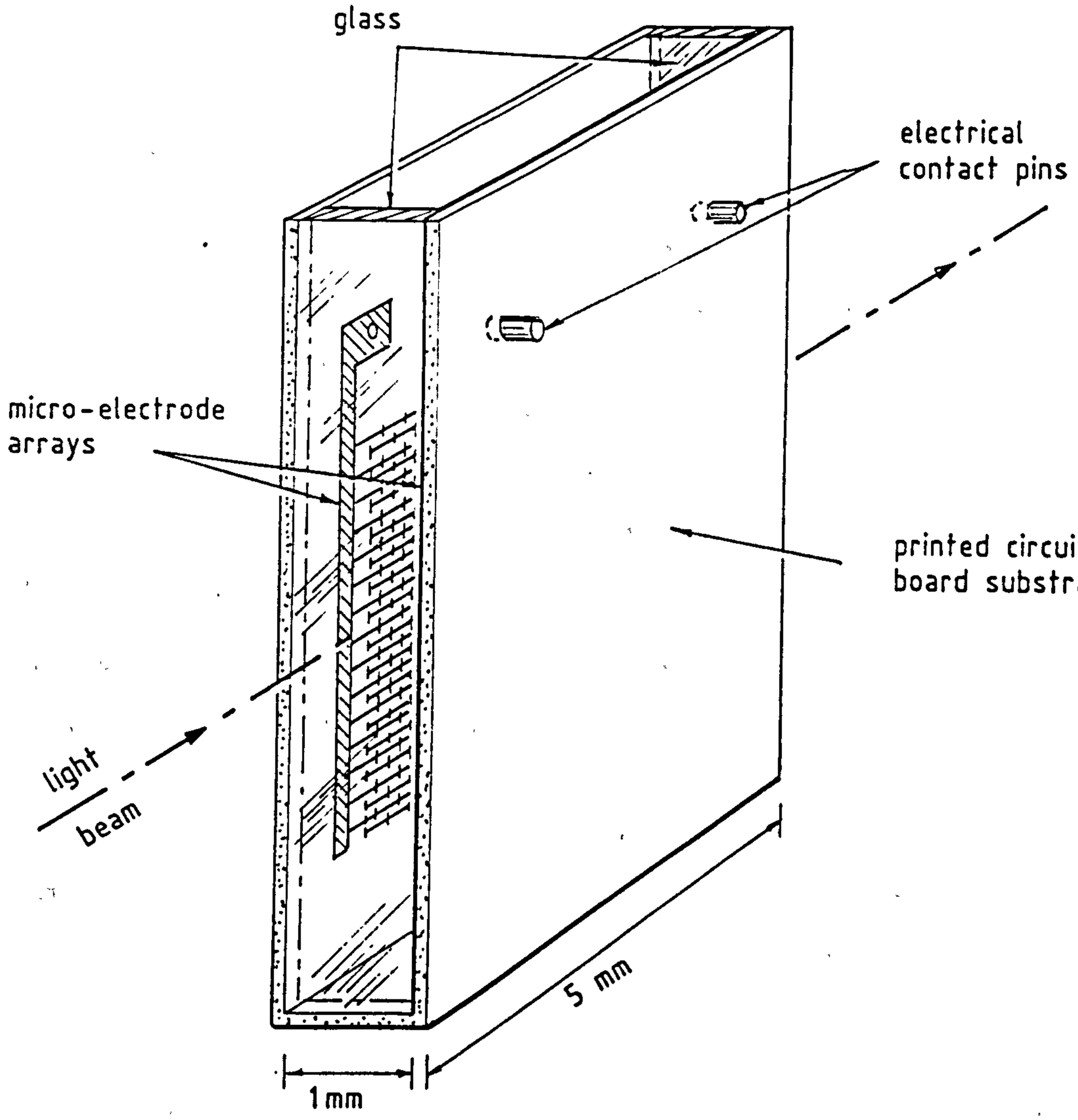

Figure 4.1 Design of the optical sample chamber and micro-electrodes.

collection rate. As the particles arrive in the plane of the electrodes, they collect as long pearl-chains between the interdigitated electrode tips as described in detail in chapter 3.

4.2.2 Instrumentation

The dielectrophoretically induced changes in optical absorbance were detected using a wide bandwidth spectrophotometer, designed to measure small changes in absorbance against a large background absorbance. The overall spectrometer design is shown in Figure 4.2. A light emitting diode (LED), with a peak wavelength of 635nm, provides a narrow beam of light focused on the sample chamber, and the transmitted light is detected using a large area photodiode. The voltage generated by the photodiode was amplified by a factor of 10^5 to produce a suitable signal for further processing.

To reduce heating effects in the photodiode, caused by optically induced current flow, the LED was switched on and off at a rate of 10kHz using a 20% duty cycle square wave. The conversion of the alternating output of the photodiode to a d.c. voltage was accomplished using a sample-and-hold amplifier and filter network. Synchronous timing signals for the light source and sample-and-hold amplifier were derived from a Read Only Memory addressed by a high speed counter. The voltage from this stage of processing is a measure of the optical transmittance of the particle suspension. To obtain an absorbance measurement signal a negative log function has to be performed on the transmittance signal, and a dedicated logarithmic amplifier (Intersil ICL8048E) was used for this because of its stability to environmental temperature changes. Small changes in the absorbance signal due to particle collection were detected by measuring a deviation from the initial bulk suspension absorbance. To do this the absorbance signal was split in two, one part going to the positive input of a difference amplifier while the other was fed, via a digital voltage sampler, to the negative input of the amplifier. The digital voltage sampler converted the signal into a binary number which was stored in a data latch and read continuously by an analogue-to-digital converter to give an output voltage equal to the input with no drift with time. By sampling the absorbance signal before a dielectrophoretic collection measurement was taken, a zero voltage reference was obtained and

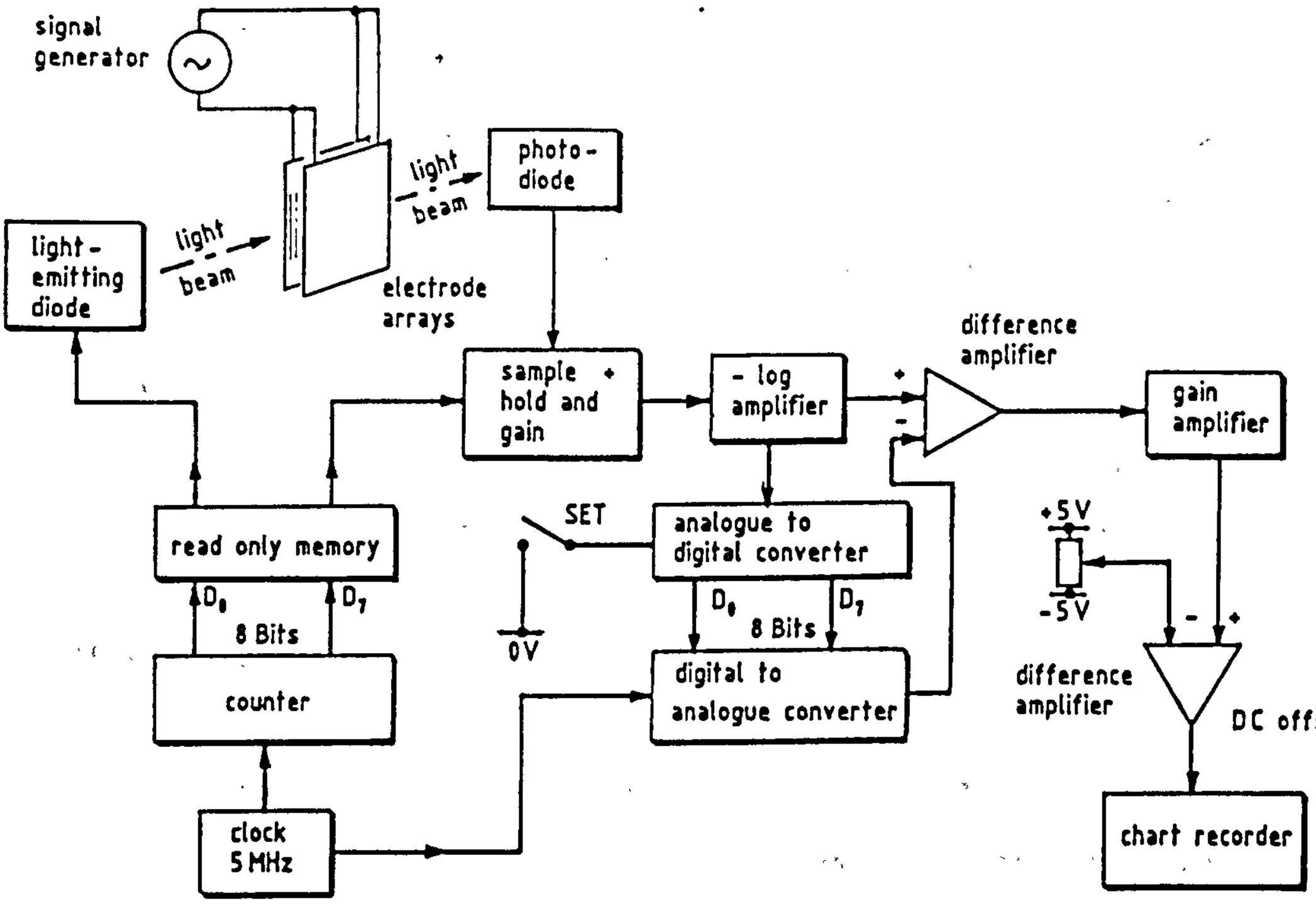

Figure 4.2 Block diagram of the dielectrophoresis spectrometer.

any change in absorbance as particles were collected appeared as a variation about this reference. This variation was amplified by known amounts (x2,x5,x10,x20) to give a signal between 0 and 1.0 volts. The final stage of the circuit is a d.c. level shifter to enable the final signal to be displayed on a chart recorder (Servogor 120).

4.2.3 Cell Suspensions

The particles used in this work were the bacteria *Micrococcus lysodeikticus* (Sigma, U.K.), dried yeast (Boots Ltd, U.K.), silicon powder (Koch Light Laboratories Ltd, U.K.) and NCYC 1110 yeast (National Collection of Yeast Cultures, U.K.). The *M. lysodeikticus* and NCYC 1110 yeast were grown for 24 hours at 37°C in 100ml of Oxoid Nutrient Broth (Oxoid, U.K.) using a standard shake flask method, while for NCYC 1110 yeast the broth was supplemented with $10gl^{-1}$ of glucose. Dried yeast was rehydrated for 1hr in 150mM NaCl and the silicon powder was filtered through Whatman 1 qualitative filter paper (Whatman U.K.) to remove particles larger than 40μm in diameter. All particle types were washed 3 times and resuspended in 280mM mannitol, equivalent in osmotic pressure to 150mM NaCl. The concentration of suspended particles was adjusted to give an initial absorbance of 1.0 at 635nm in a 1cm pathlength cuvette. The corresponding concentrations were $4.5x10^7$, $2.2x10^7$ and $2.8x10^7$ particles ml^{-1} for *M. lysodeikticus*, yeast and silicon powder respectively. At these concentrations the optical absorbance varied linearly with concentration (i.e. Beer's Law was obeyed) although for yeast suspensions a slightly higher concentration would take the absorbance into a non-linear response. Apart from the linearity of response an added advantage of operating within the Beer's Law regime was that effects associated with multiple light scattering were minimised. The optical chamber was rinsed with deionised water and refilled with a fresh particle suspension between each measurement.

Measurements of particle surface charge were made using a Malvern Instruments Zetasizer II kindly made available at Warren Spring Laboratory, Stevenage. The influence of electrode polarisation effects in modifying the electric field distribution between the electrodes was determined by measuring the effective conductivity of 280mM mannitol. For this measurement

one set of the electrode pair in the optical chamber was used and conductance values were obtained using a Hewlett Packard HP4192A Impedance Analyser.

4.3 Dielectrophoresis of Cell Suspensions

4.3.1 *Micrococcus lysodeikticus*

The dielectrophoretic collection spectrum of grown *M. lysodeikticus*, measured using the improved optical technique, is shown in figure 4.3. The response exhibited a near constant collection rate in the frequency range from 100Hz to 20kHz. Above 20kHz a gradual increase in collection was observed until at 200kHz a maximum in collection rate occurred. From 200kHz to 4MHz the dielectrophoretic response was seen to decrease in magnitude until at 4MHz virtually no collection occurred.

Also observed in figure 4.3 was a large low-frequency collection in the frequency range 1Hz to 100Hz which decreased as the applied field frequency was increased from 1Hz to reach a minimum at 70Hz. Above 70Hz the collection increased to a constant rate at 100Hz and above.

4.3.2 Yeast

Figure 4.4 shows the dielectrophoretic collection spectrum of yeast. As in the case of *M. lysodeikticus* a large low-frequency collection was observed at 1Hz which also decreased with increasing field frequency. For frequencies in the range 200Hz to 2kHz a constant collection rate was observed. Above 2kHz the dielectrophoretic response increased until a peak in collection was observed at 40kHz. At frequencies above 40kHz the magnitude of the collection decreased and appeared to approach a second region of constant collection at approximately 10MHz, which was beyond the measurement range of the optical system used here.

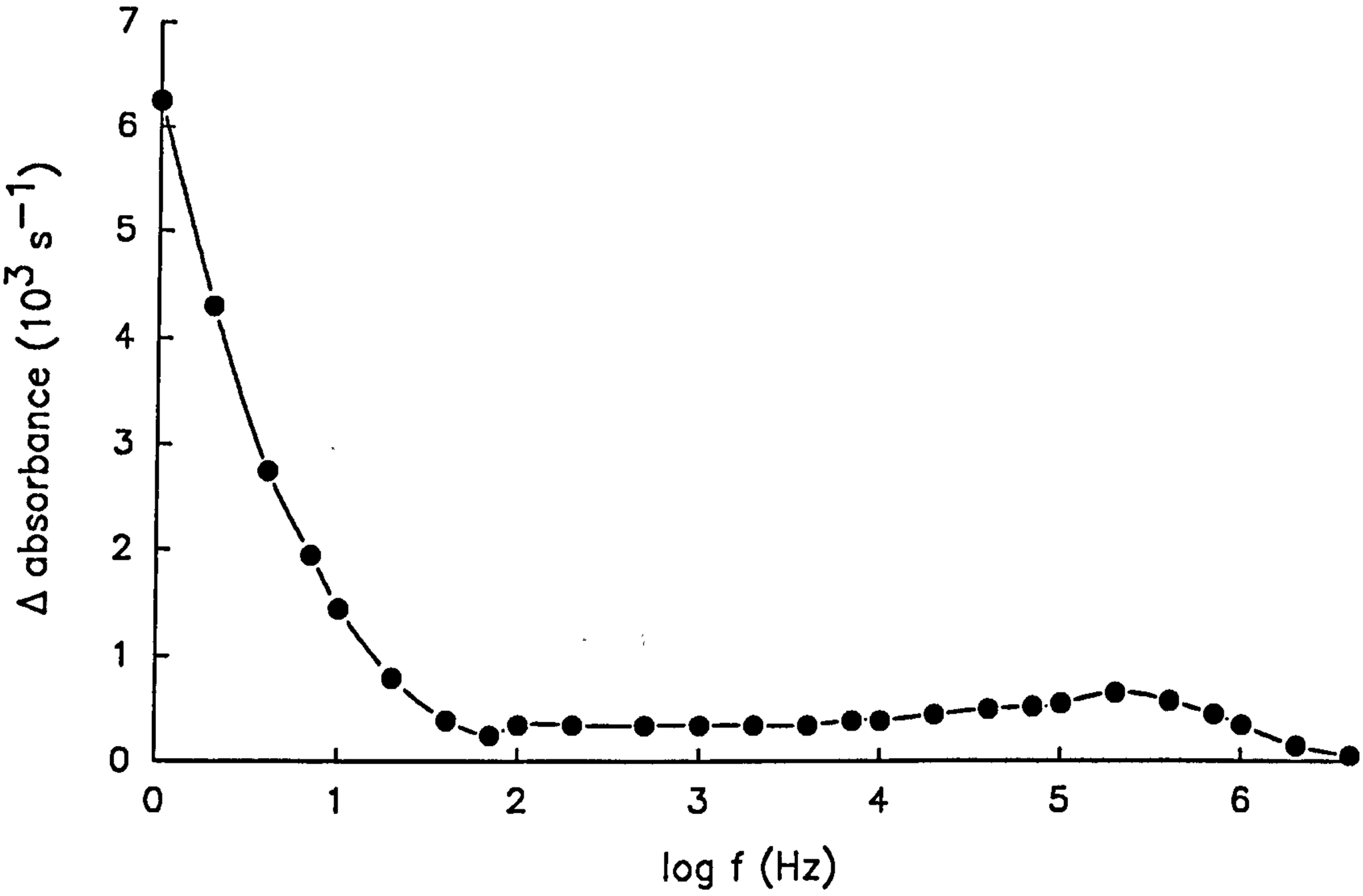

Figure 4.3 The dielectrophoretic collection spectrum for *M. lysodeikticus* suspended in 280mM mannitol solution.

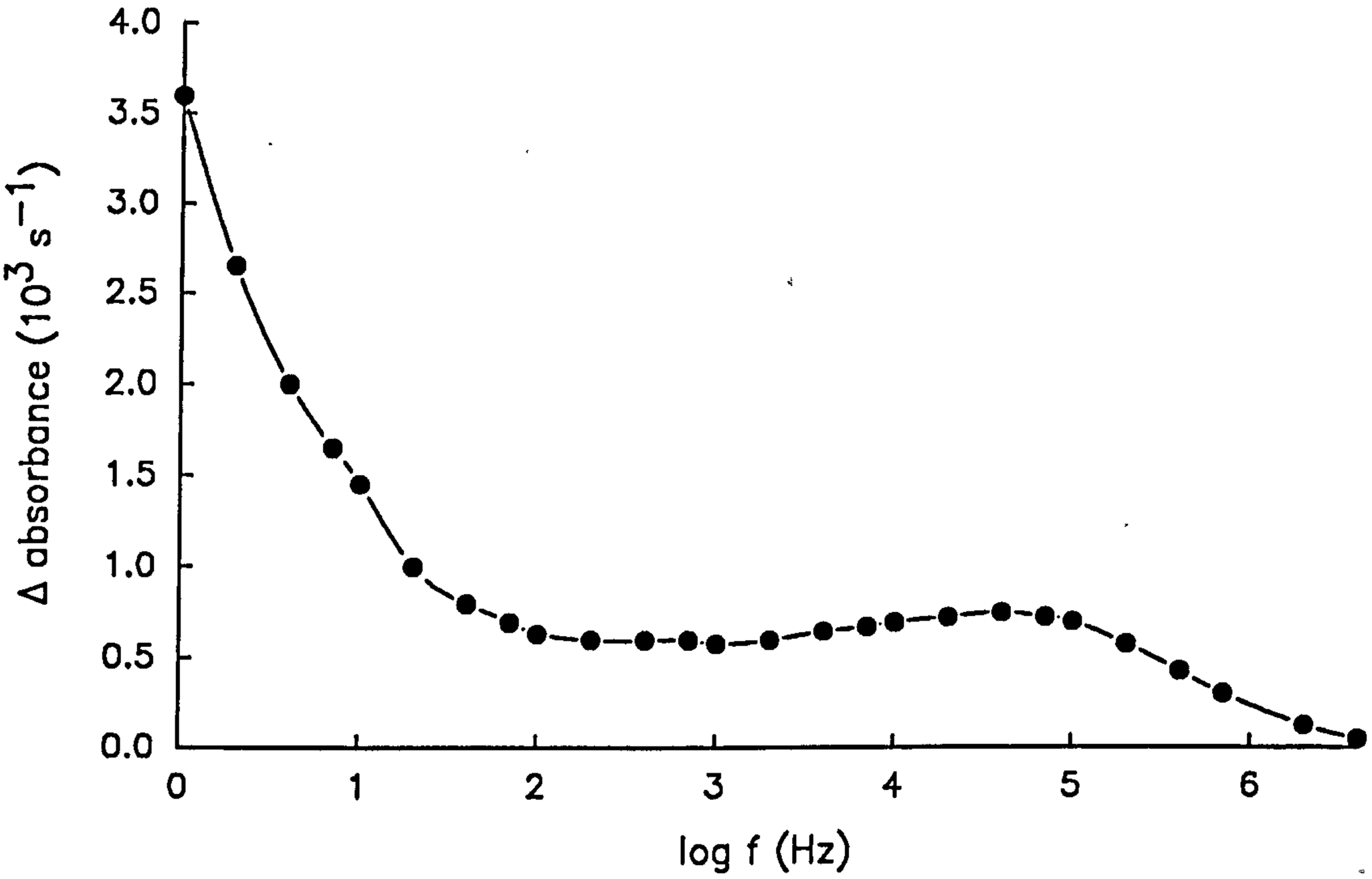

Figure 4.4 The dielectrophoretic response of yeast suspended in 280mM mannitol solution.

4.4 The Dielectrophoresis of Silicon Powder

Figure 4.5 shows the dielectrophoretic response of silicon powder. The response was similar in form to that of *M. lysodeikticus* and yeast. However, in this case the large low-frequency collection decreased linearly with the logarithm of the applied field frequency. At 1kHz a minimum in collection was observed and was followed, from 2kHz to 20kHz, by a region of constant collection rate. Above 20kHz the collection increased to a slight peak at approximately 50kHz before reducing in magnitude to virtually zero at 4MHz.

4.5 Further Investigation of the Effects of Medium Conductivity on the Dielectrophoretic Response

The dielectrophoretic response curves of NCYC 1110 yeast suspended in 0, 0.5, 1.0 and 2.0mM NaCl (equivalent to medium conductivities of 0, 0.005, 0.01, 0.02Sm^{-1} respectively) with 280mM Mannitol are shown in figure 4.6. The collection spectrum for NCYC 1110 suspended in mannitol showed the familiar characteristics of a large low-frequency collection which reduced with increasing field frequency until approximately 200Hz, above which a region of constant collection was observed. For frequencies above 50kHz the collection rate increased to reach a peak at around 100kHz before decreasing to approach a second region of constant collection out of the range of the current measurement system at frequencies above 4MHz. The dielectrophoretic responses of cells suspended in media containing NaCl were severely reduced in magnitude across the frequency range 1Hz to 100kHz. The extent of this depression in response was enough to cause the dielectrophoretic force to become negative in the region from 200Hz to 50kHz for 0.5mM NaCl and up to 300kHz for 2.0mM NaCl. The enhanced low-frequency collection from 1Hz to 100Hz observed in all particles studied in this chapter was seen to extend to a higher frequency as the medium conductivity was increased having effects as high in frequency as 10kHz for the case of 0.5mM NaCl and 20kHz for 1.0mM NaCl. At frequencies above 10kHz the collection, in general, continued at a constant, negative, rate before

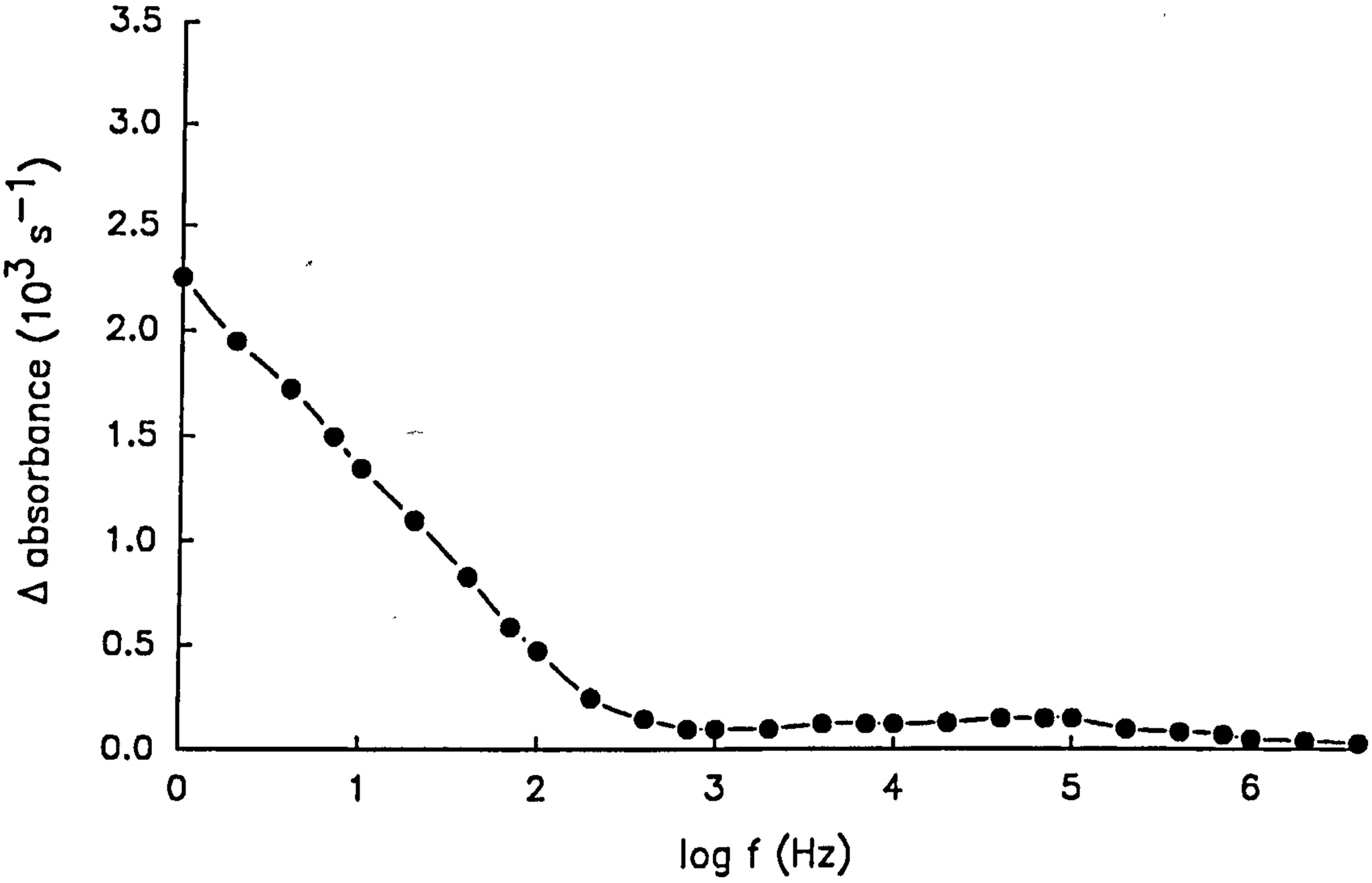

Figure 4.5 The dielectrophoretic collection spectrum of silicon powder suspended in 280mM mannitol solution.

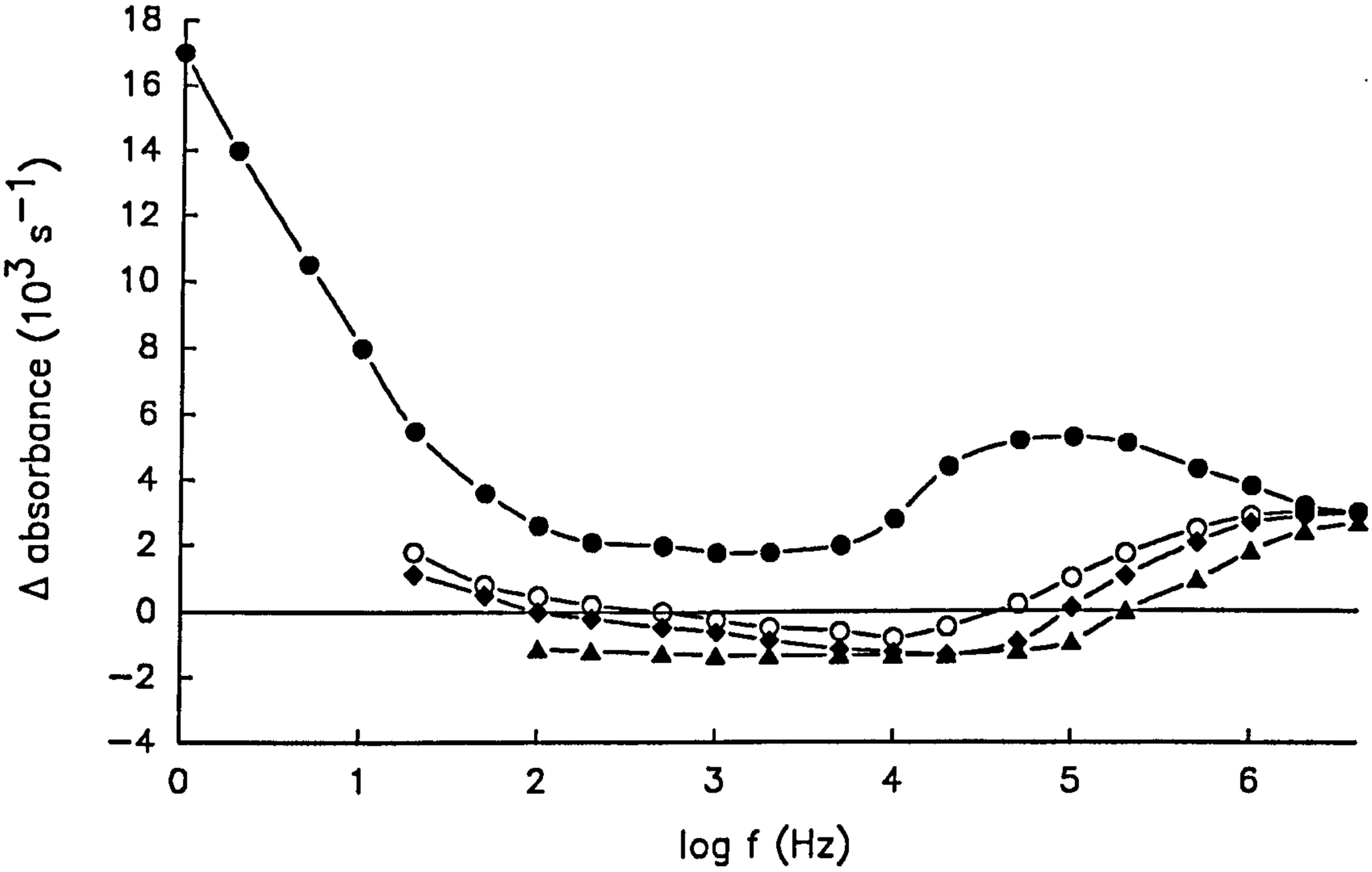

Figure 4.6 The Frequency dependence of the dielectrophoretic collection rate of NCYC 1110 yeast suspended in 280mM mannitol (●), mannitol + 0.5mM NaCl (O), mannitol + 1.0mM NaCl (◆) and mannitol + 2.0mM NaCl (▲).

increasing to become positive and in all cases tended to approach a region of constant, positive, collection at approximately 4MHz and above.

4.6 Discussion

The design of the optical chamber shown in figure 4.1 has been chosen for a number of reasons. Firstly, by positioning the field-producing-electrode arrays at the sides of the chamber and drawing particles onto the surfaces of the chamber, out of the measuring light beam, allows a measurement of the true dielectrophoretic response to be made on any particle suspension in the chamber. A major disadvantage of the original measurement system (chapter 3) was that the measuring light beam passed through the castellated electrode arrays. Hence, when studying particles of diameters greater than a few microns the pearl chain formations produced would soon fill the inter-electrode spacing and distort the measured collection rate (typically 10 yeast cells, diameter 8μm, would bridge the inter-electrode spacing). In the improved system the light beam passes through the bulk sample solution and does not pass near the electrode arrays that cause cells to be drawn from the bulk solution to collect in chains about them. A second advantage of measuring bulk solution absorbance is the removal of errors due to the observed frequency dependence of pearl chain formations. Figure 4.7 shows a series of photographs of the collection of *M. lysodeikticus* 60 second after the application of 10Hz, 1kHz and 100kHz electric fields. The 100kHz collection shows the bacteria collecting in long chains between the electrode tips as described in chapter 3. However, at 1kHz the chain formations are less prominent and cells are observed to collect along the length of the electrode as well as across the inter-electrode spacing. The tendency for cells to collect along the electrodes at lower frequencies is shown to a greater degree in figure 4.7(a) where at 10Hz cells are seen to collect entirely along the electrodes with no pearl chain formations visible across the inter-electrode spacing. The absence of pearl chains at low frequencies can be explained by the presence of a degree of 'electrophoretic' movement where cells experience a force towards one electrode during the first half cycle of the low-frequency sinusoidal field which is reversed during the next half cycle, causing the particle to oscillate about an average position. This average position

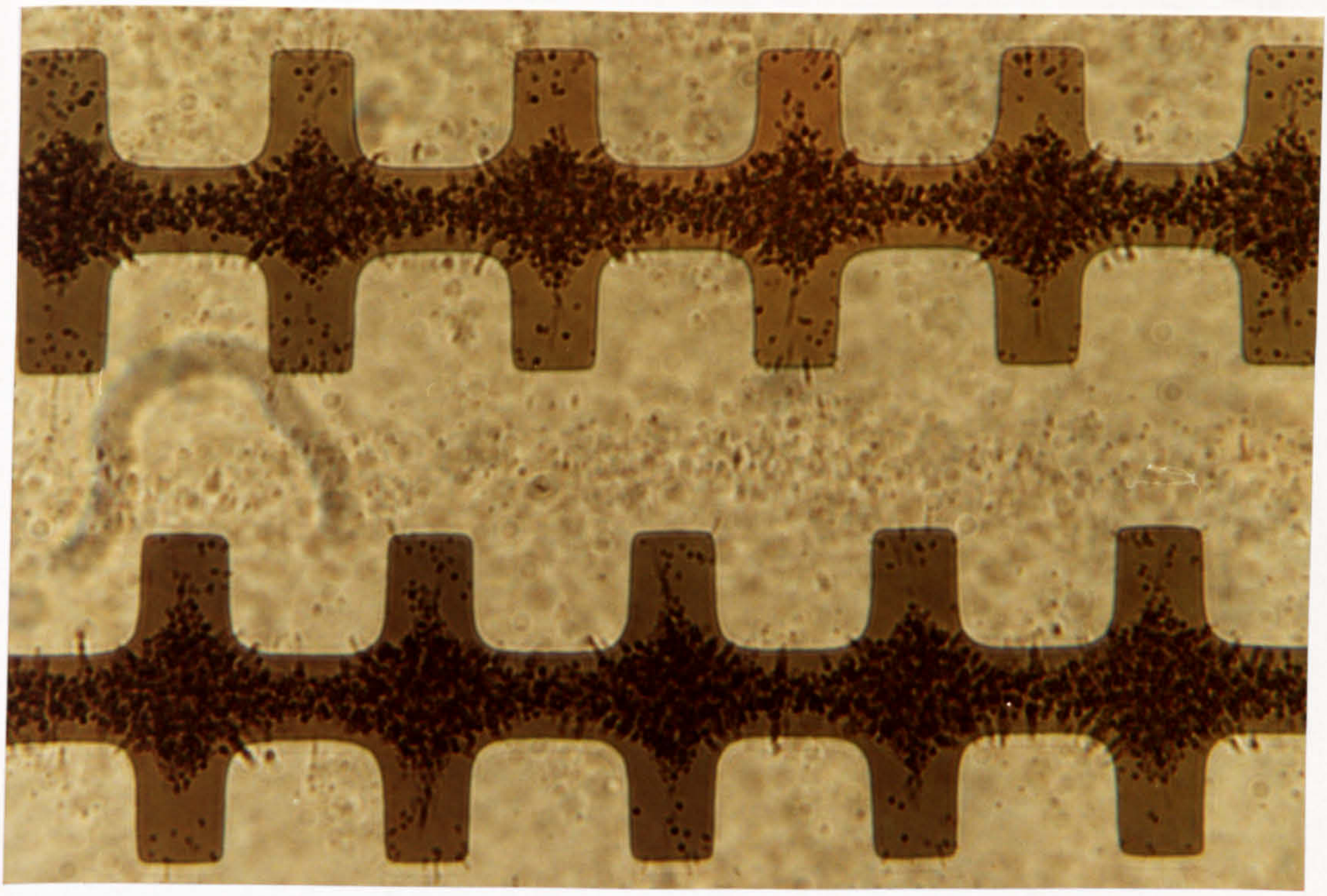

Figure 4.7(a) Microscope magnification (x130) of the micro-electrode configuration and a suspension of *M. lysodeikticus* in 280mM mannitol solution 60 seconds after the application of a 10Hz sinusoidal signal.

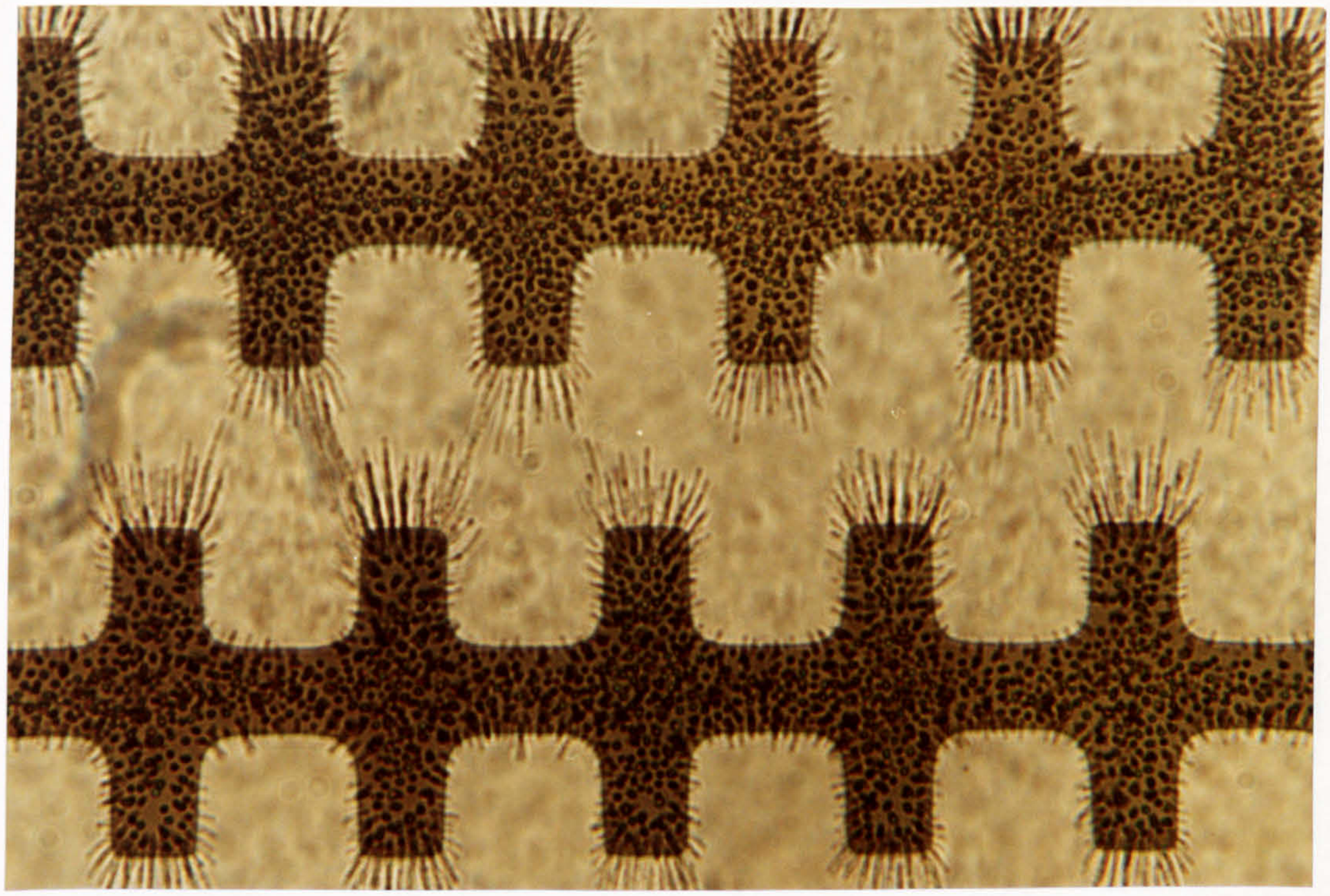

Figure 4.7(b) 60 seconds after the application of a 1kHz sinusoidal signal.

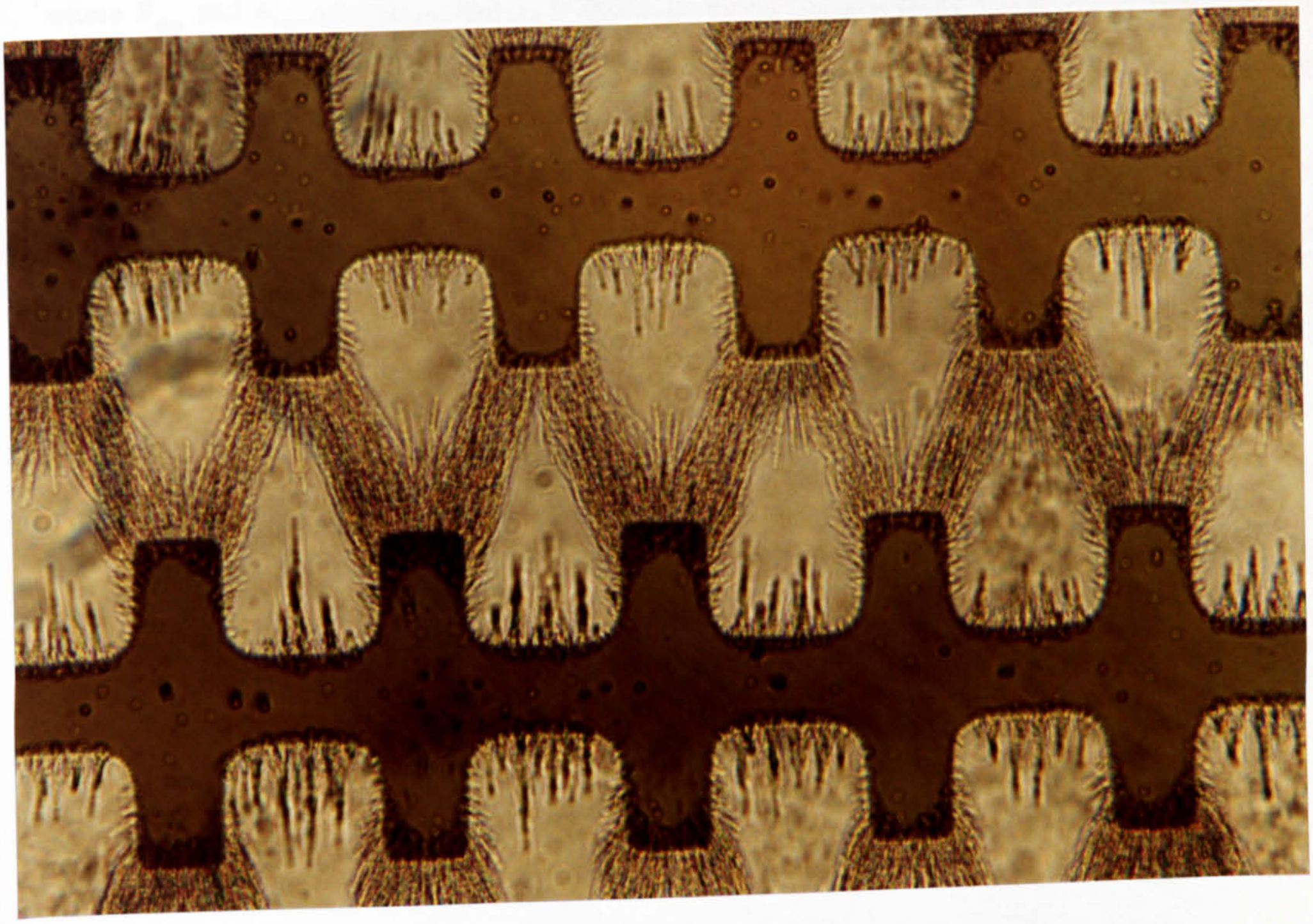

Figure 4.7(c) 60 seconds after the application of a 100kHz sinusoidal signal.

moves towards the collecting electrodes due to the dielectrophoretic force on the particle such that the total force experienced by the particle can be given as

$$F_{total} = F_{dp} + F_{ep}$$

where F_{dp} and F_{ep} are the vector dielectrophoretic and electrophoretic forces respectively.

The effects of pearl chain formation on the measured dielectrophoretic force can be seen by comparing the response of *Micrococcus lysodeikticus* using the original and improved measuring systems (figures 3.5 and 4.3) as shown in figure 4.8. At 200kHz the improved system shows a large peak in collection whereas the pearl chain formations observed in the original system mask this collection, allowing the detection of only a slight increase in collection from 5kHz to 1MHz. At frequencies below 500Hz a second factor effects the measured collection rate, namely the presence of convection currents due to the heating effects of the high field strengths around the tips of the electrodes. These convection currents help to artificially amplify the collection at frequencies below 500Hz by drawing cells onto the electrodes. However, at frequencies below 100Hz the convection currents become strong enough to severely disrupt the collection of cells causing a decreased collection and giving the overall impression of a low-frequency peak in collection at around 100Hz. In the improved system the errors due to both pearl chain formations and heating effects are reduced. The use of electrode arrays with larger electrode spacing and greater depth (17μm), together with the increased sample volume, allow heating effects to be minimised and to occur about the electrode tips out of the measuring light beam. The effects of pearl chain formations are minimised by placing the electrodes out of the measuring light beam since the majority of the errors in the original system were due to chain formation across the inter-electrode spacing.

A typical temporal change in optical absorbance of a *M. lysodeikticus* suspension, as particles are dielectrophoretically collected, is shown in figure 4.9. On application of a 20V peak-to-peak 10Hz sinusoidal voltage to the electrode arrays an initially sharp, linear, decrease in absorbance occurs. This is attributed to the rapid collection of particles close to the electrodes. As these

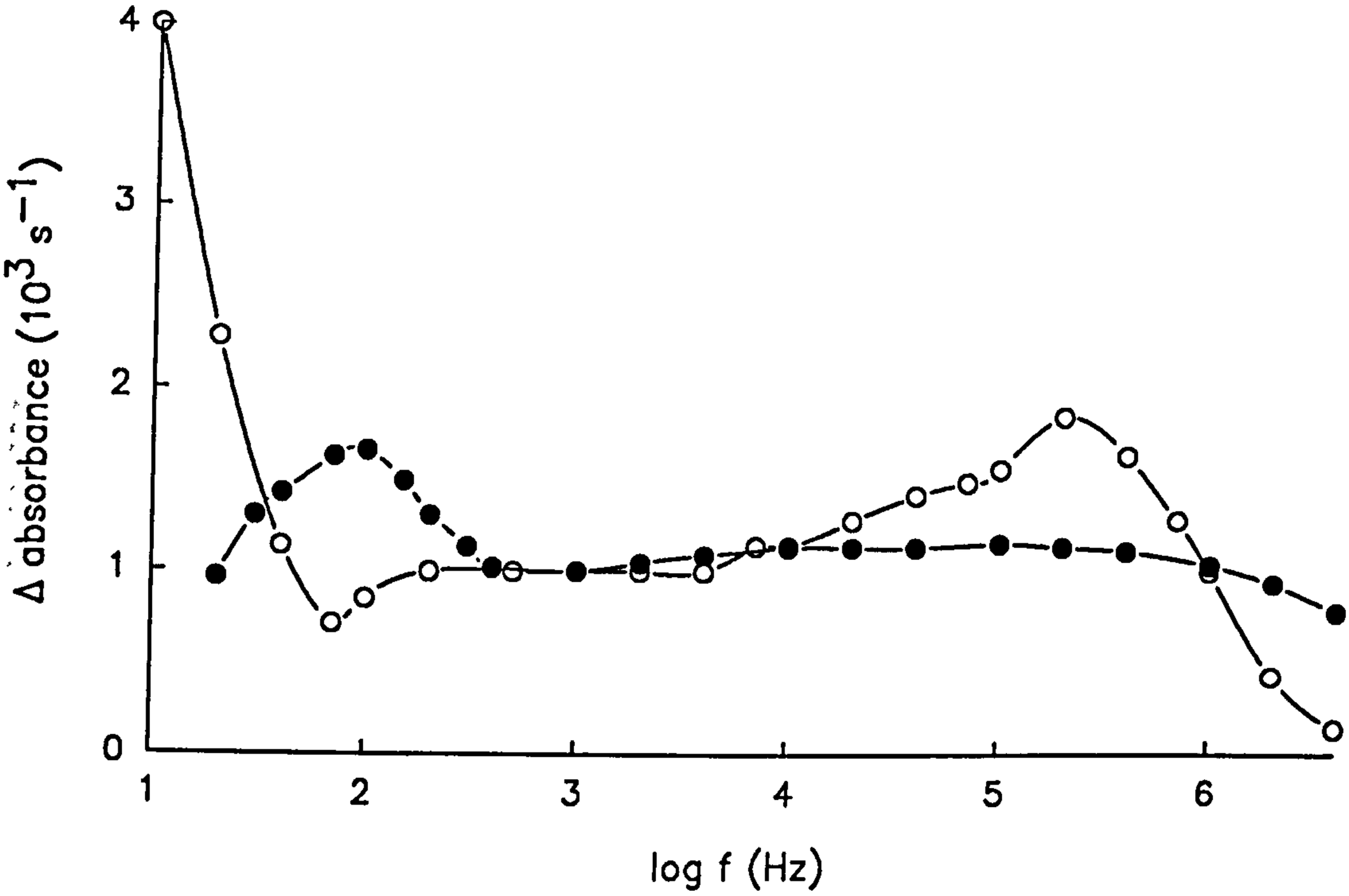

Figure 4.8 A comparison of the dielectrophoretic collection spectrum of *M. lysodeikticus* measured using the optical cell described in chapter 3 (●) and the improved optical cell described in section 4.2 (O).

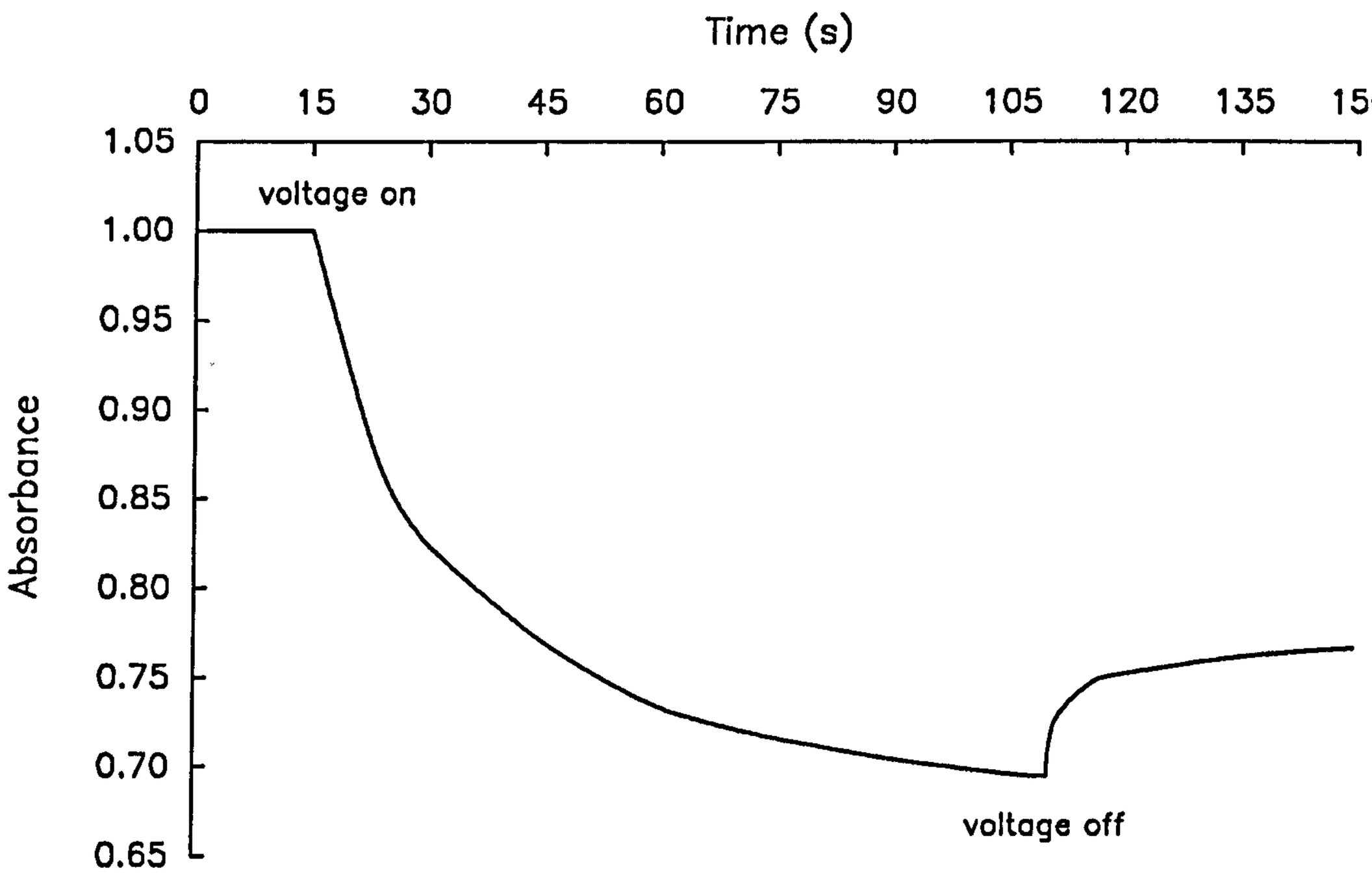

Figure 4.9 The temporal variation of the optical absorbance of *M. lysodeikticus* suspended in 280mM mannitol solution on the application and removal of a 10Hz 20 V peak-peak sinusoidal signal.

particles are collected particles further away are also being attracted to the electrodes, but at a slower rate since the dielectrophoretic force weakens with distance into the chamber. These particles experience a stronger force as they approach the electrodes and, in turn, are collected. This gradual removal of particles from the bulk solution gives rise to the decrease in the rate of change in optical absorbance that occurs within 10 to 15 seconds after the application of the a.c. field. As the particles collect at the electrodes the electric field distribution across the bulk medium can be expected to be modified, depending on the effective conductivity of the particles. By taking measurements of the initial linear decrease in optical absorbance such an effect will not influence the data. Also the particles initially collect in the plane of the 17μm deep electrodes within the castellations so that they do not obstruct the light beam to any great extent and contribute to the overall observed solution absorbance. On removal of the a.c. field the negative surface charge on the particles causes them to be electrostatically repelled from each other, so that they quickly move away from the electrodes. Further dispersion of the particles into the bulk solution occurs as a result of diffusion. The initial sharp increase in absorbance, shown in figure 4.9, when the a.c. field is removed reflects the electrostatic repulsion between particles, whilst the later, more gradual, increase in absorbance corresponds to the diffusion of the particles back into the bulk solution.

The dielectrophoretic collection spectra of *M. lysodeikticus*, yeast and silicon powder shown in figures 4.3, 4.4 and 4.5 are based on the change in absorbance over the first 15 seconds after the application of a 16V peak-to-peak sinusoidal voltage to the electrodes. All three collection spectra share a similar characteristic, namely the presence of a large low-frequency dielectrophoretic response that increases steadily as the frequency is reduced. The spectrum for each particle type also exhibits a plateau from around 100Hz to 100KHz, but there are differences in the way the responses diminish in amplitude above 100kHz. The degree to which the plateau regions extend to lower frequencies differs for the three particle types, and there are also differences in the nature of the large low-frequency responses. The dielectrophoretic collection spectrum obtained for *M. lysodeikticus* is in good agreement with that reported in chapter 3 for the frequency range 100Hz to 4MHz.

The results shown in figures 4.3, 4.4 and 4.5 are based on inspection of the changes in optical density of the colloidal suspensions and do not in themselves provide a measure of the effective polarisabilities of the test particles. From eqn. 2.16, for similar non-uniform fields, the dielectrophoretic force (related directly to the collection rates shown in figures 4.3, 4.4 and 4.5) is proportional to the product of the polarisability and volume of the particle. *Micrococcus* typically has dimensions of 0.5μm x 2.0μm, whilst the yeast cells studied here were of average diameter 8.0μm. This represents a volume difference of around 680 so that the rates of change of absorbance at 1KHz ($3.4\times10^{-4}s^{-1}$ and $5.7\times10^{-4}s^{-1}$, for *Micrococcus* and yeast respectively) indicate that the effective polarisability of *M. lysodeikticus* is about 400 times greater than that of the yeast studied here. This difference can result from the *micrococcus* having a more conductive outer surface. The silicon particles were of average diameter 40μm, so that their collection rate at 1kHz ($0.7\times10^{-4}s^{-1}$) implies that their effective polarisability at this frequency is smaller than that of *micrococcus* by a factor of 4.2×10^5.

An alternative approach to this analysis is to use Beer's law and directly relate the reduction in absorbance to the number of particles being collected. From Beer's law the absorbance A is given by

$$A = C \varepsilon \lambda$$

where C is the absorbant concentration, ε is the extinction coefficient and λ is the optical pathlength. From absorbance measurements the effective extinction coefficients for *micrococcus*, yeast and silicon are 2.22×10^{-8}, 4.54×10^{-8} and 3.57×10^{-6} cm^2 $particle^{-1}$ respectively. From the above stated changes in absorbance for a 1kHz electric field the associated particle collection rates (normalised to the initial *micrococcus* concentration) are 3.06×10^4 , 5.13×10^4 and 6.3×10^3 particles s^{-1} for *micrococcus*, yeast and silicon respectively. Taking into account the volume differences outlined above, these results show that the polarisability of *micrococcus* is larger than that of yeast and silicon powder by a factor of 408 and 4.1×10^5 respectively.

In chapter 2 the following general expression for the magnitude of the dielectrophoretic force was derived (Pohl, 1978) as

$$F = \frac{1}{2} v \varepsilon_o \varepsilon_p \frac{\varepsilon_p - \varepsilon_m}{\varepsilon_p + 2\varepsilon_m} \nabla |E|^2 \qquad 4.1$$

This formula was extended in chapter 3 to introduce the relationship between the frequency dependence of the dielectrophoretic force and the dielectric and conductometric properties of both the medium and suspended particles, eqn. 4.2.

$$\alpha = \varepsilon_o \varepsilon_m \left[\frac{\omega^2 \tau^2}{1 + \omega^2 \tau^2} \left(\frac{\varepsilon_p - \varepsilon_m}{\varepsilon_p + 2\varepsilon_m} \right) + \frac{1}{1 + \omega^2 \tau^2} \left(\frac{\sigma_p - \sigma_m}{\sigma_p + 2\sigma_m} \right) \right] \qquad 4.2$$

This equation predicts that for $\sigma_p > \sigma_m$ and $\omega\tau > 1$ the dielectrophoretic force will be positive (directed towards the regions of high field non-uniformity) and its magnitude dictated by the conductivities of the medium and particle. For the case of $\omega\tau > 1$ the force is a function of medium and particle permittivity. Further analysis of eqn. 4.2 using a single shell model of a bacteria arrived at the conclusion that equation 4.2 could be used to predict the slight peak in collection between 100kHz and 1MHz and was, in general, valid for frequencies greater than 1kHz. However, eqn. 4.2 cannot predict the large low-frequency response observed at frequencies below 1kHz for all particles studied in this chapter. (This low-frequency response was also visible in the response of *micrococcus* protoplasts studied in chapter 3, but was masked by pearl chain and heating effects for intact bacteria when using the original optical system).

An effect not included in eqn. 4.2 is that which could arise from electrostatic interactions between the charged particles and the electrodes. Most particles carry a net negative surface charge when in aqueous solution and for *M. lysodeikticus* this has been measured as $-1.5\mu Ccm^{-2}$ (Price and Pethig, 1986), while for silicon powder a value of $-0.3\mu Ccm^{-2}$ was obtained. If d.c. fields were applied then, as discussed previously, the negatively charged particles would undergo electrophoresis, moving towards the positive electrodes. At low frequencies, such electrophoretic forces are superimposed on the dielectrophoretic ones and this can be observed using an optical microscope and measured directly with the spectrometer. An example of this is shown in figure 4.10. Here the oscillatory pattern superimposed on the absorbance decay represents the low-frequency electrophoretic motion of the *micrococci*. This process can be theoretically

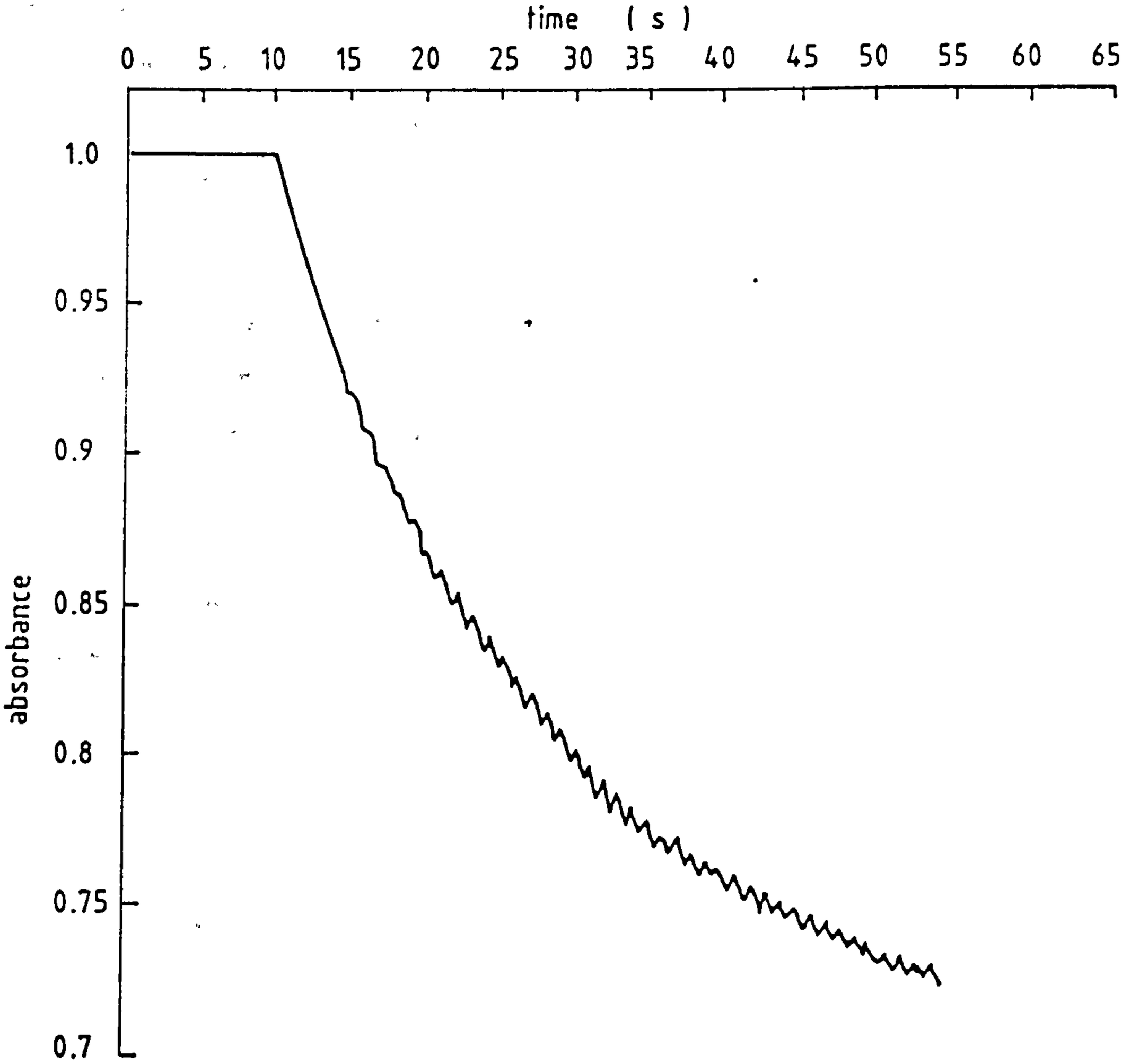

Figure 4.10 The temporal variation in the optical absorbance of *M. lysodeikticus* suspended in 280mM mannitol solution on the application of a 10V peak-peak 1Hz sinusoidal voltage.

analysed by considering the electrode array in the form of fixed point charges at the electrode tips, and representing the test colloidal particle as a mobile point charge. A simple analysis of this demonstrates that the low-frequency electrophoretic response enhances the dielectrophoretic effect by driving the particles nearer to the electrodes.

Another effect influencing the low-frequency response and not included in eqn. 4.2, could be that associated with particle surface charge and the related low-frequency dielectric dispersion. Schwarz (1962) presented a theory to describe the large dispersions observed for porous charged particles, for which relative permittivities as high as 10^6 have been observed. This theory was extended by Einolf and Carstensen (1971) and later modified by Dukhin (1971). Einolf and Carstensen presented eqn. 4.3 for the effective complex conductivity of a particle with a uniform surface charge, implying that the observed 'particle' was in fact the particle plus the region outside the particle affected by the surface charge;

$$K_p = \sigma_p + j\omega\varepsilon_o\varepsilon_p + j\omega\varepsilon_o \frac{\Delta\varepsilon_p}{1+j\omega\tau_i} + h \qquad 4.3$$

$$\Delta\varepsilon_p = \frac{q^2 a N_i}{\varepsilon_o kT} \qquad \tau_i = \left(\frac{a^2}{2\mu kT}\right)\frac{1}{M}$$

$$h = \frac{\sigma_m\varepsilon_p - \sigma_p\varepsilon_m + \sigma_m\left(\dfrac{\Delta\varepsilon_p}{1+j\omega\tau_i}\right)}{\varepsilon_m + \left(\dfrac{\sigma_m\tau_i}{\varepsilon_o}\right) + j\omega\tau_i\varepsilon_m}$$

N_i is the counter-ion concentration and μ is the effective ionic mobility at the particle surface with M being the Dukhin factor and 'a' the particle radius. M is given as

$$M = \frac{2 n_b a}{n_o \lambda_D} + 1$$

where n_b and n_o represent the equilibrium density of the bound counter-ions and the total counter-ion density, respectively, with λ_D being the Debye screening length (Dukhin, 1971).

As predicted by eqn. 4.2 the dielectrophoretic force at low frequencies ($\omega\tau>1$) is dictated solely by the particle and medium conductivity. By solving eqn. 4.3 the effective particle conductivity is given (Al-Ameen, 1990) as eqn. 4.4;

$$\sigma_p' = \sigma_p + \frac{\varepsilon_o \omega^2 \tau_i \Delta\varepsilon_p}{1+\omega^2\tau_i^2} + h' \qquad 4.4$$

$$h' = \frac{\left(\frac{\varepsilon_m}{\sigma_m}+\frac{\tau_i}{\varepsilon_o}\right)\left(\varepsilon_p - \frac{\sigma_p\varepsilon_m}{\sigma_m}+\frac{\Delta\varepsilon_p}{1+\omega^2\tau_i^2}\right) - \frac{\varepsilon_m\omega^2\tau_i^2\Delta\varepsilon_p}{\sigma_m(1+\omega^2\tau_i^2)}}{\left(\frac{\varepsilon_m}{\sigma_m}+\frac{\tau_i}{\varepsilon_o}\right)^2 + \left(\frac{\omega\tau_i\varepsilon_m}{\sigma_m}\right)^2}$$

The evaluation of eqn. 4.4 for both intact *M. lysodeikticus* and its protoplasts, from the data of Einolf and Carstensen (1969), shows that the surface charge related conductivities increase the particle conductivity by 10^{-4} - 10^{-3} Sm^{-1} at 1Hz. In the case of intact *M. lysodeikticus* this is a negligible amount compared to the measured conductivity of 0.04 Sm^{-1}. It can thus be concluded that the most significant contribution to the large low-frequency collection is an effect such as the electrophoretic movement observed at low frequencies. However, for very slightly conducting particles such as protoplasts, animal cells and, in our case, silicon powder (σ_p approx. 10^{-4} Sm^{-1}) this increase in conductivity is of the order of the conductivity of the suspending medium used in dielectrophoresis experiments (10^{-4} Sm^{-1}). This in turn could determine whether the effective dielectrophoretic force was positive or negative at low frequencies, since a negative effect occurs for the situation where the effective polarisability of the particle is less than that of the suspending medium.

Another factor which must be taken into account, and which will act equally for all particle types, is variations which might occur in the value of the field **E** in eqn. 4.1 as a function of frequency. The variation in **E** can be indirectly obtained by measuring the apparent change of

conductivity of a test solution in the optical chamber. All the particles studied were suspended in 280mM mannitol and the apparent conductivity of this solution as a function of frequency, using one set of the microelectrode arrays, is shown in figure 4.11. These results show that between 100Hz and 100kHz there is an apparent dispersion in the effective conductivity of the mannitol solution. As shown by Schwan (1966) the electrode polarisation can be represented as an equivalent series RC circuit, where R represents the true bulk resistance of the solution and C is the effective capacitance of the electrical double layer at the electrode-solution interfaces. At low frequencies the applied field acts predominantly across the electrical double layer and the effective conductance of the solution is smaller than the true bulk value. With increasing frequency the capacitive reactance of the electrical double layer decreases and the applied field increasingly acts across the bulk solution in a way that parallels the form of the conductance-frequency characteristic shown in figure 4.11. This allows simple corrections to be made of the dielectrophoretic responses shown in figure 4.3, and an example of this is shown in figure 4.12 for *Micrococcus lysodeikticus*. It can be seen that the effect of electrode polarisation extends to frequencies as high as 100kHz and that for frequencies below 1kHz the dielectrophoretic response is significantly under-valued. This simple correction can be made to all collection spectra measured by this improved system. However, because the exact effects of electrode polarisation on the field strength E in eqn. 4.1 when linked with the collection of cells on the electrode surface are not yet fully known, all following spectra will be given in an uncorrected form.

As discussed earlier, equation 4.2 can be considered accurate for field frequencies above 1kHz. Further evidence for this can be obtained by measuring the dielectrophoretic collection spectrum of grown yeast as a function of medium conductivity (figure 4.6). In the frequency range 1kHz to 10kHz a constant collection is observed. As the medium conductivity is increased the magnitude of this collection is reduced until when the medium is more conductive than the suspended cell the force becomes negative and cells are repelled from the electrodes, as predicted by equation 4.2. Above 10kHz the collection changes from being conductivity-controlled to permittivity-controlled. This is seen as an increased collection in the

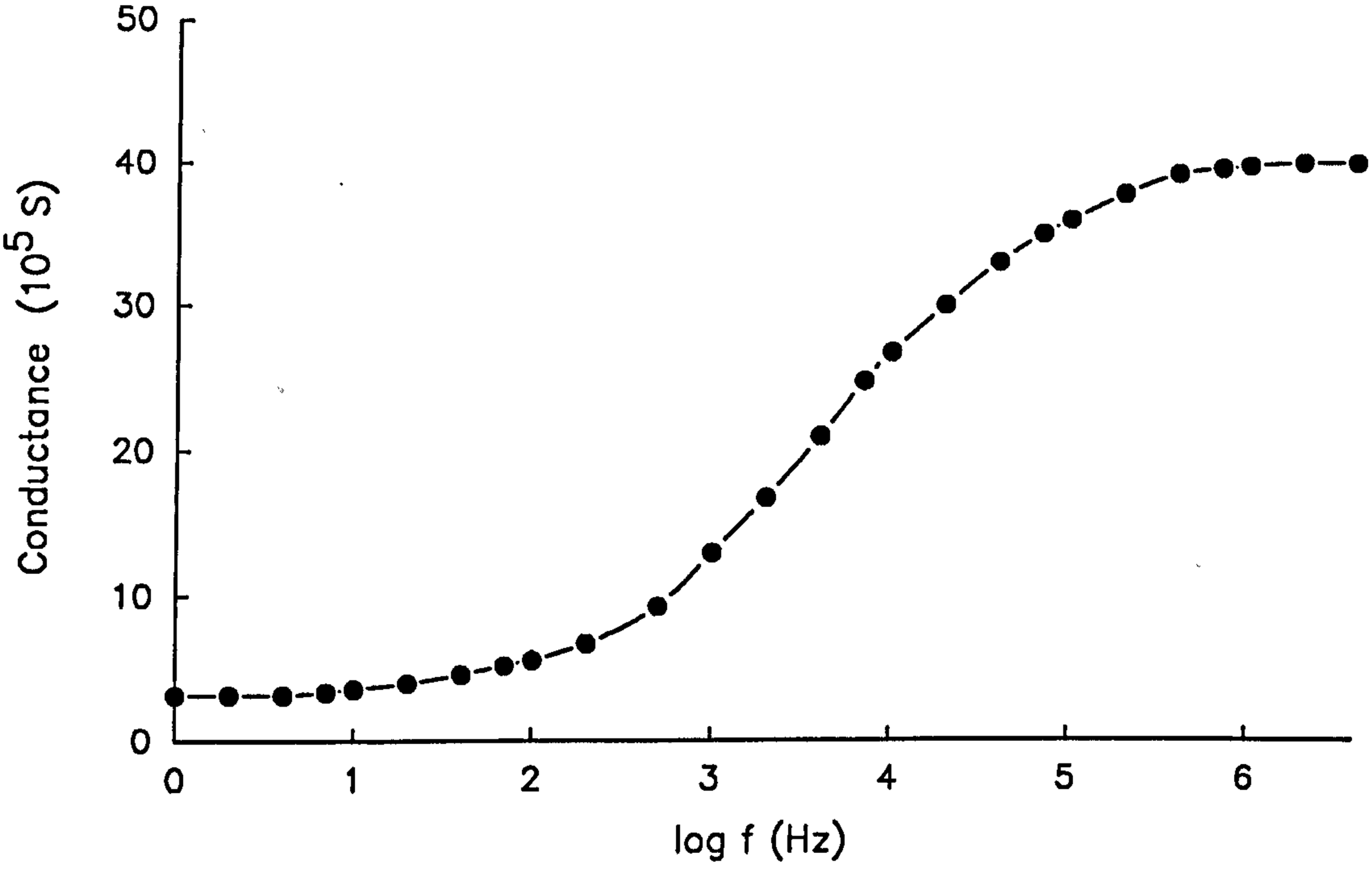

Figure 4.11 The variation in apparent conductivity of 280mM mannitol as a function of frequency.

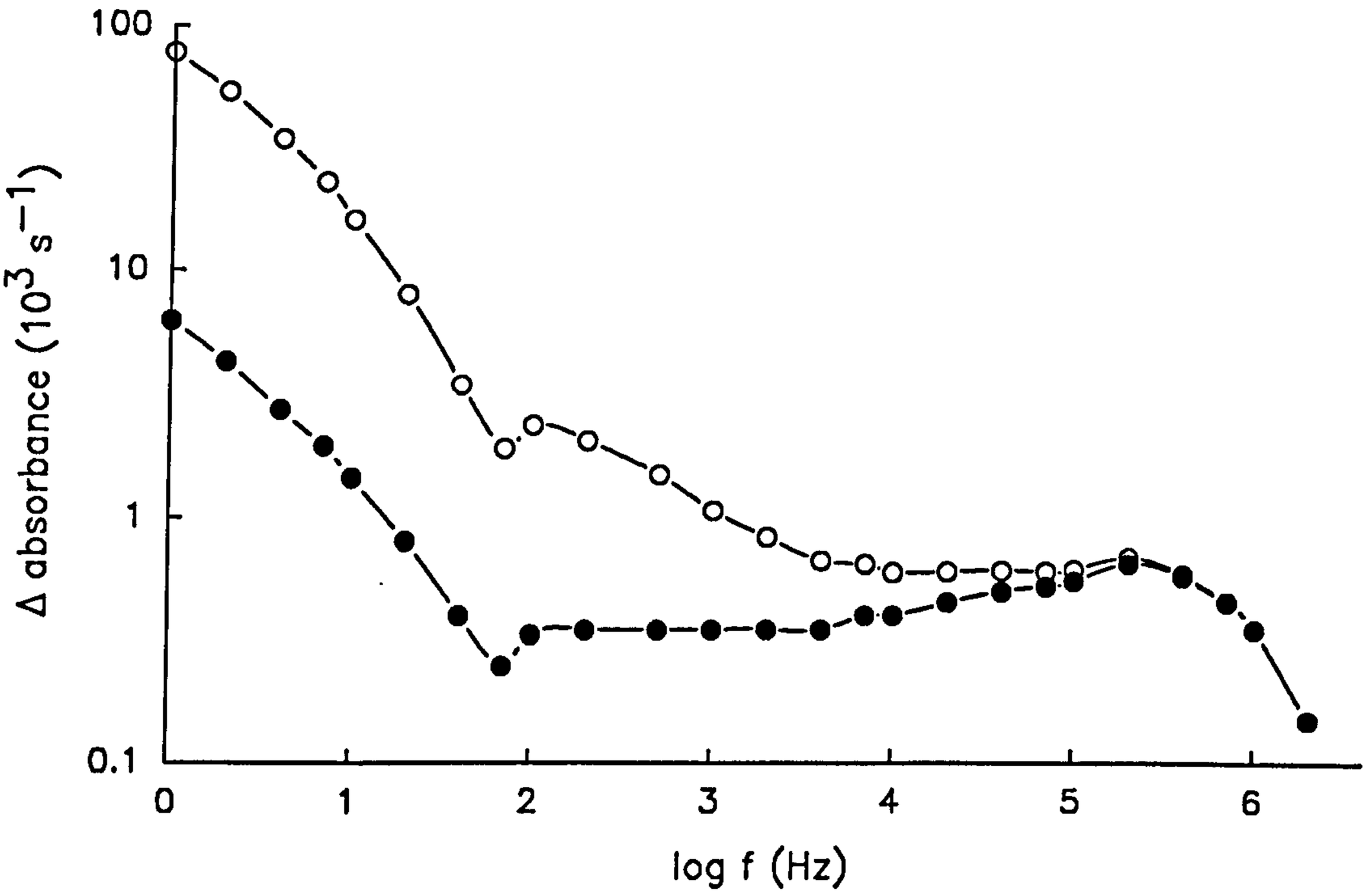

Figure 4.12 A comparison of the dielectrophoretic collection spectrum for *M. lysodeikticus* before (●) and after (O) correction for the effects of electrode polarisation.

frequency range 10kHz to 300kHz, the exact frequency being determined by the value of the substitution τ, which increases with increasing medium conductivity.

4.7 References

Al-Ameem, T.A.K. (1990) *Theoretical and Practical Aspects of Dielectrophoresis.* University of Wales Ph.D. thesis.

Dukhin, S.S. (1971) Dielectric Properties of Disperse Systems. In *Surface Colloid Science vol 3* 83-165 John Wiley and Sons, Chichester.

Einolf, C.W. and Carstensen, E.L. (1969) Passive Electrical Properties of Microorganisms, IV: Studies of the Protoplasts of *Micrococcus lysodeikticus. Biophys. J.* **9** 634-643.

Einolf, C.W. and Carstensen, E.L. (1971) Low Frequency Dielectric Dispersions in Suspensions of Ion-exchange Resins. *J. Phys. Chem.* **75** 1091-1099.

Pohl, H.A. (1978) *Dielectrophoresis.* Cambridge University Press, Cambridge.

Price, J.A.R. and Pethig, R. (1986) Surface Charge Measurements on *Micrococcus lysodeikticus* and the Catalytic Implications for Lysozyme. *Biochim. Biophys. Acta* **889** 128-135.

Schwan, H.P. (1966) Alternating Current Electrode Polarisation *Biophysik* **3** 181-201.

Schwarz, G. (1962) A Theory of the Low Frequency Dielectric Dispersion of Colloidal Particles in Electrolyte Solutions. *J. Phys. Chem.* **66** 2636-2642.

CHAPTER 5

THE CHARACTERISATION OF THE DIELECTROPHORETIC RESPONSE OF MAMMALIAN CELLS AND THE EFFECTS OF FORMALDEHYDE ON HELA CELLS

5.1 Introduction

The experiments described in chapters 3 and 4 used dielectrophoresis to study bacteria and yeasts. Although these micro-organisms are of great interest to areas of biotechnology such as the fermentation and brewing industries, they are of little use to other areas such as those involved with medical research. Mammalian cell lines are used in numerous applications for both research and the manufacture of small-scale, high-cost products including drugs and animal sera. To investigate the application of dielectrophoresis to these areas of biotechnology, a general dielectrophoretic response of mammalian cells had first to be characterised. In these experiments various mammalian cell lines were studied and characterised, including a strain of the well documented human cervical carcinoma line (designated HeLa S3). The HeLa cell line is especially suited to growth in suspension culture.

Further experiments described here were aimed at investigating the role of dielectrophoresis as a possible tool in the quality assurance of cell cultures and concentrated on two main areas of interest. The first of these was the possible use of dielectrophoresis as a sensing technique for determining the presence and the likelihood of removing mycoplasma from cell cultures. The second, and commercially more important, area investigated the use of the dielectrophoretic

force to determine the viability of a cell culture by detecting changes in the dielectric properties of the cells in suspension. The ability to either remove non-viable cells or detect the number of dead cells in a culture is of great importance in the seeding of cell cultures where the inoculum must have the highest viability possible. In these experiments cell viability was investigated as a function of the time a cell suspension was exposed to the preservative formaldehyde which is known to kill cells without changing their physical size or damaging the integrity of the plasma membrane.

At present biochemical techniques are used to determine both mycoplasma contamination and cell viability and employ a combination of staining and culture techniques using agar plates. An obvious advantage of a bioelectrical sensing/separation system would be the speed at which results could be obtained. Typically, the growth of mammalian cells on agar plates takes approximately 5-6 days, whereas a dielectrophoretic technique could take of the order of minutes.

5.2 Materials and Methods

The cell lines used in the experiments described here were all virally immortalised lines and had been designated the following names, IgG2, EL4-NOB1, EL4-Bu.Ou6, Mycl-3C7, Ox20, P815L, NS0, HeLa S3 . All the cell lines with the exception of HeLa S3 and IgG2, which are of human origin, originate from mouse tissue and were donated for these experiments by the European Collection of Animal Cell Cultures, Porton Down, U.K.

All cell lines were grown in 300ml suspension cultures. Cell lines HeLa S3, P815L and EL4-NOB1 were grown in Minimum Essential Media (Gibco, U.K.) supplemented with 10% foetal calf serum (heat activated at 56°C for 30 mins.). Lines IgG2 and EL4-Bu.Ou6 were grown in Dulbecco's Modified Eagle's Medium (Gibco, U.K.) also supplemented with 10% heat activated foetal calf serum. Mycl-3C7, Ox20 and NS0 cells were grown in RPMI 1640 media (Gibco, U.K.) with the media used for Mycl-3C7 supplemented with 10% foetal calf serum. All cell cultures were gassed with 5% CO_2/air mixture and were incubated at 37°C. The cultures

were seeded with a 5ml inoculum from a stock cell culture at a density of 10^6 cells ml^{-1}. Cells were passaged every 2-3 days to keep the cell density at approximately 10^6 cells ml^{-1}.

Cells were harvested by centrifugation (600 x g for 5mins) and were washed 3 times in a 320mM sucrose solution, made using de-ionised water, and resuspended to an optical absorbance of 0.26 at 635nm for a 1cm pathlength. A sucrose solution was found to be a better suspending medium than the 280mM mannitol used in previous experiments (chapters 3 and 4). The concentration of sucrose was determined to be 28% more hypertonic than 150mM NaCl and this caused the cells to be reduced in size very slightly giving them added mechanical strength. Such a sucrose solution is an acceptable perfusion fluid that maintains adequate cell viability both in vitro and in vivo and so was considered to be suitable for the suspending medium for the dielectrophoresis experiments. For experiments which investigated the effects of medium conductivity on the dielectrophoretic response 320mM sucrose was used to make up solutions of 0.5, 1.0, 2.0, 3.0mM sodium chloride (Sigma, U.K.).

In order to perform experiments on "dead" HeLa S3 cells, 50ml samples of the suspension culture were taken to which 0.5ml of 50% formaldehyde was added before incubation at 37°C. Dielectrophoretic collection spectra of HeLa cells were taken as a function of exposure time to the formaldehyde. Trypan blue exclusion counts were made on the treated cells when resuspended in the 320mM sucrose suspending medium to obtain an accurate measurement of cell viability for the samples.

Dielectrophoretic measurements were carried out using the dielectrophoresis spectrometer and experimental technique described in chapter 4. A 16 volt peak-to-peak sinusoidal voltage was applied to the field-producing-electrodes in the sample chamber and a fresh aliquot of cell suspension was used for each frequency reading. The dielectrophoretic response at each measurement frequency between 1Hz and 4MHz was determined from the change in optical absorbance of the cell suspension over the first 15 seconds after the application of the a.c. voltage to the electrodes. The collection spectra were measured at 20°C with each frequency reading being made twice to avoid possible errors.

5.3 Characterisation of the General Dielectrophoretic Response of Mammalian Cells

To determine the form of the general dielectrophoretic collection spectrum for mammalian cells a range of typical animal cells were characterised. The cells used in these experiments were immortal lines (i.e. virally infected) and although this results in changes in the protein composition of their membranes, no gross changes occur in the physical properties of the cells. In the frequency range studied here, 1Hz to 4MHz, the collection spectra obtained were determined by the dielectric properties of the cell surface and membrane, as discussed in the preceding chapters. However, even though there are considerable differences in the structure of animal cells and those already discussed, the dielectrophoretic responses can still be described in terms of surface charge, effective conductivity and effective permittivity.

5.3.1 IgG2 cells

Figure 5.1 shows the dielectrophoretic collection spectrum for the human hybridoma cell line IgG2, which is recognised for its expression of IgG antibodies. The spectrum shows a large positive collection at 1Hz which rapidly decreased as the electric field frequency was increased until, at 20Hz, no collection occurred. For frequencies between 20Hz and 1kHz the dielectrophoretic response was negative (i.e. the dielectrophoretic force was directed away from the field-producing-electrodes). Equation 3.6 can be used to interpret such a negative collection in terms of cell and suspending medium conductivity. This shows that for a negative collection to occur the effective conductivity of the cell must be less than that of its suspending medium (10^{-3} Sm^{-1}). Above 1kHz the collection increased, becoming positive again at 4kHz, and reached a constant rate at approximately 20kHz. The magnitude of the high-frequency plateau is determined (chapter 3) by respective magnitudes of the cell and suspending medium permittivities.

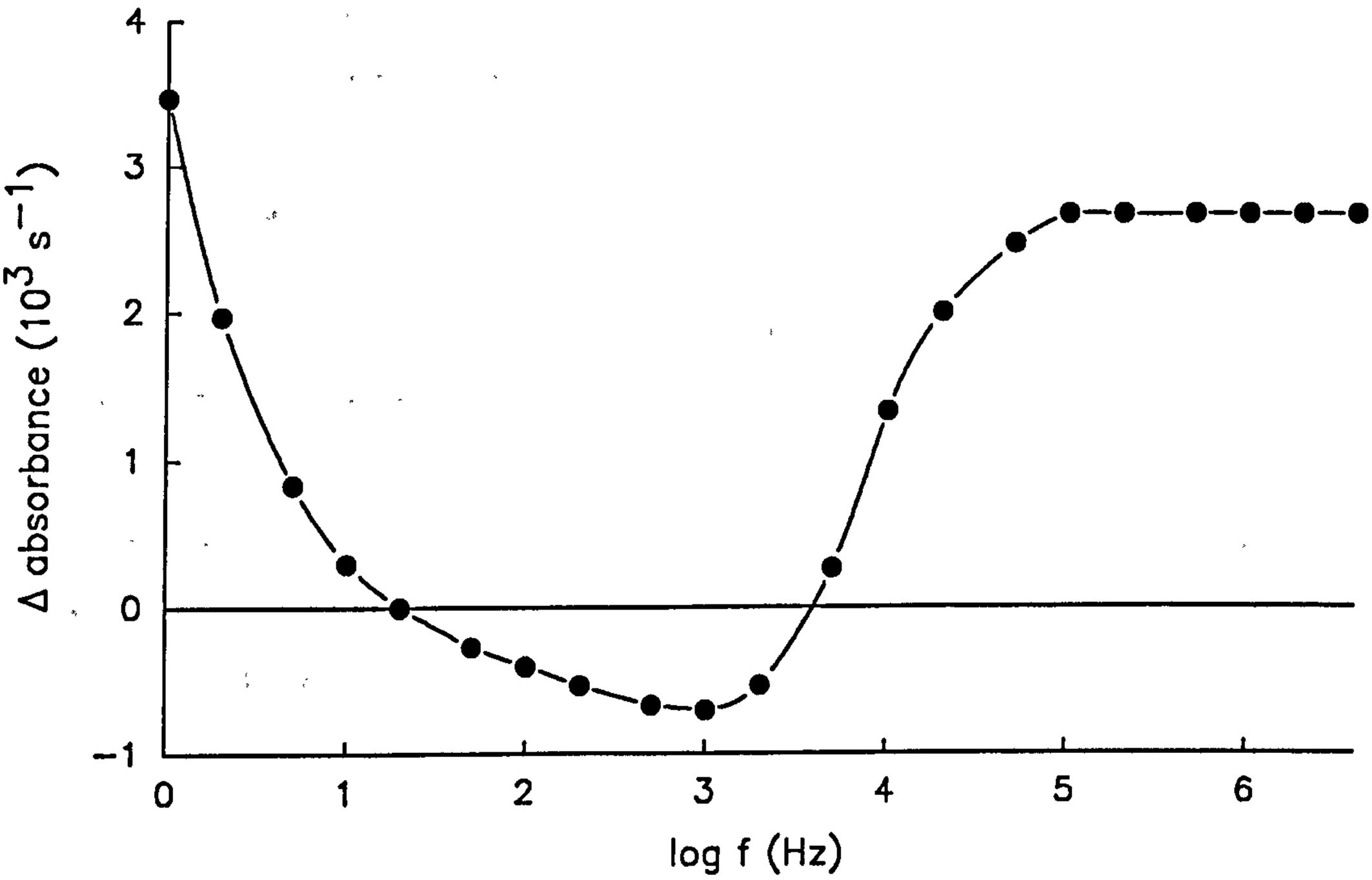

Figure 5.1 The dielectrophoretic response of IgG2 cells.

5.3.2 EL4-NOB1 cells

The dielectrophoretic response of the mouse lymphoma cell line EL4-NOB1 is given in figure 5.2. The form of this spectrum is similar to that of the IgG2 cells described in section 5.3.1. In the case of EL4-NOB1 cells the region of steady collection occurring in the mid-frequency region extended down to 200Hz and did not begin to change until 2kHz from where the collection rapidly increased to a permittivity dominated plateau region above 100kHz.

5.3.3 EL4-Bu.Ou6 cells

EL4-Bu.Ou6 mouse ascites lymphoma lymphoblast cells exhibit a similar dielectrophoretic response (figure 5.3) to those described in section 5.3.1 and 5.3.2. The low-frequency collection from 1Hz upwards reduced in magnitude as the electric field frequency was increased up to 100Hz. The mid-frequency steady collection region shown in figure 5.3 was only slightly negative implying that the effective conductivity of EL4-Bu.Ou6 cells is greater than IgG2 and EL4-NOB1 cells. Above 1kHz the response increased to reach the permittivity controlled plateau region at approximately 100kHz.

5.3.4 Mycl-3C7 cells

Figure 5.4 shows the dielectrophoretic response of the mouse balb/C hybridoma cell line Mycl-3C7. The spectrum displayed the familiar low-frequency collection from 1Hz to 70Hz. However, between 70Hz and 1kHz the dielectrophoretic response remained positive as it entered the mid-frequency constant collection region. This implies that the effective conductivity of the Mycl-3C7 cells used was greater than that of the 320mM sucrose suspending medium. At higher frequencies, above 50kHz, the collection reached a slight plateau before reducing at frequencies above 400kHz.

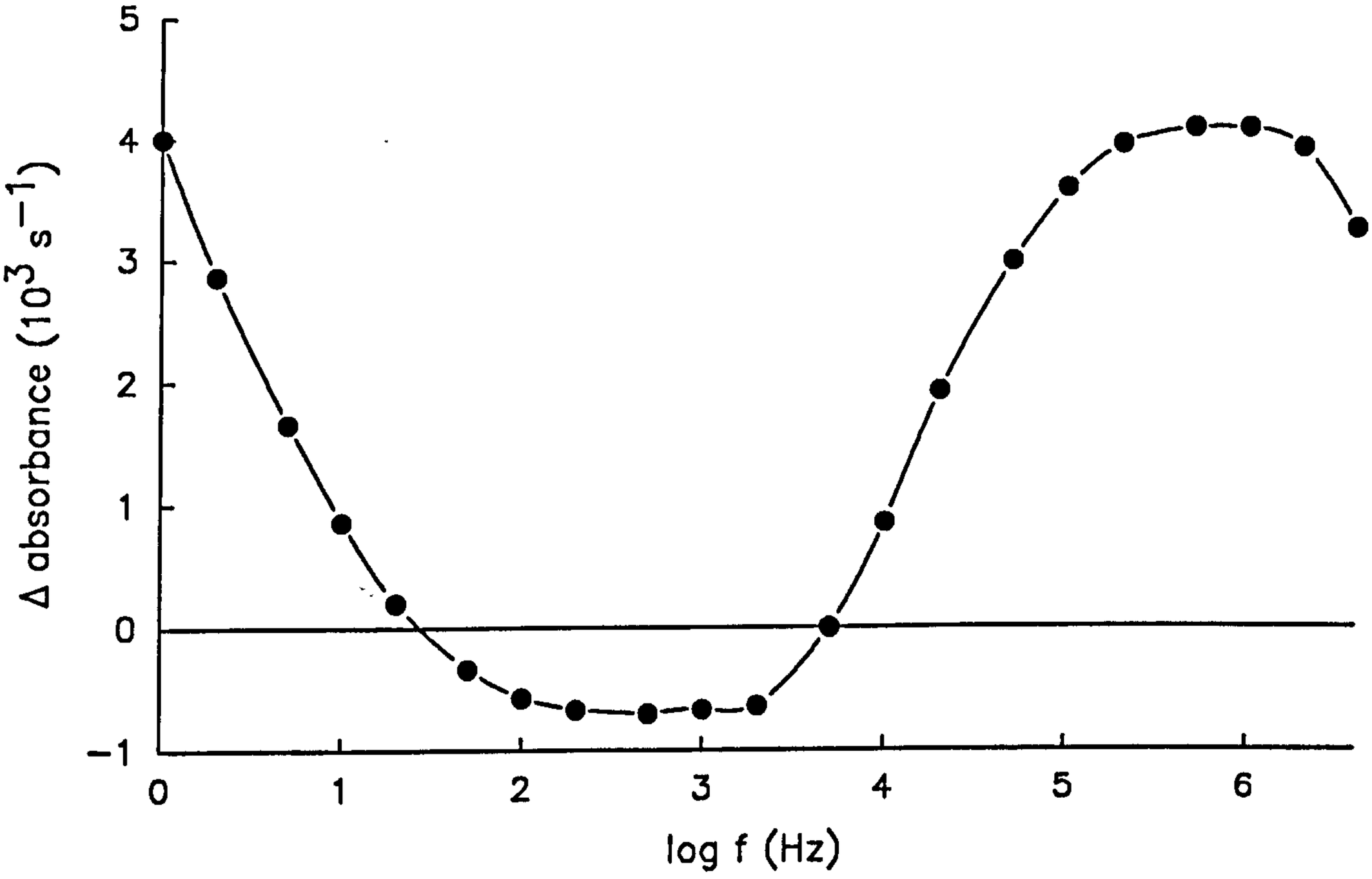

Figure 5.2 The dielectrophoretic response of EL4-NOB1 cells.

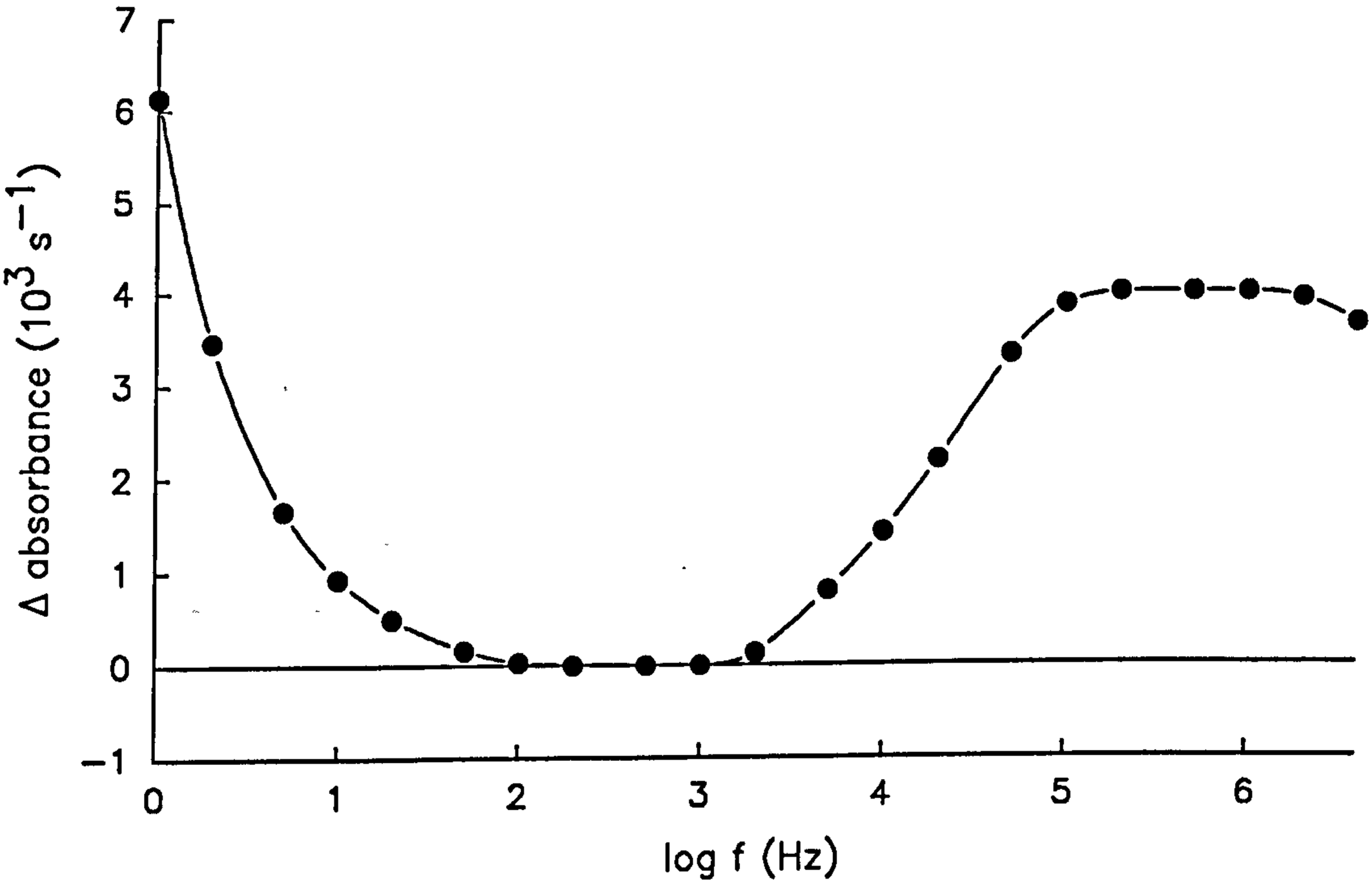

Figure 5.3 The dielectrophoretic response of EL4-Bu.Ou6 cells.

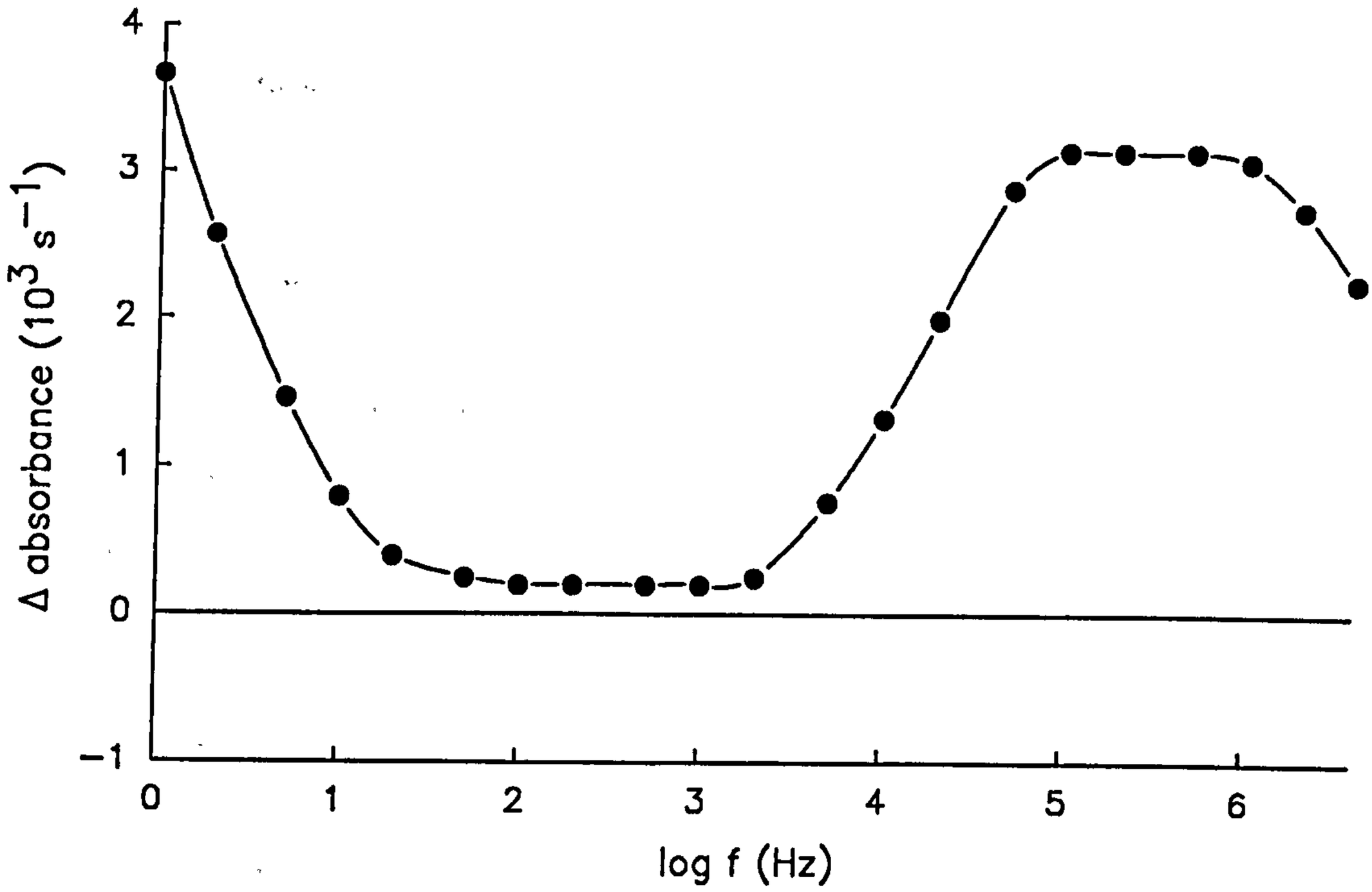

Figure 5.4 The dielectrophoretic response of Mycl-3C7 cells.

5.3.5 Ox20 cells

The dielectrophoretic response of Ox20 cells is shown in figure 5.5. Like the Mycl-3C7 line described previously Ox20 is a mouse balb/C hybridoma line. The dielectrophoretic response of these cells followed the now familiar pattern of a large low-frequency collection which reduced to a region of steady collection, as the electric field frequency was increased, before rising to a plateau at approximately 100kHz. In the case of Ox20 cells the mid-frequency region does not become appreciably negative.

5.3.6 P815L cells

The dielectrophoretic response for P815L mouse mastocytoma cells (figure 5.6) had a similar form to those of the cells previously discussed. The conductivity of these cells can be concluded to be only slightly less than that of the sucrose suspending medium because of the lack of any great amount of negative collection in the mid-frequency region.

5.3.7 NS0 cells

NS0 cells are mouse balb/C myeloma cells and their dielectrophoretic response, shown in figure 5.7, was typical of all the cells discussed in this section. They exhibited the three previously described sections to the spectrum, namely the surface charge related low-frequency collection, conductivity dominated mid-frequency steady (in this case negative) collection and the higher frequency, permittivity controlled, plateau at 100kHz.

5.3.8 HeLa S3 cells

HeLa cells are human cervical carcinoma and their collection spectrum (figure 5.8) was, like NS0, typical of that found in all the animal cells studied so far. The cells showed a surface charge related low-frequency collection which extended to approximately 100Hz, above which

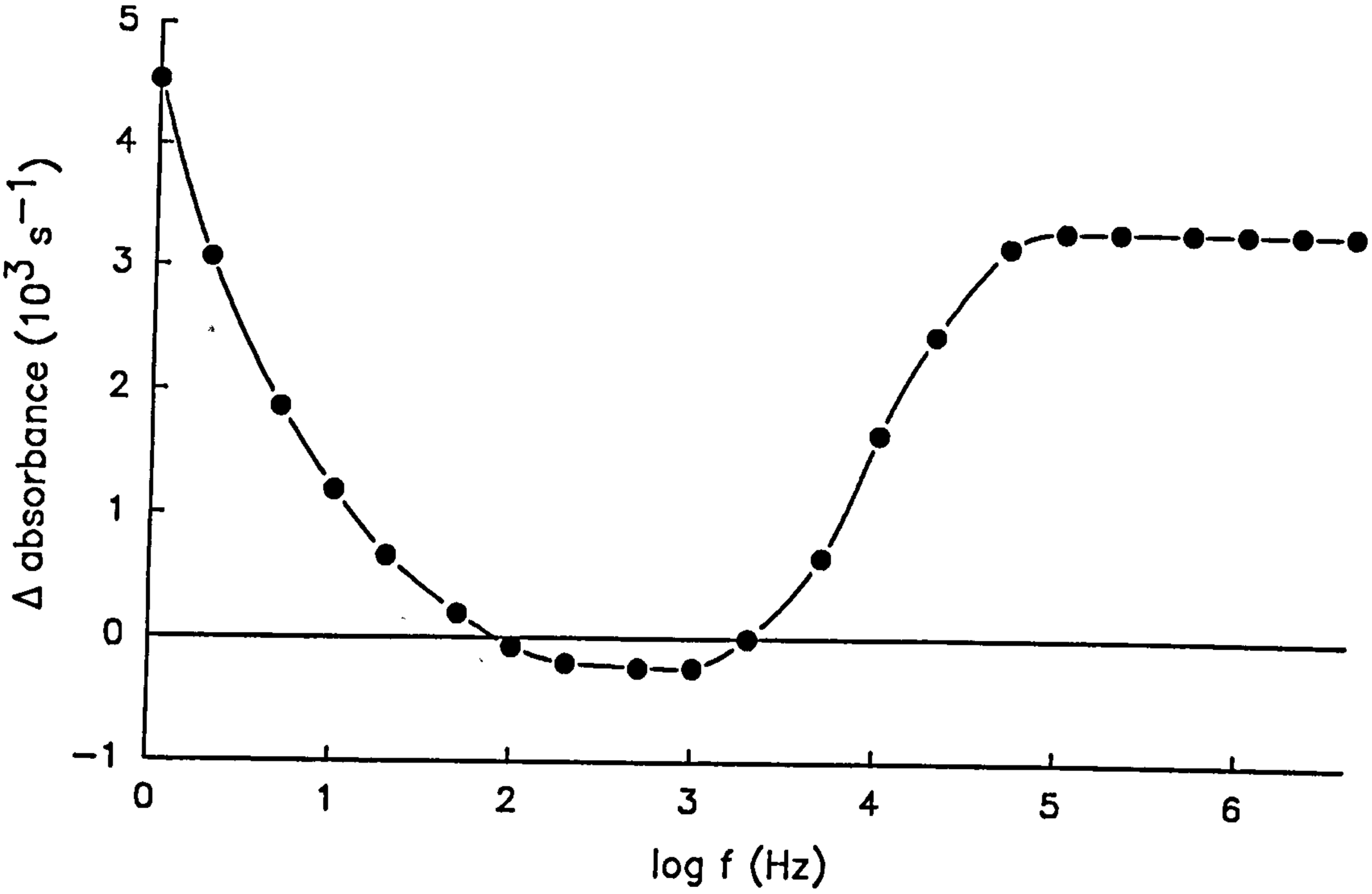

Figure 5.5 The dielectrophoretic response of Ox20 cells.

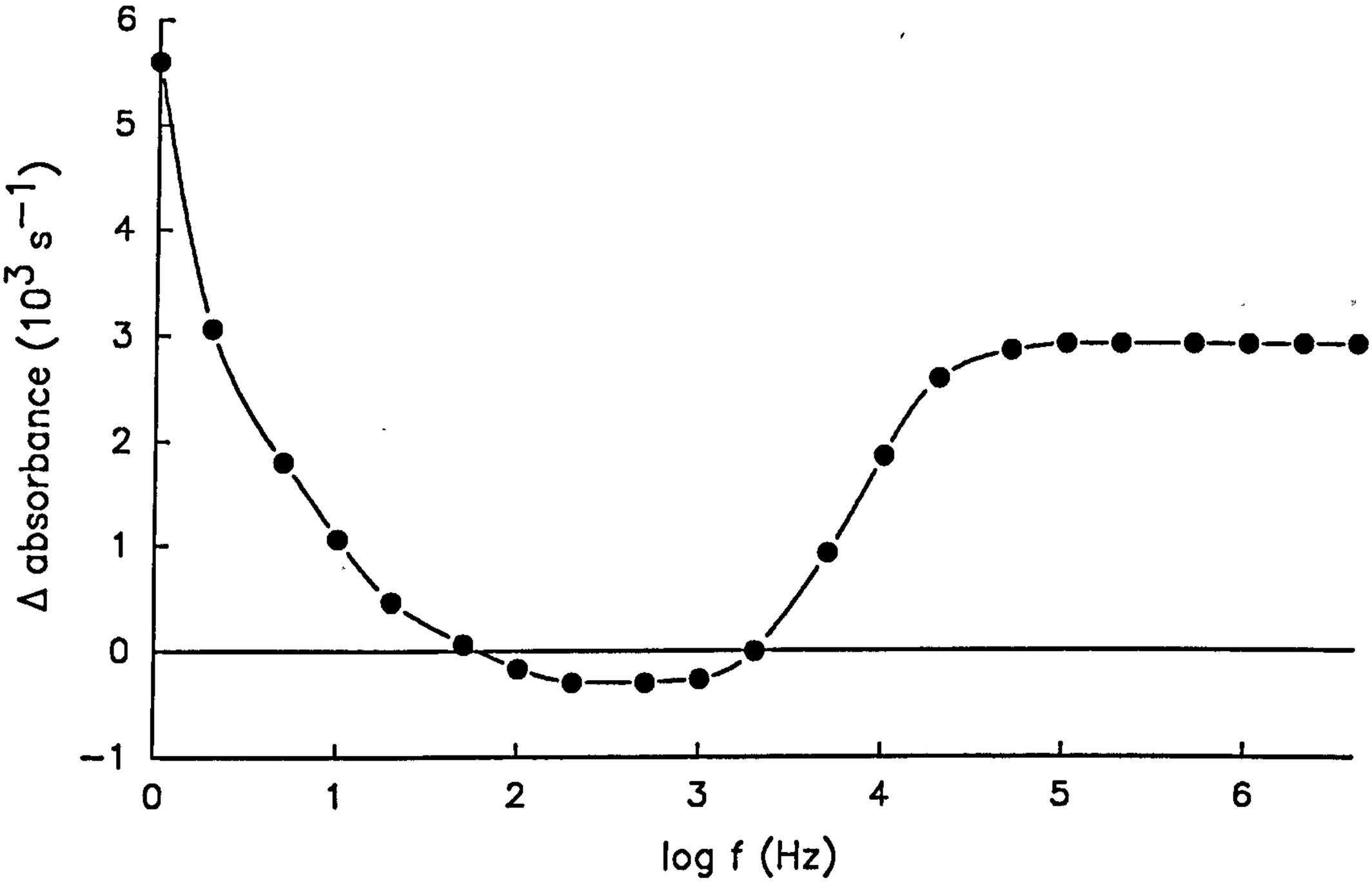

Figure 5.6 The dielectrophoretic response of P815L cells.

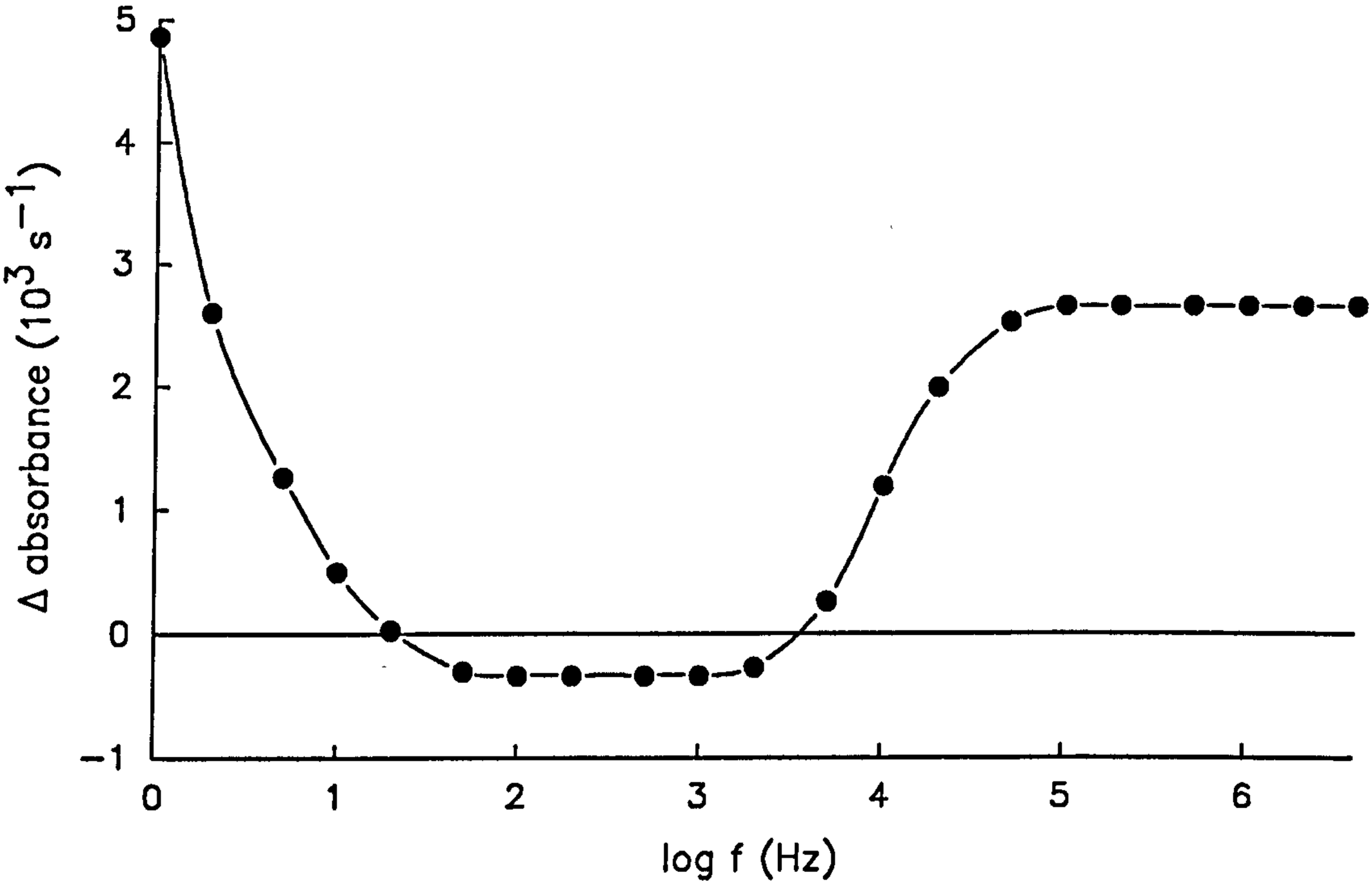

Figure 5.7 The dielectrophoretic response of NS0 cells.

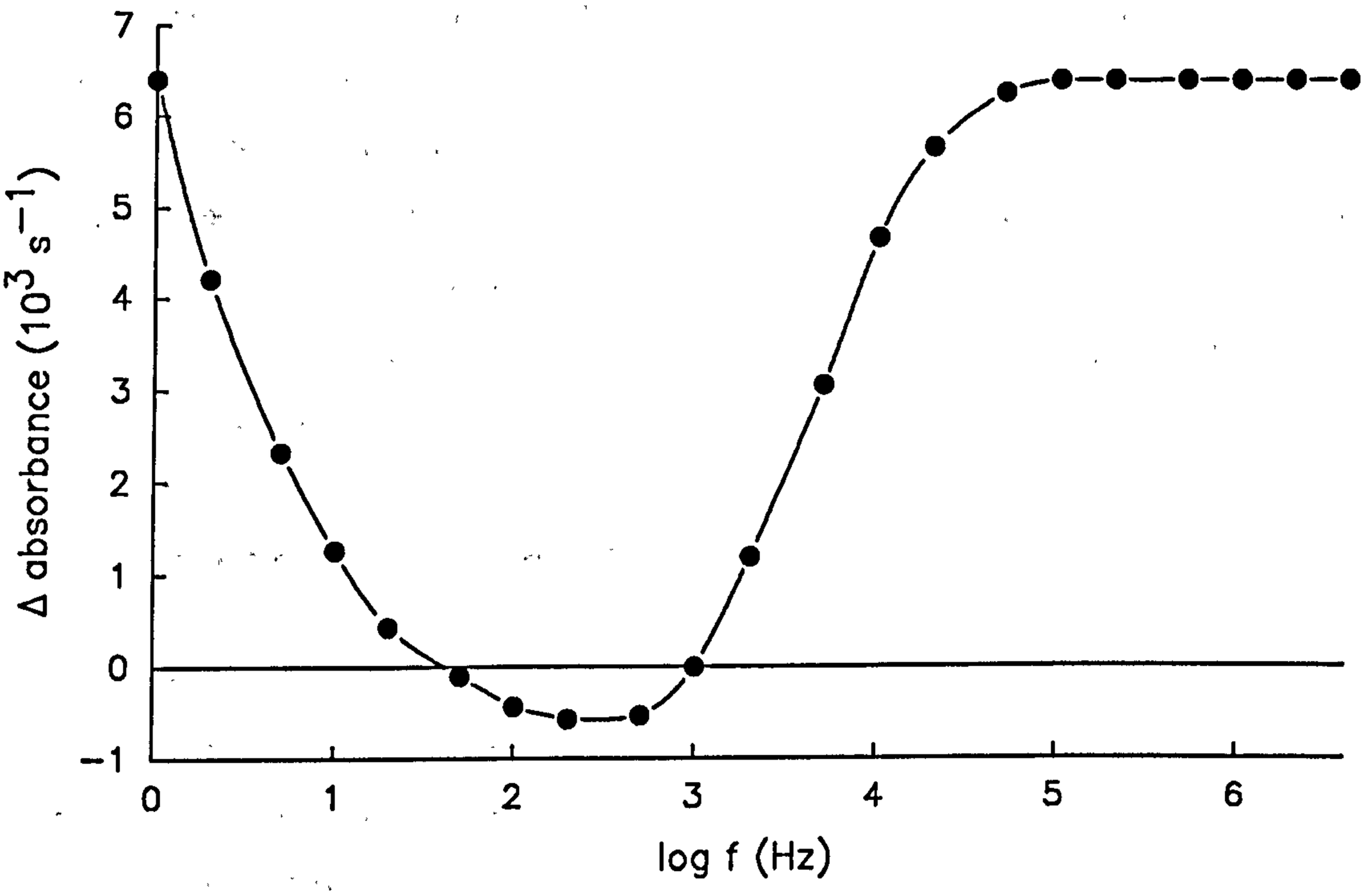

Figure 5.8 The dielectrophoretic response of HeLa S3 cells.

a steady negative collection occurred until an increase was seen at 1kHz. As the field frequency was increased the collection reached a plateau at approximately 100kHz.

5.4 Investigations of the Applications of Dielectrophoresis to Mycoplasma Determination

Mycoplasma are the simplest of cells, they are small bacterium-like organisms that normally lead a parasitic existence in close association with animal or plant cells and are approximately 0.3μm in diameter. In most cell culture systems the presence of mycoplasma may be ignored as it is generally taken that they do not affect normal cellular processes. However, when cells are used for the production of drugs or sera they are regarded as sources of product contamination. For this reason investigations into the possible use of dielectrophoresis as a technique for sensing the presence of mycoplasma or the removal of mycoplasma from a cell culture were undertaken.

5.4.1 Dielectrophoretic Response of KRO Mycoplasma

Figure 5.9 shows the dielectrophoretic collection spectra for the mycoplasma designated KRO. The cell concentration used in this experiment was approximately 10 times that normally found in a contaminated cell suspension. The membrane structure of mycoplasma is similar to that of an animal cell and because of this the response showed the familiar characteristics of a typical animal cell response with a low-frequency, surface charge related collection which extended from 1Hz to 200Hz. Above this frequency the response remained constant until 5kHz where the collection rate increased to reach the permittivity controlled plateau at 500kHz.

5.4.2 Dielectrophoretic Response of SK-4 Cells Contaminated with KRO Mycoplasma

Figure 5.10 shows the dielectrophoretic response of SK-4 cells, which have been contaminated with KRO mycoplasma at a normal concentration. The spectrum exhibited the same form as that of a typical animal cell with a slight difference in the low-frequency, surface charge controlled collection effects which extended up to 500Hz, suggesting a large surface charge was present. This spectrum is similar to that of a non-contaminated sample of SK-4 cells.

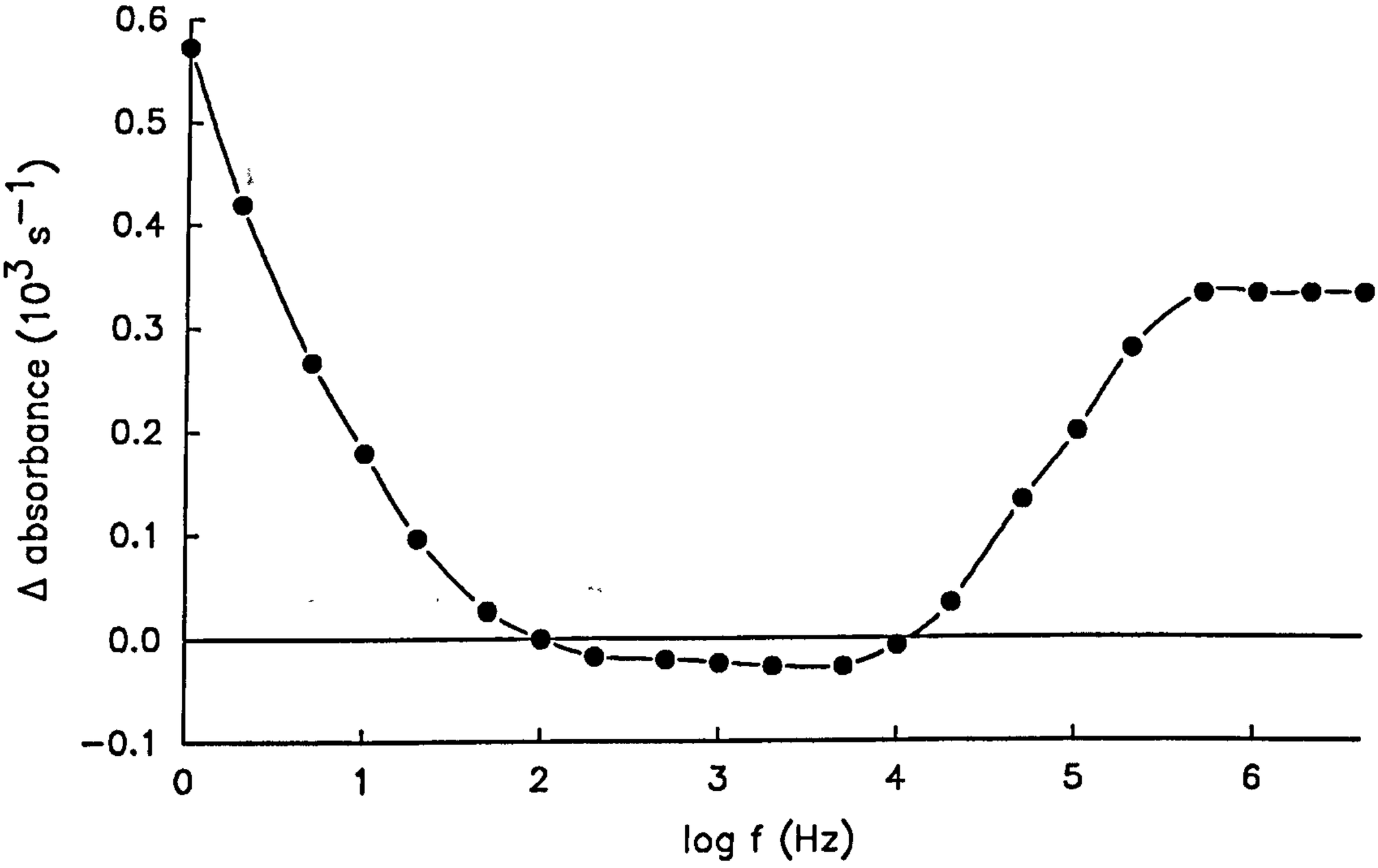

Figure 5.9 The dielectrophoretic response of the mycoplasma KRO.

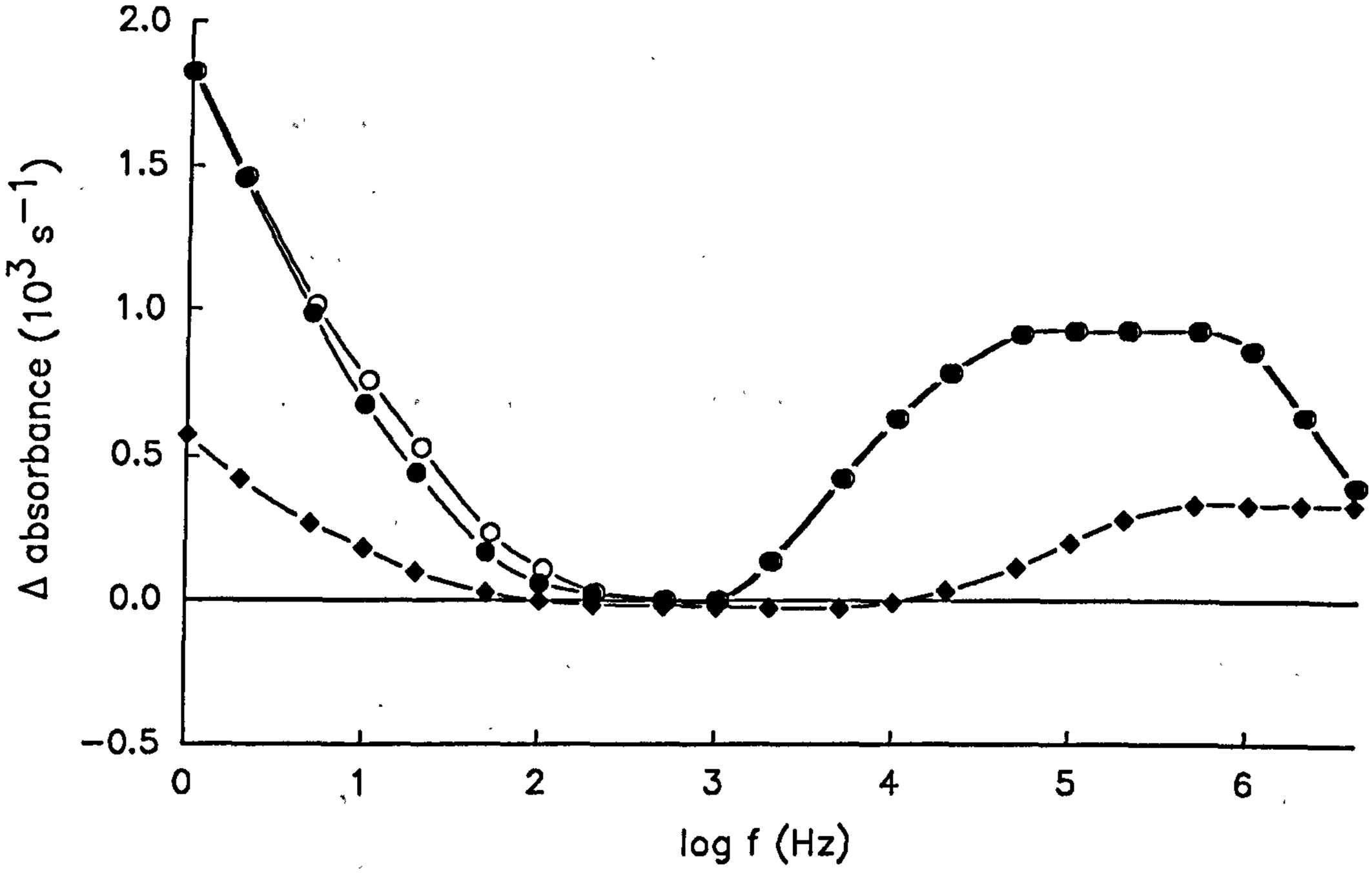

Figure 5.10 The dielectrophoretic response of SK4 cells before (●) and after (O) contamination with KRO mycoplasma. Also shown is the response for KRO mycoplasma (◆) as given in figure 5.9.

5.5 The Effects of Formaldehyde on the Dielectrophoretic Response of HeLa S3 Cells: Cell Viability Determination

The ability to determine the viability of a cell culture is of importance in the monitoring of culture growth and in the seeding of fresh cultures. Cell viability can be altered by exposure of a cell line to formaldehyde and in these experiments the dielectrophoretic response of the HeLa S3 line was measured as a function of formaldehyde treatment. The results described here were used to investigate the selective separation properties of dielectrophoresis, where dead cells would be extracted from a cell culture containing a mixture of live and dead cells, in order to remove possible sources of toxins from the culture.

5.5.1 Temporal Change in Cell Viability on Exposure to Formaldehyde

The addition of formaldehyde to a cell culture, as mentioned earlier, acts as a preservative by causing the cells to become non-viable through cessation of all normal cellular functions. The change from a viable to non-viable state does not occur instantaneously but over a period of time. Figure 5.11 shows the temporal variation in cell viability measured as a function of the time a 50ml sample of cells was exposed to formaldehyde. The graph, obtained by trypan blue exclusion counts, showed a rapid reduction in viability over the first two hours, during which the majority of cells were killed. After this the viability reduced at a much slower rate until eventually, after 24hrs, all the cells were "dead".

5.5.2 Temporal Change in Dielectrophoretic Response on Exposure to Formaldehyde

Figure 5.12 shows the dielectrophoretic spectrum of non-viable HeLa S3 cells with the spectrum of live cells (figure 5.8) reproduced for comparison. It can be seen that all three sections of the response were affected by the formaldehyde. At low frequencies the surface charge controlled collection was larger for the non-viable cells, and this observation is supported by electrophoretic measurements of both "dead" and live cells which showed "dead" HeLa S3 cells to have a slightly higher net surface charge than live cells. A second, more pronounced,

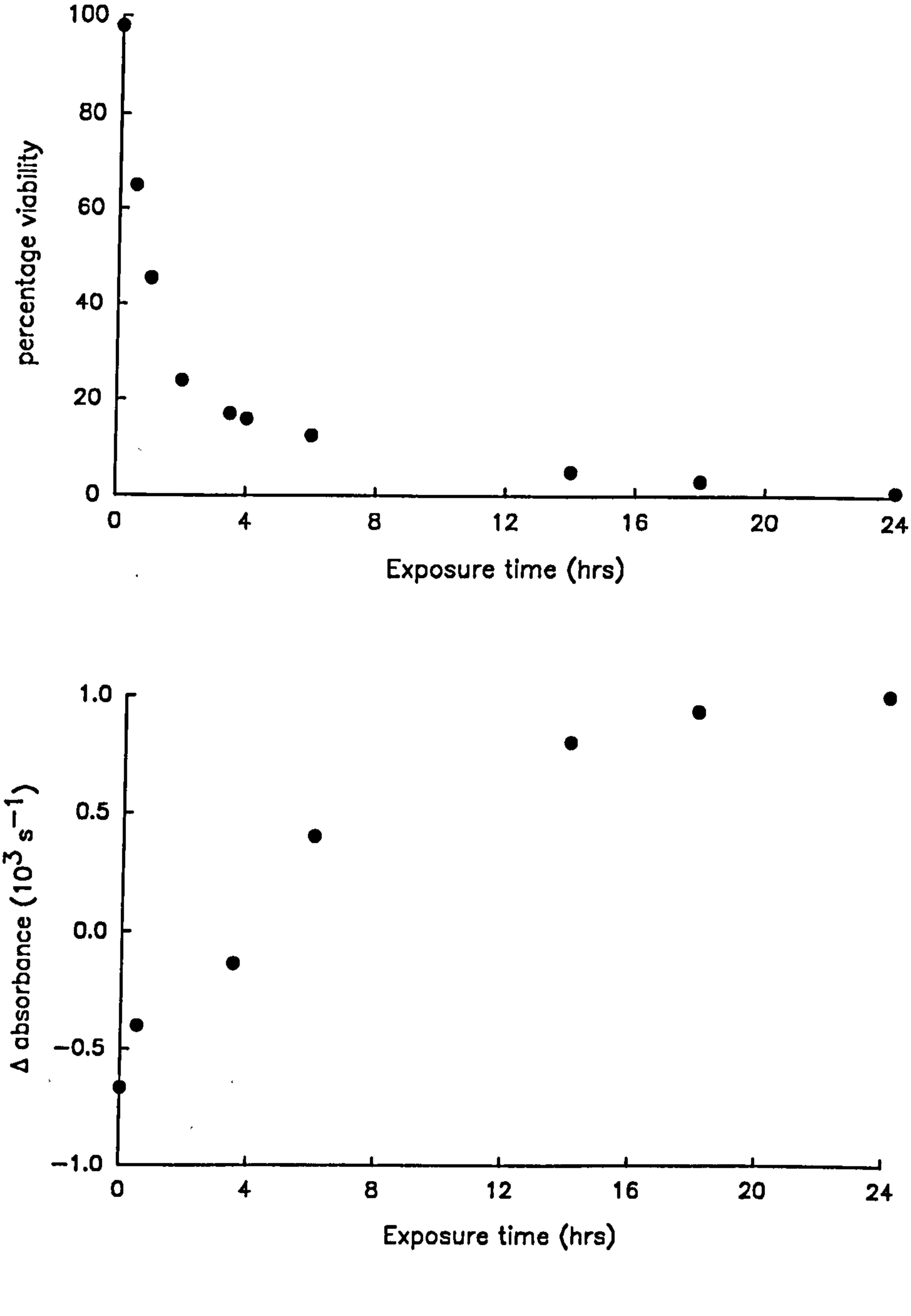

Figure 5.11 The temporal variation in (a) the percentage viability and (b) the dielectrophoretic collection rate at 1kHz of HeLa S3 cells on exposure to formaldehyde.

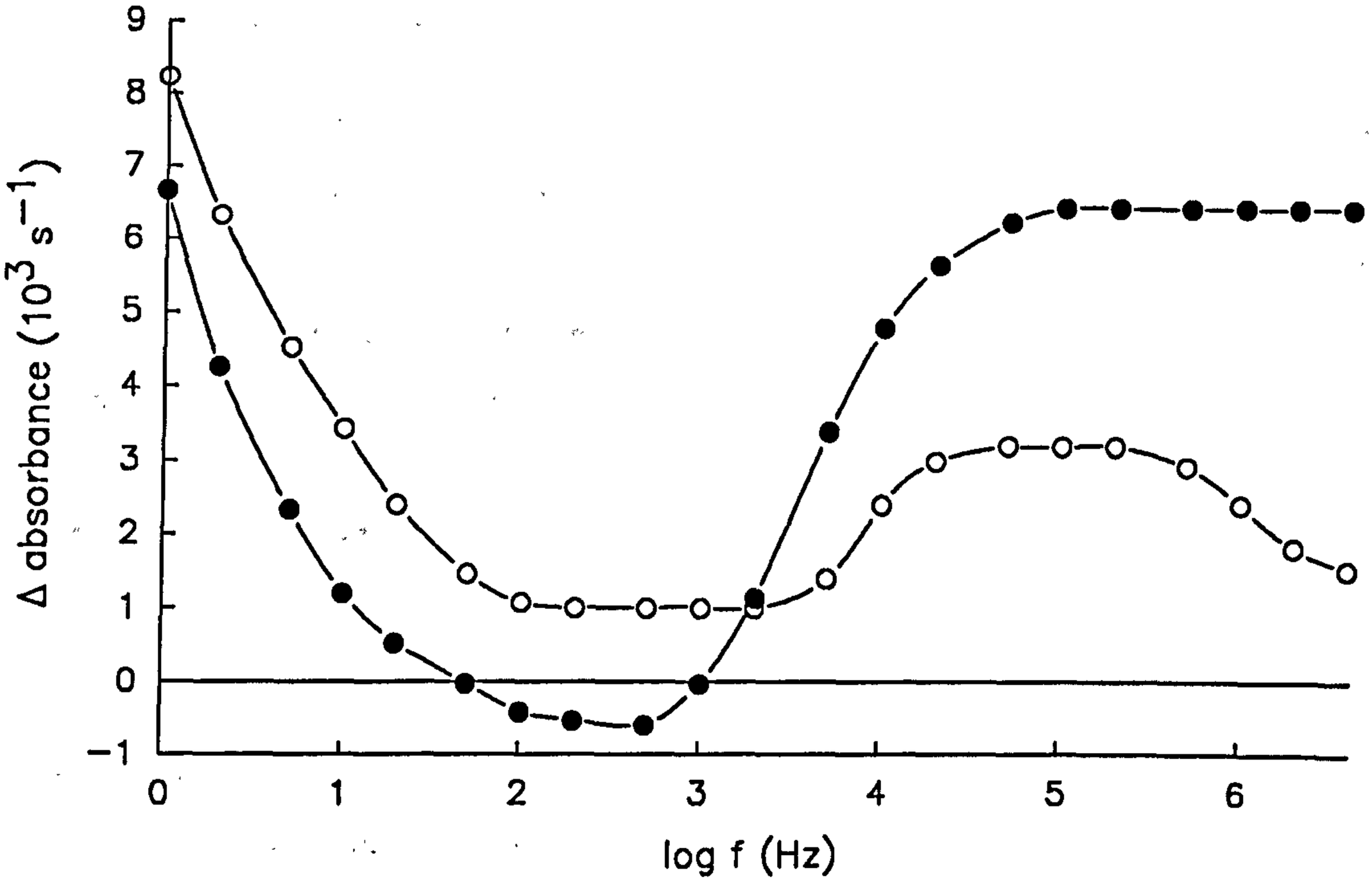

Figure 5.12 A comparison of the dielectrophoretic responses of live (●) and formaldehyde treated (O) HeLa S3 cells.

difference was that of the mid-frequency response from 100Hz to 2kHz. The "dead" cells showed no negative collection in this region but instead had a steady positive response indicating an increase in the effective conductivity of the cell. At higher frequencies, after a slightly frequency shifted increase in collection, the "dead" cells exhibited a lower response in the permittivity controlled region than the live cells, implying that formaldehyde treatment reduced the permittivity of HeLa S3 cells whilst increasing their effective conductivity.

Figures 5.13 and 5.14 show the intermediate stages between the viable and non-viable states after 0.5, 3.5, 6, 14, and 18 hours exposure to formaldehyde These graphs correspond to percentage viabilities of 65%, 17%, 12%, 5% and 2%. The responses clearly show the gradual increase in cell conductivity in the mid-frequency region and the reduction in permittivity at higher frequencies, together with changes in cell surface charge.

5.6 The Effects of Medium Conductivity on the Dielectrophoretic Response of Mammalian Cells

As discussed in chapter 3 the use of dielectrophoresis for cell separation using electric field frequencies below 1MHz is dependent on the conductivity of the medium used to suspend the cells and its magnitude relative to the effective conductivity of the cells. To investigate the effects of medium conductivity on the dielectrophoretic collection of animal cells the responses of both "dead" and live HeLa S3 cells were measured in suspending media with conductivities of 0, 0.005, 0.01, 0.02 and 0.03Sm^{-1}. The collection spectra of live and "dead" cells, shown in figures 5.15 and 5.16 respectively, both share a similar form to those described in section 5.3. As the medium conductivity was increased the most notable change in the response was the reduction in collection rate at frequencies below 1kHz (i.e. a more negative response between 100Hz and 1kHz and a reduction in the magnitude of the low-frequency response below 100Hz). An artefact of an increase in medium conductivity is a shift in the frequency at which the collection rate becomes positive again at higher frequencies. Above 100kHz differences in the responses of "dead" and live cells began to appear. In figure 5.15 the addition of NaCl to the suspending media of the live HeLa cells was seen to cause a drop in the response of the cells

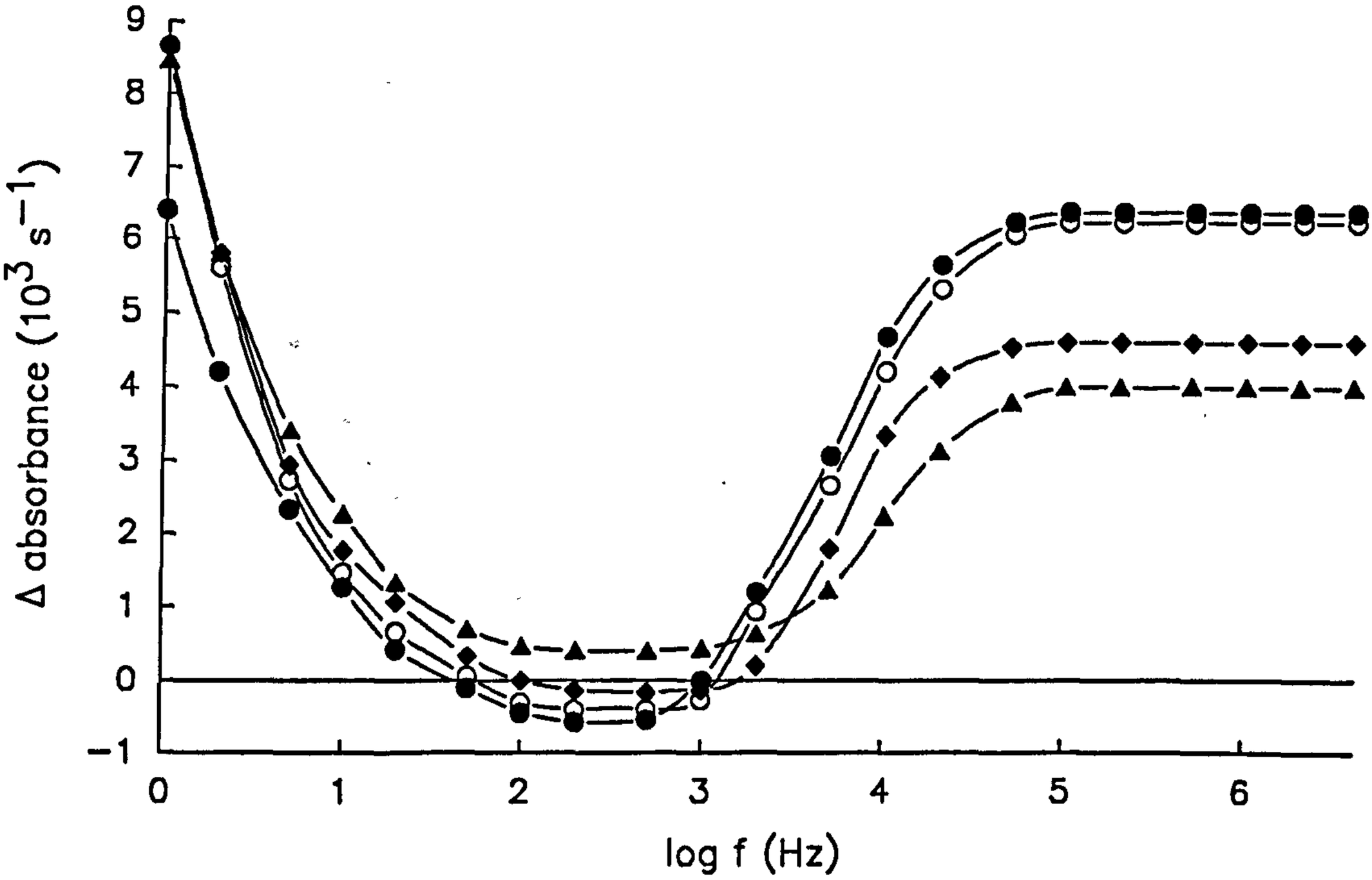

Figure 5.13 The temporal variation in the dielectrophoretic response of HeLa S3 cells on 0hrs (●), 0.5hrs (O), 3.5hrs (◆) and 6.0hrs (▲) exposure to formaldehyde.

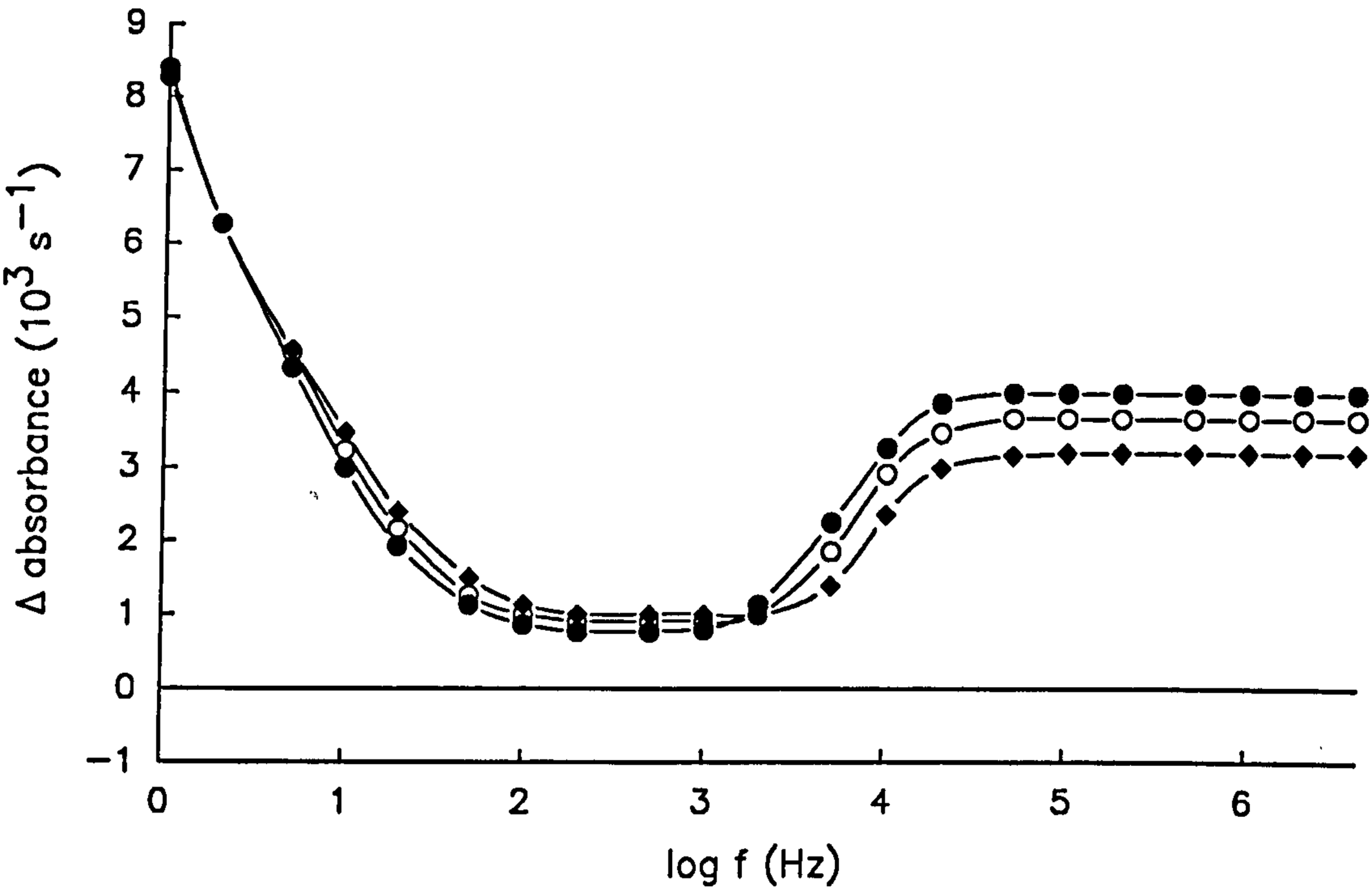

Figure 5.14 The temporal variation in the dielectrophoretic response of HeLa S3 cells on 14hrs (●), 18hrs (O) and 24hrs (◆) exposure to formaldehyde.

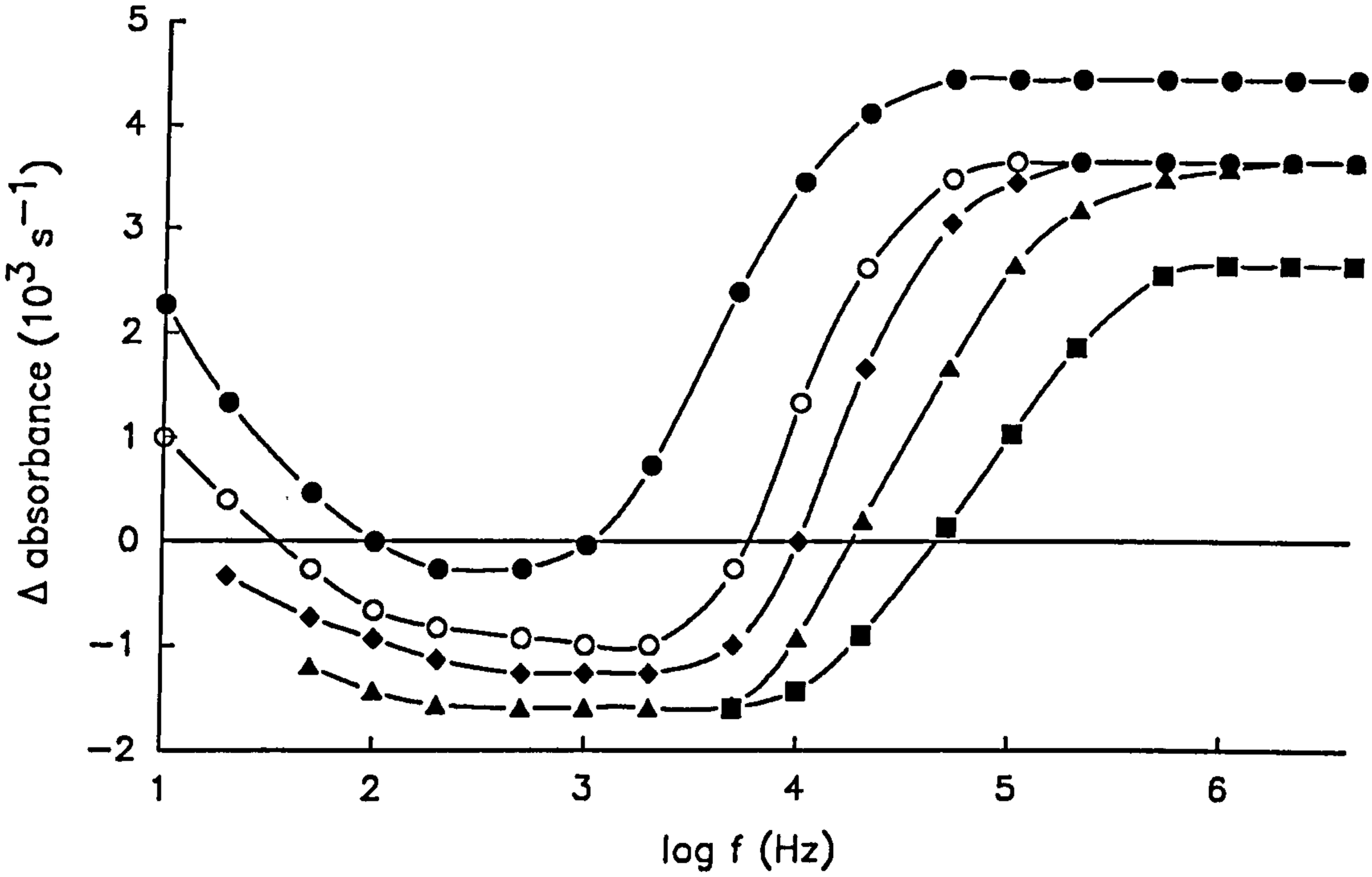

Figure 5.15 The frequency dependence of the dielectrophoretic collection rate of HeLa S3 cells suspended in 320mM sucrose (●), sucrose + 0.5mM NaCl (O), sucrose + 1.0mM NaCl (◆), sucrose + 2.0mM NaCl (▲) and sucrose + 3.0mM NaCl (■).

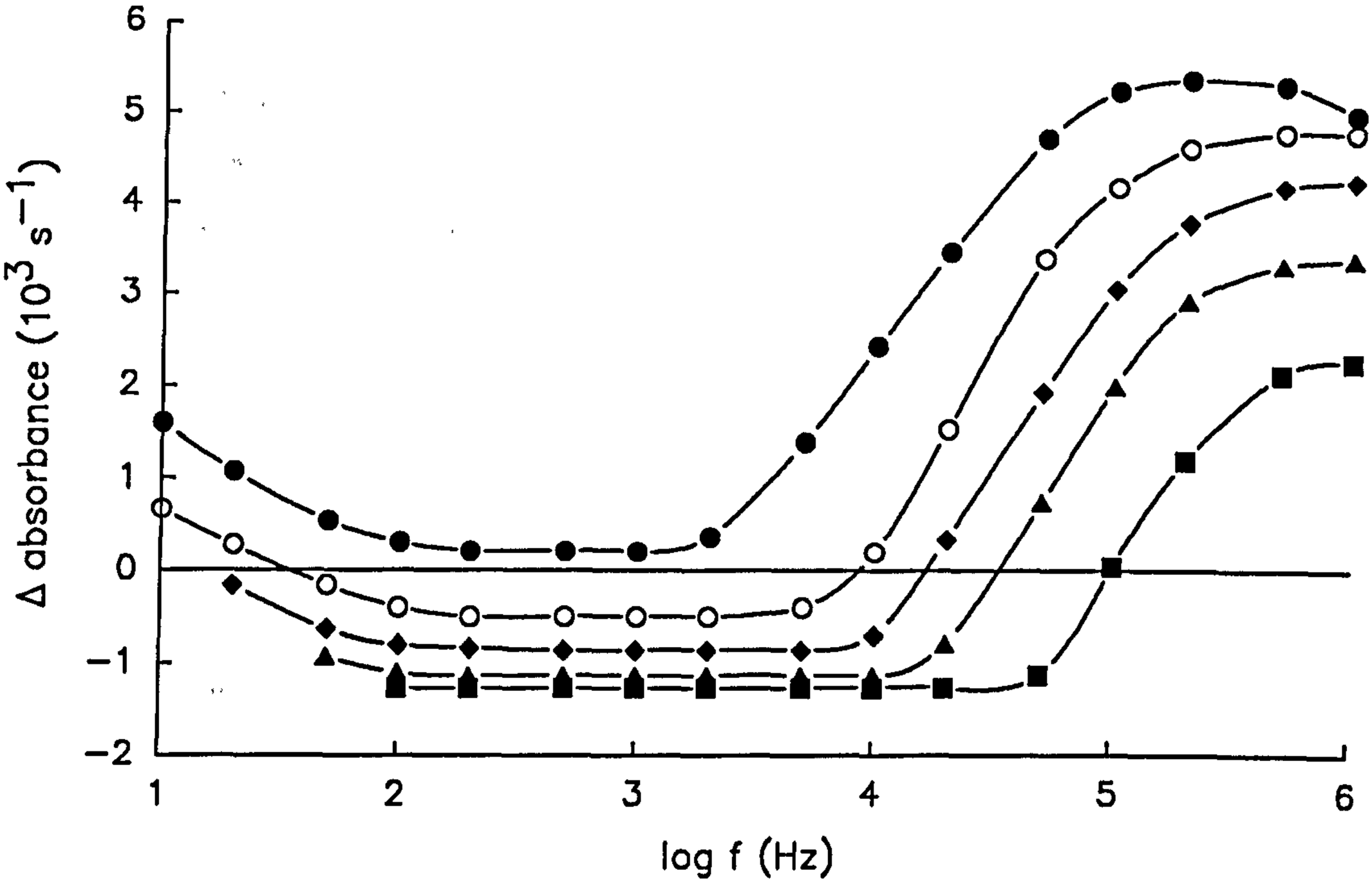

Figure 5.16 The frequency dependence of the dielectrophoretic collection rate of formaldehyde treated HeLa S3 cells suspended in 320mM sucrose (●), sucrose + 0.5mM NaCl (O), sucrose + 1.0mM NaCl (◆), sucrose + 2.0mM NaCl (▲) and sucrose + 3.0mM NaCl (■).

above 100kHz compared to that of cells in a salt free medium. This can partly be attributed to the increased conductivity of the suspending medium lowering the electrical impedance of the electrode array to produce an impedance-related drop in the output of the signal generator at high frequencies. This has been corrected for in the responses of cells in 0.005, 0.01 and 0.02Sm^{-1} media. However, in the case of 0.03Sm^{-1} medium the signal generator could not provide the 16 Volt peak to peak signal required for the experiment above 500kHz. It can be seen that for 0.005, 0.01 and 0.02Sm^{-1} media the increased medium conductivity does not affect the collection rate of live cells, whereas figure 5.16 shows the collection rate of "dead" HeLa S3 cells above 100kHz to be steadily reduced as the medium conductivity is increased.

5.7 Discussion

Figures 5.1 to 5.8 show the dielectrophoretic collection spectra of a range of mammalian cell lines. The responses can, in general, be described in the following manner. At 1Hz a large, positive, collection is observed which decreases in magnitude with increasing field frequency. Between 20Hz and 100Hz a point of zero collection occurs (except for EL4-Bu.Ou6 and Mycl-3C7) past which the collection becomes negative reaching a constant, negative, collection rate between 200Hz and 1kHz. Above 1kHz the response becomes less negative and a second zero collection point is observed at approximately 5kHz. Increasing the field frequency still further causes the collection rate to increase reaching a second region of constant, positive, collection above 100kHz. A number of cell lines also exhibited a decrease in their dielectrophoretic responses above 1MHz.

The generalised dielectrophoretic response described above can partly be explained by considering the discussions of the previous chapters. Equation 3.6 describes the polarisability of a particle in terms of the permittivity and conductivity of the particle and suspending medium and is valid for frequencies above approximately 200Hz (section 4.6). Mammalian cells do not possess a porous cell wall as do the bacteria and yeast so far studied. The surface of a typical mammalian cell consists of the polar head groups of the membrane phospholipids interspersed with the membrane proteins. On the proteins and a number of the lipids are various sugar and

carbohydrate residues (the glycocalyx of the cell) and, in some cases, these can possess a net negative charge. Asami (1989) recently presented dielectric measurements on suspended mouse lymphoma cells and erythrocytes. These measurments were analysed by means of a double shelled sphere model of a cell. Using the values of permittivity and conductivity of each shell ($\varepsilon_s=6.8\varepsilon_o$, $\varepsilon_m=\varepsilon_i=80\varepsilon_o$, $\sigma_i=0.32Sm^{-1}$, $\sigma_s=10^{-5}\sigma_i$, $\sigma_m=10^{-3}Sm^{-1}$) as given by Asami (1989) in the single shelled sphere model used in chapter 3 the dielectrophoretic response of mammalian cells can be described. In this case the Maxwell-Wagner type dispersion at the interface between the membrane surface and the suspending medium (described by eqn. 3.5) occurs at around 7kHz whereas the dispersion at the interface between the membrane and cytoplasm occurs at around 10MHz. These results are in excellent agreement with the measurements and single shelled sphere analysis of the dielectrophoretic collection of slime cells recently reported by Marszatek et al (1989) where a region of negative collection was observed from 1kHz to 20kHz followed by a region of constant positive collection between 100kHz and 5MHz above which the collection was observed to reduce. For the mammalian cells studied here the conductivity of the suspending medium was greater than that of the cells and therefore, by eqn. 3.6, the dielectrophoretic force was directed away form the field producing electrodes giving a negative collection from 200Hz to around 5kHz. Above 5kHz the effective permittivity of the particle affects the collection. Since the permittivity of the cell is much greater than that of the medium the collection is positive. Around 5MHz the permittivity of the cell decreases in correspondence with the interfacial dispersion between the membrane and cytoplasm. For frequencies above this dispersion the dielectrophoretic force should theoretically be close to zero since the permittivities of the cytoplasm and suspending medium are similar.

The discussion of chapter 4 concluded that for frequencies below 200Hz the dielectrophoretic response of a particle cannot accurately be predicted by equation 3.6. It was also mentioned that the large low-frequency collection observed in bacteria and yeasts was thought to be due to a number of effects such as the electrophoretic movement of cells in low-frequency fields together with the slight increase in effective cell conductivity associated with the surface charge related α dispersion. From the dielectrophoretic spectra shown in figures 5.1 to 5.8 it can be seen that,

at low frequencies, the dielectrophoretic response of mammalian cells is large and towards the field-producing electrodes (confirmed by microscope observations). This is contrary to the response predicted by equation 3.6. Also, the slight increase in conductivity at low frequencies predicted by eqn.4.4 is not large enough to enable the dielectrophoretic force to become positive. Therefore the model presented in chapter 4 must be incomplete. The electrical double layer around a suspended charged cell can be described in terms of two charge distributions. Close to the negatively charged surface of the cell is a layer of positive ions which are closely associated with the negative surface charge groups on the membrane lipids and proteins. Beyond these are less weakly associated ions which form the diffuse region of the double layer.

The model of the double layer put forward by Schwarz (1962) consists of a charged dielectric sphere over the surface of which is a layer of closely associated ions. These ions are permitted to move tangentially over the surface of the sphere but are unable to move normally to the surface. Einolf and Carstensen (1971) improved on this model by allowing for the movement of ions normally to the surface of the sphere and found this gave a better theoretical prediction for the low-frequency dispersions measured in ion exchange resins. The Einolf model effectively takes into account the movement of ions from the diffuse region of the double layer into the bound (Stern) region of the double layer. However, in this latter model the ions in both the surface charge associated and the diffuse regions of the double layer have been assigned the same mobility. Pethig (1979), in discussing the mechanism of charge hopping describes in detail the hydration and association of an ion in a double layer. This discussion and subsequent calculations reveal that a potassium ion closely associated with a fixed charge and separated by a single water molecule has a mobility around 1/30th of that of a potassium ion in free solution. Therefore, it is suggested that the model for the low-frequency α dispersion presented in chapter 4 may not be universally applied. Substituting this difference in ionic mobility into eqns.4.3 and 4.4 shows the increase in effective cell conductivity due to the ionic double layer to be magnified. Calculations show at low frequencies the effective conductivity of the cell to be slightly above that of the suspending medium.

A second method for the analysis of the conductive properties of the electrical double layer uses the variation in the electric potential with distance away from the surface of the particle (as described by Pethig (1986) and shown in figure 5.17(a)). This variation in potential can be described by the following expressions

$$\Psi(x) = \frac{2RT}{ZF} \ln\left[\frac{1+\alpha \exp(-x/\lambda)}{1-\alpha \exp(-x/\lambda)}\right]$$

where

$$\alpha = \frac{\exp(ZF\Psi_s/2RT) - 1}{\exp(ZF\Psi_s/2RT) + 1}$$

and

$$\lambda_D = \left(\frac{\varepsilon_o \varepsilon_r k T}{2 q^2 n_b Z^2}\right)^{1/2}$$

where R, k, F, T, Z ,n_b and Ψ_s are the gas constant, Boltzmann constant, Faraday constant, temperature, ionic valency, ionic density and surface potential, respectively. Ψ_s can be found from the surface charge density, δ, using the following relationship

$$\delta = (8 n_b \varepsilon_r \varepsilon_o k T)^{1/2} \sinh(ZF\Psi_s/2RT)$$

It can be assumed that the majority charge carriers in the 320mM sucrose suspending medium are sodium and chlorine ions (Z=1 and -1 respectively) with a bulk sodium chloride concentration of approximately 100μM to give a medium conductivity of around 10^{-3} Sm^{-1}. Under these conditions the Debye screening length (the distance at which $\Psi(x)=0.37\Psi(0)$ for low surface potentials) is around 30nm. The variation in ionic concentration with distance from the particle will follow a Boltzmann distribution as described by eqn. 5.1

$$C(x) = C_{bulk} \exp[-ZF\Psi(x)/RT] \qquad 5.1$$

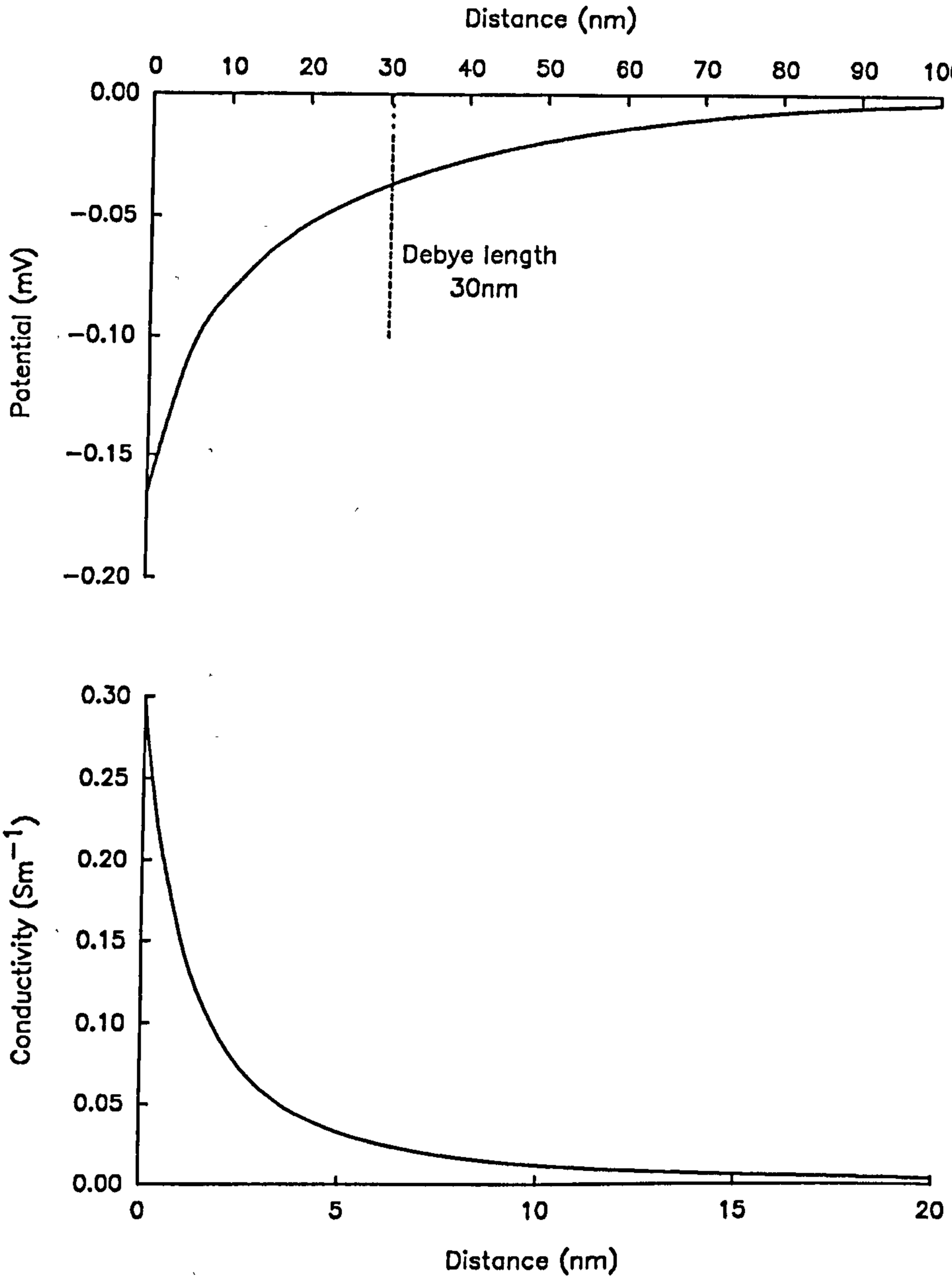

Figure 5.17 The variation in (a) electric potential and (b) conductivity of the electrical double layer with distance from the surface of a HeLa S3 cell. The high concentrations of cations in the double layer give rise to a high conductivity shell around the cell.

Using the general equation for the conductivity of a material given below

$$\sigma = n^+\mu^+q + n^-\mu^-q$$

where n^+, n^- and μ^+, μ^- are the number and mobility of cations and anions respectively it is possible to calculate the variation in double layer conductivity with distance from the particle surface. Figure 5.17 (b) shows this conductivity variation for a HeLa cell using electrophoretic measurements of the cell surface charge (discussed later in this section) to calculate the potential variation. It can be seen that close to the surface of the particle the conductivity of the double layer is almost a factor of 300 greater (equivalent to a 300 fold increase in sodium chloride concentration) than the bulk solution and for a distance up to at least 1 Debye length from the surface the conductivity is still greater than that of the bulk medium. This illustrates the limitations of considering only the bound region of the electrical double layer. It has been suggested (Al-Ameen, 1990) that the inclusion of polarisations related to the diffuse region of the double layer (Dukhin, 1974) may account for the large increase in the effective polarisability of the suspended cell enough to cause the dielectrophoretic force to become positive at low frequencies as shown in figures 5.1 to 5.8.

The dielectrophoretic response of KRO mycoplasma, shown in figure 5.9, is similar to the general response for a mammalian cell. However, the magnitude of the response is approximately 1/10th that of a mammalian cell. This can be accounted for by considering the relative sizes of the mycoplasma and mammalian cells where a typical mammalian cell has a volume approximately 4600 times that of the mycoplasma. In order to produce a sufficient change in optical absorbance to measure the dielectrophoretic response of mycoplasma, a higher concentration of cells was used than in previous experiments.

Mycoplasma (alternatively called pleuropneumonia-like-organisms after the highly infectious cattle disease) have been recognised since around 1910. However, it is only since the late 1950s that they have become a target of interest due to their interaction with mammalian cell lines. Mycoplasma are parasitic bacteria like cells which are now regarded as potential causes of

toxins to cell lines, rather than troublesome contaminants. Mycoplasma spend most of their life cycle outside cells but have an intracellular phase in this cycle. Nelson (1959) studied the effects of mycoplasma on HeLa cells. His results showed that initially the mycoplasma did not affect the cells but after three to four days a number of them were found to have degenerated, and by the twelfth to fourteenth day the cells were almost completely inactivated. The capacity of a number of mycoplasma to destroy cells in tissue culture has been well documented (Rovozzo et al, 1963, Kraemer et al, 1963 and Castrejon-Diez et al, 1963). Powelson (1961) has also reported that the metabolism of host cells is altered by the addition of mycoplasma.

In general mycoplasma are found both intracellularly and in the growth medium of a contaminated cell line. The aim of the experiments described in section 5.4 was to measure any differences between the dielectrophoretic response of mycoplasma, the host cell line and a contaminated sample of host cells. The surface of a mycoplasma is similar to that of a mammalian cell and consists of lipid head groups and protein structures. This similarity explains the almost identical form of the mycoplasma dielectrophoretic response compared to that of mammalian cells given in figures 5.1 to 5.8. In these experiments the host cell was a human nervous tissue line designated SK-4. The dielectrophoretic collection spectrum of this cell line is given in figure 5.10 together with the collection spectrum of a sample of SK-4 cells contaminated with KRO mycoplasma. The dielectrophoretic responses of the contaminated and uncontaminated samples are identical except for the frequency range 2Hz to 400Hz. In this frequency range the dielectrophoretic collection is greatly influenced by the net surface charge on the cell. The sample contaminated with mycoplasma shows a slightly increased collection from 40Hz to 200Hz. Edwards and Fogh (1959) reported that electron-micrographs of mycoplasma contaminated cells showed an intimate contact and possible joining of the cell and mycoplasma membranes. This may have the affect of increasing the overall surface charge on the host cell giving rise to slightly increased low-frequency collection. However, the spectra of figure 5.10 show that, because of the similarities in structure of mycoplasma and mammalian cells, it is unlikely that the method of dielectrophoresis can be used to selectively separate contaminating mycoplasma from a cell culture.

The second area of cell culture quality control to which dielectrophoresis was applied was that of viability determination. The viability of a cell culture is usually determined by either trypan blue exclusion counts or, more accurately, by a repeated dilution procedure and growth on nutrient agar plates. In the experiments described in section 5.5 HeLa S3 human cervical carcinoma cells were rendered non-viable by the addition of small amounts of formaldehyde to their growth medium. This technique is known to kill cells but to leave their physical structure virtually unaltered. Figure 5.11(a) shows the temporal variation in cell viability as measured from conventional exclusion counts. The rate at which cells become non-viable is exponential in form with a decay rate of approximately 1.5hrs for the first 3 hours after the addition of formaldehyde to the growth medium. After 3 hours the decay rate gradually changes to be around 6hrs at 14hrs after formaldehyde addition. Measurements of the dielectrophoretic collection rate (figure 5.11(a)) taken at a field frequency of 1kHz show the dielectrophoretic response to be negative for a fresh cell suspension sample. However, on the addition of formaldehyde to the sample the collection rate was observed to become more positive, also in an exponential manner and with a characteristic time constant of around 4.5 hrs. The difference between the forms of figures 5.11(a) and 5.11(b) shows that the mechanism for the take up of trypan blue dye and the physical parameters that control the magnitude of the dielectrophoretic force are not identical. However, figure 5.11 does show that there are measurable differences in the collection rates of cell suspensions with varying percentage viabilities. The graph of viability against collection (figure 5.18) shows it is possible to detect percentage viabilities of less that 30% with an accuracy of around 2%. However, as the collection becomes negative for higher viabilities the accuracy of detection reduces to be around 10% at 65% viability. This can be attributed to the inaccuracy of the measurement system for large negative forces due to the decrease in the magnitude of the applied electric field as the cells are repelled into the bulk suspension away from the field-producing electrodes.

Of greater interest are the graphs of figure 5.12, where a comparison of the dielectrophoretic collection spectra of both dead and live HeLa cells is made. The response of live HeLa cells is similar to that of figure 5.8 and shows the characteristic high collection at low frequencies

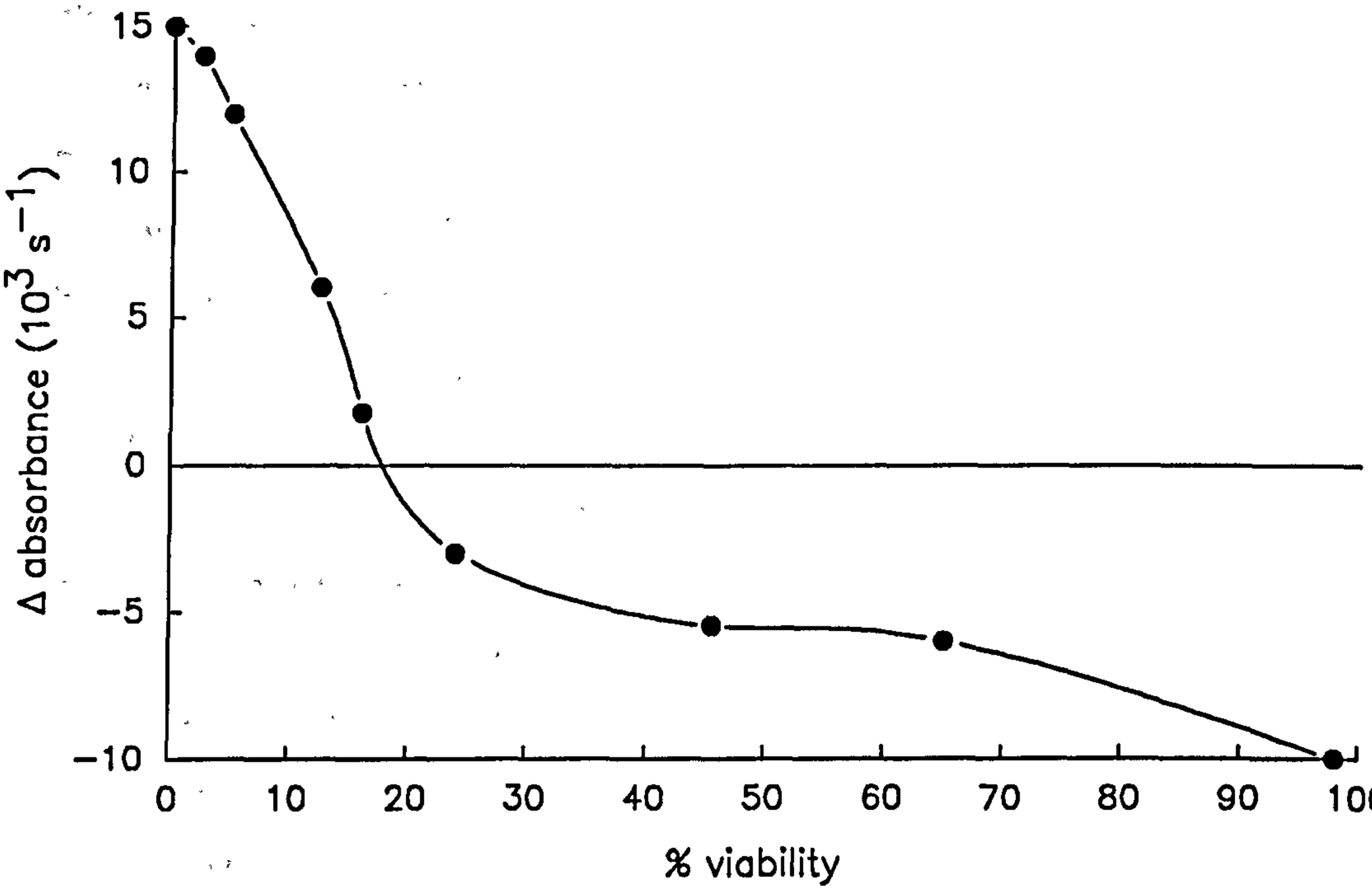

Figure 5.18 The percentage viability of HeLa S3 cells shown as a function of the dielectrophoretic collection rate at 1kHz.

followed by a region of negative collection before increasing to a constant positive collection rate at frequencies above 100kHz. The collection spectrum of dead cells has a similar form to the live HeLa cells except that it possesses no region of negative collection. In fact, in the frequency range 50Hz to 1kHz there is a relatively large positive collection. This can be attributed to the action of formaldehyde on the plasma membrane. It has long been known that aldehydes react with the amino groups of proteins and the reactions of formaldehyde in particular have been discussed in detail by French and Edsal (1945). Formaldehyde is used primarily in the fixation of cells for examination using microscopy and staining techniques. In high concentrations formaldehyde produces inter- and intra-molecular cross-linking in proteins by means of methylene (CH_2) groups (Schauenstein et al 1977, Zubay 1983). This treatment effectively stops the membrane proteins from functioning by fixing their structure and possibly their position within the membrane, so making the membrane of the cell more rigid. The results of figure 5.12 indicate that this decrease in the fluidity of the cell membrane causes an increase in the effective conductivity of the cells at frequencies below 10kHz. The exact mechanism for this increase in conductivity is not known, but is thought to be related to the cumulative effect of an increased ability for charge transport over the membrane surface caused by methylene bridge cross-linking and by a slight increase in the permeability of the membrane to ions due to a number of the trans-membrane ions channels being effectively fixed in an "open" configuration.

Figure 5.19 shows the collection spectrum of dead HeLa cells normalised to that of live cells at a frequency of 200Hz. This normalisation effectively removes the increased collection around 200Hz caused by an increase in cell conductivity and allows the low-frequency responses of both dead and live cells to be studied. A comparison shows that the rate of collection of dead cells is greater than that of live cells in the region 1Hz to 100Hz. If the conclusion that the magnitude of the low-frequency dielectrophoretic response is influenced by the magnitude of the net surface charge on the cell is correct, then according to figure 5.19, treatment with formaldehyde would be expected to increase the net cell surface charge of HeLa cells. Figure 5.20 shows electrophoretic measurements of the variation in cell surface charge for a range of

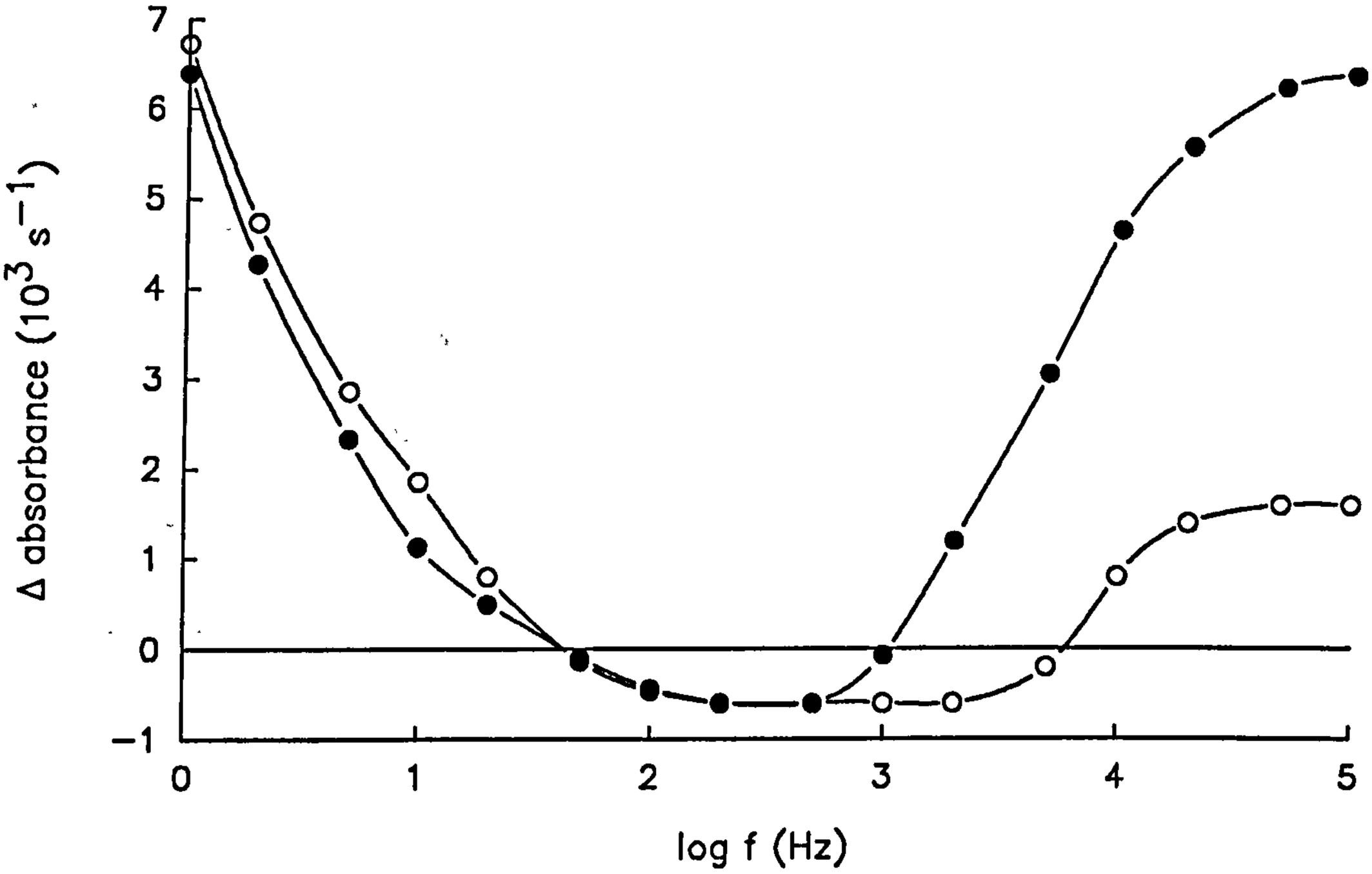

Figure 5.19 A comparison of the low-frequency collection of HeLa S3 cells. The graph shows the responses of live (●) and formaldehyde treated (O) cells normalised at a field frequency of 200Hz.

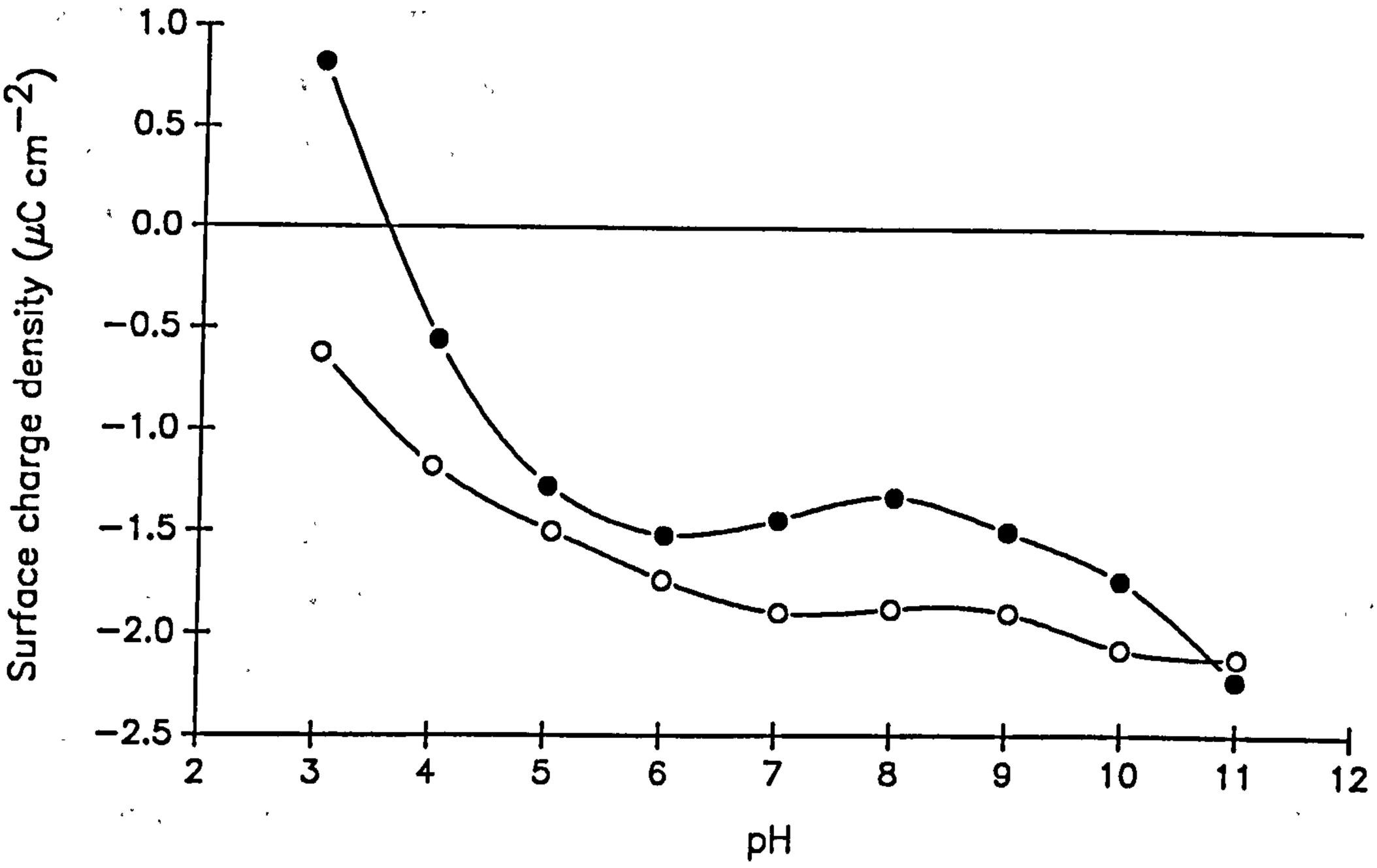

Figure 5.20 The variation in the net surface charge density of live (●) and formaldehyde treated (O) HeLa S3 cells as a function of pH.

suspending medium pHs from 3 to 11 for both live and formaldehyde treated HeLa cells. These measurements were made with the help of Mr Phil Parsonage (Warren Spring Laboratory) using a Malvern Instruments Zetasizer II microelectrophoresis and laser particle sizing system made available by the Warren Spring Laboratory, Stevenage, U.K.. The electrophoretic measurements show that over the pH range 3 to 10 the formaldehyde treated cells possess a larger (more negative) surface charge than the untreated cells being 30% larger at pH 7, a measurement in agreement with those of Mayhew and Nordling (1966). This confirms the conclusion that the low-frequency dielectrophoretic collection is, to some degree, influenced by the surface charge on the measured particles.

Figures 5.13 and 5.14 show the temporal effects of formaldehyde treatment on the collection spectra of HeLa cells. It can be seen that, with increasing treatment time, the effective conductivity of the cell is increased (shown by the increase in collection rate in the frequency range 200Hz to 1kHz). Also observable is a decrease in the effective permittivity of the cell. The decrease in permittivity can be explained in terms of the increased rigidity of the cell membrane reducing the mobility of surface dipoles and hence decreasing their ability to follow any applied alternating electric field. Figures 5.13 and 5.14 also show that although changes in cell surface charge and permittivity occur within the first 30 minutes of treatment (shown by an increased low-frequency collection) the conductivity of the cell does not change rapidly until after at least 3.5hrs (after over 75% of the cells have been rendered non-viable). This observation acts as an example of the complex mechanisms which occur on the surface of a cell membrane and their individual relationships to the viability of a cell.

In order to confirm the observed effects of medium conductivity on the dielectrophoretic response of cells, the collection spectra of live and dead (formaldehyde treatment for 24hrs) HeLa cells were measured for medium conductivities of 0, 0.005, 0.01, 0.02 and 0.03Sm^{-1}. Figures 5.15 and 5.16 show the responses obtained. For live cells the effects of medium conductivity are identical to those discussed in chapter 4 with a reduced collection rate in the frequency range 10Hz to 10kHz and an increase in the frequency at which the collection becomes positive, as described by eqn.3.5 and discussed earlier in this section. The collection

above 10kHz (that controlled by the permittivity of the cell) is reasonably unaffected by the medium conductivity, with the reduced collection observed for the $0.03Sm^{-1}$ medium being mainly due to the loading effect of the electrode system on the signal generator used in the experiments. However, the effects of medium conductivity on the response of the formaldehyde treated cells shows that in the permittivity controlled region of the collection spectrum the response reduces as the medium conductivity is increased. This may be attributed to the increased number of ions passing through the trans-membrane channels which have been fixed in an "open" configuration, where an increase in the conducting properties of a material must lead to a decrease in its dielectric properties. This final set of experiments adds experimental confirmation to the theoretically derived formula (eqn. 3.6) used in previous chapters to describe the magnitude of the dielectrophoretic force in terms of the dielectric properties of the suspended particle.

5.8 References

Al-Ameen, T.A.K. (1990) *Theoretical and Practical Aspects of Dielectrophoresis* University of Wales Ph.D. thesis.

Asami, K., Takahashi, Y. and Takashima, S. (1989) Dielectric Properties of Mouse Lymphocytes and Erythrocytes. *Biochim. Biophys. Acta* **1010** 49-55.

Castrejon-Diez, J., Fisher, T.N. and Fisher, E. (1963) Experimental Infection of Tissue Cultures with certain Mycoplasma (PPLO). *Proc. Soc. Exp. Biol. N.Y.* **112** 643-647.

Dukhin, S.S. and Shilov, V.N. (1974) *Dielectric Phenomena and the Double Layer in Disperse Systems and Polyelectrolytes.* J. Wiley and Sons, Chichester.

Edwards, G.A. and Fogh, J. (1959) Fine Structure of Pleuropneumonia-like-organisms in Pure Culture and in Infected Tissue Culture Cells. *J. Bact.* **79** 267-276.

Einolf, C.W. and Carstensen, E.L. (1971) Low Frequency Dielectric Dispersions in Suspensions of Ion-exchange Resins. *J. Phys. Chem.* **75** 1091-1099.

French, D. and Edsall, J.T. (1945) The Reactions of Formaldehyde with Amino Acids and Proteins. *Adv. Prot. Chem.* **2** 277-325.

Kraemer, P.M., Defendi, V., Hayflick, L. and Manson, L.A. (1963) Mycoplasma (PPLO) strains with Lytic Activity for Murine Lymphoma Cells in vitro. *Proc. Soc. Exp. Biol., N.Y.* **112** 381-387.

Marszalek, P., Zielinski, J.J. and Magdalena, F. (1989) Experimental Verification of a Theoretical Treatment of the Mechanism of Dielectrophoresis. *Bioelectrochem. and Bioenerg.* **22** 289-298.

Mayhew, E. and Nordling, S. (1966) The Electrophoretic Mobility of Fixed Tissue Culture Cells: Studies with Formaldehyde and Osmium Tetroxide. *Exp. Cell. Res.* **43** 72-76.

Nelson, J.B. (1959) The Behaviour of Murine PPLO in HeLa Cell Cultures. *Ann. N. Y. Acad. Sci.* **79** 450-457

Pethig, R. (1979) *Dielectric and Electronic Properties of Biological Materials.* John Wiley and Sons, Chichester.

Pethig, R. (1986) Ion, Electron, and Proton Transport in Membranes: A Review of the Physical Processes Involved. In *Modern Bioelectrochemistry* (ed.) Gutmann, F. and Keyzer, H. Plenum Publishing Corp.

Powelson, D.M. (1961) Metabolism of Animal Cells Infected with Mycoplasma. *J. Bact.* 82 288-297.

Rovozzo, G.C., Luginbuhl, R.E. and Helmboldt, C.F. (1963) A Mycoplasma from a Bovine Causing Cytopathogenic Effects in Calf Kidney Tissue Culture. *Cornell Vet.* 53 560-566.

Schauenstein, E., Esterbauer, H. and Zollner, H. (1977) *Aldehydes in Biological Systems.* Pion, London.

Schwarz, G. (1962) A Theory of the Low Frequency Dielectric Dispersion of Colloidal Particles in Electrolyte Solutions. *J. Phys. Chem.* 66 2636-2642.

Zubay, G.L. (1983) *Biochemistry.* Addison-Wesley.

CHAPTER 6

MEASUREMENTS ON NORMAL AND TRANSFORMED MAMMALIAN CELLS

6.1 Introduction

In the previous chapter the dielectrophoretic collection spectra of a number of mammalian cell lines were characterised. The information gained from this was used to help interpret differences between the dielectrophoretic responses of live and "dead" HeLa cells killed by treatment with formaldehyde. In contrast to the rather dramatic changes in physiology a cell undergoes on death are the subtle differences between normal, healthy, mammalian cells and their cancerous counterparts. In the experiments described here dielectrophoresis is used as an analytical, investigative technique to monitor differences between the electrical properties of normal and cancerous cells.

Neoplastically transformed mammalian cell membranes have frequently been observed to have electrical properties which differ from those of cells of normal phenotype. It has been suggested that these differences may be related to the genesis and maintenance of the malignant state (Bingelli et al 1980, Boonstra et al 1981, Cone 1974, Lai et al 1984 and Price et al 1987). To study such effects dielectrophoretically four transformed cell lines, which could be chemically induced to revert to a near-normal phenotype, were investigated. The cell lines used, HL60, DS19, DR10 and R1, are classified as erythroleukaemia cells and are transformed precursors of red blood cells that have not differentiated beyond the stage of colony forming cells. They are established and well-characterised (Harris and Ralph 1985, Marks et al 1987) as models for the study of cell differentiation because of their susceptibility to a variety of chemical agents which

can, in some clones, induce varying degrees of differentiation up to an advanced step of erythroid differentiation that has much in common with the late steps of the normal nuclear extrusion process (Malik et al 1985). HL60 is a human leukaemia line originally isolated from a patient with acute promyelocytic leukaemia (Gallagher et al 1979) whereas the remaining cell types are classified as Friend murine erythroleukaemia (MEL) lines due to their expression of Friend leukaemia virus (Rossi and Friend 1967).

Although the cell lines have a range of responses to inducing agents, only the agents Dimethylsulphoxide (DMSO) and Hexamethylene bisacetamide (HMBA) were used in these experiments. Clone HL60 is known to be induced to differentiate by DMSO whereas DS19 is inducible by both DMSO and HMBA. DR10 cells are, however, resistant to DMSO but inducible by HMBA and finally R1 cells are resistant to both DMSO and HMBA. This range of properties has enabled experimental comparisons to be made of the effects of each agent and allowed specific areas of the dielectrophoretic response to be further investigated.

6.2 Materials and Methods

Friend murine erythroleukaemia (MEL) clones R1, DS19 and DR10 were seeded in suspension cultures in 300ml of medium, supplemented with 10% foetal calf serum and 1mM glutamine, and gassed with 5% CO_2/air mixture. The cultures were seeded at a density of 10^5 cells ml^{-1} in Gibco minimum essential medium (Gibco, USA) containing 1μg ml^{-1} gentamycin. Cells were passaged every 2 or 3 days so that the cell density was always kept below 10^6 ml^{-1}. The cultures were harvested by centrifugation (600 x g for 7 minutes) and were counted using a haemocytometer. Cell viabilities were determined by trypan blue dye exclusion to ensure a viability greater than 95%.

To examine the effects of the inducing agents, cells were seeded in culture media supplemented with 4mM hexamethylene bisacetamide (Sigma, USA) or 1% dimethylsulphoxide (Sigma, USA) and grown for up to 4 days without refeeding. Parallel cultures were grown under identical conditions, except for the absence of inducing agents, and served as controls in all experiments.

To test the contribution of cell surface charge to the dielectrophoretic response, fresh human blood, collected in EDTA, was washed 3 times in Hank's buffered saline solution containing 3mg ml^{-1} gloucose. The cells were resuspended in 10ml of this same solution containing 0.25 units of neuraminidase (Sigma, USA n-2133 Type X from *Clostridium perfrigens*) and incubated for 40 minutes at 37°C with an occasional agitation to keep the cells suspended. A parallel sample prepared in the same manner but without the addition of neuraminidase served as a control.

Harvested cells were washed three times in a 320mM sucrose plus 3mg ml^{-1} gloucose solution made with double distilled, triple deionised water. After the final wash, cells were resuspended in this same solution, which served as the suspending medium for the dielectrophoretic measurements, to a cell concentration that gave an optical absorbance of 0.26 at 635nm for a 1cm pathlength. The conductivity of the cell suspensions, determined using a conductivity bridge (Radiometer type CDM2f, Copenhagen), was less than 650μSm^{-1} in all experiments. The use of glucose in the previously discussed (chapter 5) 320mM sucrose solution suspending media was found essential in maintaining the glycocalyx of the cells when using water of such a low conductivity. The glucose allows the cell to continue to regulate trans-membrane processes in the absence of essential ions such as calcium. Failure to maintain cell glycocalyx was found to causes a reduction in cell viability and density. In experiments using red blood cells, which are unable to self-regulate membrane processes, 1μM $CaCl_2$ was added to the suspending medium. This greatly aided the maintenance of cell integrity without significantly increasing the electrical conductivity of the final cell suspensions. Trypan Blue exclusion counts revealed that the cell viability after 3 washes and resuspension in the dielectrophoresis medium was between 89% and 94%.

Dielectrophoretic measurements were carried out using the dielectrophoresis spectrometer and associated experimental technique described in chapter 4. A 16 volt peak-to-peak sinusoidal voltage was applied to the field-producing-electrodes in the sample chamber and a fresh aliquot of cell suspension was used for each frequency reading. The dielectrophoretic response at each measurement frequency between 1Hz and 2MHz was determined from the change in optical

absorbance of the cell suspension over the first 15 seconds after the application of the a.c. voltage to the electrodes. The collection spectra were measured at 20°C with each frequency reading being made twice in order to avoid possible errors. The untreated cell responses were also repeated 2 to 3 days later on freshly grown cells to confirm the reproducibility of the results.

6.3 Effects of Inducing Agents on Transformed Cells

The collection spectra described in this section are similar in form to those of the HeLa cells discussed earlier. As previously, the form of the spectra is described in terms of cell surface charge, effective conductivity and effective permittivity. The major difference between the following collection spectra and those previously described is the lack of any region of negative collection. This can in part be explained by the use of a suspending medium of much lower conductivity than previously available.

The cell suspensions used to obtain the results described in the following sections all had an optical absorbance of 0.26 at 635nm wavelength. Figure 6.1 shows the variation in optical absorbance with cell concentration for DS19 cells. The presence of a linear region in this graph from 0.0A to 0.4A implies that Beer's Law holds in this region. The differences between the curves for treated and untreated cells is due to the induced (HMBA treated) cells containing small amounts of haemoglobin. The HL60 and MEL cells used were all of similar size and composition so it was assumed that Beer's Law held for all cell lines suspended at such low concentrations.

6.3.1 HL60 cells

Figure 6.2 shows the dielectrophoretic response of HL60 cells grown with and without 1% DMSO for 4 days. At low frequencies, up to 200Hz, the responses of the treated and untreated cells were virtually identical in shape. However, the DMSO treated cells had a response that is

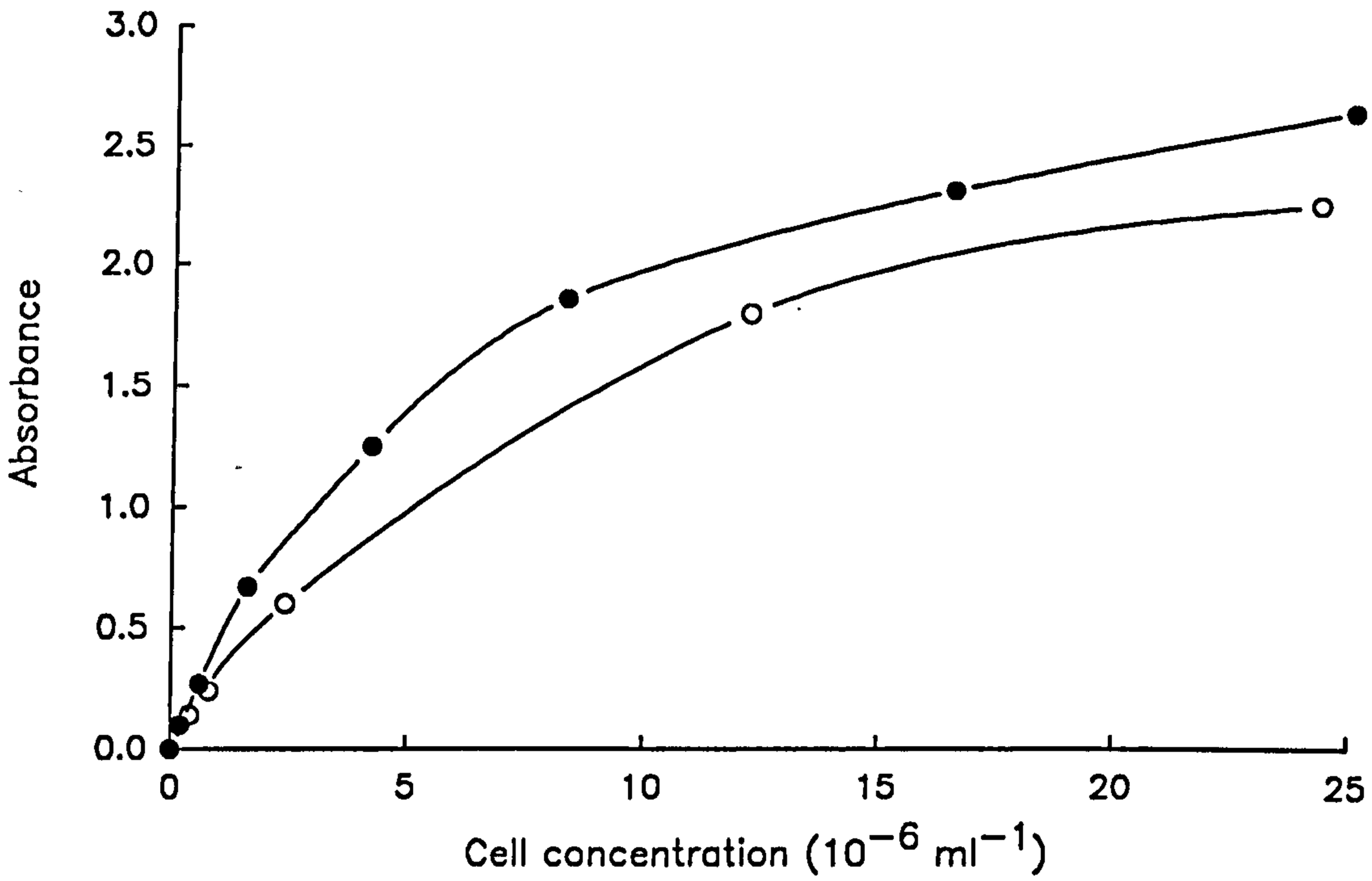

Figure 6.1 The absorbance of clone DS19 cells washed in 320mM sucrose + 3mg ml^{-1} glucose solution before (●) and after (O) treatment with HMBA.

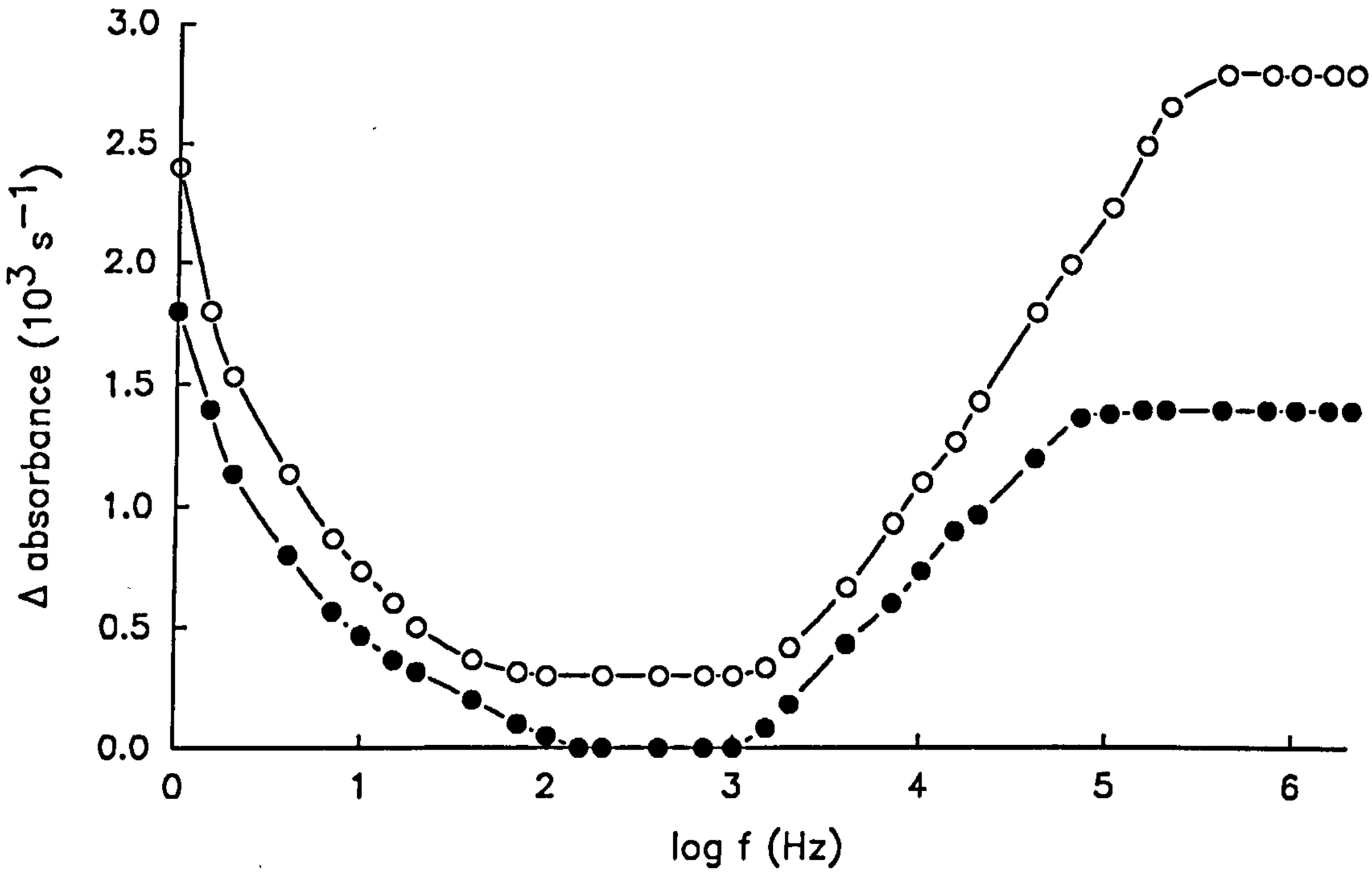

Figure 6.2 The dielectrophoretic response of clone HL60 cells before (●) and after (O) treatment with DMSO. The treated cells have an increased conductivity and permittivity.

shifted in magnitude by between 2mA and 4mA. Examining the response above 200Hz revealed consistently greater responses in the conductivity and permittivity dictated regions.

The increase in the responses of the treated cells between 1Hz and 2kHz can be explained as an increase in the effective conductivity of the cells caused by the DMSO. It has earlier been suggested that surface charge effects are responsible for the low-frequency dielectrophoretic response, up to approximately 200Hz. However, the similarity of the low-frequency responses implies that the surface charge of HL60 cells does not change on treatment with DMSO. The increase in response above 2kHz can similarly be explained as an increase in the effective permittivity of the treated cells.

6.3.2 DS19 cells

The dielectrophoretic response for clone DS19 before, and after, induction by HMBA is shown in figure 6.3. For frequencies below 30Hz the treated cells had a lower dielectrophoretic response than the untreated cells which, as indicated in chapter 4, implied that the treated cells had a reduced surface charge. This result is in agreement with cell micro-electrophoresis data for DS19 obtained by Gascoyne et al (1989). The dielectrophoretic spectrum shows a larger response for the treated cells in the frequency range 30Hz to 70kHz, which indicates that, as a result of HMBA treatment, the effective conductivity of the cells is increased. For frequencies above 70kHz the collection was independent of treatment showing that the cell permittivity was unchanged by the HMBA. It has also been noted by Gascoyne et al (1989) that as clone DS19 progresses beyond the colony-forming stage to that of terminal differentiation, as evidenced by haemoglobin production and the loss of the ability to grow in soft agar, the average diameter of the cell decreases by approximately 12%. Equation 2.16 shows that if the volume of a particle experiencing a dielectrophoretic force is reduced then the force experienced will be reduced proportionally. Hence any observed reduction in the size of the cell after treatment with HMBA serves to magnify the observed increase in effective cell conductivity.

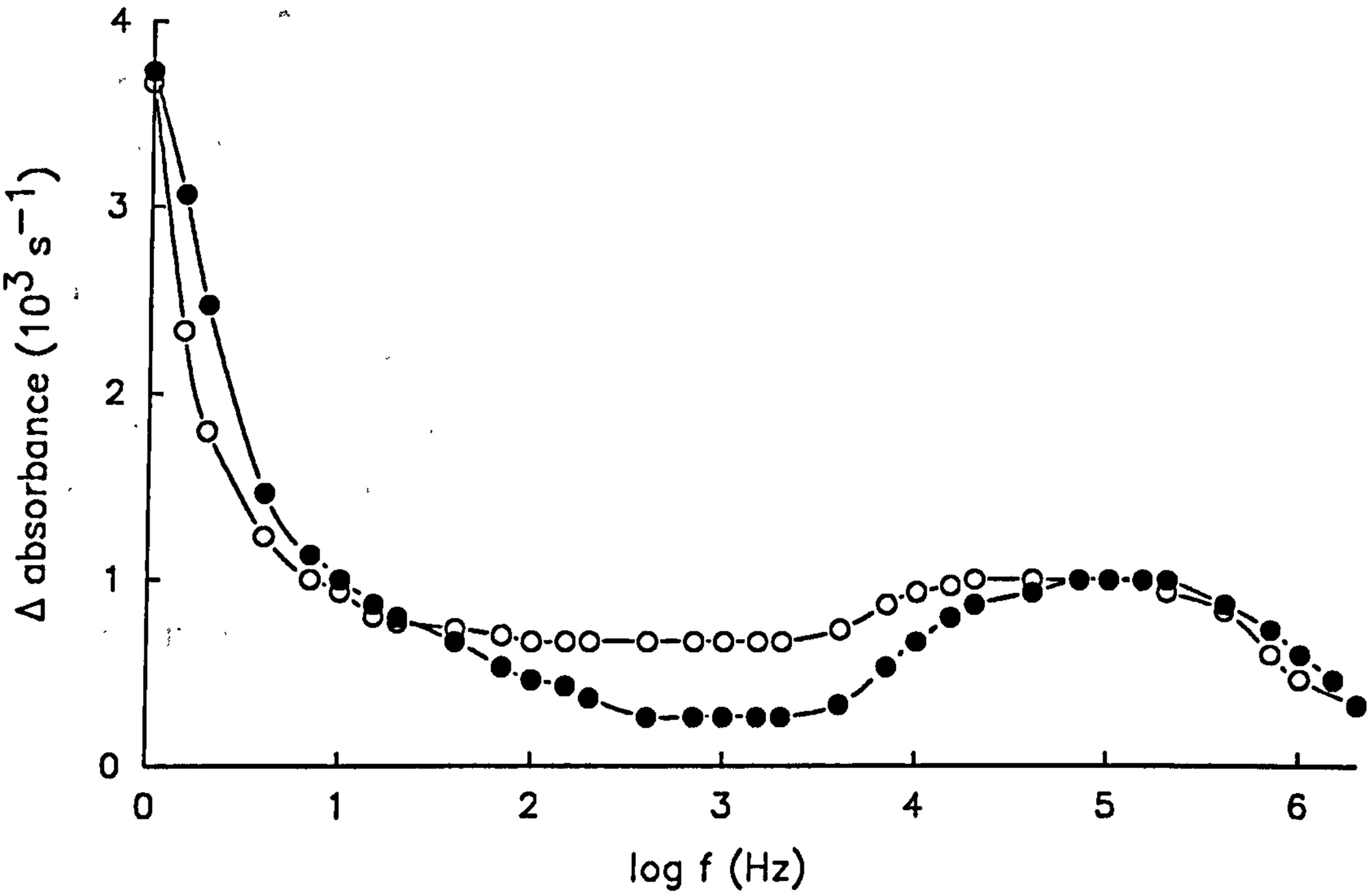

Figure 6.3 The dielectrophoretic response of clone DS19 cells before (●) and after (O) treatment with HMBA. The treated cells have a lower surface charge and larger effective conductivity.

6.3.3 DR10 cells

Clone DR10 is characterised by a differential response to the inducing agents HMBA and DMSO. Whereas this clone responds to HMBA treatment by producing haemoglobin and losing its ability to grow in soft agar, it is resistant to DMSO, which is a strong inducing agent for DS19 (Gascoyne et al, 1989). The dielectrophoretic responses in Figure 6.4 show that after treatment with HMBA the DR10 cells lost surface charge, indicated by a reduction in the response below 100Hz, and gained in effective conductivity, indicated by an increase in response between 100Hz and 5kHz. Above 5kHz the dielectrophoretic response was also increased showing an increase in the permittivity of the cells on HMBA treatment. As shown in figure 6.5, however, after treatment with DMSO the dielectrophoretic characteristics of the DR10 cells remained unchanged over the whole frequency range, implying that DMSO treatment had no effect on the surface charge, conductivity or permittivity of DR10 cells.

6.3.4 R1 cells

The dielectrophoretic responses for clone R1 with and without HMBA treatment are shown in figure 6.6. Unlike DS19, clone R1 does not produce haemoglobin or lose its ability to grow in soft agar after treatment with inducing agents and is therefore classified as being non-inducible (Gascoyne et al, 1989). Figure 6.6 shows the dielectrophoretic response below 200Hz to be reduced on HMBA treatment, indicating, as in the case of DS19, a reduction in cell surface charge. This result is also consistent with micro-electrophoresis measurements where clone R1 was found to lose net surface charge in the same way as clone DS19 after exposure to HMBA (Gascoyne et al, 1989). For frequencies above 200Hz the response remained unchanged showing that HMBA treatment had no effect on either cell conductivity or permittivity.

6.4 Investigations of Surface Charge and Conductivity Effects

The results described above have shown that inducing agents have greatest effect, electrically speaking, on the surface charge and effective conductivity of the cells. To further investigate

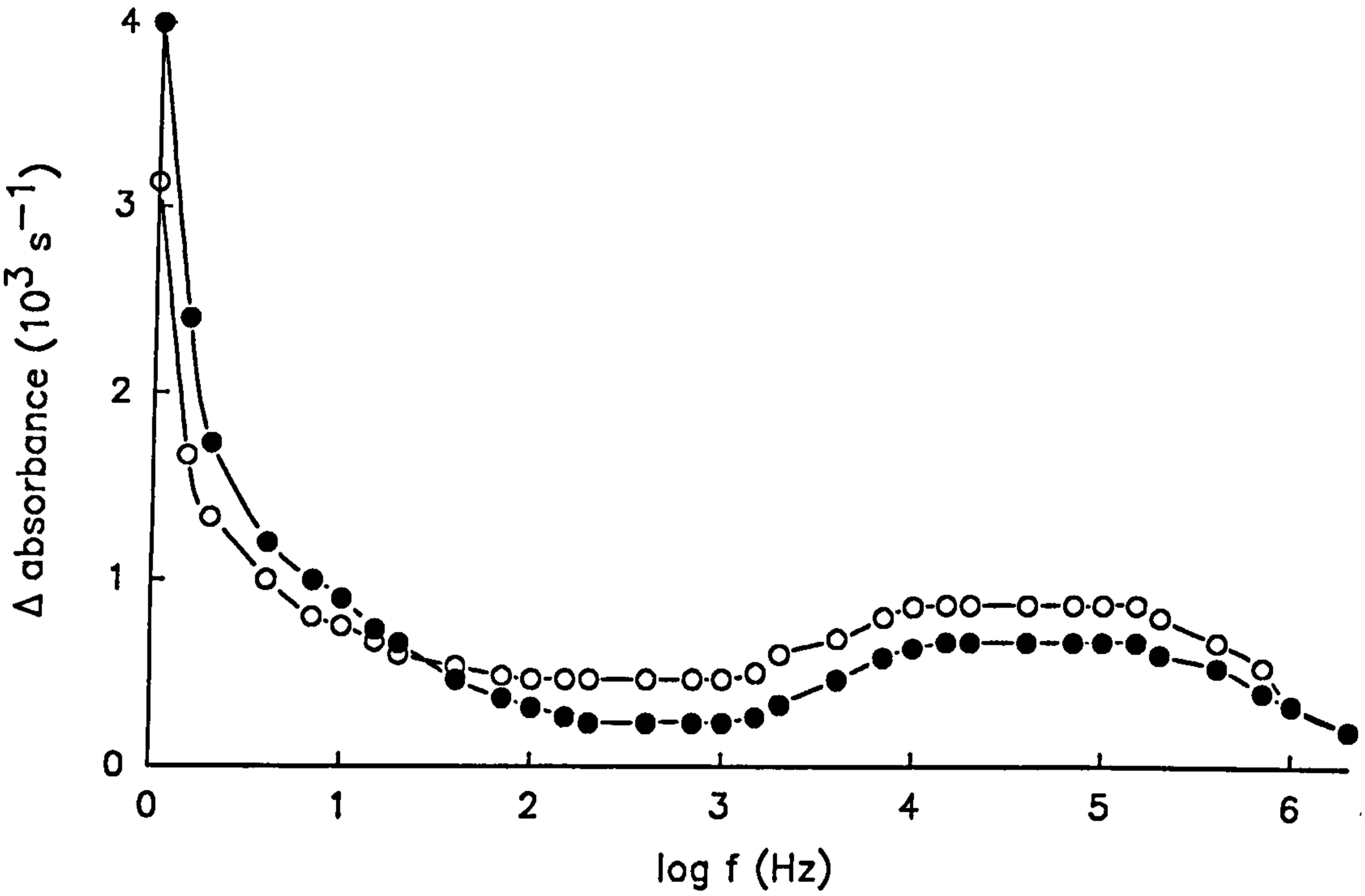

Figure 6.4 The dielectrophoretic response of clone DR10 cells before (●) and after (O) treatment with HMBA. The treated cells have a reduced surface charge and increased conductivity and permittivity.

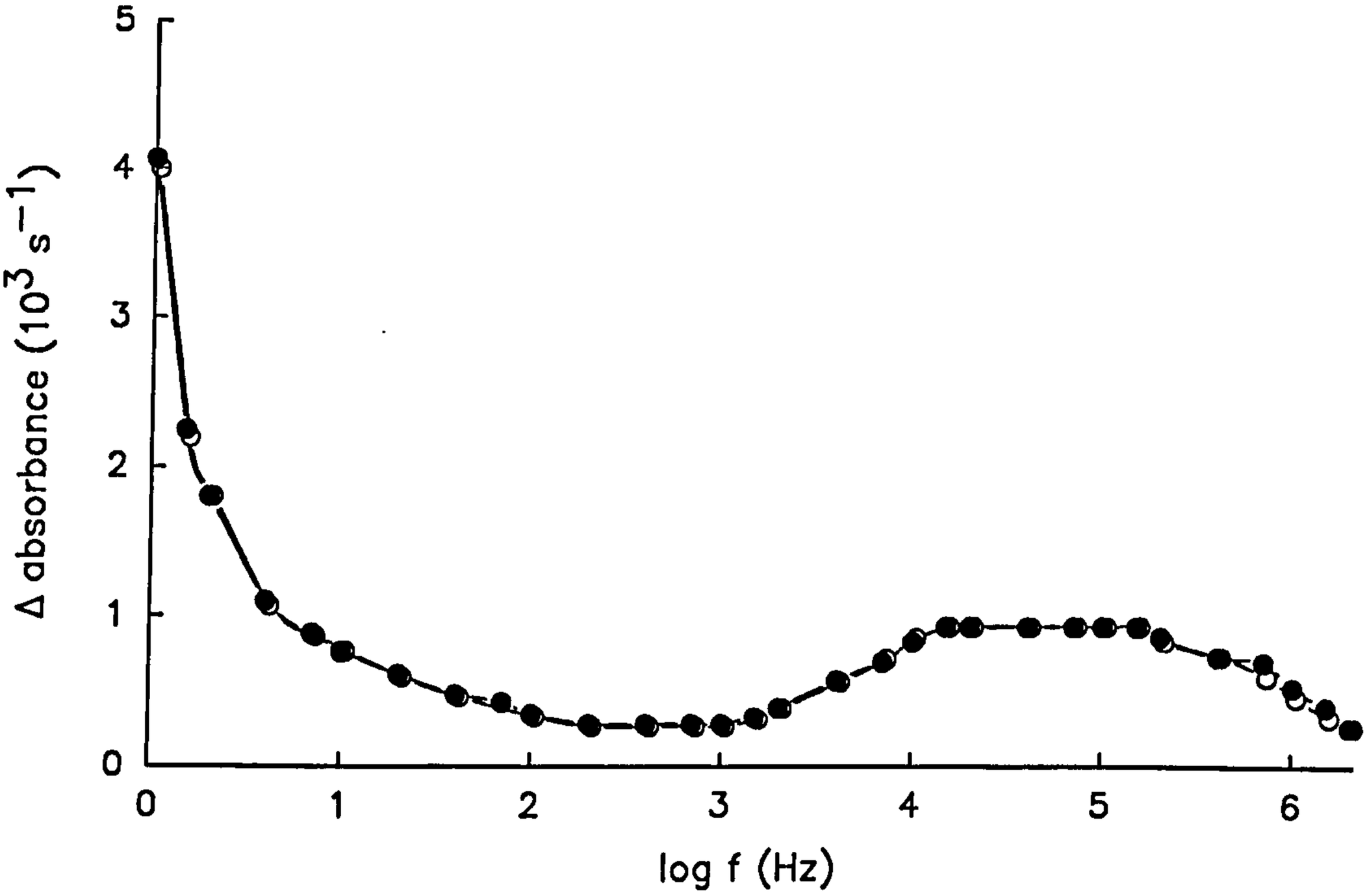

Figure 6.5 The dielectrophoretic response of clone DR10 cells before (●) and after (O) treatment with DMSO to show that no observable changes occur in the electrical properties of the cells.

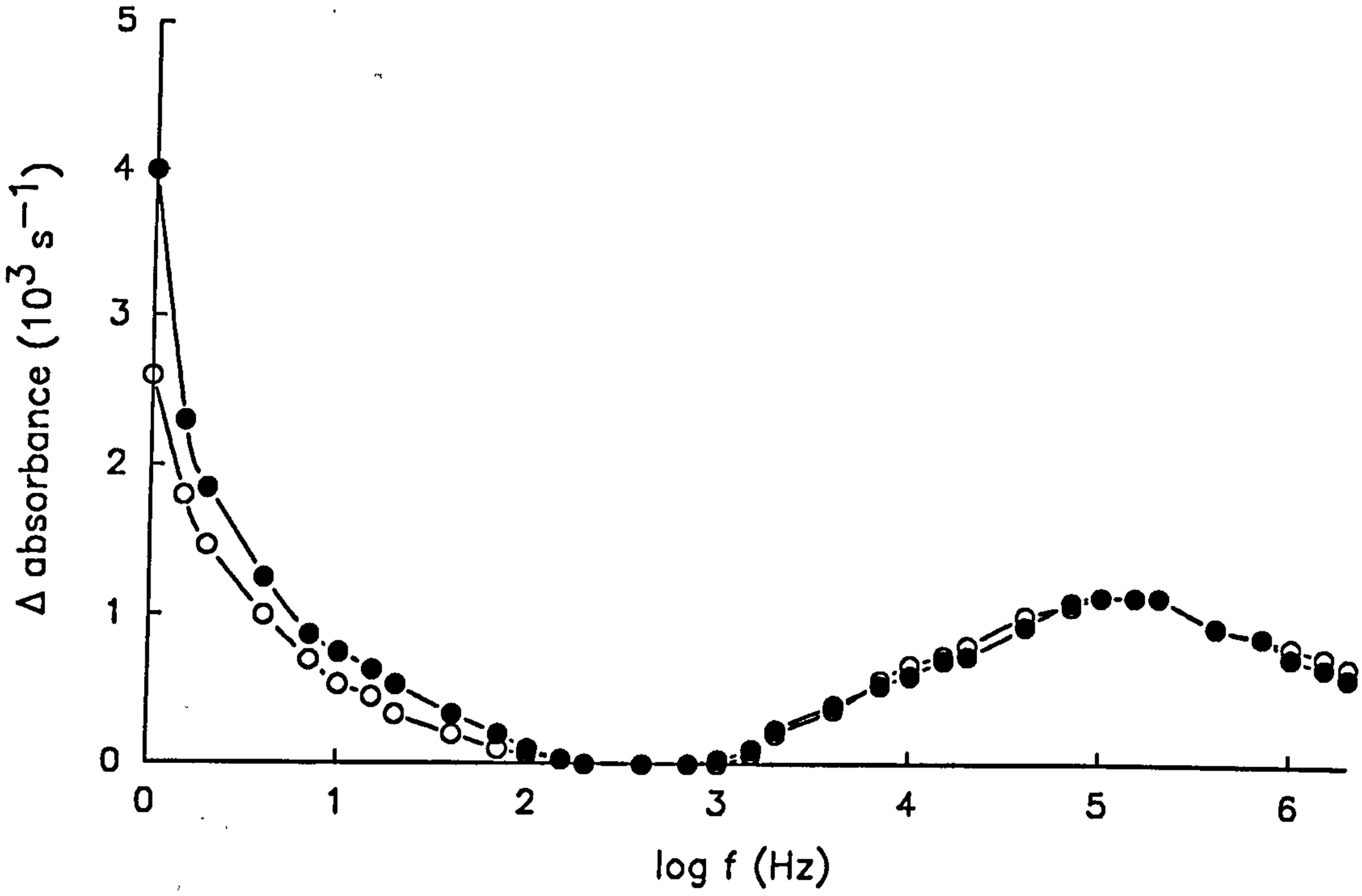

Figure 6.6 The dielectrophoretic response of clone R1 cells before (●) and after (O) treatment with HMBA. The treated cells have a slightly smaller surface charge but unchanged conductivity and permittivity.

these regions the following experiments were carried out using the enzyme neuraminidase to alter the surface charge of the cells and the soap saponin to alter the cell conductivity.

6.4.1 Effects of Neuraminidase on Cell Surface Charge

Treatment with neuraminidase is a well tested method for reducing charge associated with sialic acid residues on the cell membrane surface. Following the treatment described here the micro-electrophoretic mobility of the blood cells was found to have decreased by 50% from 1.01×10^{-8} $m^2V^{-1}s^{-1}$ to 0.56×10^{-8} $m^2V^{-1}s^{-1}$, showing that the net cell membrane surface charge had been halved. The spectra of figure 6.7 show that the neuraminidase treated cells exhibited a clear decrease in dielectrophoretic collection rate below 50Hz. The unchanged response above 50Hz demonstrates that the effective conductivity of the cell membrane was not changed by this treatment. This result supports the conclusion of chapter 4 that cell surface charge influences the dielectrophoretic behaviour only in the low-frequency range.

6.4.2 Effects of Saponin on Cell Conductivity

To investigate the contribution of membrane conductivity to the overall effective conductivity of the cell, fresh harvested R1 cells were treated with saponin (40µg ml^{-1}) for 5 minutes. This treatment has been shown (Wassler et al 1987) to porate the cell membrane and permeabilise it without causing a major loss of cytoplasmic protein. The effect of this treatment is shown in figure 6.8, where the effective membrane conductivity appeared to be slightly increased as evidenced by the increased dielectrophoretic response in the frequency range 100Hz to 1.5kHz. The saponin treatment had no effect outside this frequency range implying that saponin does not appreciably effect the cell surface charge or effective permittivity. It is of interest to note that the increase in effective conductivity due to saponin treatment is small compared to that incurred by treatment with inducing agents .

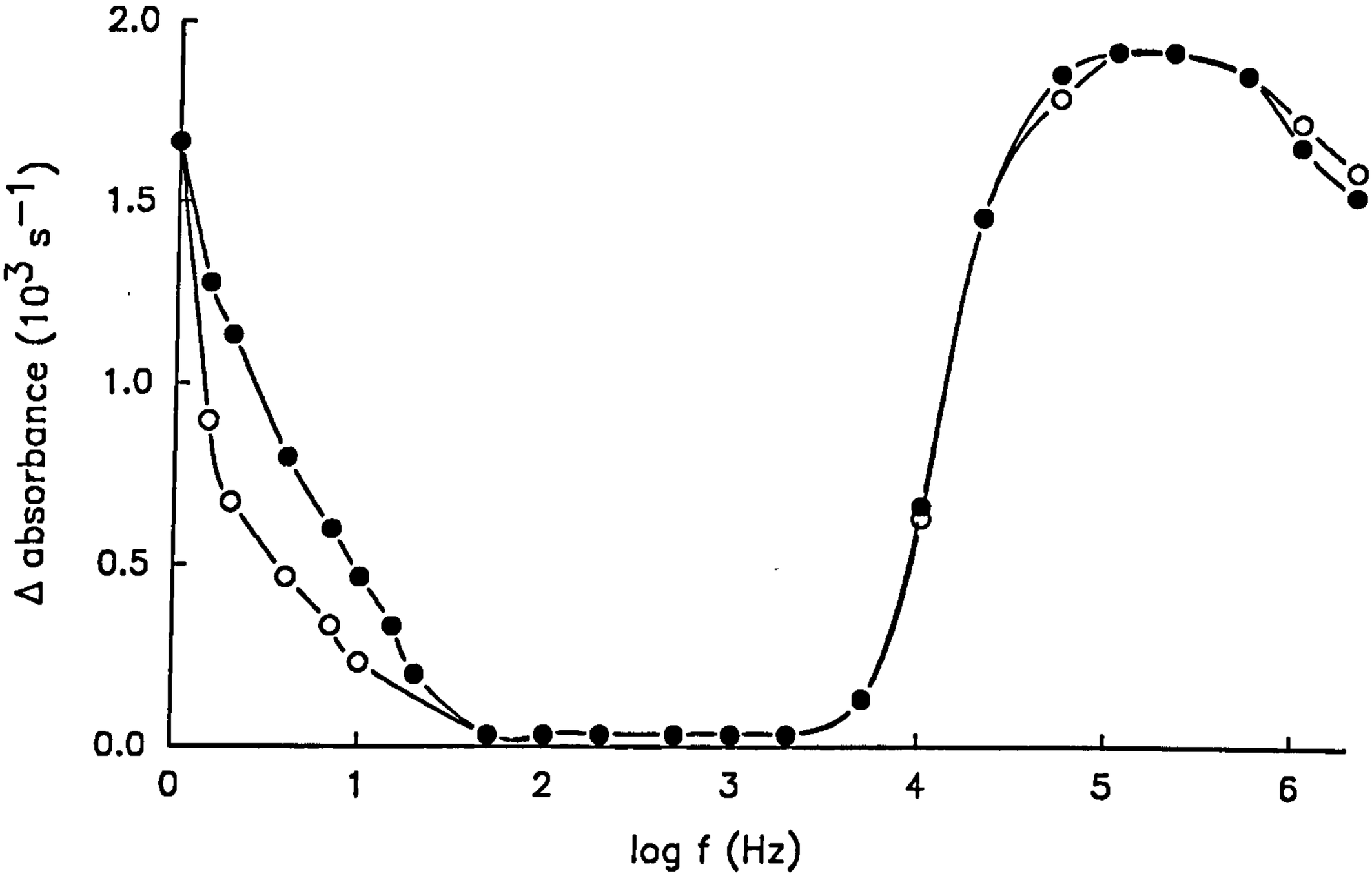

Figure 6.7 The dielectrophoretic response of human red blood cells before (●) and after (O) neuraminidase treatment. The treated cells have reduced surface charge.

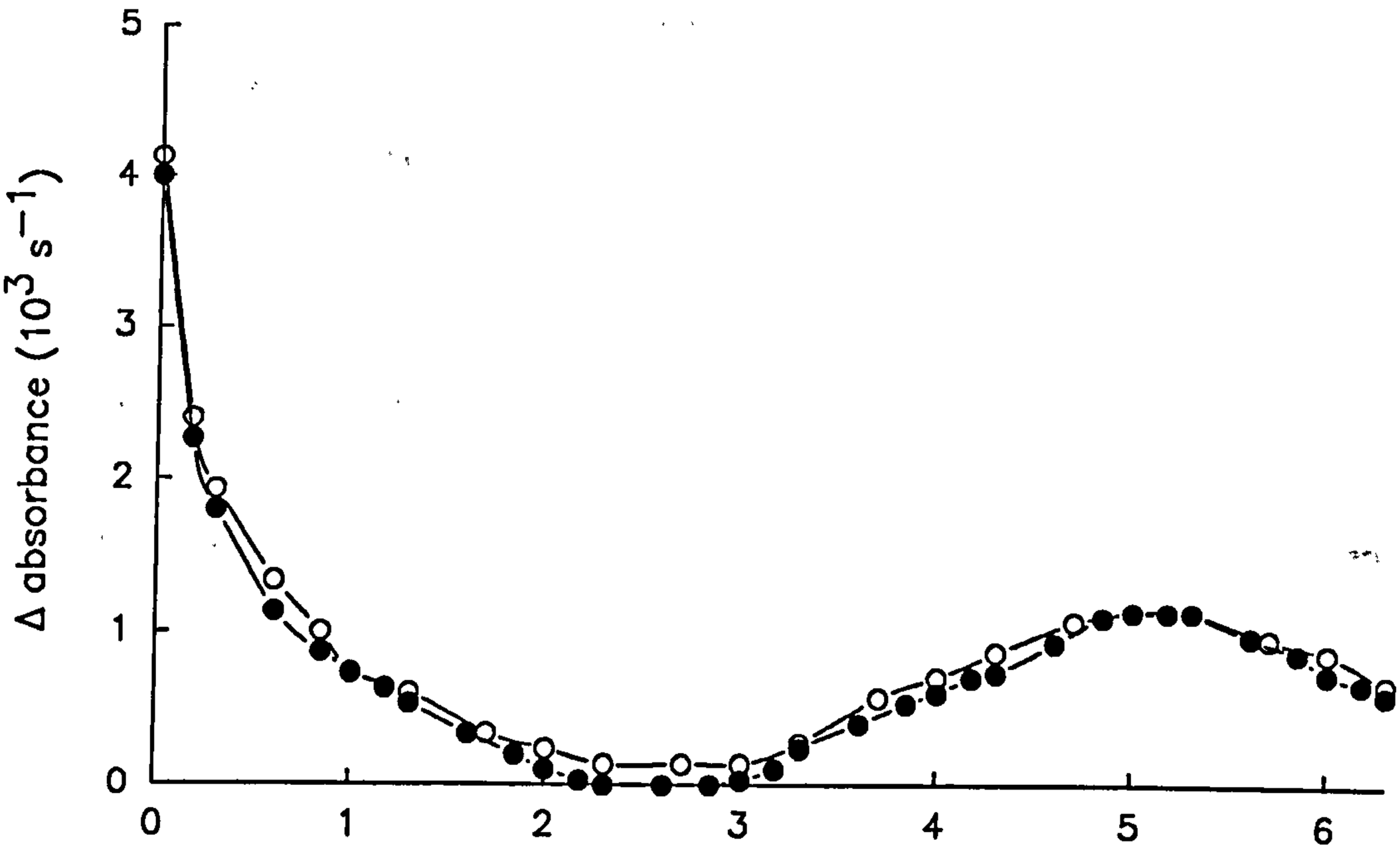

Figure 6.8 The dielectrophoretic response of clone R1 cells before (●) and after (O) saponin treatment, indicating that saponin slightly increases the effective cell conductivity.

6.5 Discussion

In general indicators of differentiation in erythroleukaemia cell lines, following treatment with inducing agents, are the expression of haemoglobin, reduction in cell and nuclear size and the inability to grow in soft agar. The results described in sections 6.3 and 6.4 show that the erythroleukaemia cell lines studied here also exhibit a number of changes in their electrical properties when treated with inducing agents. As discussed previously, in the frequency range used for these experiments the electrical changes observed are related to cell membrane processes.

It was suggested in chapters 4 and 5 that the low-frequency dielectrophoretic response is related to the presence of a net cell surface charge giving rise to a combination of dielectrophoretic forces, electrophoretic forces and various electrical double layer effects. Murine erythroleukaemia lines, DS19, DR10 and R1, all exhibited a reduction in cell surface charge when treated with HMBA. Figure 6.9 shows this reduction in surface charge as a function of growth (Gascoyne et al 1989) for DS19 and R1 cells. The change in surface charge can be explained as a cumulative effect of the many differences between normal and transformed cells. Sato et al (1979) and Brown et al (1979) presented results which investigated the form of the cell surface charge on both normal and transformed cells. These experiments, using a variety of enzymes to cleave charge groups from the cell surface, indicated that transformed cells have a greater number of anionic hyaluronidase and neuraminidase sensitive groups present than comparable normal cells. Price et al (1987) showed that temperature transformed rat kidney cells (6m2) had a higher proportion of RNAase sensitive charge groups than their non-transformed phenotype. It has also been reported (Ip and Cooper, 1980) that changes as subtle as the percentage composition of the various types of phospholipids (such as negatively charged phosphatidylserine and neutral phosphatidylethanolamine) that make up the bulk of the bilayer membrane, is altered by inducing agents such as DMSO. In previous experiments, changes in cell surface charge have been observed dielectrophoretically as a result of a treatment to the cell as a whole, as in the case of MEL cells with HMBA treatment and HeLa cells with formaldehyde treatment (chapter5). Neuraminidase is an enzyme with reacts with sialic groups

Fig 6.9

on the cell surface and does not enter or affect any other part of the cell. Figure 6.6 shows that human red blood cells treated with this enzyme had a consistently lower dielectrophoretic response from 1Hz to 100Hz, with the response being effectively halved at 4Hz. Paralleled with this are electrophoretic measurements on cells, from the same batch as that used in the dielectrophoretic experiments, which confirm reduction in cell surface charge of approximately 50% from 1.01×10^{-8} $m^2V^{-1}s^{-1}$ to 0.56×10^{-8} $m^2V^{-1}s^{-1}$ and give experimental support to these earlier conclusions.

Another significant finding (figure 6.8) is the fact that saponin produces only a small effect on the dielectrophoretic properties of R1 cells. This can be quantified by calculating the change of effective cell conductivity after saponin treatment. The theory for this has been detailed in chapter 3 where it was shown that at low frequencies the polarisability parameter α of eqn. 2.16 reduces to the expression

$$\alpha = \varepsilon_o \varepsilon_m \frac{\sigma_p - \sigma_m}{\sigma_p + 2\sigma_m}$$

where the subscripts p and m refer to the particle and suspending medium respectively. Calculations based on 1kHz measurements show that treating DS19 and DR10 cells with HMBA increases their effective conductivity (compared to that of treating R1 cells with saponin) by a factor of 3 and 1.67 respectively. Saponin, a soap, is known (Wassler et al 1987) to dissolve small holes in the phospholipid bilayer membrane of a cell large enough to allow some macromolecules to escape and to depolarise the membrane without causing a major loss of cytoplasmic protein. Such a treatment would be expected to increase the trans-membrane conductivity much more than HMBA treatment which allows the trans-membrane potential to be maintained. For frequencies below 100kHz the overall effective conductivity σ_p of the cell, can be written as (Schwan et al, 1962)

$$\sigma_p = \sigma_b + \frac{2K_s}{a} \qquad 6.1$$

where a is the cell radius. In this formula, which has been used with success in investigations of the surface conductance of latex particles (Arnold et al, 1987) and in electrorotation studies of various types of cell (Arnold and Zimmermann, 1988), the parameter σ_b can be taken to represent the membrane bulk conductivity, since the cell membrane effectively shields the cell interior from the applied electric field (Schwan, 1988). In other words the cell is considered to be a poorly conducting particle of high relative permittivity (Schwan, 1988) and σ_b represents the effective conductivity of that region of the membrane penetrated by the applied electric field. As already mentioned, the passive membrane bulk conductivity is generally very small and a typical case is the low-frequency (10Hz) anion conductance value of around $60mSm^{-2}$ for erythrocyte membranes (Takashima et al, 1988). For a membrane thickness near 8nm this gives a membrane conductivity of about $0.5nSm^{-1}$. The largest membrane conductivity value reported appears to be that of $140Sm^{-2}$ for oocytes (Arnold et al, 1989), which for a typical membrane thickness gives a σ_b value of around $1\mu Sm^{-1}$. No definite values have been derived for the surface conductance K_s of animal cells, but of possible relevance is the value of 1nS obtained for carboxylate latex particles (Arnold, 1987). For a cell radius of 5 μm and a similar K_s value, then the corresponding value for the factor $2K_s/a$ in eqn.6.1 is $400\mu Sm^{-1}$. The conductivity of the cell suspending medium was of the order $340\mu Sm^{-1}$, and for positive dielectrophoresis to be observed the effective conductivity σ_p of the cells must be greater than this.

The fact that HMBA treatment of DS19 cells produces a 3 times greater change in conductivity than the treatment of R1 cells with saponin implies, for R1 cells at least, that the effective conductivity seen in dielectrophoresis experiments is largely controlled by tangential surface conductivity processes, rather than by trans-membrane charge transport.

An interesting and new finding is that from figures 6.2 and 6.3 it can be seen that when a cell line is induced to differentiate, the mid frequency dielectrophoretic response (and hence the effective cell conductivity) is increased. Examination of figure 6.6 shows that no such effect occurs if the cell line is resistant to the inducing agent. This result is mirrored in the results of figures 6.4 and 6.5, which show that the effective conductivity of DR10 cells is increased by

HMBA treatment, but is not altered by DMSO treatment. These results suggest that cell induction is accompanied by an increase of the effective cell conductivity.

The exact mechanism for the increase in cell conductivity is not known. However, several contributing factors are suggested here. As experiments with saponin have shown, the gain in conductivity cannot arise from an increase in trans-membrane conductivity since neither HMBA nor DMSO depolarise the cell membrane, unlike saponin which does. Section 4.6 investigated the low-frequency dielectrophoretic collection from 1Hz to 200Hz and concluded this to be due to a combination of electrophoretic movements and a slight increase in effective cell conductivity around the surface of the cell due to the polarisation of the diffuse double layer. As the electric field frequency is increased from 1Hz up to 200Hz the amount of electrophoretic movement the cell experiences rapidly decreases as does the conductivity component due to the electrical double layer around the cell. Until above 200Hz these two effects have a negligible effect on the dielectrophoretic response. Following on with this argument, any increase in cell conductivity at frequencies above 200Hz must be related to the movement of charges associated with the cell membrane, since at frequencies below 5MHz the applied electric field does not penetrate the interior of the cell (e.g. Pethig and Kell, 1987)

A major factor affecting cell conductivity is that of membrane fluidity. Ip and Cooper (1980) reported that treatment with HMBA and DMSO was found to make the membranes of HL60 and MEL cells more rigid. A less fluid membrane may allow for easier charge transport over its surface since any conduction paths created by the more ordered structure are less likely to be disrupted by the movement of the lipids and proteins that make up the membrane. The main cause of the reduction in cell membrane fluidity is an increase in the cholesterol content of the membrane (up to 37% more cholesterol is present in DMSO treated HL60 cells compared to untreated cells, Ip and Cooper 1980). Cholesterol molecules orientate themselves in the bilayer with their hydroxyl groups close to the polar head groups of the phospholipid molecules; their plate-like steroid rings interact with, and partly immobilises regions of the hydrocarbon chains of the phospholipid closest to the head group leaving the rest of the chain flexible, as shown in figure 6.10. The presence of the cholesterol hydroxyl group close to the phosphate group of the

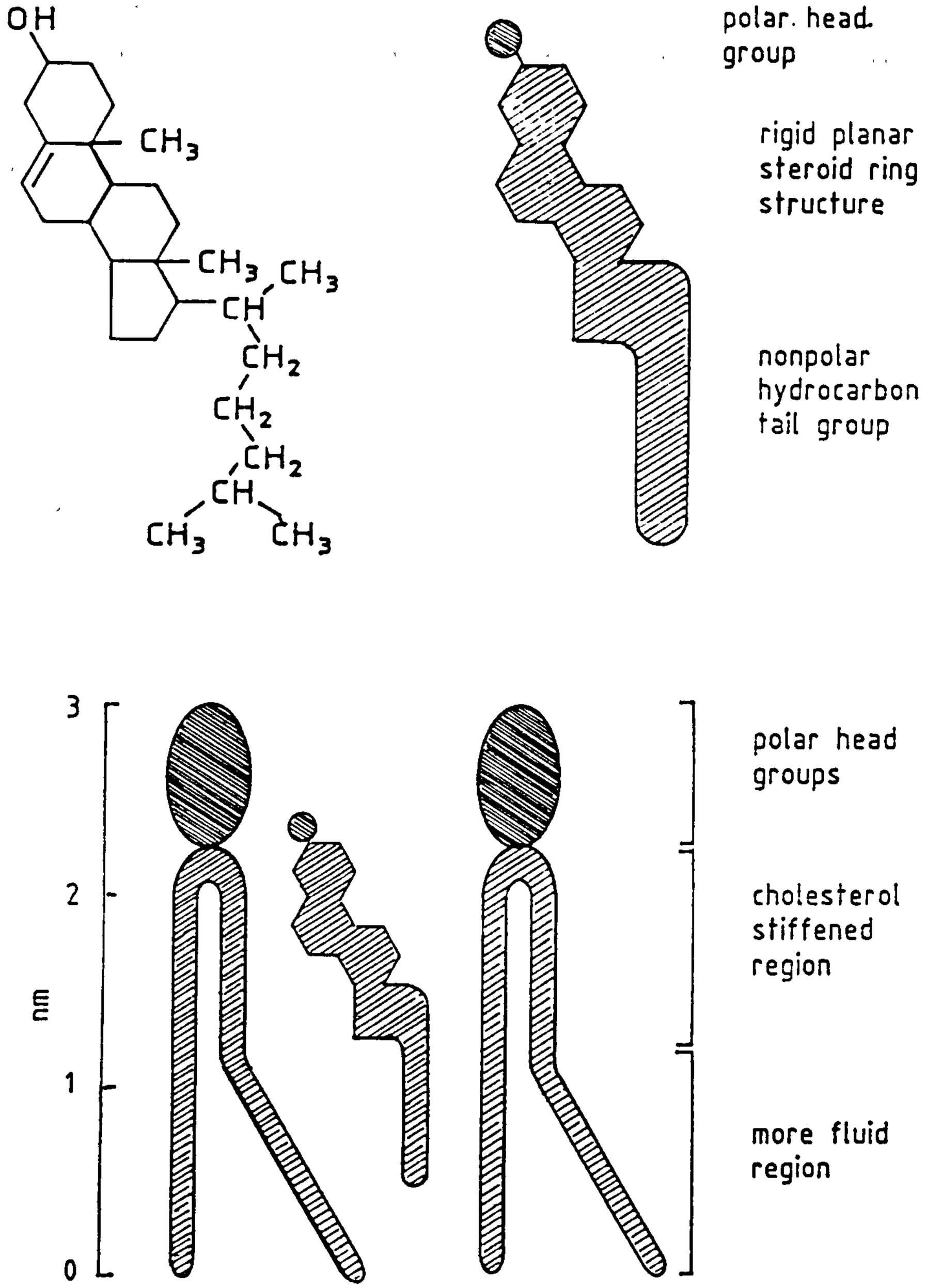

Figure 6.10 A schematic drawing of cholesterol interacting with two phospholipid molecules in a monolayer.

phospholipid may aid the movement of delocalised ions or protons over the surface of the membrane as well as acting to increase the effective length of the phospholipid dipolar head group. This increase in effective cell conductivity with increasing membrane rigidity is in agreement with the results of chapter 5 where a similar observation was made for formaldehyde treated cells

The results discussed above have shown that there are a number of electrical differences between transformed mammalian cells and cells of comparable normal phenotype. The differences in the bioelectrical properties of these cells give rise to the possibility of separating cancerous cells from body fluids (such as blood) as well as using dielectrophoresis as a possible analytical tool for the study of cells and the cancerous state.

6.6 References

Arnold, W.M., Schwan, H.P. and Zimmermann, U. (1987) Surface Conductance and Other Properties of Latex Particles Measured by Electro-rotation. *J. Phys. Chem.* **91** 5093-5098.

Arnold, W.M. and Zimmermann, U. (1988) Electro-rotation: Development of a Technique for Dielectric Measurement on Individual Cells and Particles. *J. Electrostastics* **21** 151-191.

Arnold, W.M., Schmutzler, R.K., Al-Hasani, S., Krebs, D. and Zimmermann, U. (1989) Differences in Membrane Properties Between Unfertilised Single Rabbit Oocytes Demonstrated by Electro- rotation Comparison with Cells from Early Embryos. *Biochim. Biophys. Acta* **979** 142-146.

Bingelli, R. and Cameron, I.V. (1980) Cellular Potentials of Normal and Cancerous Fibroblasts and Hepatocytes. *Cancer Res.* **40** 1830-1845.

Boonstra, J., Mummery, C.L., Tertoolen, L.G.J., Van Der Saag, P.T. and DeLaat, S.W. (1981) Cation Transport and Growth Regulation in Neuroblast Cells. Modulation of K^+ Transport and Electrical Membrane Properties During Cell Cycle. *J. Cell Physiol.* **238** 420-435.

Brown, A.E., Case, K.R., Bosmann, H.B. and Sartorelli, A.C. (1979) Cell Surface Charge Alterations Occurring during Dimethylsulfoxide -Induced Erythrodifferentiation of Friend Leukemia Cells. *Biochem. Biophys. Res. Commun.* **86** 1281-1287.

Cone, C.D. (1974) The Role of Surface Electrical Trans-Membrane Potential in Normal and Malignant Mitogenesis. *Ann. N.Y. Acad. Sci* **107** 75-83.

Gallagher, R., Collins,S., Trajillo, J., McCredie, K., Ahearn, M. Tsai,S., Metzgar, R., Aulakh, G., Ting, R., Rucetti, F. and Gallo, R. (1979) Characterisation of the Continuous Differentiating Myeloid Cell Line HL60 from a Patient with Acute Promyelocytic Leukaemia. *Blood* **54** 713.

Gascoyne, P.R.C. and Becker, F.F. (1989) Alterations in Electrophoretic Mobility, Diaphorase Activity and Terminal Differentiation Induced in Murine Erythroleukemia Lines by Differentiating Agents. *J. Cell Physiol.* **142** 309-315.

Harris, P. and Ralph, P. (1985) Human Leukaemic Models of Myelomonocytic Development: A Review of the HL60 and U937 Cell Lines. *J. Leuk. Biol.* **37** 407-422.

Ip, S.H.C. and Cooper, R.A. (1980) Decreased Membrane Fluidity During Differentiation of Human Promyelocytic Leukaemia Cells in Culture. *Blood* **56** 227-232.

Lai, C-N., Gallick, G.E., Arlinghaus, R.B. and Becker F.F. (1984) Temperature-Dependent Trans-Membrane Potential Changes in Cells Infected with a Temperature-Sensitive Maloney Sarcome Virus. *J. Cell Physiol.* **121** 139-142.

Malik, Z., Lugaci, H. and Hanania, J. (1985) Stimulation of Friend Erythroleukaemic Cell Cytodifferentiation by 5-aminolevulinic Acid: Porphyrins, Cell Size, Segregation of Sialogycoproteins and Nuclear Translocation. *Exp. Hematol.* **16** 330-335.

Marks, P.A., Sheffery, M. and Rifkind, R.A. (1987) Induction of Transformed Cells to Terminal Differentiation and the Modulation of Gene Expression. *Cancer Res.* **47** 659-660.

Pethig, R. and Kell, D.B. (1987) The Passive Electrical Properties of Biological Systems: their Significance in Physiology, Biophysics and Biotechnology. *Phys. Med. Biol.* **32** 933-970.

Price, J.A.R., Pethig, R., Lai, C-N., Becker, F.F., Gascoyne, P.R.C. and Szent-Gyorgyi, A. (1987) Changes in Cell Surface Charge and Trans-Membrane Potential Accompanying Neoplastic Transformation of Rat Kidney Cells. *Biochim. Biophys. Acta.* **898** 129-136.

Rossi, G.B. and Friend, C. (1967) Erythrocytic Maturation of (Friend) Virus-Induced Leukaemic Cells in Spleen Clones. *Proc. Natl. Acad. Sci. USA* **58** 173-1380.

Sato, C., Kojima, K., Nishizawa and K. Ikawa, Y. (1979) Early Decrease in Hyaluronidase-Sensitive Cell Surface Charge during the Differentiation of Friend Murine Erythroleukemia Cells by Dimethylsulfoxide. *Cancer Res.* **39** 1113-1117.

Schwan, H.P., Schwarz, G., Maczuk, J. and Pauly, H. (1962) On the Low-frequency Dielectric Dispersion of Colloidal Particles in Electrolyte Solution. *J. Phys. Chem.* **66** 2626-2635

Schwan, H.P. (1988) Dielectric Spectroscopy and Electro-rotation of Biological Cells. *Ferroelectrics* **86** 205-223.

Takashima, S., Asami, K. and Takahashi, Y. (1988) Frequency Domain Studies of Impedance Characteristics of Biological Cells Using Micropipet Techniques. *Biophys. J.* **54** 995-1000.

Wassler, M., Jonasson, I., Persson, R. and Fries, E. (1987) Differential Permeabilization of Membranes by Saponin Treatment of Isolated Rat Hepatocytes: Release of Secretory Proteins. *Biochem. J.* **247** 407-415.

CHAPTER 7

CONCLUSIONS

In this work a number of experiments have been carried out with the aim of further understanding the physical parameters which determine the properties of the dielectrophoretic force. Through the design of a novel optical measurement system for obtaining the dielectrophoretic collection rate of particles it has been possible to quickly and accurately measure the responses of a range of cell lines. These experiments have investigated responses for bacteria, yeasts and mammalian cells using a range of medium conductivities and have assessed how medium conductivity affects the collection of cells. Other experiments have investigated the effects of specific treatments such as chemical inducement and cell wall removal on the responses of cells. The results of these experiments have enabled the large amount of general background information for the application of dielectrophoresis to biotechnology to be amassed, as well as allowing a number of observations on the electrical properties of cells to be made. These experiments can be summarised as follows:

Initial experiments studied the responses of three bacteria, *Micrococcus lysodeikticus*, *Escherichia coli* and *Bacillus subtilis*. It was found that each bacteria possessed a broadly similar collection characteristic with differences noted at frequencies below 100Hz and around 100kHz. Further experiments to study the effects of medium conductivity on the dielectrophoretic response suggested that below a characteristic frequency the dielectrophoretic force was controlled by the differences in cell and medium conductivities (eqn. 3.7). For a cell conductivity greater than that of its suspending medium the force was directed towards the regions of highest field strength, whereas a cell conductivity less than the medium conductivity caused the force to be directed away from the regions of highest field intensity. These

experimental observations were verified by a theoretical consideration of the dielectrophoretic force. Throughout the work described here experiments were carried out on different cell lines to assess the limitations of this conductivity dependence to biotechnological applications of dielectrophoresis.

Improvement to the optical measurement system enabled measurements to be carried out on particles up to 40μm in diameter over the frequency range 1Hz to 4MHz. Low frequency measurements revealed a large, previously unreported, increase in collection with decreasing field frequency below 100Hz. This collection was interpreted as an increase in the effective low-frequency conductivity of the cell caused by the polarisation of the electrical double layer around a cell, a conclusion verified by experiments using the enzyme neuraminidase, which is known to cleave charge groups form the surface of red blood cells . Results from studies using mammalian cells revealed that this increase in conductivity could, close to the surface of the cell, be a factor of 300 greater than the conductivity of the suspending sucrose medium used.

Other experiments with mammalian cells studied the effects of the preservative formaldehyde on the response of HeLa cells. Here the formaldehyde rendered the cells non-viable by "fixing" proteins in the cell. The effect of this was to cause the plasma membrane to become more rigid. Dielectrophoretically the formaldehyde caused an increase in the mid frequency (100Hz to 1kHz) region, an effect comparable to an increase in the effective conductivity of the cell. Also noted in the dielectrophoretic spectrum was a increase in the large low-frequency collection which was attributed to an increase in the net cell surface charge and verified by micro-electrophoresis measurements of the cell surface charge. Changes in the surface charge properties of cell lines contaminated with mycoplasma were also detected. However, because of the small size of mycoplasma and their similarity to the surface structure of mammalian cells, these effects could not be fully investigated.

The final set of experiments investigated the dielectrophoretic response of normal and transformed cell lines. The cells used here were able to change phenotype as a response to incubation with inducing agents. The dielectrophoretic responses of these cells showed that,

when in the near-normal state, the cells exhibited a larger dielectrophoretic response in the frequency range 100Hz to 5kHz than in their cancerous state. Also observed were changes in the large low-frequency collection, which correlated to known changes in the surface charge density of the cells. The increased collection in the mid frequency range was accompanied by an increase in the rigidity of the plasma membrane, supporting the earlier conclusion that increased rigidity of the membrane leads to an increased effective cell conductivity. It has been suggested that this increased conductivity is associated with the movement of ions tangentially across the membrane surface rather than transversely through the membrane. Treatment with the porating agent saponin showed that increasing the ability for ions to travel through the membrane had only a slight effect on the collection rate. This provided evidence that tangential charge movement dominates the effective conductivity of a cell at low frequencies.

The implications of these finding to the application of dielectrophoresis to biotechnology can also be summarised. The necessary use of highly conductive cell suspending media in manufacturing processes restricts the ability to directly collect cells by dielectrophoresis when using electric fields at frequencies less than 1MHz. Examination of the collection spectrum of *M. lysodeikticus* suspended in high ($1.0Sm^{-1}$) conductivity media shows the force to be negative (away for the regions of high field strength). *M. lysodeikticus* was the most conductive of the particles studied and, applying the equations derived in chapter 3, to obtain a usable positive dielectrophoretic force to collect bacteria, the conductivity of the suspending medium would have to be at least a factor of 10 less conductive. This does not take into account the fact that the more biotechnological important cell lines such as *E. coli* and yeasts are much less conducting than *M. lysodeikticus*. However, the negative force can be utilised to separate cells by concentrating them in regions of low field intensity. Although this would not completely separate cells it may be possible to use this technique to improve the efficiency of conventional processes. It is possible, however, that direct collection could find applications in the manufacture of high-cost low-yield products where a degree of de-salting can be carried out on the suspending media to reduce its conductivity.

A more probable application for dielectrophoresis is in the areas of general diagnostics and quality control. Use of the optical measurement system described here has shown that it is possible to detect differences in the physico-chemical properties of cells and therefore this type of system may have uses in the study of, for instance, cancer cells or be used in the removal of abnormal cells from a mixture of abnormal and normal cells. The experiments detecting the viability of HeLa cells after formaldehyde treatment show that, by the careful choice of suspending medium, it may be possible to selectively separate non-viable cells from a suspension. This would be of use in maximising the efficiency of culture inoculation.

It is hoped that this work will be continued to further investigate the large dielectrophoretic effect observed on colloidal particles at low frequencies, and to supplement dielectrophoretic measurements with dielectric and electrophoretic measurements on cell suspensions.

APPENDIX

PUBLICATIONS RESULTING FROM THIS WORK

Burt, J.P.H., Pethig R. and Price J.A.R. (1987) Fundamental Studies of Dielectrophoresis Applied to Biotechnological Problems (Part 1). BIOSEP/87/PS/RN6 Warren Spring Laboratory, Stevenage, U.K.

Price, J.A.R., Burt, J.P.H. and Pethig, R. (1987) An Optical Technique for the Measurement of Cell Dielectrophoresis. *Proceedings of the Institute of Physics Conference* Ser. No. 85: Section 1 75-79.

Burt, J.P.H., Pethig, R. and Price, J.A.R. (1987) Fundamental Studies of Dielectrophoresis Applied to Biotechnological Problems (Part 2). BIOSEP/87/PS/RN7 Warren Spring Laboratory, Stevenage, U.K.

Price, J.A.R., Burt, J.P.H. and Pethig, R. (1988) Applications of a New Optical Technique for Measuring the Dielectrophoretic Behaviour of Micro-organisms. *Biochim. Biophys. Acta* 964 221-230.

Burt, J.P.H., Pethig, R., and Price, J.A.R. (1988) Fundamental Studies of Dielectrophoresis Applied to Biotechnological Problems (Part 3). BIOSEP/88/PS/RN12 Warren Spring Laboratory, Stevenage, U.K.

Inoue, T., Pethig, R., Al-Ameen, T.A.K., Burt, J.P.H.and Price, J.A.R. (1988) Dielectrophoretic Studies of Micrococcus Lysodeikticus and its Protoplasts. *J. Electrostatics* 21 215-223.

Burt, J.P.H. and Pethig, R. (1988) Fundamental Studies of Dielectrophoresis Applied to Biotechnological Problems (Part 4). BIOSEP/88/PS/RN Warren Spring Laboratory, Stevenage, U.K.

Burt, J.P.H. and Pethig, R. (1989) Applications of Dielectrophoresis to the Study of Colloidal Suspensions. In *Electric Field Phenomena in biological Systems* (ed. R. Paris) Inst. of Physics Short Meeting Series No. 21 15-26.

Burt, J.P.H., Al-Ameen, T.A.K. and Pethig, R. (1989) An Optical Dielectrophoretic Spectrometer for Low-Frequency Measurements on Colloidal Suspensions. *J. Phys E: Sci. Instrum.* 22 952-957.

Burt, J.P.H., Al-Ameen, T.A.K. and Pethig, R. (1990) An Optical Dielectrophoretic Spectrometer for Low-Frequency Measurements on Colloidal Suspensions. *Engineering Optics* February issue 83-88. (Reprint of J. Phys. E: Sci. Instrum. Publication)

Burt, J.P.H., Pethig, R. Gascoyne, P.R.C. and Becker, F.F. (1990) Dielectrophoretic Characterisation of Friend Murine Erythroleukaemic Cells as a function of Induced Differentiation. *Biochim. Biophys. Acta* (In Press) 1034 93-101

Pethig, R. and Burt, J.P.H. (1990) Manipulation of Solid, Semi-solid or Liquid Materials. U.K. Patent Application No.9002092.6